ORDERING AND SEGREGATION IN LIQUID ALLOYS

A THESIS SUBMITTED TO THE

CENTRAL DEPARTMENT OF PHYSICS

INSTITUTE OF SCIENCE AND TECHNOLOGY

TRIBHUVAN UNIVERSITY

NEPAL

FOR THE AWARD OF

DOCTOR OF PHILOSOPHY

IN PHYSICS

BY

SHASHIT KUMAR YADAV

MAY 2018

ORDERING AND SEGREGATION IN LIQUID ALLOYS

A THESIS SUBMITTED TO THE

CENTRAL DEPARTMENT OF PHYSICS

INSTITUTE OF SCIENCE AND TECHNOLOGY

TRIBHUVAN UNIVERSITY

NEPAL

FOR THE AWARD OF

DOCTOR OF PHILOSOPHY

IN PHYSICS

BY

SHASHIT KUMAR YADAV

MAY 2018

DECLERATION

Thesis entitled "**Ordering and Segregation in Liquid Alloys**" which is being submitted to the Central Department of Physics, Institute of Science and Technology (IOST), Tribhuvan University, Nepal for the award of the degree of Doctor of Philosophy (Ph. D.), is a research work carried out by me under the supervision of Prof. Dr. Lok Narayan Jha, Central Department of Physics, Tribhuvan University, Kirtipur, Nepal and co−supervised by Prof. Dr. Devendra Adhikari, Department of Physics, Mahendra Morang Adarsha Multiple Campus, Tribhuvan University, Biratnagar, Nepal.

This research is original and has not been submitted nor published earlier in part or full in this or any other form to any university or institute, here or elsewhere, for the award of any degree.

……

Shashit Kumar Yadav
Research Scholar
Central Department of Physics
Tribhuvan University, Kirtipur
Kathmandu, Nepal

RECOMMENDATION

This is to recommend that **Shashit Kumar Yadav** has carried out research entitled "**Ordering and Segregation in Liquid Alloys**" for the award of Doctor of Philosophy (Ph. D.) in **Physics** under our supervision. To our knowledge, neither this work nor any part of it has been submitted for the award of any other degree elsewhere.

He has fulfilled all the requirements laid down by the Institute of Science and Technology (IOST), Tribhuvan University, Kirtipur for the submission of the thesis for the award of Ph. D. degree.

.....
Dr. Lok Narayan Jha
Supervisor
Professor
Central Department of Physics
Tribhuvan University, Kirtipur
Kathmandu, Nepal

.....
Dr. Devendra Adhikari
Co−Supervisor
Professor
Department of Physics
Mahendra Morang Adarsha Multiple Campus, Tribhuvan University
Biratnagar, Nepal

Date: 15/05/2018

ACKNOWLEDGEMENTS

Firstly, I would like to express my immense gratitude to my research supervisor Prof. Dr. Lok Narayan Jha, Central Department of Physics, Tribhuvan University, Kirtipur, Nepal and co−supervisor Prof. Dr. Devendra Adhikari, Department of Physics, Mahendra Morang Adarsha Multiple Campus, Tribhuvan University, Biratnagar, Nepal for their support, scientific as well as motivational inspirations, guidance and mentorship to carry this research work.

I would also like to express my sincere gratitude to Prof. Dr. B. P. Singh (University Department of Physics, T. M. Bhagalpur University, India) and Dr. Indu Shekhar Jha (Department of Physics, Mahendra Morang Adarsha Multiple Campus, Tribhuvan University, Biratnagar, Nepal) for providing database, valuable suggestion and inspirations to pursue the work.

I must express my sincere gratitude to Prof. Dr. Binil Aryal (HoD), Prof. Dr. Narayan Prasad Adhikari, Prof. Dr. Raju Khanal and Dr. Gopi Chanda Kaphle, Central Department of Physics, Tribhuvan University, Kirtipur, Nepal for their continuous supports, encouragements and inspirations to handle the work. I am also appreciative to all the faculty members and non−teaching staffs of the department for their motivational supports.

I express my sincere gratitude to Prof. Dr. Pradeep Raj Pradhan, Prof. Dr. Ashok Kumar (HoD), Prof. Dr. Saroj Nepal, Dr. Ram Prasad Koirala and all the faculty members of Department of Physics, Mahendra Morang Adarsha Multiple Campus, Tribhuvan University, Biratnagar for their valuable suggestion and encouragements. I am also thankful to all the non−teaching staffs of the department for their good wishes.

I am thankful to my seniors and colleagues Ganesh Kumar Shrestha (Pulchowk Campus, Institute of Engineering, Tribhuvan University, Latitpur, Nepal) and Saran Lamichhane (Central Department of Physics, Tribhuvan University, Kirtipur, Nepal) for their helps. I am also much thankful to my colleagues Milan Koirala (Missouri University of Science

and Technology, Physics Building, MO 65409, U. S. A.) and Lokendra Raj Khanal (Department of Physics, University of Idaho, Moscow, Idaho, U. S. A.) for their efforts to collect literatures related to this work.

My sincere thanks go to Sarita Adhikari for her continuous support, encouragement and inspiration during this work.

For the love, understanding and support, I would like to thank my beloved wife Jyoti and offsprings Piyusha and Chandan. I would also like to thank my elder brother Ramendra and his wife Bimal Devi for their love, support and good wishes during my ups and downs. Moreover, I would like to show my gratitude to my father−in−law Damodar Khadga, mother−in−law Anila Devi and brother−in−law Shambhu Nandan Khadga for their continuous supports and encouragements. Last but not the least, I would like to show my immense gratitude to my father Yogendra Prasad for the encouragement and inspirations and my mother late Ramkumari Devi for nurturing and standing there for me during her physical presence.

Shashit Kumar Yadav

April, 2017

ABSTRACT

The design and fabrication of new alloys is usually approached by a method that combines theoretical analysis and experimental observation (composition−structure−property), but in many cases, due to the experimental difficulties related to high temperatures, the theoretically predicted property values are of key importance. This is particularly relevant for all industrial processes, such as casting, joining, crystal growth, etc. that involves the presence of the liquid phase, i.e. liquid metals and alloys. Alloying processes have been evolved as one of robust tool to achieve desired materials with required characteristics. The thermal treatments of materials, chemical compositions and operating parameters (temperature, pressure and working atmosphere) overrule the microstructure of an alloy. The in−depth knowledge of thermodynamics, kinetics and thus, the energetic of the alloy prototypic process has great significance in metallurgical science and engineering.

In view of the aforementioned, we have studied and explained the mixing behaviour of two Al−based (Al−Fe at 1873 K and Al−Mg at 1073 K) as well as two Bi−based (Bi−Tl at 750 K and In−Bi at 900 K) liquid binary alloys with the help of theoretical modeling. The thermodynamic properties, such as free energy of mixing (G_M), activity (a), enthalpy of mixing (H_M) and entropy of mixing (S_M), structural properties, such as concentration fluctuation in long wave length limit ($S_{CC}(0)$), chemical short range order parameter (α_1) and ratio of diffusion coefficients (D_M/D_{id}) for above mentioned liquid alloys at chosen temperatures have been analyzed in the fame work of regular associated solution model. For this purpose, we have determined the model parameters which are the interaction energy parameters ($\omega_{1,2}$, $\omega_{1,3}$ and $\omega_{2,3}$), equilibrium constant (k), mole fractions of complex ($x_{A_\mu B_\nu}$) and free monomers (x_A and x_B). The compositional contribution from the heat associated with the formation of the complex and the heat of mixing of species to the net enthalpy change has been studied for each system. The comparative studies of the thermodynamic properties of these systems reveal that the Al−Fe being the most interacting system followed by the Bi−Tl, the Al−Mg and the In−Bi, in which the

interactions are the weakest. Theoretical investigations of structural properties show that all the preferred liquid alloys show complete ordering nature at least close to their respective melting temperatures. The interaction energy parameters are found to be temperature dependent. The surface properties of the chosen liquid alloys have been explained with the help of Renovated Butler model. The trends of surface segregations in these liquid binary alloys have been studied by computing surface tension (σ) and surface concentrations (x_A^S and x_B^S). Theoretical investigations confirm the segregation of the alloy component having a lower surface tension, i.e. the extent of segregation of Bi−atoms at the surface layer, which is more pronounced in In−Bi melts with respect to that of liquid Bi−Tl alloys. Moreover, in case of two Al−based melts, the Al−atoms segregate on the Al−Fe surface phase whereas they remain in the bulk region of Al−Mg.

Additionally, the regular associated solution model has been extended to study and predict the thermodynamic and structural properties of concerned liquid alloys at different temperatures. For this purpose, $\omega_{1,2}$, $\omega_{1,3}$ and $\omega_{2,3}$ for each of the system have been computed at different temperatures keeping $x_{A_\mu B_\nu}$, x_A, x_B and k invariant. The modeling equations obtained by the polynomial fitting of different orders along with the values of parameters to forecast these properties have also been included in this work. Theoretical computations indicate that the excess Gibbs free energy of mixing (G_M^{XS}) of the alloys gradually decreases with an increase in temperature above melting temperatures. Accordingly, at higher temperatures, the ordering or the compound formation tendencies of these alloy systems gradually decrease and sometimes show segregating nature. These findings are further supported by decrease in deviations between the computed and observed values of $S_{CC}(0)$ at higher temperatures. The liquid alloys thus show the maximum tendency towards complex formation at their respective melting temperatures, however, these tendencies significantly decreases at elevated temperatures. Thermodynamic properties have been then correlated with the Renovated Butler model to explain the surface properties at different temperatures. The computed values for the surface concentrations of the segregating components of the liquid alloys approach respective ideal values at higher temperatures. Similarly, the surface tension of metallic melts metals and alloys, decrease at elevated temperatures.

LIST OF SYMBOLS

A, B	Components of a liquid binary alloy
A–B	Type of liquid alloy
$A_\mu B_\nu$	Type of complex
μ, ν	Stoichiometry indices of a complex
x_1, x_2	Bulk concentrations of respective constituent atoms an alloy
x_q	Mole fractions of a component (q =A or B)
$x_{A_\mu B_\nu}$	Mole fraction of complex $A_\mu B_\nu$
$\omega_{i,j}$	Interaction energy parameters (i, j =1, 2, 3; i ≠ j)
γ_q	Activity coefficient of free monomers
a_q	Activity of free monomer
K	Equilibrium constant
G_M	Free energy of mixing
G_q^{XS}	Partial excess free energy
G_M^{XS}	Excess free energy of mixing
H_M	Heat of mixing
S_M	Entropy of mixing
$S_{CC}(0)$	Concentration fluctuation in long wavelength limit
α_1	Chemical short range order parameter
D_M/D_{id}	Ratio of mutual to intrinsic diffusion constant
α_q^0	Molar surface area of a pure component
σ_q^0	Surface tension of pure alloy component
σ	Surface tension of the liquid alloy
x_q^S	Surface concentration of an alloy component

LIST OF TABLES

LIST OF FIGURES

TABLE OF CONTENTS

CHAPTER 1

INTRODUCTION

1.1 Preface

The prime goal for researchers and engineers in metallurgical science is to design and/or optimize alloy microstructure in order to obtain the required properties and thus, desired performances. The chemical compositions, processing route and thermal processing/treatments of materials together with operating parameters (temperature, pressure, working atmosphere) govern the microstructure of an alloy. Though alloys have profound utilizations in the solid state, their properties are originated in the liquid state. Eventually, the understanding of energetic of the initial melt serves as fundamental basis to develop new alloys with desired characteristics. Thus in metallurgical synthesis, design and characterization, the determination of alloying behaviour, such as thermodynamic, electrical, magnetic, surface, bulk and structural properties of mixing of binary liquid alloys are one of the basic field of research.

To understand the mixing behaviour of complex alloys, a comprehend knowledge about the phase stability and thermodynamics of the binary subsystems is mandatory. This information cannot be exclusively obtained from experiments as they are expensive, time consuming, cumbersome, and often face difficulties related to high reactivity of melts at high temperatures. With these regards, the thermodynamic modeling is a useful tool to understand the nature and to predict the alloying behaviour of liquid alloys reflecting theme of the appropriate phase equilibria are most essential. Moreover, the asymmetries as well as the anomalies in the mixing properties of the liquid alloys have drawn considerable attentions of researchers in the field of Materials Science since century. Both the theoreticians (Butler, 1932; Hume-Rothery & Powell, 1935; McLean, 1957; Bhatia et al., 1974; Overbury et al., 1975; Burton & Machlin, 1976; Lele & Ramchandrarao, 1981; Singh, 1987; Jha et al., 1990; Saboungi et al., 1990; Singh et al., 1993; Prasad & Singh, 1991; Prasad et al., 1996; Srikanth et al., 1999; Anusionwu, 2010; Novakovic, 2002,

Adhikari, 2011; Adhikari et al., 2014; Kaptay, 2015; Yadav et al., 2015, 2016) and the experimentalists (Harris, 1968; Brongersma & Buck, 1975; Tamaki et al., 1984; Lee et al., 2004; Giuranno, 2002, Mekler & Kaptay, 2008; Yakymovych et al., 2008) have been devising models and experimental techniques to get through the anomalies in thermodynamic, microscopic structural and surface properties of alloys since decades.

Eventually, we intend to study the mixing properties of two Bi−based (Bi−Tl and In−Bi) and two Al−based (Al−Fe and Al−Mg) binary liquid alloys on the basis of theoretical modeling. The thermodynamic properties, such as Gibbs free energy of mixing, activity, heat of mixing and entropy of mixing and the structural properties expressed by the microscopic functions, such as the concentration fluctuation in long wavelength limit, chemical short range order parameter and ratio of diffusion coefficients for the above mentioned liquid alloys have been studied in the framework of the regular associated solution model. The surface properties, such as the surface tension and surface segregation have been studied by means of Renovated Butler model. The details of these models along with their advancements are highlighted in literature survey in the next Chapter. In this work, we intend to extend regular associated solution model to predict the thermodynamic and structural properties of the liquid alloys at different temperatures which will definitely serve as a database in case of unavailability of experimental data. On the same contest, we have combined the thermodynamic functions with Renovated Butler model to predict the surface properties of above mentioned systems at different temperatures.

Following Guggenheim (1952), the regular or presumably conformal solution theories are generally considered to be valid when the size factor ($\Omega_{A-B} = \Omega_A/\Omega_B$; Ω being the atomic volumes of the components of alloy at its melting temperature) is less than 2. The size factors of the systems preferred in the present study are found to be 0.87, 0.82, 1.50 and 0.73 for Bi−Tl, In−Bi, Al−Fe and Al−Mg respectively. We, therefore, have employed the regular solution theories to study and explain the mixing behaviours of above mentioned systems. Moreover, the compound forming alloys are characterized by large electronegativity difference and show ionic behaviours. The electronegativity difference

($d = E_{A-B} = E_A - E_B$; E_A and E_B are the electronegativity of components A and B respectively for $E_A > E_B$) and hence the ionic character [IC = 1-exp*(-0.25d*^{2})] for the preferred systems are 0.40, 0.24, 0.22, 0.30 and 0.0392, 0.0010, 0.0120, 0.0223 respectively for Bi−Tl, In−Bi, Al−Fe and Al−Mg liquid alloys. Hence, the preferred systems do not show ionic character leading to the complex formation. Eventhough, the phase diagrams of the solid state clearly indicate the stable complexes at one or more stiochiometric compositions (Hultgren *et al*. 1973; Desai, 1987).

The liquid alloys investigated in the present study have great depth of deviations with respect to their mixing behaviours and with no doubt will provide wide spectrum of information. Due to the desirable properties, they have found to have space in numerous applications. The alloys of bismuth (Bi) have low melting points and hence are preferred over lead in solders as lead being hazardous to mankind and nature (Mc Cormack et al., 1994; Suganuma, 2001; Gnecco et al., 2007; Plevachuk et al., 2011). Iron aluminides are used as high temperature structural and functional materials. They possess good oxidation resistance, weight reduction and good ductility and hence have numerous applications in present day technology (Cubero−Sesin & Horita, 2012). Nevertheless, the advantage of the regular associated solution model is that the model parameters (pairwise interaction energies and equilibrium constant) are calculated with the aid of experimental values of the activity coefficients at infinite dilution of the components of the binary liquid alloys irrespective of the most of other models where they are just fitting parameters. The mole fractions of the complex and the unassociated species are calculative parameters in this model which govern the entire mixing properties of the system in addition to most of the other models where gross mole concentrations overrule these properties.

1.2 Alloying behaviours of binary liquid alloys

The thermodynamic functions of liquid alloys provide the fundamental information relating to the extent of interaction in the light of which the tendency towards complex formation or demixing in the initial melt can be understood. The structural properties give microscopic view of arrangement of atoms in nearest neighborhood in the melt whereas

the information about the surface phenomenon can be withdrawn from surface properties. However, the expressions for the structural and surface properties have direct dependence on thermodynamic functions especially partial excess free energy or Gibbs free energy of mixing for binary liquid alloys (Gibbs, 1875-1878; Butler, 1932; Bhatia & Thornton, 1970; Singh & Sommer, 1997; March & Alonso, 2008; Novakovic, 2010; Kaptay, 2015).

The activity (a) can be coined as the fundamental thermodynamic property to qualify and quantify the thermodynamic, structural and surface properties of liquid alloys. It can be directly measured from experiments as a function of concentration and temperature. Any deviations from the ideal behaviour can be lumped into the activities of the monomers of the liquid alloys. Their magnitudes are considered to predict the extent of interactions among the species of the liquid mixture which in turn determine the stability of the complex. The free energy of mixing (G_M) of liquid alloys in general determines the strength of bonding between the atoms of complex. A compound formation tendency in alloy melts can be "quantified" by the normalized form of the Gibbs free energy of mixing expressed as G_M/RT and its values varying between 0 and -1 are characteristic for weakly interacting systems, those between -1 and -2 characterize moderate interacting systems, while the systems with (G_M/RT) ≤ -2.5 are strongly interacting. According to the thermodynamics, the phase assemblage with the lowest free energy determines the equilibrium state of the system at given temperature, pressure and chemical composition. It can be expressed as the function of activity for binary liquid alloy as

$$G_M = RT \sum x_l a_i \tag{1.1}$$

where R is universal gas constant, T is absolute temperature, *l* (=0.1−0.9) is concentration and i (=1, 2) is the number of species of the liquid alloy.

The heat of mixing (H_M) is another important thermodynamic parameter which is directly measurable from calorimetric experiments. The short−range ordered liquid alloys are characterized by large negative values of heat of mixing whereas the low negative and positive values of heat of mixing reflect the tendency towards demixing and segregation.

Likewise, the entropy (S_M) is another essential thermodynamic function which determines the equilibrium state of the system. The system with an increase in entropy is featured with transfer from stable to unstable state. In general, it is not directly measurable from experiments and hence needs to be comprehended by theoretical modeling. The theoretical modeling equations of both H_M and S_M are derivable from G_M as

$$H_M = G_M - T\left(\frac{\partial G_M}{\partial T}\right)_p \tag{1.2}$$

and, $$S_M = -\left(\frac{\partial G_M}{\partial T}\right)_p \tag{1.3}$$

where p is pressure.

Talking about the structural properties, the concentration fluctuation in long wavelength ($S_{CC}(0)$) has been devised as a powerful tool to peep into the nature of local arrangements of atoms in the liquid mixture at microscopic level. The quantitative statistical concept of $S_{CC}(0)$ was introduced by Bhatia and Thornton (1970), since then several researchers (Bhatia & Hargrove, 1974; Bhatia & March, 1975; Singh, 1987; Prasad et al., 1991; Singh and Sommer, 1997; Akinlade et al., 2000; Novakovic et al., 2004, 2011; Awe et al., 2008; Adhikari et al., 2010; Adhikari, 2011; Adhikari et al., 2014) have profoundly studied it to understand the hetero−coordinating or homo−coordinating asymmetry in liquid alloys. As stated earlier, it can be expressed as the function of G_M by the relation

$$S_{CC}(0) = \left[RT\left(\frac{\partial^2 G_M}{\partial {x_1}^2}\right)^{-1}\right]_{T,p,N} \tag{1.4}$$

where x_1 is concentration of species A in the liquid mixture and N is total number of atoms. The ideal value of $S_{CC}(0)$ can be expressed as

$$S_{CC}^{id}(0) = x_1 x_2 \tag{1.5}$$

where $x_2 = (1 - x_1)$ is the concentration of atom B in the liquid mixture.

The deviation of $S_{CC}(0)$ from $S_{CC}^{id}(0)$ is gateway to understand the nature of interaction between the species in the initial melt. At a specific composition, if $S_{CC}(0) \gg S_{CC}^{id}(0)$ corresponds to tendency towards segregation which leads to phase separation and if $S_{CC}(0) \ll S_{CC}^{id}(0)$ refers to tendency towards ordering or tendency towards formation of complex in the initial melt.

The chemical short range order (α_1) and ratio of mutual to intrinsic diffusion coefficients (D_M/D_{id}) helps to understand the nature of local arrangement of atoms in the liquid mixture. Both of these parameters can be expressed in terms of $S_{CC}(0)$. At a given composition, if $\alpha_1 > 0$ refers to segregation for which $\frac{D_M}{D_{id}} < 1$ and if $\alpha_1 < 0$ corresponds to ordering for which $\frac{D_M}{D_{id}} > 1$.

The information about the surface phenomena can be obtained with the study of surface properties, such as surface tension (σ) and surface segregations (x_q^S; q =A or B). They are important to understand the processes, such as wetting or decomposition, nucleation, etc. Following Gibbs (1875−1878), the surface tension in terms of thermodynamics can be expressed as

$$\sigma \equiv \left(\frac{dG}{dA}\right)_{p,T,N} \tag{1.6}$$

where G is absolute Gibbs energy and A is absolute surface area. This expression has been serving as the epicenter for all the theoretical modeling equations as well as devising experimental tools to study surface tension of liquid metals or alloys till date.

1.3 Classification of binary liquid alloys

The binary liquid alloys can be broadly categorized on the basis of position of the extremum values of thermo−physical functions and their deviations from ideal behaviour. They are classified as mentioned in the following sub−sections.

1.3.1 Asymmetric and symmetric binary liquid alloys

With regards to the symmetry of curves describing thermodynamic functions, such as G_M, H_M, $S_{CC}(0)$, etc. at the equiatomic composition $x_1 = x_2 = 0.5$, the binary liquid alloys can be grouped into two classes: symmetric and asymmetric. In the former class, these functions are symmetric at the equiatomic composition and are termed as regular alloys. The binary liquid alloys, such as In−Bi; Cu−Zn, Al−Zn, Bi−Pb, Al−Fe, etc. belong to this class (Hultgren *et al.*, 1973; Desai, 1987; Singh, 1987; Adhikari et al., 2014). Fig. 1.1(a) shows the plot of compositional dependence of the Gibbs free energy of mixing (G_M/RT) for Al−Fe liquid alloys at 1873 K representing symmetric binary liquid alloy.

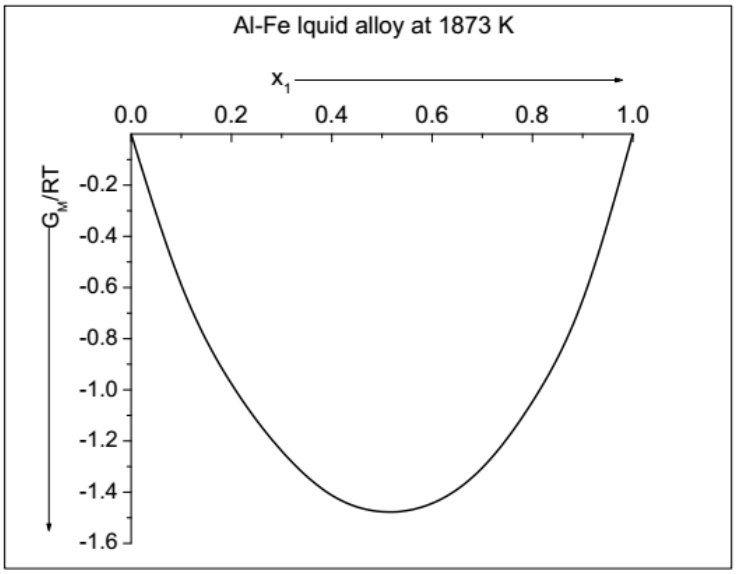

Figure 1.1 (a): The Gibbs free energy of mixing (Hultgren *et al.*, 1973) versus concentration of Al (x_1) for Al−Fe liquid alloys at 1873 K.

Whereas in the later class of liquid alloys, the thermo−physical functions are not symmetric at the equiatomic composition such that their extremum values lie at other

stoichiometric compositions. The binary liquid alloys, such as Bi−Tl, Ag−Al, Cu−Sn, Mg−Tl, Ag−Ge, Ag−Sb, etc. (Hultgren *et al.*, 1973; Yadav et al., 2015) fall under asymmetric category. Figure 1.1 (b) shows the plot of compositional dependence of the Gibbs free energy of mixing (G_M/RT) of Bi−Tl liquid alloy at 750 K corresponding to the asymmetric class of alloy.

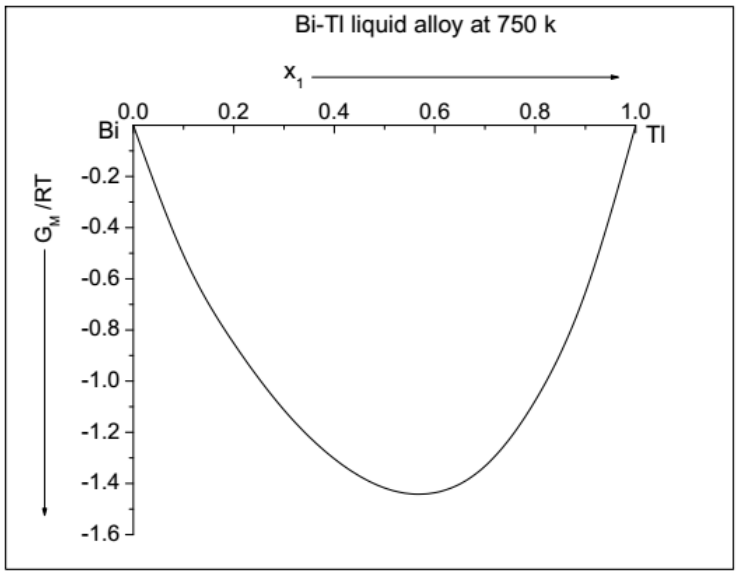

Figure 1.1 (b): The Gibbs free energy of mixing (Hultgren *et al.*, 1973) versus concentration of Tl (x_1) for Bi−Tl liquid alloys at 750 K.

1.3.2 Ordering and segregation in liquid binary alloys

On the basis of deviation of thermo−physical functions from ideal mixing conditions, the binary liquid alloys can be further grouped into two classes: ordering and segregating liquid alloys (Alblas, 1983; Singh & Sommer, 1997). In the former class, the liquid alloys show negative deviation from ideal Raoult's law and are characterized as short−range ordered. For these alloys, if $S_{CC}(0) \ll S_{CC}^{id}(0)$, then it correspods to ordering nature or tendency towards compound formation in the melt (Alblas, 1983; Singh & Sommer, 1997). Al−Fe, Al−Mg, In−Bi, Bi−Tl, Mg−Ga, etc. (Hultgren *et al.*, 1973) are compound forming liquid alloys. Fig. 1.2 (a) shows the plots compositional dependence of $S_{CC}(0)$ for Al−Fe liquid alloy at 1873 K referring to this class (Desai, 1987).

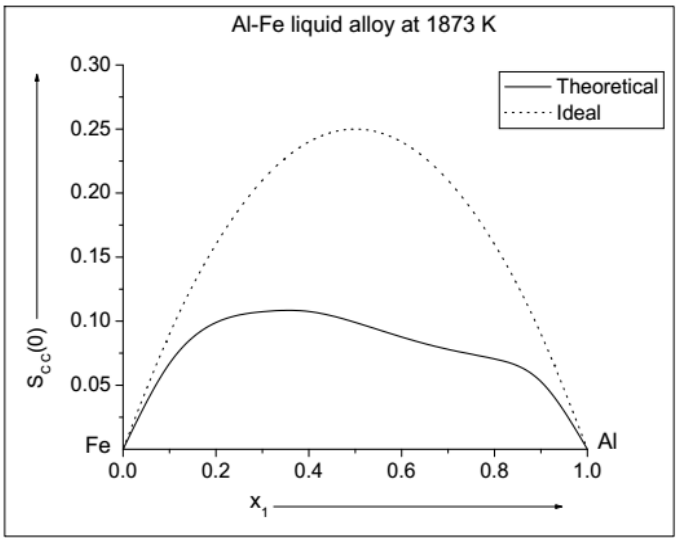

Figure 1.2 (a): The computed values of $S_{CC}(0)$ versus concentration of Al (x_1) for Al–Fe liquid alloy at 1873 K.

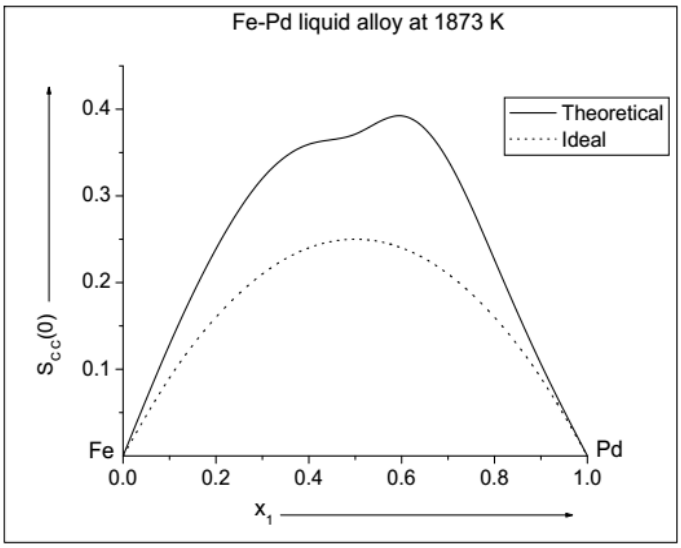

Figure 1.2 (b): The computed values of $S_{CC}(0)$ versus concentration of Pd (x_1) for Fe–Pd liquid alloy at 1873 K.

In the case of the later class, the liquid alloys show positive deviation from Raoult's law and are characterized as segregating systems. The values of $S_{CC}(0) \gg S_{CC}^{id}(0)$ for these liquid alloys referring to the homo–coordinating tendency in the initial melt. If the deviations are noticeably large, these alloys lead to phase separation. Fe–Pd, Co–Sn, Bi–Ga, Bi–Zn, Li–Na, etc. alloys falls under this group (Hultgren *et al.*, 1973; Singh &

Sommer, 1997). Fig. 1.2 (b) corresponds to the plots of compositional dependence of $S_{CC}(0)$ for Fe−Pd liquid alloy at 1873 K indicating the present class of alloys.

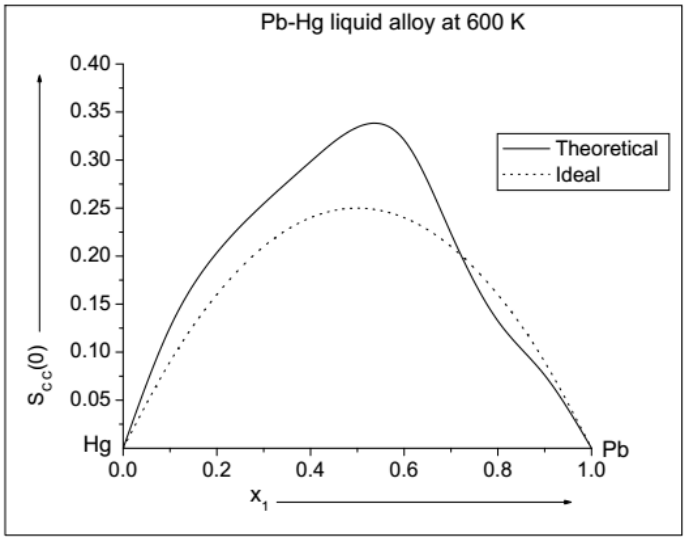

Figure 1.2 (c): The computed values of $S_{CC}(0)$ versus concentration of Pb (x_1) for Pb−Hg liquid alloy at 600 K.

While some of the liquid alloys, such as In−Sn, Pb−Hg, Cd−Na, Ag−Al, etc. also show the transformation from segregating to ordering behaviours (Hultgren *et al.*, 1973, Yadav et al., 2015). Fig. 1.2 (c) shows the plots of compositional dependence of $S_{CC}(0)$ for Pb−Hg liquid alloys showing segregation to ordering transformation. Their heat of mixing ranges from positive or low negative values to high positive values indicating transformation from homo−coordinating system to hetero−coordinating.

1.4 Organization of the work

The present work has been divided into following Chapters:

Chapter 2: It consists of a brief review of literatures by going through with the present work is organized and carried out.

Chapter 3: The necessary theories about the regular associated solution model have been presented in this chapter. It includes theoretical modeling equations derived in the frame

work of above stated model to compute the model parameters, such as mole fraction of complex ($x_{A_\mu B_\nu}$), interaction energy parameters (ω_{ij}), equilibrium constant (k), temperature derivative terms of interaction energy parameters ($\partial\omega_{ij}/\partial T$) and heat of dissociation ($RT^2 d\ln k/dT$) and; the thermodynamic functions, such as free energy of mixing (G_M), activity (a), heat of mixing (H_M) and entropy of mixing (S_M). The derivations of the expressions for the evaluations of the structural functions, such as concentration fluctuation in long wavelength limit ($S_{CC}(0)$), chemical short range order parameter (α_1) and ratio of mutual to intrinsic diffusion coefficients (D_M/D_{id}) are also presented in this Chapter. Further, it includes the formulations to evaluate the surface properties, such as surface tension (σ) and surface segregations (surface concentrations of liquid components, x_A^S and x_B^S) in the frame work of Renovated Butler model.

Chapter 4: The results and discussion of the thermodynamic, structural and surface properties for Bi−Tl, In−Bi, Al−Fe and Al−Mg liquid alloys are included in this chapter. The theoretical modeling equations obtained by extending regular associate solution model to predict the thermodynamic and structural functions of above mentioned liquid alloys at different temperatures along with their results and discussion are also included in the same Chapter. Additionally, it includes the results and discussion for the prediction of structural properties of the liquid alloys at different temperatures.

Chapter 5: It contains the conclusion and recommendations of the present work.

Chapter 6: It amends the brief summary of the present work.

CHAPTER 2

LITERATURE REVIEW

2.1 Introduction

The alloying as the processing route for metals has been developed as a robust tool in achieving desired materials with predetermined characteristics. The alloying of two metals usually results into a new material with improved properties, such as superiority in mechanical and electrical properties, an increased resistance to oxidation and radioactive processes, etc. These exemplify the needs of an in−depth understanding of energetic and kinetics of alloy prototypic process. In this limelight, the researchers in the field of material science have been long attempting to understand and access the alloying behaviours of binary liquid alloys by employing and developing different approaches. These approaches can be distinctly divided into two theories: free electron theory of mixing and statistical theory of mixing.

2.2 A brief review of electronic approaches for mixing properties of binary alloys

The initialization of the concept of free electron theory is accredited to Sommerfeld (1933) and was a breakthrough for paving the path to comprehend the thermodynamic properties of metals and alloys. Following this concept, several other empirical models have been devised (Hume−Rothery et al., 1934; Hume−Rothery & Powell, 1935; Darken & Gurry, 1953; Brewer, 1967; Miedema et al., 1980; Hume−Rothery *et al.*, 1988) to study the trends of alloying metals and correlating the electronic properties to physical stability or phase stability of pure metals as well as alloys. Meanwhile, Hume−Rothery et al. (1934) put forwarded some rules based on size mismatch, crystal structures, electrochemical factors and valence effect regarding the trends of alloying of pure metals; and applied the concept to study the formation of compound in alloys of copper and silver (Hume−Rothery et al., 1934). Later this concept was extended by Darken and Gurry (1953) to predict solid solubility on ionic radii and electro negativity of metals for Mg

which created a road map in metallurgical processes. The Engel−Brewer method was then developed by Brewer (1967) by correlating the Hildebrand (Hildebrand & Scott, 1950) formulations to the Engel method and used it to compute the mixing properties and phase transformations in binary and multi−component systems. This model has been broadly used to study and predict the phase diagrams of actinides and transition metals (Brewer, 1965; Brewer & Lamoreaux, 1980; Ogawa, 1993; Wu & Brewer, 1996). Another approach then profoundly used was Miedema model to calculate the enthalpy of formation of compounds and enthalpy of mixing of solutions by several workers (Bangwei, 1983; Zhang & Jesser, 2002; Lin et al., 2010; Zhou et al., 2010; Arzpeyma et al., 2013). Further substitutions were then made by formulating volume−based expression for excess entropy of mixing (Kleppa, 1960). The empirical methods relating the entropy of mixing to heat of mixing, melting and boiling temperatures were put forwarded by another group of researchers (Kubaschewski, 1976; Tanaka et al., 1990; Witusiewicz, 1995; Witusiewicz & Sommer, 2000; Sommer et al, 2001).

Based on the electron theory, pseudopotential model developed by Harrison (1966) and hard sphere model (Young, 1976; Mansoori et al., 1971; Umar et al., 1976; Singh & Choudhary, 1981; Mishra et al., 1993; Vora, 2010; Kumar & Ojha, 2011; Arzpeyma et al., 2013) were used as robotic tool for an in−depth study of energetic of alloying materials. The cyclopedic study of energetic of binary liquid alloys based on these approaches have been done by Stroud (1973) on the phase separation in lithium−sodium alloys, Umar et al. (1974) on the enthalpy and entropy of sodium−potassium alloys, Joarder et al. (1984) on noble metal alloys, Stevenson 1975) on liquid hydrogen helium and Hafner (1977) on some liquid mixtures. Moreover, the parameterization of the excess entropy of formation of binary liquid alloys in terms of pseudopotential and hard sphere models have been done by Umar et al. (1974, 1976). The hard sphere theory has been employed by Schwitzgebel and Langen (1981) to study the diffusion of binary liquid alloy systems, such as Bi−Sn, Sn−Zn, Li−Ag, Hg−Zn and Li−Pb. Several other researchers employed this concept to study the trends of alloying behaviour, such as electrical resistivity and thermodynamic properties of Na−K, Na−Rb, Na−Cs, K−Rb and K−Cs (Mishra et al., 1993; Wang et al., 1980; Singh, 1981), entropy of mixing of Na−Sn

(Hoshino, 1982), Li−Pb (Hoshino & Young, 1980), Al−Mg, Cd−In, Cd−Tl, In−Zn, Cd−Zn and Mg−Zn (Singh & Choudhary, 1981), electrical resistivity of Na−Pb (Thakur et al., 2005), structure and electrical resistivity of liquid alkali alloys (Singh et al., 1991), etc. Even though the above approach does not contains any adjustable parameter, the information about the structural properties, such as segregation and phase separation cannot be obtained purely on the basis of hard sphere models which deals fundamentally with negative potentials (Singh & Sommer, 1997). This concept was later modified by Osman and Singh (1993, 1995) by introducing the role of interactive potentials in the framework of a hard sphere like approach to phase stability of a binary mixture. The segregation and phase separation in binary liquid alloys can be explained on the basis of this modified hard sphere potential for an attractive interaction (Singh & Sommer, 1997).

2.3 A brief review of statistical approaches for the mixing properties of binary alloys

2.3.1 Modeling of thermodynamic and structural properties

Besides electronic theory, different statistical models have been so far devised by researchers in this field to access the energetics of liquid mixtures since decades (Prigogine & Defay, 1954; Jordan, 1970; Bhatia et al., 1974; Lele & Ramchandrarao, 1981; Alonso et al., 1982; Alblas, 1983; Singh & Mishra, 1988; Jha, 1989; Singh et al., 1990; Singh & Sommer, 1997; Jha & Mishra, 2001; Anusionwu et al., 2003; Adhikari et al., 2010; Adhikari, 2013; Yadav et al., 2015, 2016; Koirala, 2016). They have derived analytical expressions for the various thermodynamic and structural functions based on different assumptions. As a first approximation, an ideally associated solution model was devised as an initial tool to comprehend the thermodynamic mixing functions of liquid alloys (Hildebrand & Scott, 1950; Prigogine & Defay, 1954; Bhatia et al., 1974). In this model, ideal mixture of the free atoms and the associate or complex are assumed to be in tranquility. Herein, the interactions between the different species in the liquid mixture are ignored and the only unknown parameters are the free energy of formation of the complex and its temperature dependence terms which can be determined from the experimental data. Therefore, the interchange energy parameter, $\omega = 0$ and hence the

heat of mixing, $H_M = 0$. As a result, the free energy of mixing is determined from the configuration entropy and the later can be expressed as (Alblas, 1983)

$$S_M = -R\{x_1 \ln x_1 + x_2 \ln x_2\} \tag{2.1}$$

For $H_M = 0$, from Eqs. (1.2) and (1.3) one can get

$$G_M = RT\{x_1 \ln x_1 + x_2 \ln x_2\} \tag{2.2}$$

where the terms have usual meanings. The expression for $S_{CC}(0)$ is similar to Eq. (1.5).

Later the conformal solution model developed by Longuet-Higgins (1951) was employed by several workers (Bhatia et al., 1973; Alonso & March, 1982) to study and explain $S_{CC}(0)$ of regular alloys in which the liquid mixture with the particles of nearly same size are assumed to interact with each other so that $\omega \neq 0$. In case of regular mixture, both the enthalpy of mixing and entropy of mixing contribute to the free energy of mixing. Following Alblas (1983), H_M and G_M can be give as

$$H_M = RTx_1x_2\omega \tag{2.3}$$

$$G_M = RT\{x_1 \ln x_1 + x_2 \ln x_2\} + RTx_1x_2\omega \tag{2.4}$$

The expression for $S_{CC}(0)$ then becomes

$$S_{CC}(0) = x_1x_2/\{1 - 2x_1x_2\omega\} \tag{2.5}$$

This approach has been broadly used to study the thermodynamics of regular alloys. However, it ignores the local ordering and hence chemical short range order parameter (α_1) cannot be studies under this assumption as $\alpha_1 \to 0$. Additionally, the concentration fluctuations in binary liquid alloys characterized with a small heat of mixing but with a sizeable atomic volume mismatch between the components of liquid mixtures cannot be

explained by the conformal solution theory. This discrepancy suggests the necessity of developing further more statistical tools to investigate the mixing properties of binary liquid alloys. To overcome the above incomprehensibility, Bhatia and March (1975) have introduced Flory–Huggins model (Flory, 1942; Huggins, 1942, Guggenheim, 1952) for the binary liquid alloys. This model was initially devised for a lattice model of polymers. In this approach, the free energy of mixing of a liquid alloy can be given as

$$G_M = Nk_BT[x_1 \ln \phi + x_2 \ln(1-\phi) + \omega x_1(1-\phi)] \tag{2.6}$$

where the first term is $(-T)$ times the entropy of mixing and the second term is the heat of mixing. N stands for number of atoms in the alloy, k_B is Botzmann constant, ω is the interchange energy parameter and $\phi = x_1/(x_1 + \gamma x_2)$ such that $\gamma = V_B/V_A$, V being the atomic volume and B stands for the larger atom of the alloy.

The activity (a) in terms of ω can be expressed as (Bhatia & March, 1975)

$$\ln a_1 = \ln\left(\frac{x_1}{\gamma}\right) - \ln\left\{\frac{x_1+\gamma x_2}{\gamma}\right\} + \frac{(\gamma-1)x_2}{x_1+\gamma x_2} + \frac{\gamma^2 x_2^2 \omega}{\{x_1+\gamma x_2\}^2} \tag{2.7}$$

With the help of Eqs. (2.6) and (1.4), the expression for $S_{CC}(0)$ can be given as (Bhatia & March, 1975)

$$S_{CC}(0) = x_1x_2/\{1 - x_1x_2\delta\} \tag{2.8}$$

$$\text{where, } \delta = \{2\gamma^2\omega - (\gamma-1)^2[\gamma - x_1(\gamma-1)]\}[\gamma - x_1(\gamma-1)]^{-3} \tag{2.9}$$

They further emphasized that this model is only valid for the liquid alloys having large volume ratios ($\gamma \geq 2$). On the basis of this theory, the concentration fluctuation in liquid Na–Cs alloy (for which $\gamma = V_{Cs}^0/V_{Na}^0 = 3.03$) was successfully explained by Bhatia & March (1975). However, this model failed to explain $S_{CC}(0)$ for liquid alloys for which $\gamma < 2$, such Na–K where $\gamma = V_K^0/V_{Na}^0 = 1.96$. This model was later modified by Alonso

et al., (1982) by introducing the concentration dependence of the heat of mixing given by the semi−emperical theory of Miedema (Miedema, 1973; Miedema et al., 1977) into the Flory's expression for the free energy of mixing for liquid alloys having small atomic size mismatch. The Flory−Miedema theory was used to explain the concentration fluctuation in Na−K (Alonso et al., 1982).

Meanwhile a simple statistical mechanical model was proposed by Singh and Mishra (1988). It is based on pairwise interaction energies to obtain conditional probabilities for the occupation of neighbouring atoms in binary liquid alloys. On this floor the analytical expressions for activity, free energy of mixing, concentration fluctuation in long wavelength limit and the chemical short range order parameters have been derived. In this statistical framework the concentration dependent thermodynamic functions were explained by evaluating ordering energy for Cu−Pb, Na−K, Li−Mg and Cd−Mg (Singh & Mishra, 1988). This approximation was further extended by Singh et al. (1990) to explain the extent of hetero−coordination in Cd−based regular binary liquid alloys, such as Cd−Bi, Cd−Mg and Cd−Ga.

Another statistical model called quasi−chemical approximation has been profoundly used to explain the energetic of regular binary liquid alloys by many researchers (Bhatia & Singh, 1982, 1984; Singh et al., 1987, 1990; Anusionwu, 2000; Awe et al., 2008; Passerone et al., 2009; Novakovic, 2010; Adhikari et al., 2012; Awe & Olawole, 2012, Koirala et al., 2013, 2014, Singh et al., 2015; Koirala, 2016). This approximation is found to explain the thermodynamics of liquid alloys with negative chemical short range order which are termed as ordering alloys (Singh et al., 1987, 1990). But this model stands poor for the liquid alloys with positive chemical short range order which are assumed to be homo−coordinating (Singh, 1987).Even though; the mixing behaviour of two segregating liquid Cd−Pb and In−Pb alloys have been studied by Odusote et al. (2007) on the basis of this theoretical framework. Following the constraints of quasi−chemical approximation, the concentration fluctuations and chemical complexes in Zn−Au liquid alloy has been studied by Anusionwu in 2000. Awe et al. (2008) has studied the surface properties of Bi−Pb and Sb−Sn and the thermodynamic properties of Ga−based liquid alloys based on

this approximation. Passerone et al. (2009) used this approximation to explain the mixing behaviour of liquid Cu-B alloys. Novakovic (2010) have employed this approximation to explain the energetic of two Nb−based (Al−Nb and Nb−Ti) alloys. Awe and Olawole (2012) studied the correlation between bulk properties and surface properties in Cd−X (X=Hg, Mg) liquid alloys, Koirala (2016) have studied the mixing properties of Al−Ga, Cd−In, Cd−Zn, Fe−Pd, Ga−Zn, In−Tl and K−Na liquid alloys on the basis of quasi−chemical approximation.

Since decades different experimental techniques have also been designed and carries out to study the thermodynamics of mixing of a number of alloys by the experimentalists (Taylor & Jones, 1958; Belton & Fruehan, 1969; Predel, 1982; Komarek et al., 1973; Tamaki et al., 1984, Harada et al., 1988; Yakymovych et al., 2008; Cubero−Sesin & Horita, 2012) in the field of material science and engineering. Most of them reported the anomalies in the thermodynamics behaviours of a great numbers of alloys. These experimental database were then compiled by Hultgren *et al.* (1973) which distinctly indicate the asymmetry in the thermodynamic properties, such as heat of mixing, excess free energy of mixing, entropy of mixing, etc., of binary alloys. These alloys are generally characterized by large negative thermodynamic quantities and compositional dependence of partial excess free energy of mixing and entropy of mixing show S−like curvature (Hultgren *et al.*, 1973). Moreover, the minima in the heat of mixing and the point of inflection in the partial entropy of mixing plots most often occur at the stoichiometric composition where the stable intermetallic compound exist in the solid state under equilibrium conditions (Darken, 1967). The plots of compositional dependence of concentration fluctuation in long wavelength limit for these alloys show eutectic around the stoichiometric composition followed by two maxima on either side. These observations clearly indicate the existence of complex in the initial melt of the binary liquid alloys. Additionally, several experimentalists (Faber & Ziman, 1964; Busch & Guntherodt, 1974; Calaway & Saboungi, 1983) have studied electrical properties of compound forming binary alloys and reported the anomalous behaviour. The deviations in compositional dependence of magnetic susceptibility from linearity have also been reported for compound forming alloys (Matsunaga et al., 1983).

The compound forming trends or short range ordering in the liquid binary alloys have been further detected by the neutron diffraction experiments (Ruppersberg & Egger, 1975; Wagner, 1978; Ruppersberg & Reiter, 1982; Alblas et al., 1983; Saboungi et al., 1990; Vander Aart, 2000; Blagoveshchenskii et al., 2002). The neutron diffraction experiment provides the direct insight of structural properties at microscopic level of alloys basically concentration fluctuations in long wavelength limit and short range order parameters. These experiments for different alloy systems reveal the presence of associations at atomic level or complexes in the initial melts of alloys at one or more stoichiometric compositions. Additionally, the anomalies in the structural properties have also been reported in most of the experiments.

These discussion stands in favour of the presence of atomic clusters in the molten state of alloys and also clarify that these alloys show anomalous behaviour with respect to different thermodynamic or structural properties at or near the compound forming concentration. These asymmetric trends might be due to presence of strong interactions between constituent atoms of the liquid mixture which in turn resulted in the existences of intermetallic compounds at one or more stoichiometric compositions in solid state (Sommer, 1990; Young, 1992). Eventually, many researchers believed in the presence of atomic associations in the initial melt of the binary liquid alloys and these associations were called as 'clusters' or 'associations' or 'pseudomolecules' or 'complexes' (Jordan, 1970; Bhatia & Hargrove, 1974; McAlister & Crozier, 1974; Hoshino & Young, 1980; Lele & Ramchndrarao, 1981; Gerling et al., 1983; Arpshofen, 1984; Bhatia & Singh, 1984; Hoch et al., 1984; Prasad & Singh, 1990; Singh & Sommer, 1992; Mishra et al., 1994; Prasad et al., 1995; Srikanth et al., 1999; Akinlade et al., 2000; Awe et al., 2003; Godbole et al., 2004; Kumar et al., 2005; Singh et al., 2010; Adhikari et al., 2010, 2012; Adhikari 2011, 2013; Adhikari et al., 2014; Yadav et al., 2015, 2016). The different theoretical models were then devised to study the thermodynamic and structural properties of binary liquid alloys based on the presence of chemical complex called complex formation models and are enlisted as follows.

The expression for the free energy of mixing, the activity and the concentration fluctuation in long wavelength limit were derived by Bhatia and Hargrove (1974) by assuming the existence of complex of the type $A_\mu B_\nu$ (μ and ν are small integers) on the basis of conformal solution model and Flory's approximation. The expressions for G_M and $S_{CC}(0)$ so derived can be given as

$$G_M = -n_3 g + RT \sum_{i=1}^{3} n_i \ln\left(\frac{n_i}{n}\right) + \sum_{i<j} \frac{n_i n_j}{n} \omega_{ij} \tag{2.10}$$

and, $$S_{CC}(0) = \left[\sum_{i=1}^{3} \left\{\frac{n_i'^2}{n_i}\right\} - \frac{n'^2}{n} + \frac{2n}{RT} \sum_{i<j} \left(\frac{n_i}{n}\right)' \left(\frac{n_j}{n}\right)' \omega_{ij}\right]^{-1} \tag{2.11}$$

where g denotes the energy of formation of the complex, n_1, n_2 and n_3 represents the atoms of unassociated atoms of respective species A, B and the complex $A_\mu B_\nu$, $n = n_1 + n_2 + n_3$ and ω_{ij} $(i, j = 1, 2, 3)$ are the interaction energy parameters. The prime stands for the differentiations with respect to concentration, x_1. The Flory's expression for G_M and $S_{CC}(0)$ can be given as (Jha, 1989)

$$G_M = -n_3 g + RT[n_1 \ln n_1 + n_2 \ln n_2 + n_3 \ln(\mu + \nu) n_3] + \sum_{i<} \sum_{j} n_i n_j v_{ij} \tag{2.12}$$

and, $$S_{CC}(0) = \left[\sum_{i=1}^{3} \left\{\frac{n_i'^2}{n_i}\right\} + \frac{2}{RT} \sum_{i<j} n_i' n_j' v_{ij}\right]^{-1} \tag{2.13}$$

where $v_{12} = \chi'_{12}$, $v_{13} = (\mu + \nu)\chi'_{13}$ and $v_{23} = (\mu + \nu)\chi'_{23}$; and χ'_{ij} are analogue to ω_{ij}.

Bhatia and Hargrove (1974) explained concentration dependent asymmetry in Tl–Te, Mg–Bi, Cu–Sn and Ag–Al binary liquid alloys in the framework of the complex formation model. Since then several theoreticians (Bhatia & Singh, 1980; Hoshino & Young, 1980; Jha, 1989; Mishra et al., 1990; Singh et al., 1991; Awe et al., 2003; Godbole et al., 2004; Novakovic et al., 2011; Ali et al., 1999) have used this model to study and explain the compositional dependence of asymmetry in the mixing behaviour of various binary liquid alloys assuming the existence of chemical ordering or complex in

the initial melt. From these literatures, it can be concluded that the individual metals of the alloys undergo major structural changes in atomic and electronic behaviour on alloying. But the procedure to be amended in this model while solving the modeling equations for determining the model fit parameters is tedious as it involves the selection of initial values for these unknown parameters and continuous iteration to obtain the best fit values to explain the experimental data (Srikanth & Jacob, 1988).

The complex formation model was further extended by Bhatia and Singh (1982) by introducing the concept of grand partition function and considering the energy of AB, AA or BB bond pairs relying whether the bond is part of the complex $A_\mu B_\nu$ or not. They formulated the expressions for different thermodynamic functions on this assumption and the model was then named as quasi-chemical theory. This model is superior to complex formation model in the sense that it can be used to obtain the chemical short range order parameter for compound forming binary liquid alloys, however, is applicable for weakly interacting alloys. In the framework of this model, Singh et al. (1987) studied the thermodynamics of Li−Mg liquid alloy; Akinlade (1994) explained the thermodynamics of K−Te liquid alloy; Anusionwu (2006) explained the thermodynamic and surface properties of Sb−Sn and In−Sn liquid alloys; Anusionwu et al. (2009) explained the thermodynamics of Al−Ge and Al−Ga liquid alloys, etc.

The complex formation model of Bhatia and Hargrove (1974) to explain the thermodynamic properties of compound forming alloys was reformulated by Bhatia and Singh (1984) using quasi−lattice picture. The formulation was basically carried out to an approximation where the peudo−ternary alloy (of free atoms A and B, and the complex $A_\mu B_\nu$) envisaged in Bhatia and Hargrove treatment in quasi−chemical approximation. This approximation was names as quasi−lattice theory wherein the expressions reduces to the expressions of conformal solution approximation (Bhatia & Hargrove, 1974) and Flory's approximation by simply going to lower (zeroth) approximation and by substituting the coordination number (z) of the alloy to be $z = 2$ and $z = \infty$ respectively (Bhatia & Singh, 1984). Further, this model also provides the expression for chemical short range parameter order unlike Bhatia and Hargrove approximation. On the basis of

this model, Prasad and Singh (1990) explained the mixing properties of Au−Zn liquid alloy, Novakovic et al. (2005) studied the surface and transport properties of Ag−Cu liquid alloy, Novakovic (2010) explained thermodynamic, surface and structural functions of Al−Nb and Nb−Tl liquid alloys, Kumar et al. (2011) explained the thermodynamic and structural properties of molten Fe−Si alloy, Koirala et al. (2012) mixing properties of Al−Ga liquid alloy, Kumar et al. (2013) studied the mixing properties of Mg−Bi liquid alloy, and so on. Hoch and Arpshofen (1984) have also proposed complex formation model to explain the thermodynamic properties of liquid alloys. The expression for the excess free energy of mixing G_M^{XS} in the first approximation can be given as

$$G_M^{XS} = n(x - x^n)\omega \tag{2.14}$$

where n is the number of atoms, ω is the interaction energy parameter and x is the atom fraction of the component with the lower binding capacity. Based on this models Hoch and Coworkers (Hoch & Arpshofen, 1984) have successfully explained the mixing behaviours of alloys.

Jordan (1970) suggested more realistic model for associated liquid mixtures taking into account the interaction between the different species (A, B and AB) and derived equations for the thermodynamic and the liquidus curve in the Zn−Te and Cd−Te with predominant AB−type clusters. In the first approximation, he suggested that departure from ideality in an associated solution due to short−range nearest neighbour interactions and these interactions should be taken into account by identifying the activity coefficients of free atoms and the complexes of the ternary liquid mixture. The expressions for the ternary activity coefficients suggested by him are similar to that proposed by Prigogine and Defay (1954). Jordan (1970) termed the solution as regular associated solution wherein the unknown parameters to be estimated are the three interaction energies between the species, the free energy of mixing and the enthalpy of dissociation of the complex. For the mathematical simplification, he assumed the interactions between the unassociated atoms (A and B) and the complex (AB) to be equal and determined the

model parameters from the experimental liquidus data. Osamura and Predel (1977) employed Jordan's approximation to the In−Sb system; however, he solved the necessary equations by ignoring higher order terms in the concentration of the complex.

A comprehensive analytical procedure for the treatment of regular associated solution without invoking any simplistic approximation was provided by Lele and Ramchandrarao (1981). They determined the model parameters which are the interaction energy parameters and the equilibrium constant with the aid of the observed activity coefficients of the components at infinite dilution of the binary liquid alloy and the activity data at one other intermediate composition. Using this approximation, they successfully explained the thermodynamic properties of Mg−Sn and In−Sb liquid alloys. However, they treated the interaction energy parameters to be temperature independent and the information regarding the microscopic structural properties, such as concentration fluctuation in long wavelength limit and chemical short range order parameter is lacking. Later Adhikari (2013) further assumed the interaction between the unassociated atoms and complex to be unequal and pairwise interaction energy parameters to be temperature dependent. Adhikari (2013) extended regular associated solution model by presenting the expressions for $S_{CC}(0)$ and α_1 to study and explain the structural properties of the binary liquid alloys at atomic level. With the help of these expressions and as stated further assumptions, the thermodynamic and structural properties of few binary liquid alloys, such as Cd−Na, Ag−Sb, Cu−Sn, Ag−Al, Mg−Tl, Fe−Si and Hg−Na were explained. Additionally, based on this model Adhikari (2011) explained the inhomogeneity in structure of Mg−Pb liquid alloy, Adhikari (2010) explained the disorder in Cu−Pd liquid alloy, Jha et al. (2012) explained the mixing behaviour of Na−based (In−Na and Na−Pb) and Al−Mn liquid alloys, etc. However, they assumed the complex of the type $A_\mu B_\nu$ ($\mu > 1$ and $\nu = 1$) or $A_\mu B$ as the most stable complex in the liquid mixture.

The regular associated solution model of Jordan (1970) has been extended by Kellogg and Coworkers (Goel et al., 1980; Kellogg, 1987) by incorporating asymmetric interaction among the species and temperature dependence of interaction energy parameters. The proposed model has fourteen unknown model fit parameters to be

determined from experimental thermodynamic data. Kellogg (1991) has applied this model to study the energetic of copper−indium system. Chang and Coworkers (Sharma & Chang 1980; Schmid & Chang, 1985) used a sub−regular solution model to describe the thermodynamics of complex forming alloys. However, their model has even more model fit parameters than that of Kellogg and Coworkers. The procedure of obtaining the model fit parameters involves simultaneous optimization of the available thermodynamic and phase equilibrium data by least square regression analysis which proves to be difficult when there is insufficient thermodynamic information available on the alloy. Srikanth and Jacob (1988) incorporated the volume effect to the regular associated solution model relaxing the constraints in Bhatia and Hargrove (1974) treatment regarding the volume of the clusters. They formulated the expressions for thermodynamic mixing functions using this modified approach and used it to describe the thermodynamic properties of Al−Ca alloy. Further, Srikanth and Coworkers (Srikanth & Jacob, 1988; Srikanth et al., 1999) used this approach to describe the thermodynamics of complex forming alloys.

2.3.2 Modeling of surface properties

Like thermodynamic properties, the study of surface properties reveals the information about the kinetics of phase transformation, catalytic activities of alloys catalysts and several other metallurgical phenomena, such as crystal growth, wettability or deposition, gas absorption, nucleation, etc. It can be, therefore, stated that the knowledge of surface properties and phenomena are of outmost important in material design and characterization (Singh & Sommer, 1997; Akenlade et al., 2001; Aqra et al., 2011; Pstrus′ et al. 2011; Gasior et al., 2012; Gancarz & Gasior, 2015; Kaptay, 2015; Yadav et al., 2016; Gancarz, 2017). In this limelight, both theoreticians and experimentalist in the field of metallurgical science are working to access the thermodynamic and structural behaviour of materials on the basis surface properties, such as surface tension and surface segregation. The initialization of the concept of expressing surface tension in terms of thermodynamic is accredited to Gibbs (1875−1878) and the relation can be given as (Kaptay, 2015, 2016)

$$\sigma \equiv \left(\frac{dG}{dA}\right)_{p,T,n_i} \tag{2.15}$$

where σ is the surface tension of a liquid solution phase, G is absolute Gibbs energy of the liquid solution and A is its absolute surface area. The above expression can be further elaborated at constant pressure (p), constant absolute temperature (T) and constant number of matter in liquid phase (n_i). Eq. (1) leads to the physical interpretation that there should be gradual change in the shape of the liquid droplet which leads to the gradual change in its surface area which in turn leads to gradual change in its Gibbs energy.

Butler (1932) derived the expression for the surface tension of binary alloys under taking Eq. (1) as epicenter and redefining the arrangement of atoms on the surface of liquid phase. He assumed that the surface of the liquid is planar or linearly planar monoatomic layer which exists as a separate phase and is in thermodynamic equilibrium with the homogeneous bulk phase. According to this approach expression for the surface tension can be expressed equivalent to (Hoar & Melford, 1957; Gasior et al., 2012; Mekler & Kaptay, 2008; Picha et al., 2004; Yadav et al., 2016)

$$\sigma = \sigma_A + \frac{RT}{\alpha_A^0}\ln\left(\frac{x_A^S}{x_A^b}\right) + \frac{G_{S(A)}^{xs} - G_{b(A)}^{xs}}{\alpha_A^0} = \sigma_B + \frac{RT}{\alpha_B^0}\ln\left(\frac{x_B^S}{x_B^b}\right) + \frac{G_{S(B)}^{xs} - G_{b(B)}^{xs}}{\alpha_B^0} \tag{2.16}$$

where σ is the surface tension of the alloy, σ_A^0 and σ_B^0 are the surface tensions of the respective pure component A and B, α_A^0 and α_B^0 are the molar surface areas of the respective components, x_A^S and x_B^S are the surface concentrations of the respective components, x_A^b and x_B^b are the bulk surface concentration of the respective components, $G_{S(A)}^{xs}$ and $G_{S(B)}^{xs}$ are the surface partial excess free energy of the respective components; and $G_{b(A)}^{xs}$ and $G_{b(B)}^{xs}$ are the bulk partial excess free energy of the respective components.

Belton and Evans (1945) applied statistical approach to a quasi−lattice model by assuming the same surface phase as monolayer and also considering additional restriction

that $\alpha_A^0 = \alpha_B^0 = \alpha^0$ obtained a relation similar to Eq. (2.16). Guggenheim (1945) applying the method of grand partition function derived the more elegant symmetrical expression as

$$\exp\left(\frac{-\sigma\,\alpha^0}{RT}\right) = x_1 \exp\left(\frac{-\sigma_1\,\alpha^0}{RT}\right) + x_2 \exp\left(\frac{-\sigma_2\,\alpha^0}{RT}\right) \tag{2.17}$$

Meanwhile, Guggenheim (1952) proposed another statistical approach called quasi−crystalline model based on the assumption of the existence of double layered atoms on the surface of a binary solution that are similar to a particular plane of a crystal lattice such that the composition of only outer layer differ from that of the bulk. He designated the surface coordination numbers p and q to the layers and assumed the similar arrangements of atoms in the surface as well as in the bulk. Further, he assigned the interchange energy as $w = z(2\varepsilon_{AB} - \varepsilon_{AA} - \varepsilon_{BB})/2$, herein ε_{AB}, ε_{AA} and ε_{BB} are bond energies of A−B, A−A and B−B respectively and z is the coordination number and derived the expression for the surface tension in terms of w and surface composition by constructing grand partition function in the quasi−crystalline model as (Guggenheim, 1952; Prasad & Singh, 1991)

$$\sigma = \sigma_A + \frac{k_B T}{\alpha}\ln\left(\frac{x_A^S}{\gamma_A x_A^b}\right) + \left[p\left(x_B^S\right)^2 + q\left(x_B^b\right)^2\right]\frac{w}{\alpha} = \sigma_B + \frac{k_B T}{\alpha}\ln\left(\frac{x_B^S}{\gamma_B x_B^b}\right) + \left[p\left(x_A^S\right)^2 + q\left(x_A^b\right)^2\right]\frac{w}{\alpha} \tag{2.18}$$

where γ_A and γ_B are the activity coefficients of the free components A and B respectively, $\alpha = (x_A^b\alpha_A + x_B^b\alpha_B)$ is the mean atomic surface area and α_A and α_B can be estimated from Eq. (2.18). The values of p and q are chosen depending upon the types of crystal structures of the components of the alloy such that $p + 2q = 1$ (Guggenheim, 1952). Additionally, for closed−packed crystal structures, such as fcc and hcp lattices ($z = 12$), $p = 0.5$ and $q = 0.25$ whereas for simple cubic lattice ($z = 6$), $p = 2/3$ and $q = 1/6$; and for bcc lattice ($z = 8$), $p = 3/5$ and $q = 1/5$ (Guggenheim, 1952). On the basis of this model several researchers (Hoar & Melford, 1957; Prasad & Singh, 1991;

Prasad et al., 1994, 1998; Novakovic & Brillo, 2014; Yadav et al., 2016; Koirala, 2016) have explained the surface properties of different binary liquid alloys.

Hoar and Melford (1957) formulated another expression based on the formation energy change of the surface as follows

$$\sigma = \sigma_A \frac{\alpha_A^0}{\alpha_A} + \frac{RT}{\alpha_A} \ln\left(\frac{x_A^S}{x_A^b}\right) + \frac{G_{S(A)}^{xs} - G_{b(A)}^{xs}}{\alpha_A} = \sigma_B \frac{\alpha_B^0}{\alpha_B} + \frac{RT}{\alpha_B} \ln\left(\frac{x_B^S}{x_B^b}\right) + \frac{G_{S(B)}^{xs} - G_{b(B)}^{xs}}{\alpha_B} \quad (2.19)$$

where α_A and α_B are the partial molar surface areas of the respective components A and B of the alloy. The rest of the symbols carry the same meanings as in Eq. (2.16). However, in the case $\alpha_A = \alpha_A^0$ (Hoar & Melford, 1957; Gasior et al., 2012; Kaptay, 2016; Yadav et al., 2016), the Eq. (2.16) and Eq. (2.19) take the same form. The molar surface area of the component A can be given as

$$\alpha_A^0 = L\, N^{1/3} V_A^{2/3} \quad (2.20)$$

where L (=1.091) is a dimensionless geometrical constant, N is the Avogadro's number and V_A is the molar volume of the component A at the temperature T. The molar surface area of the component B can be obtained from the same expression. The surface excess free energy of the component i in the monoatomic surface in terms of its bulk partial excess free energy can be given as (Bulter, 1932; Tanaka et al., 1996; Picha et al., 2004; Gasior, 2012; Kaptay, 2015; Yadav et al., 2016)

$$G_{S(i)}^{xs} = \beta G_{b(i)}^{xs} \quad (2.21)$$

where β is a constant and to determine the surface tensions of the liquid alloys its values has been adapted in the range $0.5 - 0.84$. Hoar and Melford (1957) has described the surface tension of Sn-Pb and Pb-In systems by taking the value of β in the range from 0.5 to 0.667. Monma and Sudo (1961) have assumed the value of β in the range from 0.80 to 0.84 to describe the surface tensions of Cu−Ni and Ni−Mo systems. Likewise, Lee at al.

(1993) have taken the value of β to be 0.75 for Fe–Ni alloy; Tanaka and Iida (1994) have taken the value of β to be in the range $0.5 - 1.0$ for Ag–Pb, Cu–Al, Cu–Pb, Cu–Fe, Ni–Si, Sn–Pb and several Fe–based alloys to accordance the results obtained from theoretical modelings with the experimental; and Tanaka et al. (1996) have suggested the value of β to be 0.83 for Cu–Pb and Fe–Si alloys by devising experimental techniques. Since then several researchers (Balton & Evans, 1945; Hoar & Melford, 1957; Speiser et al., 1987; Gasior et al., 2001, 2012; Picha et al., 2004; Liu et al., 2004; Lee et al., 2004; Schmitz et al., 2009; Adhikari et al., 2012; Garzel et al., 2012; Trybula et al., 2014; Koirala, 2016) have employed Butler's model with $\beta = 0.83$ and described the surface tensions of different systems both theoretically and experimentally.

Another theoretical model that has been commonly used to determine the surface properties of binary liquid alloys is quasi–chemical approximation (Prasad et al., 1994; Prasad & Jha, 2005; Koirala, 2016). This expression is also derived on the floor of quasi–crystalline approximation of Guggenheim (1952) and can be expressed as (Prasad & Jha, 2005)

$$\sigma = \sigma_i + Y(2 - pZ)\ln\left(\frac{x_i^S}{x_i}\right) + YZ\left[p\ln\left\{\frac{(\beta+1)(\beta^S+2x_i^S-1)}{(\beta^S+1)(\beta+2x_i-1)}\right\} - q\ln\left\{\frac{(\beta+2x_i-1)}{(1+\beta)x_i}\right\}\right] \tag{2.22}$$

where $i = A, B$; $Y = k_B T/2\alpha$ and the rest of the terms carry their usual meanings as stated earlier. The term β can be expressed as

$$\beta = [4x_i(1 - x_i)\exp(2w/Zk_BT) + (1 - 2x_i)^2]^{1/2} \tag{2.23}$$

The expression for the computation of β^S can be obtained by replacing the bulk concentration x_i by the surface concentration x_i^S in the above expression. Employing this model several researchers (Prasad & Jha, 2005; Kaptay, 2005; Novakovic, 2010; Koirala et al., 2014; Koirala, 2016) have explained the surface properties of different systems.

Kaptay (2015) reformulated Butler's expression (1932) for the surface tension of the binary alloys undertaking the Gibb's equation as epicenter and resting the constraints assumed by Butler called Renovated Butler model (the details of the derivation is included in Chapter 6). He also provided the definitions for the partial surface tensions and the information about the substantial knowledge gap lacking in Butler's assumption (Kaptay, 2015, 2016). More precisely, when the shape of the liquid solution is changed slowly and gradually at constant pressure, constant temperature and constant numbers of components in it, this will enhance the gradual change in the partial surface area of the components and the partial Gibbs energies of the components of the mixture resulting in the gradual change in the surface tension of the liquid solution (Kaptay, 2015). However, the nature tends to minimize the total Gibbs energy of the liquid solution and also its surface tension due to which the partial surface tensions corresponding to all atomic or molecular sites along the surface minimizes. In case of the non−equilibrium condition, Marangoni flow will start due to which the subsurface with lower surface tension replaces the subsurface with higher surface tension leading to the global equilibrium of the surface thereby minimizing the partial surface tensions of the components of liquid mixture. Moreover, he reformulated the value of constant L used in Eq. (2.18) as follows and redefined its values (Kaptay, 2008, 2016; Yadav et al., 2016)

$$L = \left(\frac{3\,f_b}{4}\right)^{2/3} \frac{\pi^{1/3}}{f_S} \tag{2.24}$$

where f_b is the volume packing fraction and f_S is the surface packing fraction. Following Kaptay (2008), the bulk packing fraction of a melted bcc crystal is obtained by lowering its crystal bulk packing fraction (0.68) by 9.6% due to volume expansion from 0 K till the melting point at liquid state and hence for bcc, $f_{b,bcc} = 0.62$. Likewise, for fcc and hcp crystals each having the value of bulk packing fraction of 0.74 should be reconsidered to be $f_b = 0.66$. In an average, for simple liquid metals, $f_b = 0.65 \pm 0.02$ and is in accordance with the experimental results obtained for random dense packing of macroscopic equal spheres (Topuridze et al., 1978). The surface packing fraction of the $\{1\,1\,1\}$ plane of the fcc crystal is $f_S = 0.906$ (Skapski, 1948; Kaptay, 2008) and hence

with all these considerations the value of $L \approx 1.00 \pm 0.02$ (calculated from Eq. (2.22)). Additionally, Kaptay (2008) suggested the value of β to be 0.8282 and these values ($L \approx 1.00 \pm 0.02$ and $\beta = 0.8181$) Kaptay and Coworkers (Mekler & Kaptay, 2008; Kaptay, 2008; Kaptay, 2012; Sandor et al., 2013; Kaptay, 2016) have explained the surface tensions of bcc, fcc and hcp crystal structured different liquid metals as well as different liquid alloys.

In this work, the thermodynamic and microscopic structural properties of compound forming liquid binary alloys have been studied in the theoretical framework of the regular associated solution model. The initial priority has been given to study and to explain the thermodynamic and structural properties of compound forming binary liquid alloys assuming the chemical complex of the type $A_\mu B_\nu$ ($\mu > 1$ and $\nu > 1$) as energetically favoured in the initial melt. Though Srikanth et al. (1999) presented the thermodynamic expressions for the $A_\mu B_\nu$ chemical complex, its applicability is lacking till date as per literature survey. In this thesis, firstly the expressions for different thermodynamic and structural properties in the constrained framework of regular associated solution model have been presented for the complex of the type $A_\mu B_\nu$ following the trends of literatures (Lele & Ramchandrarao, 1981; Srikanth et al., 1999; Adhikari, 2013). With the help of these expressions the thermodynamic and structural properties of Al−Mg liquid alloys have been explained assuming the complex Al_3Mg_2. Moreover, the validity of the regular associated solution has been established by employing it to study the thermodynamic and structural properties of few binary liquid alloys, such as Bi−Tl, In−Bi and Al−Fe. Secondly, the regular associated solution has been extended to predict the thermodynamic and structural properties of herein included binary liquid alloys at different temperatures. Finally, these thermodynamic properties at different temperatures have been correlated with the Renovated Butler model (Kaptay, 2015, 2016) to predict the surface properties of these binary liquid alloys at different temperatures.

Besides free electron theory and statistical modelings, the molecular dynamic approaches have also been used by several researchers to explain the macroscopic properties of different systems from the microscopic behaviours using computer simulation techniques

(Allen & Tildesley, 1987; Chushak & Baumketner, 1999; Adebayo & Anusionwu, 2006; Mendelev, 2009). Young (1992) explained the structural and thermodynamic properties of NFE liquid metals and binary alloys from the first principle approximations. Woodward et al. (2012) studied the fundamental parameters of liquid metal alloys using first principles approach based on Density Functional Theory and Ab-initio molecular dynamic simulation. Based on molecular dynamics, the properties of Al−Fe alloys have been studied by Rehn at al. (1978), Li et al. (2001), etc. Similarly, the properties of Al−Mg have been studied by Liu & Adams (1998), Mendelev et al. (2009), Wang & Wong (2011), etc and electric transport and thermodynamic properties of binary liquid alloys was studied by Kumar & Ojha (2010).

2.4 Objectives

2.4.1 Problem statement and objective selection

From the brief overview of the literature survey, it can be stated that since decades several efforts so far have been put forwarded by many researchers in the field of metallurgical science to comprehend the energetic of liquid alloys. The knowledge of the thermodynamic, structural and surface properties of liquid alloys helps to select the micro−ingredients for the alloys preparation in order to obtain predetermined properties. In this work, we have applied regular associated solution model to study the thermodynamic and structural properties of two Bi−based (Bi−Tl and In−Bi) liquid alloys and two Al−based (Al−Fe and Al−Mg) liquid alloys. The preferred model has also been extended to predict these properties of concerned liquid alloys at different temperatures. The surface properties of these alloys have been studied in the frame work of Renovated Butler model. The thermodynamic properties of the concerned systems have been then correlated with Renovated Butler model to predict the surface properties at different temperatures. The problem statements and objective related in selecting the theoretical models as well as these liquid alloys in the present study can be highlighted as follows:

(i) Since last three decades, a numerous of world projects have been dedicated to investigate lead free solders as lead being hazardous to mankind and nature. Arising from the transition to Pb−free and the EU Reduction of Hazardous substance (RoHs) Directive, safety and environmental compliances issues exercise a dominant role and it was addressed aiming to develop new lead free alloys having equal characteristics or better than Sn−Pb solders widely used in the electronic industries. The alloys of bismuth (Bi) have low melting points which make them suitable to be used as solders and toxic solders containing lead can be replaced by safer bismuth (Mc Cormack et al., 1994; Suganuma, 2001; Gnecco et al., 2007; Plevachuk et al., 2011). Additionally, Pb is being replaced from its alloys by Bi in many applications, such as pigments for paints, fishing sinkers, bullets and shots, brass for plumbing and as ingredients in grease for lubrications for safety purposes. In spite of all these, the In−Bi alloy is a crystalline solid which is used as a semiconductor and in photo−optic applications. It also possesses the superconducting behaviour (Kirschner et al., 1974). We, therefore, have preferred two Bi−based liquid alloys in this thesis.

(ii) Al−based alloys have light weight and high corrosion resistance which makes them suitable to be used in engineering structures and components. The alloys of Al are extensively used in aircrafts and automotive engines particularly cylinder blocks and crankcases due to their high strength−to−weight ratio. Among them, Al−Mg alloy has light weight, high mechanical strength, excellent resistance to high−temperature oxidation, good crack resistance, low cost maintenance and is much less inflammable than other Al−based alloys due to which it is profoundly used in electrical industry, memory chips, roofing sheets, vehicle paneling, etc. Likewise, Al−Fe alloy is preferred as high temperature structural and functional materials in many modern technologies (Taylor & Jones, 1958; Cubero−Sesin & Horita, 2012). Eventually, the investigations of energetic of two Al−based alloys are preferred in this work.

(iii) The energetic of initial melt provide in−depth knowledge about the equilibrium conditions, annealing conditions and arrangements of atoms in the alloy. These information helps in selection of micro−constituents for the materials synthesis, design and characterization to obtain predetermine properties as per the demands of modern technological world.

(iv) The knowledge of surface properties of the liquid alloys reveal various physical information relating to the kinetics of phase transformations, catalytic activities of alloy catalysts, wettability, annealing conditions, grain boundary separation, etc.

(v) Obtaining the above mentioned information solely through experiments is very cumbersome, costly and tedious. Moreover, an experimental phase equilibrium result does not most often link to the important thermodynamic properties of the phases. The experimental databases for the most of the alloys at different temperatures are lacking as such techniques being difficult to handle at higher temperatures. Eventually, it is mandatory to construct and devise theoretical models to study and predict the energetic of binary liquid alloys at a temperature and different temperatures. The prediction of thermodynamic, structural and surface properties of the liquid alloys by extending theoretical models preferred in this work, with no doubt, will provide references to obtain database thereby avoiding long term experimental works.

2.4.2 Objectives of the present work

The main features of the work carried out in this thesis can be summarized as follows:

(i) The thermodynamic and structural properties of above mentioned liquid alloys have been studied in the frame work of regular associated solution model. The preferred model is fundamentally based on the existence of chemical complex in the initial melt. In this work, we have assumed the existence of chemical

complexes of the types $A_\mu B_\nu$ with $\mu, \nu > 1$, $\mu > 1$, $\nu = 1$ and $\mu = \nu = 1$ and derived the expressions for the various thermodynamic and structural functions. The interactions among the various species of the liquid mixture are assumed to be unequal in this work.

(ii) The thermodynamic behaviour of the liquid alloys have been studied by computing free energy of mixing, activity, heat of mixing and entropy of mixing. For consistency, we have used the same set of model parameters to compute all the thermodynamic functions. To establish the validity of the model, we have compared the theoretical results with the experimental results. The interacting natures of the preferred liquid alloys have also been compared on the floor of thermodynamic properties.

(iii) The ordering and segregation natures of the preferred liquid alloys have been explained by computing concentration fluctuation in long wavelength limit ($S_{CC}(0)$), chemical short range order parameter (α_1) and ratio of mutual to intrinsic diffusion coefficients (D_M/D_{id}). The modeling equations for these functions are also included in this work. Herein a theoretical investigation of concentration dependence of $S_{CC}(0)$ has considerable significance as its experimental determination is still far from reality. The tendency towards the complex formation in the liquid alloys has also been compared on the basis of structural behaviour.

(iv) The surface properties, such as surface tension (σ) and surface concentrations of constituent atoms (x_A^S and x_B^S) of the concerned liquid alloys have explained in the frame work of Renovated Butler model. The modeling equations relating to these functions are also derived in this work. Due to the lack of experimental data, our theoretical findings could not be compared with that of experimental results. The surface segregation in these alloys has also been explained.

(v) The regular associated solution model has been extended to obtain the interaction energy parameters of the liquid alloys at different temperatures. With the help of these model parameters, the thermodynamic and structural properties of the concerned liquid alloys have been predicted at different temperatures. The mathematical equations to predict the thermodynamic and structural properties of these alloys along with the values of input parameters are also presented in this work. These predictions equations are obtained by polynomial fittings of different orders. The strength of interactions or the complex formation tendency of these liquid alloys have been forecasted and compared at different temperatures. The ordering and segregation behaviour of these alloys have been predicted and analyzed at high temperatures.

(vi) Finally, the thermodynamic properties have been correlated with Renovated Butler model to predict the surface properties of concerned liquid alloys at different temperatures. The mathematical equations to predict the surface properties obtained by polynomial fitting of different orders along with the values of input parameters are also included in this work. The change in surface properties with the increase in temperatures of these liquid alloys beyond their respective melting temperatures have also explained and analyzed.

CHAPTER 3

MATERIALS AND METHODS

In this thesis, thermodynamic and microscopic structural properties of the lower (of the type: $A_\mu B_\nu$, where $\mu \geq 1$ and $\nu = 1$) as well as higher order stoichiometry (of the type: $A_\mu B_\nu$, where $\mu > 1$ and $\nu > 1$) binary liquid alloys have been studied at a temperature on the basis of regular associated solution model. These properties have also been predicted at different temperatures by extending regular associated solution model. The thermodynamic properties have been then correlated with the renovated Butler model to determine and to predict the surface properties of the binary liquid alloys at a temperature and at different temperatures. For the determination of afore mentioned properties and their discussion, the greater insight of the fundamental concepts of these theoretical models are outmost essential. This Chapter is basically presented to provide the theories and advancements made in them with the assistance of which the thermodynamic, microscopic structural and surface properties of the binary liquid alloys at different have been determined and discussed.

3.1 Regular associated solution model for binary liquid alloys

It has been already mentioned that the binary liquid alloys can be broadly classified into two classes; ordering or hetero−coordinating alloys which show negative deviation from Raoult's law (Wilson, 1965; Singh & Sommer, 1997; Akinlade & Singh, 2001) and segregating or homo−coordinating alloys which show positive deviation from Raoult's law (Lele & Ramchandrarao, 1981; Singh, 1987; Shrikanth & Jacob, 1988; Novakovic et al., 2004; Awe et al., 2011; Adhikari et al., 2012, 2014; Yadav et al., 2015, 2016). The former class of alloys leads to mixing or compound formation whereas the later class leads to demixing or phase separation in the liquid alloys. Moreover, on the basis of thermodynamic properties, these alloys can also be categorized as either symmetric or asymmetric alloys. The most of the symmetric alloys show normal behaviour respective

to their thermodynamic and structural properties and the plots of these properties with compositions are generally C−shaped (Hultgren, *et al*., 1973). But in case of the alloys of second kind, thermodynamic, electrical and several other physical properties show anomalous behaviour (Wilson, 1965; Busch & Guntnerodt, 1974). Their plots of thermodynamic properties, such as partial excess free energy of mixing, entropies and heat of mixing with the compositions show S−like curvatures and are asymmetric (Hultgren, *et al*., 1973; Darken, 1967; Ramchandrarao et al., 1971; Adhikari et al., 2010).

On the basis of thermodynamics, it can be said that the equilibrium state of an alloy at a given conditions is depicted by the phase assemblage with the lowest Gibbs energy (Luka et al., 2007). The different conditions, such as temperature, pressure, chemical composition and history of thermal processing of the materials determine the microstructure of the alloy. The appropriate phase diagram describing the state of equilibrium in the system under above mentioned conditions serves as visual graph to the researchers working in the field of material science. It can be regarded as one of the most important tool which aids in understanding the formation of complex or compounds at one or more stoichiometric compositions in the solid state. As a result, several theoreticians (Jordan, 1970; Bhatia & Hargrove, 1974; McAlister & Crozier, 1974; Hoshino & Young, 1980, Bhatia & Singh, 1980; Lele & Ramchandrarao, 1981; Gerling et al., 1983; Singh, 1987; Srikanth & Jacob, 1988; Jha et al., 1990; Sommer et al., 2001; Miki et al., 2001; Awe et al., 2003; Anusionwu & Echendu, 2010; Adhikari et al., 2010, 2014) assumed the existence of strong associations among the constituent species of the alloy near the melting temperature in the initial melt. These associations have been named as 'complexes', 'pseudomolecules', 'clusters', etc. The initial melt of binary alloys thus can be assumed as the ternary mixtures of unassociated atoms of the constituents of the alloy and complexes in thermodynamic and chemical equilibrium.

The details of the development of regular associated solution model and advancements made in it to explain and to predict the energetic of binary liquid alloys have been presented in the Chapter 2. The model for associated liquid mixtures by considering the interaction between the constituent species of the alloy was proposed by Jordan in 1970.

Jordan termed such solutions as regular associated solutions. Moreover, the specific interactions, such as hydrogen bonding, acid−base association and charge transfer do not occur in the regular solution. However, these assumptions were made by considering the equal interactions between the unassociated atoms and complex and the expressions for the different thermodynamic functions, such as free energy of mixing and enthalpy of dissociation of the complex were derived on this basis. As the complex has comparatively large volume than that of the free monomers in the liquid mixtures, the model proposed by Jordan may not be adequate to explain the experimental thermodynamic properties of mixing (Srikanth & Jacob, 1988). We, therefore, have assumed that the free monomers and complex do not interact equally. Also the interaction energy parameters are assumed to be temperature dependent. The expressions for different thermodynamic functions are derived on these fundamentals.

3.2 For the Binary Liquid Alloys of Type: $A_\mu B_\nu$ $(\mu, \nu > 1)$

Consider a mole of binary solution consists of x_1 moles of atoms A and x_2 moles of atoms B. In the initial melt, there is preferable association of the types $A_\mu B_\nu$ ($\mu A + \nu B \Leftrightarrow A_\mu B_\nu$), where μ and ν are small integers values indicating the stoichiometry of an energetically favoured intermetallic compound, and are determined from the phase diagram at complex formation composition (= μ/ μ + ν) of the alloy in the solid state. The formation of the complex reduces the concentrations of the unassociated atoms A and B or free monomers. The liquid mixture thus consists of free atoms of A and B and the complex $A_\mu B_\nu$ in chemical as well as thermodynamic equilibrium. Due to the association, the thermodynamic behaviour of the components A and B is ruled by the true mole fractions x_A, x_B and $x_{A_\mu B_\nu}$ in spite of the gross mole fractions x_1 and x_2. The operation thus can be carried out by choosing two reference frames, one attributed to the gross mole fractions x_1 and x_2 and the other attributed to true mole fractions of each species of the mixture (x_A, x_B and $x_{A_\mu B_\nu}$). Moreover, let there be n_1 moles of species A, n_2 moles of species B and n_3 moles of species $x_{A_\mu B_\nu}$ in one mole of the binary solution. The two reference frames can be related on the basis of conservation of mass as follows:

$$n_1 = x_1 - \mu n_3,\ n_2 = x_2 - \nu n_3 \text{ and, } n = n_1 + n_2 + n_3 = 1 - (\mu + \nu - 1)n_3 \qquad (3.1)$$

The number of moles of each species and the species true mole fractions can be interrelated as follows:

$$x_A = \frac{n_1}{n_1+n_2+n_3} = \frac{n_1}{1-(\mu+\nu-1)n_3}$$

$$x_B = \frac{n_2}{n_1+n_2+n_3} = \frac{n_2}{1-(\mu+\nu-1)n_3}$$

and, $$x_{A_\mu B_\nu} = \frac{n_3}{n_1+n_2+n_3} = \frac{n_3}{1-(\mu+\nu-1)n_3} \qquad (3.2)$$

where, $$\frac{1}{n} = \frac{1}{1-(\mu+\nu-1)n_3} = 1 + \frac{(\mu+\nu-1)n_3}{1-(\mu+\nu-1)n_3} = 1 + (\mu + \nu - 1)\, x_{A_\mu B_\nu} \qquad (3.3)$$

Using Eq. (3.3) in Eq. (3.2), yields

$$n_1 = \frac{x_A}{1+(\mu+\nu-1)\, x_{A_\mu B_\nu}},\ n_2 = \frac{x_B}{1+(\mu+\nu-1)\, x_{A_\mu B_\nu}} \text{ and, } n_2 = \frac{x_{A_\mu B_\nu}}{1+(\mu+\nu-1)\, x_{A_\mu B_\nu}} \qquad (3.4)$$

Both of these reference frames are considered in regular associated solution model.
The true mole fractions of the species x_A, x_B and $x_{A_\mu B_\nu}$ can be interrelated as below

$$x_1 x_2 = x_2 x_1$$

With help of Eq. (3.1), the above Eq. takes the form

$$(n_1 + \mu n_3)x_2 = (n_2 + \nu n_3)x_1$$

After performing some algebraic operations and rearranging the terms, we get

$$n_1(x_1 + x_2) + \mu x_2 n_3 = x_1(n_1 + n_2 + n_3)$$

and, $x_A = x_1\left[1 + (\mu + \nu - 1)x_{A_\mu B_\nu}\right] - \mu x_{A_\mu B_\nu}$ (3.5)

Following similar procedure, one can obtain

$$x_B = x_2\left[1 + (\mu + \nu - 1)x_{A_\mu B_\nu}\right] - \nu x_{A_\mu B_\nu} \quad (3.6)$$

3.2.1 Thermodynamic mixing functions

3.2.1.1 Free energy of mixing (G_M)

The free of mixing (G_M) of binary alloys in terms of n_3 (complex mole fraction) can be given as

$$G_M = -n_3 g + G' \quad (3.7)$$

where $(-n_3 g)$ represents the reduction of the free energy due to the association or formation of the chemical complex $x_{A_\mu B_\nu}$and g is the formation energy of the complex. The term G' is the free energy of mixing of a ternary solution having species A, B and $x_{A_\mu B_\nu}$, which are considered to interact relatively weakly with one another as the strong bonding interaction between A and B atoms have been already taken in to account through the formation of the complex $x_{A_\mu B_\nu}$. If it is assumed that the ternary mixture forms an ideal solution, then G' can be simply expressed as

$$G' = G - \sum_i n_i G_i^{(0)} \quad (3.8)$$

where i (= 1, 2, 3), G is the total Gibbs free energy of the mixture and $G_i^{(0)}$ stands for the chemical potentials per atoms of the species i in its pure state. The Gibbs free energy of mixture can also be expressed as a function of temperature, pressure and number of moles

of the species. On the basis of Euler's theorem, the identity between the extensive variable and the corresponding partial quantities can be expressed as

$$G = \sum_i n_i G_i \tag{3.9}$$

where G_i is the chemical potential of the species i (per mole) and can be given as

$$G_i = \left(\frac{\partial G}{\partial n_i}\right)_{T,p,n_j} \tag{3.10}$$

where i = j; i = 1, 2, 3. With the aid of Eq. (3.9), Eq. (3.8) takes the form

$$G' = \sum_i n_i (G_i - G_i^{(0)}) \tag{3.11}$$

where $(G_i - G_i^{(0)})$ represents the change in chemical potential of the species of mixture. This change in chemical potential in terms of the activity a_i or the activity coefficient γ_i can be expressed as

$$G_i - G_i^{(0)} = RT \ln a_i = RT \ln x_i \ \gamma_i \tag{3.12}$$

where R is the universal gas constant and $x_i = (n_i / \sum_i n_i)$ is the mole fractions of species (x_A, x_B and $x_{A_\mu B_\nu}$). In case of ideal solution, $a_i = x_i$ or $\gamma_i = 1$. In this approximation Eq. (3.12) reduces to the form

$$G_i - G_i^{(0)} = RT \ln\left(\frac{n_i}{\sum_i n_i}\right) = RT \ln\left(\frac{n_i}{n}\right) \tag{3.13}$$

The expression for G' can be made simpler by using Eq. (3.13) in Eq. (3.11) and becomes

$$G' = RT \sum_i n_i \ \ln(n_i / n) \tag{3.14}$$

The above expression is valid only for ideal mixing in which the effects of differences in sizes of the constituents of the solution is ignored and the differences in the interaction energies ω_{ij} (which describes whether a like atom pair or an unlike atom pair is energetically favoured at the nearest neighbour) between different species is zero. But we have assumed that the interaction energies ω_{ij} are not zero. Following Longuest-Higgins (Longuest-Higgins, 1951), the expression for G' as per above mentioned condition can be given as

$$G' = RT \sum_i n_i \ln(n_i/n) + \sum_{i<j} \frac{n_i n_j}{n} \omega_{ij} \tag{3.15}$$

where ω_{ij} (= 0 for i = j) are the pairwise interaction energies which can be defined as $2\omega_{ij} = \omega_{AA} + \omega_{BB} - 2\omega_{AB}$, etc. The interaction energies ω_{12}, ω_{13} and ω_{23} respectively represents the interaction energies for the specific pairs A, B; A, $x_{A_\mu B_\nu}$ and B, $x_{A_\mu B_\nu}$. The equilibrium constant k and the formation of energy g are correlated as

$$k = e^{(-\frac{g}{RT})} \tag{3.16}$$

From Eqs. (3.7), (3.15) and (3.16), the free energy of mixing (G_M) of the alloy can be given as

$$G_M = RT \sum_i n_i \ln(\frac{n_i}{n}) + \sum_{i<j} \frac{n_i n_j}{n} \omega_{ij} + RTn_3 \ln k \tag{3.17}$$

The free energy of mixing can be expressed in terms of true mole fractions x_A, x_B and $x_{A_\mu B_\nu}$ by using Eqs. (3.3) and (3.4) in Eq. (3.17) as follows (Yadav et al., 2016)

$$G_M = \frac{1}{1+(\mu+\nu-1)x_{A_\mu B_\nu}} \Big[\left(x_A x_B \omega_{12} + x_A x_{A_\mu B_\nu} \omega_{13} + x_B x_{A_\mu B_\nu} \omega_{23} \right) + RT \left(x_A \ln x_A + x_B \ln x_B + x_{A_\mu B_\nu} \ln x_{A_\mu B_\nu} \right) + x_{A_\mu B_\nu} RT \ln k \Big] \tag{3.18}$$

This is the required expression for the free energy of mixing in regular associated solution model for binary liquid alloys. If there is no complex formation or association among the species in the liquid mixture, then $\omega_{ij} = 0$ and hence $x_{A_\mu B_\nu} = 0$ and the Eq. (3.18) takes the form

$$G_M = RT[x_1 \ln x_1 + x_2 \ln x_2] \tag{3.19}$$

As obvious, this is the expression for the free energy of mixing of an ideal alloy. It has been mentioned earlier that the conditions $\omega_{ij} = 0$ and $x_{A_\mu B_\nu} = 0$ represent to the situation of ideal mixing.

3.2.1.2 Activity coefficients (γ_A, γ_B and $\gamma_{A_\mu B_\nu}$)

The deviation from ideality in an associated solution model can be considered in terms of activity coefficients γ_A, γ_B and $\gamma_{A_\mu B_\nu}$ of the monomers and complex respectively in a strictly regular pseudo−ternary solution (Jordan, 1970; Bhatia & Hargrove, 1974). According to Jordan, these activity coefficients can be obtained by the following relations

$$RT \ln \gamma_1 = \left(\frac{\partial G'}{\partial n_i}\right)_{T,P,n_j} - RT \ln \left(\frac{n_i}{n}\right) \tag{3.20}$$

Therefore, the above expression becomes

$$RT \ln \gamma_A = \left(\frac{\partial G'}{\partial n_1}\right)_{T,P,n_2,n_3} - RT \ln \left(\frac{n_1}{n}\right) \tag{3.21}$$

From Eq. (3.15), we have

$$\left(\frac{\partial G'}{\partial n_1}\right)_{T,P,n_2,n_3} = RT \frac{\partial}{\partial n_1}\left\{n_1 \ln\left(\frac{n_1}{n}\right) + n_2 \ln\left(\frac{n_2}{n}\right) + n_3 \ln\left(\frac{n_3}{n}\right)\right\} + \frac{\partial}{\partial n_1}\left\{\left(\frac{n_1 n_2}{n}\right)\omega_{12} + \left(\frac{n_1 n_3}{n}\right)\omega_{13} + \left(\frac{n_2 n_3}{n}\right)\omega_{23}\right\}$$

$$= \mathrm{RT}\ln\left(\frac{n_1}{n}\right) + \frac{n_2^2}{n^2}\omega_{12} + \frac{n_3^2}{n^2}\omega_{13} + \frac{n_2 n_3}{n^2}(\omega_{12} - \omega_{23} + \omega_{13}) \quad (3.22)$$

Using Eq. (3.22) in Eq. (3.21), we have

$$\mathrm{RT}\ln\gamma_A = \frac{n_2^2}{n^2}\omega_{12} + \frac{n_3^2}{n^2}\omega_{13} + \frac{n_2 n_3}{n^2}(\omega_{12} - \omega_{23} + \omega_{13}) \quad (3.23)$$

Therefore, using Eqs. (3.3) and (3.4) in Eq. (3.23), we get

$$\mathrm{RT}\ln\gamma_A = x_B^2\omega_{12} + x_{A_\mu B_\nu}^2\omega_{13} + x_B x_{A_\mu B_\nu}(\omega_{12} - \omega_{23} + \omega_{13}) \quad (3.24a)$$

By the similar procedure, we can obtain the following relations (Yadav et al., 2016)

$$\mathrm{RT}\ln\gamma_B = x_{A_\mu B_\nu}^2\omega_{23} + x_A^2\omega_{12} + x_A x_{A_\mu B_\nu}(\omega_{23} - \omega_{13} + \omega_{12}) \quad (3.24b)$$

and, $$\mathrm{RT}\ln\gamma_{A_\mu B_\nu} = x_A^2\omega_{13} + x_B^2\omega_{23} + x_A x_B(\omega_{13} - \omega_{12} + \omega_{23}) \quad (3.24c)$$

3.2.1.3 Equilibrium constant (k)

It is assumed that the equilibrium between the complex and free atoms corresponding to the association reaction of the $A_\mu B_\nu$ complex of the type $A_\mu B_\nu \Leftrightarrow \mu A + \nu B$ exists in regular associated solution model. The equilibrium constant for this reaction can be expressed as (Osmura & Predel, 1977; Srikanth & Jacob, 1988; Yadav et al., 2014)

$$k = \frac{a_A^\mu\, a_B^\nu}{a_{A_\mu B_\nu}} = \frac{x_A^\mu\, x_B^\nu}{x_{A_\mu B_\nu}}\,\frac{\gamma_A^\mu\,\gamma_B^\nu}{\gamma_{A_\mu B_\nu}} \quad (3.25)$$

where a_A and a_B are the activities of the free monomers A and B in the liquid mixture. Also in regular associated solution model $a_A = x_A\gamma_A$ and $a_B = x_B\gamma_B$. Taking logarithm on both sides of Eq. (3.25), we get

$$\ln k = \ln\left(\frac{x_A^{\mu} x_B^{\nu}}{x_{A_\mu B_\nu}}\right) + \ln\left(\frac{\gamma_A^{\mu} \gamma_B^{\nu}}{\gamma_{A_\mu B_\nu}}\right) = \ln\left(\frac{x_A^{\mu} x_B^{\nu}}{x_{A_\mu B_\nu}}\right) + \ln\left(\gamma_A^{\mu}\, \gamma_B^{\nu}\right) - \ln \gamma_{A_\mu B_\nu}$$

$$= \ln\left(\frac{x_A^{\mu} x_B^{\nu}}{x_{A_\mu B_\nu}}\right) + \mu \ln \gamma_A + \nu \ln \gamma_B - \ln \gamma_{A_\mu B_\nu} \tag{3.26}$$

With the help of Eqs. (3.24), the above Eq. takes the form

$$\begin{aligned}\ln k = \ln\left(\frac{x_A^{\mu} x_B^{\nu}}{x_{A_\mu B_\nu}}\right) &+ \mu\left[\mathrm{x_B^2}\omega_{12} + \mathrm{x_{A_\mu B_\nu}^2}\omega_{13} + \mathrm{x_B x_{A_\mu B_\nu}}(\omega_{12} - \omega_{23} + \omega_{13})\right] \\ &+\nu\left[\mathrm{x_{A_\mu B_\nu}^2}\omega_{23} + \mathrm{x_A^2}\omega_{12} + \mathrm{x_A x_{A_\mu B_\nu}}(\omega_{23} - \omega_{13} + \omega_{12})\right] \\ &+[\mathrm{x_A^2}\omega_{13} + \mathrm{x_B^2}\omega_{23} + \mathrm{x_A x_B}(\omega_{13} - \omega_{12} + \omega_{23})\,]\end{aligned} \tag{3.27}$$

After performing some algebraic operations and rearranging the terms, we get

$$\begin{aligned}\ln k = \ln\left(\frac{x_A^{\mu} x_B^{\nu}}{x_{A_\mu B_\nu}}\right) &+ \frac{\omega_{12}}{\mathrm{RT}}\left[\mu \mathrm{x_B}(1 - \mathrm{x_A}) + \nu \mathrm{x_A}(1 - \mathrm{x_B}) + \mathrm{x_A x_B}\right] \\ &+ \frac{\omega_{13}}{\mathrm{RT}}\left[\mu \mathrm{x_{A_\mu B_\nu}}(1 - \mathrm{x_A}) - \mathrm{x_A}\left(1 - \mathrm{x_{A_\mu B_\nu}}\right) - \nu \mathrm{x_A x_{A_\mu B_\nu}}\right] \\ &+ \frac{\omega_{23}}{\mathrm{RT}}\left[\nu \mathrm{x_{A_\mu B_\nu}}(1 - \mathrm{x_B}) - \mu \mathrm{x_B x_{A_\mu B_\nu}} - \mathrm{x_B}\left(1 - \mathrm{x_{A_\mu B_\nu}}\right)\right]\end{aligned} \tag{3.28}$$

3.2.1.4 Activity

The activity is a fundamental thermodynamic quantity on the basis of which the stability of the complex in terms of its constituent atoms can be interpreted. The different thermodynamic properties as well as structural properties can also be expressed and explained on the basis of activity. Any deviation of the liquid binary alloys from the ideal behaviour can be incorporated into the activity. It can be measured as a function of the alloy composition and/or temperature (Saboungi et al., 1990). It can be measured directly from several experimental techniques, such as measurements of electromotive force, vapour pressure, chemical equilibria, etc. (Richardson & Alcock, 1959; Komarek, 1973; Kubaschewski, 1981; Predel, 1982; Kubaschewski et al., 1993) depending upon the

physicochemical properties of the system. The thermodynamic activities of the components of liquid alloys can be directly obtained from the electromotive force of a galvanic cell or partial vapour pressures.

The activity a_A of the monomer or unassociated atom A in the liquid alloy at constant temperature T in terms of its partial vapour pressure p_A can be related as

$$RT \ln a_A = \frac{p_A}{p_A^0} \tag{3.29}$$

Here p_A^0 stands for the vapour pressure of pure liquid A at T. The activity of the monomers can also be related with electromotive force E of galvanic cell by the following expression

$$RT \ln a_i = -z F E \tag{3.30}$$

where F is the Faraday constant and z is the valence of the ion in the liquid or solid electrolyte which exhibit exclusively ion conductivity and i carry the usual values as mentioned above. The activities of each component of the liquid alloy can be related via the Gibbs–Duhem equation as follows (Prigogine & Defay, 1954)

$$\sum_i \left(\frac{\partial \ln a_1}{\partial x_i}\right) = 0 \tag{3.31}$$

Here x_i represents the mole fraction of i^{th} component. But in case of regular associated solution, the gross chemical potentials of components 1 and 2 are equal to the chemical potentials of the monomeric species A and B (Prigogine & Defay, 1954). Thus in regular associated solution

$$x_1\gamma_1 = x_A\gamma_A \tag{3.32a}$$

and, $$x_2\gamma_2 = x_B\gamma_B \tag{3.32b}$$

where γ_1 and γ_2 are the gross activity coefficients of components A and B respectively of the binary liquid alloys. Taking logarithm of Eq. (3.32a), we get

$$\ln \gamma_1 = \ln\left(\frac{x_A}{x_1}\right) + \ln \gamma_A \tag{3.33}$$

Substituting the value of γ_A from Eq. (3.24a), we have

$$\ln \gamma_1 = \ln\left(\frac{x_A}{x_1}\right) + \frac{1}{RT}\left[x_B^2\omega_{12} + x_{A_\mu B_\nu}^2\omega_{13} + x_B x_{A_\mu B_\nu}(\omega_{12} - \omega_{23} + \omega_{13})\right]$$

or, $$\gamma_1 = \exp\left\{\frac{1}{RT}\left[x_B^2\omega_{12} + x_{A_\mu B_\nu}^2\omega_{13} + x_B x_{A_\mu B_\nu}(\omega_{12} - \omega_{23} + \omega_{13})\right] + \ln\left(\frac{x_A}{x_1}\right)\right\} \tag{3.34}$$

The activity of pure component A then can be given as

$$a_1 = x_1\gamma_1 \tag{3.35}$$

Using Eq. (3.34) in Eq. (3.35), we get

$$a_1 = x_1 \exp\left\{\frac{1}{RT}\left[x_B^2\omega_{12} + x_{A_\mu B_\nu}^2\omega_{13} + x_B x_{A_\mu B_\nu}(\omega_{12} - \omega_{23} + \omega_{13})\right] + \ln\left(\frac{x_A}{x_1}\right)\right\} \tag{3.36}$$

Similarly, the activity of pure component B in the liquid mixture can be obtained by using Eqs. (3.24b), (3.32b) and in the approximation $a_2 = x_2\gamma_2$. Taking logarithm of Eq. (3.32b), we get

$$\ln \gamma_2 = \ln\left(\frac{x_B}{x_2}\right) + \ln \gamma_B \tag{3.37}$$

Substituting Eq. (3.24b) in Eq. (3.37) and in the approximation $a_2 = x_2\gamma_2$, the activity of B can be given as

$$a_2 = x_2 \exp\left\{\frac{1}{RT}\left[x_{A_\mu B_\nu}^2\omega_{23} + x_A^2\omega_{12} + x_A x_{A_\mu B_\nu}(\omega_{23} - \omega_{13} + \omega_{12})\right] + \ln\left(\frac{x_B}{x_2}\right)\right\} \tag{3.38}$$

3.2.1.5 Heat of mixing (H_M)

Heat of mixing of binary liquid alloy is one of the important thermodynamic functions which give the knowledge of the nature and strength of bonding of the liquid alloy. Eventually, the theoretical investigations and predictions of the heat of mixing of binary liquid alloys plays prominent role in metallurgical processing, characterization and design. The heat of mixing of the binary liquid alloys can be expressed in terms of free energy of mixing (G_M) by standard thermodynamic relation as

$$H_M = G_M - T\left(\frac{\partial G_M}{\partial T}\right)_P \tag{3.39}$$

In regular associated solution model, it is assumed that the interaction energies are temperature dependent. From Eq. (3.18), we have

$$\begin{aligned}\left(\frac{\partial G_M}{\partial T}\right)_P &= \frac{1}{1+(\mu+\nu-1)x_{A_\mu B_\nu}}\left(x_A x_{\mathbf{B}} \frac{\partial \omega_{12}}{\partial T} + x_A x_{A_\mu B_\nu} \frac{\partial \omega_{13}}{\partial T} + x_{\mathbf{B}} x_{A_\mu B_\nu} \frac{\partial \omega_{23}}{\partial T}\right) \\ &+ \frac{R}{1+(\mu+\nu-1)x_{A_\mu B_\nu}}\left(x_A \ln x_A + x_{\mathbf{B}} \ln x_{\boldsymbol{B}} + x_{A_\mu B_\nu} \ln x_{A_\mu B_\nu}\right) \\ &+ \frac{x_{A_\mu B_\nu}}{1+(\mu+\nu-1)x_{A_\mu B_\nu}} R \ln k + \frac{x_{A_\mu B_\nu}}{1+(\mu+\nu-1)x_{A_\mu B_\nu}} RT \frac{d\ln k}{dT}\end{aligned} \tag{3.40}$$

Substituting the values from Eqs. (3,18) and (3.40) in Eq. (3.39), we get

$$\begin{aligned}H_M &= \frac{1}{1+(\mu+\nu-1)x_{A_\mu B_\nu}}\left(x_A x_{\mathbf{B}} \omega_{12} + x_A x_{A_\mu B_\nu} \omega_{13} + x_{\mathbf{B}} x_{A_\mu B_\nu} \omega_{23}\right) - \frac{T}{1+(\mu+\nu-1)x_{A_\mu B_\nu}} \\ &\left(x_A x_{\mathbf{B}} \frac{\partial \omega_{12}}{\partial T} + x_A x_{A_\mu B_\nu} \frac{\partial \omega_{13}}{\partial T} + x_{\mathbf{B}} x_{A_\mu B_\nu} \frac{\partial \omega_{23}}{\partial T}\right) - \frac{x_{A_\mu B_\nu}}{1+(\mu+\nu-1)x_{A_\mu B_\nu}} RT^2 \frac{d\ln k}{dT}\end{aligned} \tag{3.41}$$

The term $RT^2 \frac{d\ln k}{dT}$ represents the heat of dissociation due to the formation of the complex $x_{A_\mu B_\nu}$. The Eq. (3.41) is the required expression for the heat of mixing of the binary liquid alloys. The second and third term of right hand side of above expression represents the heat of mixing of the species of the liquid alloy. Therefore, the total enthalpy or heat of mixing of the liquid alloy arises from the mixing of the species and the formation of the

complex. If there is no association or when $x_{A_\mu B_\nu} = 0$ and hence $\omega_{ij} = 0$, Eq. (3.40) reduces to that for binary regular solution, a case of ideal mixing.

3.2.1.6 Entropy of mixing (S_M)

The study of the entropy of mixing of the liquid alloys provides various structural information. As the entropy functions are difficult to be determined experimentally, the necessities of the theoretical models are of outmost essential. The entropy of mixing of the binary liquid alloy on the basis of regular associated solution model can be obtained from the standard thermodynamic relation given below

$$S_M = -\left(\frac{\partial G_M}{\partial T}\right)_P \tag{3.42}$$

Substituting Eq. (3.40) in Eq. (3.42), we get

$$\begin{aligned} S_M = & -\frac{1}{1+(\mu+\nu-1)x_{A_\mu B_\nu}}\left(x_A x_{\mathbf{B}} \frac{\partial \omega_{12}}{\partial T} + x_A x_{A_\mu B_\nu} \frac{\partial \omega_{13}}{\partial T} + x_{\mathbf{B}} x_{A_\mu B_\nu} \frac{\partial \omega_{23}}{\partial T}\right) \\ & -\frac{R}{1+(\mu+\nu-1)x_{A_\mu B_\nu}}\left(x_A \ln x_A + x_{\mathbf{B}} \ln x_{\boldsymbol{B}} + x_{A_\mu B_\nu} \ln x_{A_\mu B_\nu}\right) \\ & -\frac{x_{A_\mu B_\nu}}{1+(\mu+\nu-1)x_{A_\mu B_\nu}} R \ln k - \frac{x_{A_\mu B_\nu}}{1+(\mu+\nu-1)x_{A_\mu B_\nu}} RT \frac{d \ln k}{dT} \end{aligned} \tag{3.43}$$

Eq. (3.43) is the required expression for the entropy of mixing of the binary liquid alloys.

The entropy of mixing of binary liquid alloys can also be obtained from another standard thermodynamic relation and is

$$S_M = \frac{H_M - G_M}{T} \tag{3.44}$$

Therefore, the theoretical values of S_M can be directly computed with the aid of determined values of heat of mixing (H_M) and free energy of mixing (G_M).

3.2.2 Estimation of model parameters

The model parameters in regular associated solution model are the pairwise interaction energies (ω_{12}, ω_{13} and ω_{23}), equilibrium constant (k) and the mole fraction of the complex ($x_{A_\mu B_\nu}$). All the thermodynamic as well as structural functions depend upon these parameters. The modeling equations relating these functions and parameters are transcendental and cannot be solved independently. This complexity has been greatly simplified by Lele & Ramchandrarao in 1981. The pairwise interaction energies and the equilibrium constant for the formation of complex can be determined with the knowledge of observed activity coefficients of the components at infinite dilution of the binary liquid alloy and the activity data at one other intermediate composition (Lele & Ramchandrarao, 1981). In this section, the modeling equations have been derived to determine the above mentioned parameters by assuming the complex $x_{A_\mu B_\nu}$ in which both μ and ν are greater than one, i.e., $\mu > 1$and $\nu > 1$.

Substituting Eq. (3.5) in Eq. (3.33), we have

$$\ln \gamma_1 = \ln \gamma_A + \ln \left\{ \frac{x_1 \left[1+(\mu+\nu-1)x_{A_\mu B_\nu}\right] - \mu x_{A_\mu B_\nu}}{x_1} \right\} \tag{3.45}$$

And, substituting Eq. (3.6) in Eq. (3.37), we have

$$\ln \gamma_2 = \ln \gamma_B + \ln \left\{ \frac{x_2 \left[1+(\mu+\nu-1)x_{A_\mu B_\nu}\right] - \nu x_{A_\mu B_\nu}}{x_2} \right\} \tag{3.46}$$

In the limit $x_1 \to 0$, $x_A \to 0$ and $x_{A_\mu B_\nu} \to 0$, consideration of Eq. (3.45) under these conditions require the application of L' Hospital's rule and evaluation of $\left(\frac{dx_{A_\mu B_\nu}}{dx_1}\right)$ at $x_1 \to 0$ from the implicit relationship among the variables in Eq. (3.28). Eq. (3.28) can be written in the form

$$\ln\left(\frac{x_A^{\mu}x_B^{\nu}/x_{A_\mu B_\nu}}{k}\right) = -\frac{\omega_{12}}{\mathrm{RT}}\left[\mu x_B - \mu x_A x_B + \nu x_A - \nu x_A x_B + x_A x_B\right]$$
$$-\frac{\omega_{13}}{\mathrm{RT}}\left[\mu x_{A_\mu B_\nu} - \mu x_A x_{A_\mu B_\nu} - x_A + x_A x_{A_\mu B_\nu} - \nu x_A x_{A_\mu B_\nu}\right]$$
$$-\frac{\omega_{23}}{\mathrm{RT}}\left[\nu x_{A_\mu B_\nu} - \nu x_B x_{A_\mu B_\nu} - \mu x_B x_{A_\mu B_\nu} - x_B + x_B x_{A_\mu B_\nu}\right] \quad (3.47)$$

Substituting $x_1 \to 0$, $x_1 \to x_A \to 0$, $x_{A_\mu B_\nu} \to 0$ and $x_2 = x_B = 1$ and applying L' Hospital's rule in the above Eq. (3.47), it can be shown that

$$\left(\frac{dx_{A_\mu B_\nu}}{dx_1}\right)_{x_1 \to 0} = 0 \quad (3.48)$$

Similarly, in the limit $x_2 \to 0$, $x_2 \to x_B \to 0$, $x_{A_\mu B_\nu} \to 0$ and $x_1 = x_A = 1$; and applying L' Hospital's rule in the Eq. (3.28), we get

$$\left(\frac{dx_{A_\mu B_\nu}}{dx_2}\right)_{x_2 \to 0} = \left[1 + k \exp\left(\frac{\omega_{13} - \nu\omega_{13}}{RT}\right)\right]^{-1} \quad (3.49)$$

Using Eqs. (3.48) and (3.49) in Eqs. (3.45) and (3.46) respectively, we get

$$\ln \gamma_1^0 = \ln \gamma_A^0 \quad (3.50)$$

and, $\ln \gamma_2^0 = \ln \gamma_B^0 + \ln\left[1 - \left(1 + k \exp\frac{\omega_{13} - \nu\omega_{12}}{RT}\right)^{-1}\right]$ (3.51)

The activity coefficients of A and B in the limits $x_1 \to 0$ and $x_2 \to 0$, respectively assumes an identical values of $\frac{\omega_{12}}{\mathrm{RT}}$ from Eq. (3.24). Substituting these limiting values in Eqs. (3.50) and (3.51), we get

$$\ln \gamma_1^0 = \frac{\omega_{12}}{\mathrm{RT}} \quad (3.52)$$

and, $\ln \gamma_2^0 = \frac{\omega_{12}}{\mathrm{RT}} + \left[1 - \left(1 + k \exp\frac{\omega_{13} - \nu\omega_{12}}{RT}\right)^{-1}\right]$ (3.53)

Solving Eqs. (3.52) and (3.53), we have

$$\mathrm{k}\exp\left(\frac{\omega_{13}}{RT}\right) = \frac{\gamma_1^0\gamma_2^0}{\gamma_1^0-\gamma_2^0} \tag{3.54}$$

The model parameters ω_{12}/RT and $\mathrm{k}\exp(\omega_{13}/RT)$ thus can be determined with the knowledge of activity coefficients of monomers at infinite dilutions (γ_1^0 and γ_2^0) which are extrapolated from experiments on concentrations. The specific values of the models parameters can be obtained from the expressions and methodologies as follows.

Solving Eqs. (3.24a) and (3.24b) for ω_{13}/RT by substituting $\mathrm{x_A} + \mathrm{x_B} + \mathrm{x_{A_\mu B_\nu}} = 1$, yields

$$\frac{\omega_{13}}{\mathrm{RT}} = \frac{\mathrm{x_B}\ln\left(\frac{a_2}{x_B}\right)+(1-\mathrm{x_B})\ln\left(\frac{a_1}{x_A}\right)-\mathrm{x_B}(1-\mathrm{x_B})\frac{\omega_{12}}{\mathrm{RT}}}{\mathrm{x_{A_\mu B_\nu}}^2} \tag{3.55}$$

which is the required expression for ω_{13}/RT in terms of activities of the free monomers and ω_{12}/RT. Similarly, the expression for ω_{23}/RT can be obtained by solving Eqs. (3.24a) and (3.24b), and expression so obtained is as follows

$$\frac{\omega_{23}}{\mathrm{RT}} = \frac{\mathrm{x_A}\ln\left(\frac{a_1}{x_A}\right)+(1-\mathrm{x_A})\ln\left(\frac{a_2}{x_B}\right)-\mathrm{x_A}(1-\mathrm{x_A})\frac{\omega_{12}}{\mathrm{RT}}}{\mathrm{x_{A_\mu B_\nu}}^2} \tag{3.56}$$

The expression for the mole fraction of the complex in terms of the mole fractions of the unassociated atoms can be then obtained by using Eqs. (3.55) and (3.56) in Eq. (3.28) along with algebraic simplification as follows

$$\ln k + \frac{\omega_{13}}{\mathrm{RT}} = \left(\frac{1+\mathrm{x_A}}{\mathrm{x_{A_\mu B_\nu}}}\right)\ln\left(\frac{a_1}{x_A}\right) + \left(\frac{\mathrm{x_B}}{\mathrm{x_{A_\mu B_\nu}}}\right)\left[\ln\left(\frac{a_2}{x_B}\right) - \frac{\omega_{13}}{\mathrm{RT}}\right] + \ln\left(\frac{a_1^\mu a_2^\nu}{x_{A_\mu B_\nu}}\right) \tag{3.57}$$

Thus the values of mole fractions of the complex ($\mathrm{x_{A_\mu B_\nu}}$) at all concentrations can be obtained by expressing $\mathrm{x_A}$ (in Eq. (3.5) and $\mathrm{x_B}$ (in Eq. (3.6) in terms of $\mathrm{x_{A_\mu B_\nu}}$, and with

the known values of ω_{12}/RT and $\ln k + \omega_{13}/RT$ (which are determined from the observed values of γ_1^0 and γ_2^0) by following iterative procedure. The optimized values of the other model parameters k, ω_{13} and ω_{23} then can be determined by using the respective Eqs. (3.28), (3.55) and (3.56). Once the mole fraction of the complex is determined, the mole fractions of the free monomers can be obtained from the respective Eqs. (3.5) and (3.6).

3.3 For the binary liquid alloys of type: $A_\mu B_\nu$ ($\mu > 1, \nu = 1$)

Let a mole of binary liquid alloy consists of x_1 moles of atoms A and x_2 moles of atoms B. There is a probable association between these atoms of the type $A_\mu B$ ($\mu A + B \Leftrightarrow A_\mu B$). The formation of the complex thus results in the reduction of concentrations of free atoms of A and B in the initial melt. The unassociated atoms of A and B and the complex $A_\mu B$ are assumed to be in chemical equilibrium. The thermodynamic properties of the alloy is thus governed by their true mole fractions x_A, x_B and $x_{A_\mu B}$ respectively of free atoms A and B and the complex AB, rather than their gross mole fractions x_1 and x_2. The theoretical modeling equations for the thermodynamic and structural functions are based on the two reference frames, one related to the gross mole fractions (x_1 and x_2) and the other related to the actual mole fractions (x_A, x_B and $x_{A_\mu B}$). Moreover, if it is assumed that there are n_1 moles of unassociated monomer A, n_2 moles of unassociated monomer B and n_3 moles of the complex $A_\mu B$, then from the conservation mass the reference frames can be related as

$$n_1 = x_1 - \mu n_3 \text{ , } n_2 = x_2 - n_3 \text{ and } n = n_1 + n_2 + n_3 = 1 - \mu n_3 \tag{3.58}$$

The true mole fractions of A, B and AB can be then given as

$$x_A = \frac{n_1}{n_1+n_2+n_3} = \frac{n_1}{1-\mu n_3}, \; x_B = \frac{n_2}{n_1+n_2+n_3} = \frac{n_2}{1-\mu n_3} \text{ and } x_{A_\mu B} = \frac{n_3}{n_1+n_2+n_3} = \frac{n_3}{1-\mu n_3} \tag{3.59}$$

where, $$\frac{1}{n} = \frac{1}{1-\mu n_3} = 1 + \frac{\mu n_3}{1-\mu n_3} = 1 + \mu x_{A_\mu B} \tag{3.60}$$

Then using Eq. (3.60) in Eq. (3.59), we obtain

$$n_1 = \frac{x_A}{1+\mu x_{A_\mu B}},\ n_2 = \frac{x_B}{1+\mu x_{A_\mu B}} \quad \text{and} \quad n_3 = \frac{x_{A_\mu B}}{1+\mu x_{A_\mu B}} \tag{3.61}$$

The true mole fractions x_A, x_B and $x_{A_\mu B}$ then can be correlated as follows

$$x_1 x_2 = x_2 x_1 \tag{3.62}$$

Substituting the values of n_1 and n_2 from Eq. (3.58), the above Eq. (3.62) takes the form

$$(n_1 + \mu x_{A_\mu B})x_2 = (n_2 + n_3)x_1$$

After performing some algebraic operations and rearranging the terms, yields

$$n_1(x_1 + x_2) + \mu x_2 n_3 = x_1(n_1 + n_2 + n_3)$$

and, $$x_A = x_1 - \mu\, x_2\, x_{A_\mu B} \tag{3.63a}$$

By following the similar procedure, the expression for x_B can be obtained as

$$x_B = x_2 - (1 - \mu\, x_2)\, x_{A_\mu B} \tag{3.63b}$$

3.3.1 Thermodynamic functions

3.3.1.1 Free energy of mixing (G_M)

The details of the theory related to the free energy of mixing of the binary liquid alloys have been presented in the former Section 3.2.1.1. The expression for the free energy of mixing of the binary liquid alloys can be obtained by using Eqs. (3.60) and (3.61) in Eq. (3.17) as given below

$$G_M = \frac{1}{\left(1+\mu x_{A_\mu B}\right)}\left(x_A x_B \omega_{12} + x_A x_{A_\mu B}\omega_{13} + x_B x_{A_\mu B}\omega_{23}\right) + \frac{RT}{\left(1+\mu x_{A_\mu B}\right)}\left(x_A \ln x_A + x_B \ln x_B + x_{A_\mu B} \ln x_{A_\mu B}\right) + \frac{x_{A_\mu B}}{\left(1+\mu x_{A_\mu B}\right)} RT \ln k \quad (3.64)$$

The Eq. (3.64) is the required expression for the free energy of mixing for the binary liquid alloy under regular associated solution model approximation.

3.3.1.2 Activity coefficients (γ_A, γ_B and $\gamma_{A_\mu B}$)

The necessary theory and initial procedure to obtain the activity coefficients are outlined in the above mentioned Section 3.2.1.2.

The activity coefficient of the free species A in the liquid mixture can be obtained by using Eqs. (3.60) and (3.61) in Eq. (3.23) and is

$$RT \ln \gamma_A = x_B^2 \omega_{12} + x_{A_\mu B}^2 \omega_{13} + x_B x_{A_\mu B}(\omega_{12} - \omega_{23} + \omega_{13}) \quad (3.65a)$$

In the same manner, the activity coefficients of free species B and the complex $A_\mu B$ can be expressed as

$$RT \ln \gamma_B = x_{A_\mu B}^2 \omega_{23} + x_A^2 \omega_{12} + x_A x_{A_\mu B}(\omega_{23} - \omega_{13} + \omega_{12}) \quad (3.65b)$$

and, $$RT \ln \gamma_{A_\mu B} = x_A^2 \omega_{13} + x_B^2 \omega_{23} + x_A x_B(\omega_{13} - \omega_{12} + \omega_{23}) \quad (3.65c)$$

3.3.1.3 Equilibrium constant (k)

Following Osmura and Predel (1977), the equilibrium constant k for the association reaction of the type $A_\mu B \Leftrightarrow \mu A + B$ in regular associated solution can be expressed as

$$k = \frac{a_A^{\mu} a_B}{a_{A_{\mu}B}} = \frac{x_A^{\mu} x_B}{x_{A_{\mu}B}} \frac{\gamma_A^{\mu} \gamma_B}{\gamma_{A_{\mu}B}} \tag{3.66}$$

where the terms carry their usual meanings. Also in regular associated solution model $a_A = x_A\gamma_A$ and $a_B = x_B\gamma_B$. Taking logarithm on both sides of Eq. (3.66), we get

$$\begin{aligned} \ln k &= \ln\left(\frac{x_A^{\mu} x_B}{x_{A_{\mu}B}}\right) + \ln\left(\frac{\gamma_A^{\mu} \gamma_B}{\gamma_{A_{\mu}B}}\right) = \ln\left(\frac{x_A^{\mu} x_B}{x_{A_{\mu}B}}\right) + \ln\left(\gamma_A^{\mu}\, \gamma_B\right) - \ln \gamma_{A_{\mu}B} \\ &= \ln\left(\frac{x_A^{\mu} x_B}{x_{A_{\mu}B}}\right) + \mu \ln \gamma_A + \ln \gamma_B - \ln \gamma_{A_{\mu}B} \end{aligned} \tag{3.67}$$

Using Eqs. (3.65) in Eq. (3.67) and after performing some algebraic operations along with rearranging the terms, we get

$$\begin{aligned} \ln k = \ln\left(\frac{x_A^{\mu} x_B}{x_{A_{\mu}B}}\right) &+ \frac{\omega_{12}}{RT}\left[\mu x_B(1 - x_A) + x_A\right] + \frac{\omega_{13}}{RT}\left[\mu x_{A_{\mu}B}(1 - x_A) - x_A\right] \\ &+ \frac{\omega_{23}}{RT}\left[x_{A_{\mu}B}(1 - \mu x_B) - x_B\right] \end{aligned} \tag{3.68}$$

Eq. (3.68) is the required expression for the equilibrium constant.

3.3.1.4 Activities of unassociated species (a_A and a_B)

The detailed literatures including the basic relations between the free energy of mixing and activities of unassociated species are highlighted in afore mentioned Section 3.2.1.4.

Substituting the value of $\ln \gamma_A$ from Eq. (3.65a) into Eq. (3.33), we get

$$\ln \gamma_1 = \ln\left(\frac{x_A}{x_1}\right) + \frac{1}{RT}\left[x_B^2\omega_{12} + x_{A_{\mu}B}^2\omega_{13} + x_B x_{A_{\mu}B}(\omega_{12} - \omega_{23} + \omega_{13})\right] \tag{3.69}$$

Similarly, using Eq. (3.65b) in Eq. (3.37), we get

$$\ln \gamma_2 = \ln\left(\frac{x_B}{x_2}\right) + \frac{1}{\mathrm{RT}}\left[\mathrm{x}_{\mathrm{A_\mu B}}^2 \omega_{23} + \mathrm{x}_{\mathrm{A}}^2 \omega_{12} + \mathrm{x_A x_{A_\mu B}}(\omega_{23} - \omega_{13} + \omega_{12})\right] \tag{3.70}$$

The expression for the activity of unassociated atoms A in the liquid state can be obtained by using Eq. (3.69) in Eq. (3.35), one obtains

$$\mathrm{a}_1 = \mathrm{x}_1 \exp\left\{\frac{1}{RT}\left[x_B^2 \omega_{12} + x_{A_\mu B}^2 \omega_{13} + x_B x_{A_\mu B}(\omega_{12} - \omega_{23} + \omega_{13})\right] + \ln\left(\frac{x_A}{x_1}\right)\right\} \tag{3.71a}$$

Likewise, the activity of the unassociated atoms of B can be obtained with the aid of Eq. (3.70) as

$$\mathrm{a}_2 = \mathrm{x}_2 \exp\left\{\frac{1}{RT}\left[x_{A_\mu B}^2 \omega_{23} + x_A^2 \omega_{12} + x_A x_{A_\mu B}(\omega_{23} - \omega_{13} + \omega_{12})\right] + \ln\left(\frac{x_B}{x_2}\right)\right\} \tag{3.71b}$$

3.3.1.5 Heat of mixing ($\mathbf{H_M}$)

The necessary literature associated with the heat of mixing of the binary liquid alloys has been indicated in the aforementioned Section 3.2.1.5. The expression for the heat of mixing of binary liquid alloys on the basis of regular associated solution model can be obtained with the aid of Eqs. (3.39) and (3.64). Evaluating the term $(\partial \mathrm{G_M}/\,\partial \mathrm{T})_\mathrm{P}$ from Eq. (3.64), we get

$$\begin{aligned}\left(\frac{\partial \mathrm{G_M}}{\partial \mathrm{T}}\right)_\mathrm{P} = {} & \frac{1}{\left(1+\mu \mathrm{x_{A_\mu B}}\right)}\left(\mathrm{x_A\, x_B}\,\frac{\partial \omega_{12}}{\partial \mathrm{T}} + \mathrm{x_A\, x_{A_\mu B}}\,\frac{\partial \omega_{13}}{\partial \mathrm{T}} + \mathrm{x_B\, x_{A_\mu B}}\,\frac{\partial \omega_{23}}{\partial \mathrm{T}}\right) \\ & + \frac{\mathrm{R}}{\left(1+\mu \mathrm{x_{A_\mu B}}\right)}\left(\mathrm{x_A \ln} x_A + \mathrm{x_B \ln}\, x_B + \mathrm{x_{A_\mu B} \ln}\, x_{A_\mu B}\right) \\ & + \frac{\mathrm{x_{A_\mu B}}}{\left(1+\mu \mathrm{x_{A_\mu B}}\right)}\mathrm{RT}\,\frac{\partial \ln k}{\partial \mathrm{T}} + \frac{\mathrm{x_{A_\mu B}}}{\left(1+\mu \mathrm{x_{A_\mu B}}\right)}\mathrm{R} \ln k\end{aligned} \tag{3.72}$$

Then using Eq. (3.72) in Eq. (3.39), we get

$$\begin{aligned}\mathrm{H_M} = {} & \frac{1}{\left(1+\mu \mathrm{x_{A_\mu B}}\right)}\left(\mathrm{x_A\, x_B}\,\omega_{12} + \mathrm{x_A\, x_{A_\mu B}}\,\omega_{13} + \mathrm{x_B\, x_{A_\mu B}}\,\omega_{23}\right) - \frac{\mathrm{T}}{\left(1+\mu \mathrm{x_{A_\mu B}}\right)} \\ & \left[\left(\mathrm{x_A\, x_B}\,\frac{\partial \omega_{12}}{\partial \mathrm{T}} + \mathrm{x_A\, x_{A_\mu B}}\,\frac{\partial \omega_{13}}{\partial \mathrm{T}} + \mathrm{x_B\, x_{A_\mu B}}\,\frac{\partial \omega_{23}}{\partial \mathrm{T}}\right) - \mathrm{x_{A_\mu B}RT^2}\,\frac{\mathrm{d} \ln K}{\mathrm{dT}}\right]\end{aligned} \tag{3.73}$$

where the terms carry their usual meanings. The above Eq. (3.73) is the required expression for the heat of mixing of liquid alloys in regular associated solution model.

3.3.1.6 Entropy of mixing (S_M)

The expression of entropy of mixing can be obtained by substituting Eq. (3.72) in Eq. (3.42) and is of the form

$$S_M = -\frac{1}{\left(1+\mu x_{A_\mu B}\right)}\left(x_A\, x_B\, \frac{\partial \omega_{12}}{\partial T} + x_A\, x_{A_\mu B}\, \frac{\partial \omega_{13}}{\partial T} + x_B\, x_{A_\mu B}\, \frac{\partial \omega_{23}}{\partial T}\right) - \frac{1}{\left(1+\mu x_{A_\mu B}\right)}$$
$$\left[R\left(x_A \ln x_A + x_B \ln x_B + x_{A_\mu B} \ln x_{A_\mu B}\right) + x_{A_\mu B}\left(T\, \frac{\partial \ln K}{\partial T} - R \ln k\right)\right] \qquad (3.74)$$

The theoretical value of entropy of mixing can also be determined with help of Eq. (3.44) with the aid of determined values of free energy of mixing and heat of mixing.

3.3.2 Estimation of model parameters

It has been already mentioned (in the Section 3.2.2) that the thermodynamic as well as the microscopic structural properties of the binary liquid entirely rely upon the model fitting parameters, such as interaction energy parameters (ω_{12}, ω_{13} and ω_{23}), equilibrium constant (k) and the mole fractions of the free species (x_A and x_B) and the complex ($x_{A_\mu B}$). In this section, the modeling equations have been derived to determine the above mentioned parameters by assuming the complex $x_{A_\mu B}$ in which μ is greater than one and $\nu = 1$, i.e., $\mu > 1$and $\nu = 1$. Using Eq. (3.63a) in Eq. (3.33), we have

$$\ln \gamma_1 = \ln \gamma_A + \ln\left\{1 - \frac{\mu\, x_2\, x_{A_\mu B}}{x_1}\right\} \qquad (3.75)$$

And, substituting Eq. (3.63b) in Eq. (3.37), we have

$$\ln \gamma_2 = \ln \gamma_B + \ln\left\{1 - \frac{(1-\mu\, x_2) x_{A_\mu B}}{x_2}\right\} \qquad (3.76)$$

3.3.2.1 Case I ($\mu > 1$)

In the limit $x_1 \to 0$, $x_A \to 0$ and $x_{A_\mu B} \to 0$, consideration of Eq. (3.75) under these conditions require the application of L' Hospital's rule and evaluation of $\left(\frac{dx_{A_\mu B}}{dx_1}\right)$ at $x_1 \to 0$ from the implicit relationship among the variables in Eq. (3.68).

Using the conditions $x_1 \to 0$, $x_1 \to x_A \to 0$, $x_{A_\mu B} \to 0$ and $x_2 = x_B = 1$ and applying L' Hospital's rule in the above Eq. (3.68), it can be shown that

$$\left(\frac{dx_{A_\mu B}}{dx_1}\right)_{x_1 \to 0} = 0 \tag{3.77}$$

Similarly, using the conditions $x_2 \to 0$, $x_2 \to x_B \to 0$, $x_{A_\mu B} \to 0$ and $x_1 = x_A = 1$; and applying L' Hospital's rule in the Eq. (3.68), it can be shown that

$$\left(\frac{dx_{A_\mu B}}{dx_2}\right)_{x_2 \to 0} = \left[1 + k \exp\left(\frac{\omega_{13} - \omega_{13}}{RT}\right)\right]^{-1} \tag{3.78}$$

Using Eqs. (3.77) and (3.78) in Eqs. (3.75) and (3.76) respectively, we get

$$\ln \gamma_1^0 = \ln \gamma_A^0 \tag{3.79}$$

and, $$\ln \gamma_2^0 = \ln \gamma_B^0 + \ln\left[1 - \left(1 + k \exp\frac{\omega_{13} - \omega_{12}}{RT}\right)^{-1}\right] \tag{3.80}$$

where γ_1^0 and γ_2^0 represent the activity coefficients of the unassociated atoms A and B respectively in the liquid mixture.

In the limiting conditions $x_1 \to 0$ and $x_2 \to 0$, the activity coefficients of A and B respectively assumes an identical values of $\frac{\omega_{12}}{RT}$ from Eq. (3.65). Using these limiting values in Eqs. (3.79) and (3.80), we obtain

$$\ln \gamma_1^0 = \frac{\omega_{12}}{\mathrm{RT}} \tag{3.81}$$

$$\text{and, } \ln \gamma_2^0 = \frac{\omega_{12}}{\mathrm{RT}} + \left[1 - \left(1 + \mathrm{K} \exp \frac{\omega_{13} - \omega_{12}}{RT}\right)^{-1}\right] \tag{3.82}$$

Solving Eqs. (3.81) and (3.82), yields

$$\mathrm{k} \exp\left(\frac{\omega_{13}}{RT}\right) = \frac{\gamma_1^0 \gamma_2^0}{\gamma_1^0 - \gamma_2^0} \tag{3.83}$$

Once the model parameters ω_{12}/RT and k exp(ω_{13}/RT) are evaluated, the specific values of ω_{13}/RT and ω_{23}/RT can be obtained from the expressions and methodology as presented below.

In the assumption $\mathrm{x_A} + \mathrm{x_B} + \mathrm{x_{A_\mu B}} = 1$, Eqs. (3.65a) and (3.65b) can be solved for ω_{13} and ω_{23} as follows

$$\frac{\omega_{13}}{\mathrm{RT}} = \frac{\mathrm{x_B} \ln\left(\frac{a_2}{x_B}\right) + (1 - \mathrm{x_B}) \ln\left(\frac{a_1}{x_A}\right) - \mathrm{x_B}(1 - \mathrm{x_B}) \frac{\omega_{12}}{\mathrm{RT}}}{\mathrm{x_{A_\mu B}^2}} \tag{3.84}$$

$$\text{and, } \quad \frac{\omega_{23}}{\mathrm{RT}} = \frac{\mathrm{x_A} \ln\left(\frac{a_1}{x_A}\right) + (1 - \mathrm{x_A}) \ln\left(\frac{a_2}{x_B}\right) - \mathrm{x_A}(1 - \mathrm{x_A}) \frac{\omega_{12}}{\mathrm{RT}}}{\mathrm{x_{A_\mu B}^2}} \tag{3.85}$$

The expression for the mole fraction of the complex by using the above expressions for ω_{13} and ω_{23} in Eq. (3.28) along with algebraic simplification as follows

$$\ln k = \frac{\omega_{13}}{\mathrm{RT}} = \left(\frac{1 + \mathrm{x_A}}{\mathrm{x_{A_\mu B}}}\right) \ln\left(\frac{a_1}{x_A}\right) + \left(\frac{\mathrm{x_B}}{\mathrm{x_{A_\mu B}}}\right) \left[\ln\left(\frac{a_2}{x_B}\right) - \frac{\omega_{12}}{\mathrm{RT}}\right] + \ln\left(\frac{a_1^\mu a_2}{x_{A_\mu B}}\right) \tag{3.86}$$

The further procedures of obtaining the mole fractions of the complex ($\mathrm{x_{A_\mu B}}$) and unassociated species ($\mathrm{x_A}$ and $\mathrm{x_B}$) are similar to that mentioned in the Section 3.2.2.

3.3.2.2 Case II ($\mu = 1$)

The procedure of evaluating the limiting values of $\left(dx_{A_\mu B}/dx_1\right)$ at $x_1 \to 0$ and $\left(dx_{A_\mu B}/dx_2\right)$ at $x_2 \to 0$ when $\mu = 1$ are similar to that stated in the Section 3.3.2.1 for when $\mu > 1$. Following as in aforementioned Section, we get

$$\left(\frac{dx_{A_\mu B}}{dx_1}\right)_{x_1 = 0} = \left[1 + k \exp\left(\frac{\omega_{23} - \omega_{12}}{RT}\right)\right]^{-1} \tag{3.87}$$

and, $$\left(\frac{dx_{A_\mu B}}{dx_2}\right)_{x_2 = 0} = \left[1 + k \exp\left(\frac{\omega_{13} - \omega_{12}}{RT}\right)\right]^{-1} \tag{3.88}$$

With the help of Eq. (3.87), Eq. (3.75) takes the form

$$\ln \gamma_1^0 = \frac{\omega_{12}}{RT} + \ln\left[1 - \left\{1 + K \exp\left(\frac{\omega_{23} - \omega_{12}}{RT}\right)\right\}^{-1}\right] \tag{3.89}$$

Likewise, with help of Eq. (3.88), Eq. (3.76) takes the form

$$\ln \gamma_2^0 = \frac{\omega_{12}}{RT} + \ln\left[1 - \left\{1 + K \exp\left(\frac{\omega_{13} - \omega_{12}}{RT}\right)\right\}^{-1}\right] \tag{3.90}$$

The mole fraction of the complex $A_\mu B$ in this case is obtained from Eq. (3.90) by rearranging the terms and by algebraical simplification as

$$\ln k + \frac{\omega_{13}}{RT} = \ln \gamma_2^0 - \ln\left[1 - \gamma_2^0 \exp\left(-\frac{\omega_{12}}{RT}\right)\right] \tag{3.91}$$

Likewise, Eq. (3.89) takes the form

$$\ln k + \frac{\omega_{23}}{RT} = \ln \gamma_1^0 - \ln\left[1 - \gamma_1^0 \exp\left(-\frac{\omega_{12}}{RT}\right)\right] \tag{3.92}$$

Solving Eqs. (3.91) and (3.92), yields

$$\frac{\omega_{23}-\omega_{13}}{RT} = \ln\left[\frac{\gamma_1^0}{\gamma_2^0}.\frac{1-\gamma_2^0\exp\left(-\frac{\omega_{12}}{RT}\right)}{1-\gamma_1^0\exp\left(-\frac{\omega_{12}}{RT}\right)}\right] \tag{3.93}$$

Moreover, Eqs. (3.84) and (3.85) can be solved for equiatomic composition ($x_1 = x_2 = 0.5$ and $x_A = x_B$) to get

$$\frac{\omega_{23}-\omega_{13}}{RT} = \frac{\ln\left(\frac{\gamma_2}{\gamma_1}\right)_{x_1=x_2=0.5}}{x_{A_{\mu B}}} \tag{3.94}$$

Equating Eqs. (3.93) and (3.94), we get

$$x_{A_{\mu B}} = \frac{\ln(\gamma_2/\gamma_1)_{x_1=x_2=0.5}}{\ln\left[\frac{\gamma_1^0}{\gamma_2^0}.\frac{1-\gamma_2^0\exp(-\omega_{12}/RT)}{1-\gamma_1^0\exp(-\omega_{12}/RT)}\right]} \tag{3.95}$$

The values of the mole fraction of the complex ($x_{A_{\mu B}}$) and the interaction energy parameter ω_{12} at equiatomic composition are obtained by simultaneously solving Eqs. (3.86), (3.92) and (3.95) by iterative procedure. With the help of determined values of $x_{A_{\mu B}}$ and ω_{12}, the values of other model parameters (ω_{13}, ω_{23} and k) are then estimated respectively from Eqs. (3.84), (3.85) and (3.86).

3.4 Modeling of structural properties

The complex formation tendency of the liquid alloys can be further analyzed from the study of their structural properties. As the alloys are grown from the liquid state, are termed as disorder having only interaction in nearest neighbourhood. Further, the local arrangements of atoms in the initial melt can be interpreted in terms of structural functions, such as concentration fluctuation in long wavelength limit ($S_{CC}(0)$), chemical short range order parameter (α_1) and ratio of diffusion coefficients (D_M/D_{id}). The

necessary methods to obtain the expressions for the structural functions are enlisted in the following sub−sections.

3.4.1 Expression for concentration fluctuation in long wavelength limit ($S_{CC}(0)$)

The structural information at the atomic level can be directly extracted from the diffraction experiments. Following Guiner (1963) and March (1968), the fundamental expression for the amplitude of the radiation scattered from an arbitrary collection of atoms can be given as

$$A(\vec{q}) = \sum_i f_i(\vec{q}) \exp(-i\vec{q}.\vec{R}_i) \tag{3.96}$$

where $f_i(\vec{q})$ stands for the atomic scattering factor of the atoms labeled i, $\vec{R}_i$ is a position vector and $\vec{q}$ is the scattering vector, Herein, $q = |\vec{q}_2 - \vec{q}_1| = 4\pi \sin\Theta/\lambda$, $\vec{q}_2$ and $\vec{q}_1$ are the wave vectors of incident and scattered radiation, 2Θ is scattering angle and λ is the wavelength of the incident beam. The scattering factor $f_i(\vec{q})$ rely upon the type of diffraction performed. For the neutron scattering, the quantity b appears instead of $f_i(\vec{q})$ where b is called the scattering length and it is independent of $\vec{q}$.

Following Alblas (1983), the idealized intensity $I(\vec{q})$ can be related to the structure of the sample as

$$I(\vec{q}) = < |A(\vec{q})|^2 > = < f_i(\vec{q}) f_j(\vec{q}) \exp\{-i\vec{q}.(R_i - R_j)\} > \tag{3.97}$$

where the brackets indicate the thermal average.

On the basis of weak scattering approximation and the Van Hove (1954) correlation technique, Bhatia and Thornton (1970) showed that the scattering function for the binary alloy is generally expressible in terms of three structure factors for the respective atom pairs (A−A, B−B, and A−B) $S_{NN}(\vec{q})$, $S_{NC}(\vec{q})$ and $S_{CC}(\vec{q})$ (Faber & Ziman, 1965; Ashcroft & Langreth, 1967; Alblas, 1983), such that

$$S_{NN}(q) = 1 + \rho_0 \int (g_{NN}(r) - 1) \exp(i\vec{q}.\vec{r}) d\vec{r} \quad (3.98)$$

$$S_{CC}(q) = x_1 x_2 + \rho_0 \int g_{CC}(r) \exp(i\vec{q}.\vec{r}) d\vec{r} \quad (3.99)$$

$$S_{NC}(q) = \rho_0 \int g_{NC}(r) \exp(i\vec{q}.\vec{r}) d\vec{r} \quad (3.100)$$

where $g_{NN}(r)$, $g_{CC}(r)$ and $g_{NC}(r)$ are radial distribution functions and ρ_0 is the number density of the particles. The terms x_1 and x_2 represent the concentrations of the components A and B in binary alloys. These functions are devised from Fourier transforms of the local number density and concentration in the alloy.

In the limit $q \to \infty$, the Bhatia and Thornton structure factors can be given as (Ratti and Bhatia, 1978)

$$S_{NN}(q \to \infty) = 1, S_{CC}(q \to \infty) = x_1 x_2 \text{ and } S_{NC}(q \to \infty) = 0$$

The total scattered intensity per atom of the scattered beam $I(\vec{q})$ can be expressed as the linear combination of these structural factors as (Alblas, 1983; Jha et al., 1990; Adhikari, 2011)

$$I(q) = < f(q) >^2 S_{NN}(q) + \{f_1(q) - f_2(q)\}^2 S_{CC}(q) + 2. < f(q) >. \{f_1(q) - f_2(q)\}. S_{NC} \quad (3.101)$$

where, $f(q) = x_1 f_1(q) + x_2 f_2(q)$ (3.102)

Among them, $S_{NN}(0)$ and $S_{CC}(0)$ at the temperature above Debye temperature in the long wavelength limit represent the mean square thermal fluctuation in the particle number and concentration. Whereas $S_{NC}(0)$ stands for the correlation between these fluctuations. Further, they can be written as

$$S_{NN}(0) = < (\Delta N)^2 > / N \quad (3.103)$$

$$S_{CC}(0) = N < (\Delta x_1)^2 > \tag{3.104}$$

and, $$S_{NC}(0) =< (\Delta N\, \Delta x_1)^2 > \tag{3.105}$$

where $< (\Delta N)^2 >$ represents the mean square fluctuation in the number of particles in the given element of volume V, $N < (\Delta x_1)^2 >$ stands for the mean square fluctuation in the concentration and Δx_1 can be obtained as follows:

If $N = N_1 + N_2$ is the total number of atoms of the alloy, where N_1 and N_2 are the number of atoms of the constituent species, then $x_1 = N_1/N$ and $x_2 = N_2/N$. A fluctuation in x_1 is then expressed in terms of fluctuations of N_1 which is ΔN_1 and N_2 which is ΔN_2 as

$$\Delta x_1 = \left(\frac{\partial C_1}{\partial N_1}\right)_{N_2} \Delta N_1 + \left(\frac{\partial C_1}{\partial N_2}\right)_{N_1} \Delta N_2 = \frac{1}{N_2}(N_2 \Delta N_1 - N_1 \Delta N_2) \tag{3.106}$$

Neglecting the contribution from the second order terms of fluctuation, the fluctuation in x_1 can be expressed as

$$\Delta x_1 = (x_2 \Delta N_1 - x_1 \Delta N_2)/N \tag{3.107}$$

Likewise, $< \Delta N \Delta x_1 >$ can be expressed in terms of correlation between the fluctuations Δx_1 and ΔN_1, where $\Delta N = \Delta N_1 + \Delta N_2$. The fluctuation $< (\Delta x_1)^2 >$ can be expressed in terms of the second order derivative of the Gibb's free energy as (Bhatia & Thornton, 1970; March & Tosi, 1976; Adhikari, 2011; Yadav et al., 2015, 2016)

$$< (\Delta x_1)^2 > = N^{-1} \left[N K_B T \left(\frac{\partial^2 G}{\partial^2 x_1}\right)^{-1} \right]_{T,P,N} \tag{3.108}$$

where K_B is Boltzmann's constant and G is the free energy of binary mixture consisting of Nx_1 and Nx_2 g moles of species A and B respectively. The free energy of binary mixture can be expressed as

$$G = G_M + N\left[x_1 G_1^{(0)} + x_2 G_2^{(0)}\right] \tag{3.109}$$

Here, the terms $G_1^{(0)}$ and $G_2^{(0)}$ are for the Gibb's energies per atoms of the species A and B respectively and G_M is for the free energy of mixing of the binary mixture.

With the help of Eqs. (3.108) and (3.109), Eq. (3.104) can be written in the form

$$S_{CC}(0) = \left[NK_B T\left(\frac{\partial^2 G}{\partial^2 x_1}\right)^{-1}\right]_{T,P,N} \tag{3.110}$$

The terms $G_1^{(0)}$ and $G_2^{(0)}$ do not contribute for the evaluation of $\frac{\partial^2 G}{\partial^2 x_1}$. With the aid of standard thermodynamic relations, the above Eq. (3.110) can be expressed as

$$S_{CC}(0) = \left[NK_B T\left(\frac{\partial^2 G}{\partial^2 x_1}\right)^{-1}\right]_{T,P,N} = x_2 a_A \left[\left(\frac{\partial a_A}{\partial x_1}\right)_{T,P,N}\right]^{-1} = x_1 a_B \left[\left(\frac{\partial a_B}{\partial x_2}\right)_{T,P,N}\right]^{-1} \tag{3.111}$$

where a_A and a_B are thermodynamic activities of the species A and B in the mixture. Following Darken (1967), the term $(\partial^2 G/\partial^2 x_1)$ is also known as the stability of the liquid mixture. Eq. (3.111) is used to determine the experimental values of $S_{CC}(0)$ with the help of experimentally determined values of activity of species A and B or free energy of mixing of the binary mixture.

In case of ideal alloys,

$$G_M = RT\sum_i x_i \ln x_i \tag{3.112}$$

Therefore, the expression for $S_{CC}(0)$ for ideal alloys takes the form

$$S_{CC}^{id}(0) = x_1\, x_2 \tag{3.113}$$

The study of concentration fluctuation in long wavelength limit serves as the fundamental tool to peep into the structural properties of binary liquid alloys. The deviation of $S_{CC}(0)$ from $S_{CC}^{id}(0)$ provides the basis to visualize the degree of interaction among the constituent atoms of the liquid alloy (Singh, 1987; Singh & Mishra, 1988; Adhikari, 2011). At a given concentration, if $S_{CC}(0) > S_{CC}^{id}(0)$, then segregation (association among the like atoms) in the liquid alloy is expected and if $S_{CC}(0) < S_{CC}^{id}(0)$, then ordering (association among the unlike atoms) in the liquid mixture is expected. The mixing behaviour of the liquid alloys can be thus analyzed by the study of $S_{CC}(0)$.

3.4.2 Expression for $S_{CC}(0)$ in regular associated solution model

The methodology to obtain the expression for the concentration fluctuation in long wavelength limit in the frame work of regular associated solution model has been discussed in the present section. In the present work, we have assumed the existence of three different types of complexes in the liquid binary alloys, such as $A_\mu B_\nu$ (in which $\mu > 1$ and $\nu > 1$), $A_\mu B_\nu$ (=$A_\mu B$, in which $\mu > 1$ and $\nu = 1$) and $A_\mu B_\nu$ (=AB, in which both $\mu = \nu = 1$). At first, the procedure to obtain the theoretical expression for $S_{CC}(0)$ of the complex of the type $A_\mu B_\nu$ on the basis of the preferred model is presented.

3.4.2.1 Expression for $S_{CC}(0)$ for the complex of the type $A_\mu B_\nu$ ($\mu > 1; \nu > 1$)

Eq. (3.110) can be written of the form

$$S_{CC}(0) = \left[NRT \left(\frac{\partial^2 G}{\partial^2 x_1} \right)^{-1} \right]_{T,P,N} \tag{3.114}$$

The above expression clarifies that necessity of second derivative of G_M to obtain the formulation of $S_{CC}(0)$. The expression of G_M in Eq. (3.18) can be arranged in the form

$$\left[1+(\mu+\nu-1)x_{A_\mu B_\nu}\right]G_M=\left[\left(x_A x_B\omega_{12}+x_A x_{A_\mu B_\nu}\omega_{13}+x_B x_{A_\mu B_\nu}\omega_{23}\right)+RT\left(x_A\ln x_A+x_B\ln x_B+x_{A_\mu B_\nu}\ln x_{A_\mu B_\nu}\right)+x_{A_\mu B_\nu}RT\ln k\right] \quad (3.115)$$

Applying the condition $\frac{\partial G_M}{\partial x_1}=0$ for $\frac{\partial^2 G_M}{\partial {x_1}^2}>0$,the second derivative of above expression with respect to concentration gives

$$\left[1+(\mu+\nu-1)x_{A_\mu B_\nu}\right]\frac{\partial^2 G_M}{\partial {x_1}^2}=RT\left[\frac{2}{RT}\left(x'_A x'_B\omega_{12}+x'_A x'_{A_\mu B_\nu}\omega_{13}+x'_B x'_{A_\mu B_\nu}\omega_{23}\right)+\left(\frac{{x'_A}^2}{x_A}+\frac{{x'_B}^2}{x_B}+\frac{{x'_{A_\mu B_\nu}}^2}{x_{A_\mu B_\nu}}\right)\right] \quad (3.116)$$

where x'_A, x'_B and $x'_{A_\mu B_\nu}$ are the differentiations of x_A, x_B and $x_{A_\mu B_\nu}$ with respect to concentration (x_1). Using Eq. (3.116) in Eq. (3.114), we get

$$S_{CC}(0)=1/\left[\left(\frac{1}{1+(\mu+\nu-1)x_{A_\mu B_\nu}}\right)\left\{\frac{2}{RT}\left(x'_A x'_B\omega_{12}+x'_A x'_{A_\mu B_\nu}\omega_{13}+x'_B x'_{A_\mu B_\nu}\omega_{23}\right)+\left(\frac{{x'_A}^2}{x_A}+\frac{{x'_B}^2}{x_B}+\frac{{x'_{A_\mu B_\nu}}^2}{x_{A_\mu B_\nu}}\right)\right\}\right] \quad (3.117)$$

The expression for $x'_{A_\mu B_\nu}$ is obtained by differentiating Eq. (3.28) and using the condition $\frac{d\ln K}{dx_1}=0$. The expression so obtained can be written as

$$x'_{A_\mu B_\nu}=-\frac{M_1}{M_2} \quad (3.118a)$$

where

$$M_1=\left[1+(\mu+\nu-1)x_{A_\mu B_\nu}\right]\left\{\frac{\mu}{x_A}-\frac{\nu}{x_B}-\frac{\omega_{12}}{RT}[(\mu-(\mu+\nu-1)x_A)-(\nu-(\mu+\nu-1)x_B)]+(\frac{\omega_{13}}{RT}-\frac{\omega_{23}}{RT})\left[1+(\mu+\nu-1)x_{A_\mu B_\nu}\right]\right\} \quad (3.118b)$$

and

$$M_2 = \frac{\mu[x_1(\mu+\nu-1)-\mu]}{x_A} + \frac{\nu[\mu-(\mu+\nu-1)x_1-1]}{x_B} - \frac{1}{x_{A_\mu B_\nu}} + [\mu-(\mu+\nu-1)x_1-1]$$
$$\left\{\frac{\omega_{12}}{RT}[\mu-(\mu+\nu-1)x_A] - \frac{\omega_{23}}{RT}\left[1+(\mu+\nu-1)x_{A_\mu B_\nu}\right]\right\} + [x_1(\mu+\nu-1)-\mu]$$
$$\left\{\frac{\omega_{12}}{RT}[\nu-(\mu+\nu-1)x_B] - \frac{\omega_{13}}{RT}\left[1+(\mu+\nu-1)x_{A_\mu B_\nu}\right]\right\} + \left\{\frac{\omega_{13}}{RT}[\mu-(\mu+\nu-1)x_A]\right.$$
$$\left. + \frac{\omega_{23}}{RT}[\nu-(\mu+\nu-1)x_B]\right\} \quad (3.118c)$$

The expressions for x'_A and x'_B are obtained by differentiating Eq. (3.5) and Eq. (3.6) respectively with respect to concentration. The expressions so obtained are as follows

$$x'_A = 1+(\mu+\nu-1)x_{A_\mu B_\nu} + x'_{A_\mu B_\nu}[x_1(\mu+\nu-1)-\mu] \quad (3.119a)$$

and, $$x'_B = [(1-x_1)(\mu+\nu-1)-\nu]x'_{A_\mu B_\nu} - [1+(\mu+\nu-1)x_{A_\mu B_\nu}] \quad (3.119b)$$

where the terms carry their usual meanings.

3.4.2.2 Expression for $S_{CC}(0)$ for the complex of the type $A_\mu B_\nu$ ($\mu > 1$; $\nu = 1$)

Following the similar procedure as mentioned in the former section, the expression for $S_{CC}(0)$ for the complex of the preferred type can be derived. For this purpose, Eq. (3.64) can be rearranged in the form

$$\left(1+\mu x_{A_\mu B_\nu}\right)G_M = \left[\left(x_A x_B \omega_{12} + x_A x_{A_\mu B}\omega_{13} + x_B x_{A_\mu B}\omega_{23}\right)\right.$$
$$\left. + RT\left(x_A \ln x_A + x_B \ln x_B + x_{A_\mu B}\ln x_{A_\mu B}\right) + x_{A_\mu B} RT \ln k\right] \quad (3.120)$$

Differentiating Eq. (3.120) twice with respect to concentration and under the constraints $\frac{\partial G_M}{\partial x_1} = 0$ for $\frac{\partial^2 G_M}{\partial {x_1}^2} > 0$, one can obtain

$$\left[1+\mu x_{A_\mu B_\nu}\right]\frac{\partial^2 G_M}{\partial {x_1}^2} = RT\left[\frac{2}{RT}\left(x'_A x'_B \omega_{12} + x'_A x'_{A_\mu B}\omega_{13} + x'_B x'_{A_\mu B}\omega_{23}\right)\right.$$
$$\left. + \left(\frac{{x'_A}^2}{x_A} + \frac{{x'_B}^2}{x_B} + \frac{{x'_{A_\mu B}}^2}{x_{A_\mu B}}\right)\right] \quad (3.121)$$

where the terms carry their usual meanings as stated earlier. The expressions for x'_A, x'_B and $x'_{A_\mu B}$ can be obtained by differentiating x_A, x_B and $x_{A_\mu B}$ with respect to concentration.Using Eq. (3.121) in Eq. (3.114), the expression for $S_{CC}(0)$ can be given as

$$S_{CC}(0) = 1/\left[\left(\frac{1}{1+\mu x_{A_\mu B}}\right)\left\{\frac{2}{RT}\left(x'_A x'_B \omega_{12} + x'_A x'_{A_\mu B}\omega_{13} + x'_B x'_{A_\mu B}\omega_{23}\right) + \left(\frac{x'^2_A}{x_A} + \frac{x'^2_B}{x_B} + \frac{x'^2_{A_\mu B}}{x_{A_\mu B}}\right)\right\}\right] \quad (3.122)$$

The term $x'_{A_\mu B}$ can be evaluated from Eq. (3.68) using the condition $\frac{d\ln K}{dx_1} = 0$ and expression so obtained is

$$x'_{A_\mu B} = -\frac{R_1}{R_2} \quad (3.123a)$$

where,

$$R_1 = \left(1 + \mu x_{A_\mu B}\right)\left\{\frac{\mu}{x_A} - \frac{1}{x_B} - \frac{\omega_{12}}{RT}[\mu(1 - x_A) + (\mu x_B - 1] - \left[\frac{\omega_{13}}{RT} - \frac{\omega_{23}}{RT}\right]\left(1 + \mu x_{A_\mu B}\right)\right\} \quad (3.123b)$$

and,

$$R_2 = \left\{\frac{\mu(\mu\, x_1 - \mu)}{x_A} + \frac{(\mu - \mu\, x_1 - 1)}{x_B} - \frac{1}{x_{A_\mu B}} + \frac{\omega_{12}}{RT}[\mu(\mu - \mu\, x_1 - 1)(1 - x_A) - (\mu x_B - 1)(\mu\, x_1 - \mu)] + \frac{\omega_{13}}{RT}\left[\mu(1 - x_A) - \left(1 + \mu x_{A_\mu B}\right)(\mu x_1 - \mu)\right] + \frac{\omega_{23}}{RT}[(1 - \mu x_B) - (\mu - \mu x_1 - 1)(1 + \mu x_{A_\mu B})]\right\} \quad (3.123c)$$

Further, the expressions for x'_A and x'_B can be obtained by differentiating Eq. (3.63) with respect to concentration and are

$$x'_A = 1 - \mu x'_{A_\mu B} + \mu x_1 x'_{A_\mu B} + \mu x_{A_\mu B} \quad (3.124a)$$

and, $$x'_B = \mu x'_{A_\mu B} - 1 - x'_{A_\mu B} - \mu x_1 x'_{A_\mu B} - \mu x_{A_\mu B} \quad (3.124b)$$

The concentration fluctuation in long wavelength limit for the complex of the type $A_\mu B_\nu$ (=AB, for both $\mu = \nu = 1$) can be evaluated by putting $\mu = 1$ in the above expressions mentioned in the Section 3.4.2.2.

3.4.3 Chemical short range order parameter (α_1)

To have a greater insight of the degree of ordering in binary liquid alloys, the knowledge of the Warren–Cowley short range order parameter is most essential (Cowley, 1950; Warren, 1969; Adhikari, 2011; Adhikari et al., 2014; Yadav et al., 2015). The information about the local arrangement of atoms in the liquid mixture at microscopic level can be obtained from α_1. Moreover, the tendency towards mixing (ordering or compound formation and demixing (segregation or phase separation) of the liquid mixture can be obtained from the quantitative investigation of α_1. In terms of conditional probability P_{AB}, the chemical short range order parameters for first–neighbour shell is given as

$$\alpha_1 = 1 - \frac{P_{AB}}{x_1} \tag{3.125}$$

Here P_{AB} represents the conditional probability of finding an atom A in the nearest neighbourhood of atom B. Thus the above expression, Eq. (3.125), provides immediate microscopic information about the local arrangement of atoms in the liquid mixture. At a given concentration, if $\alpha_1 > 0$, then association between A–A and A–B are preferred over A–B; if $\alpha_1 < 0$, then association between A–B is preferred over A–A and B–B; and if $\alpha_1 = 0$, then random distribution of only x_1 takes place. Following the probabilistic approach, the range of α_1 can be given as

$$-\frac{x_1}{x_2} \leq \alpha_1 \leq 1 \qquad x_2 \leq 0.5 \tag{3.126a}$$

$$-\frac{x_2}{x_1} \leq \alpha_1 \leq 1 \qquad x_1 \geq 0.5 \tag{3.126b}$$

The value of α_1 at an equiatomic concentration which is $x_1 = 0.5$ lies between –1 and +1 ($-1 \leq \alpha_1 \leq 1$. The minimum possible value of α_1 is –1 which represents the complete ordering in the nearest neighbours with preferenciable association between A and B whereas the maximum possible value of α_1 is +1 which represents the complete segregation with preferrenciable association between A, A and B, B. If $\alpha_1 = 0$, it

represents the complete randomness of atoms in the liquid state. In terms of generalized probability X_{AB}, the Eq. (3.124) can be expressed as

$$\alpha_1 = 1 - \frac{X_{AB}}{x_1 x_2} \quad \text{with } x_{AB} = x_1 x_2 P_{AB} \tag{3.127}$$

where generalized probability X_{AB} based on the assumption that one lattice of a nearest pair consists of an atom A and the other consists of atom B. This probability can also be expressed in relation with the thermodynamic functions as given below (Singh et al., 1987; Novakovic, 2010; Adhikari, 2011; Yadav et al., 2016)

$$\alpha_1 = \frac{S-1}{S(Z-1)+1} \text{ where } S = \frac{S_{CC}(0)}{S_{CC}^{id}(0)} \tag{3.128}$$

Here the term Z represents the coordination number of the alloy concerned. It should be noted that varying the value of Z does not have any effect on the position of the minima of α_1; the effect is to vary the depth while the overall features remain unchanged.

3.4.4 Ratio of diffusion coefficients (D_M/D_{id})

The local arrangement of atoms in the liquid mixture of binary alloys at microscopic level can be understood with the knowledge of ratio of diffusion coefficients. Following Darken (1948), the intrinsic diffusion coefficients D_A or D_B can be expressed in terms of the observed tracer diffusion coefficients D_A^* or D_B^* as

$$D_A = D_A^* \frac{d \ln a_A}{d \ln x_1} \tag{3.129a}$$

$$D_B = D_B^* \frac{d \ln a_B}{d \ln(1-x_1)} \tag{3.129b}$$

where the terms have their usual meanings. The above expressions are useful where these tracer diffusion coefficients are directly determined from the experiments by the

measurement of the evolving concentration features of a dilute radioactive isotopes A^* or B^* in the liquid alloy (Darken, 1948; Singh & Sommer, 1997). The chemical or mutual diffusion or inter diffusion coefficient in relation with the Eq. (3.129) is expressible in the form

$$D_M = x_1 D_B + (1 - x_1) D_A \tag{3.130a}$$

According to the Gibbs–Duhem relation, we get

$$D_M = (x_1 D_B^* + (1 - x_1) D_A^*) \frac{d \ln a_A}{d \ln x_1} \tag{3.130b}$$

where, $\frac{d \ln a_A}{d \ln x_1} = \frac{d \ln a_B}{d \ln(1-x_1)}$ (3.130c)

Eq. (3.130b) can also expressed in terms of $S_{CC}(0)$ as

$$D_M = (x_1 D_B^* + (1 - x_1) D_A^*) \frac{S_{CC}^{id}(0)}{S_{CC}(0)} \tag{3.131}$$

For the case of ideal alloys, $S_{CC}^{id}(0) = x_1(1 - x_1) = S_{CC}(0)$, then

$$D_M = x_1 D_B + (1 - x_1) D_A = (x_1 D_B^* + (1 - x_1) D_A^*) = D_{id} \tag{3.132}$$

For ideal mixture the intrinsic diffusion coefficient D_{id} and the tracer diffusion coefficients D_{id}^* are identical by virtue of Eq. (3.129), therefore, Eq. (3.131) becomes

$$D_M / D_{id} = S_{CC}^{id}(0) / S_{CC}(0) \tag{3.133}$$

At a reference concentration if $\frac{D_M}{D_{id}} > 1$, it reveals the ordering tendency of the liquid alloy as $S_{CC}(0) < S_{CC}^{id}(0)$; if $\frac{D_M}{D_{id}} < 1$, it notifies the segregating tendency of the liquid alloy as $S_{CC}(0) > S_{CC}^{id}(0)$ and if $\frac{D_M}{D_{id}} = 0$, it notifies random mixing.

3.5 Modeling of surface properties

The study of the surface properties of liquid alloys provides information about various the mechanical properties. The surface properties, such as surface tension (σ) and surface concentrations (x_A^S and x_B^S) of the preferred liquid alloys have been computed in the framework of Renovated Butler model. In the following sub−sections, the methods to obtain the expressions for the surface properties have been presented.

3.5.1 Renovated Butler model for binary liquid alloys

The necessity for the development of Renovated Butler model has been already mentioned in the Chapter 2. Herein, we intend to obtain the mathematical working expressions in the frame work of Renovated Butler model to the study of the surface properties, such as surface tension and surface segregation of liquid binary alloys preferred in this work.

The irrigation of fundamental stream leading to the oceans of investigations about the surface properties is accredited to Gibbs (1875−1878). The noble expression devised by him which serves as epicenter till date is the relation between the surface tension and Gibbs energy, and is

$$\sigma \equiv \left(\frac{dG}{dA}\right)_{p,T,n_i} \tag{3.134}$$

where σ is the surface tension of a liquid solution phase, G is its absolute Gibbs energy and A is its absolute surface area. Eq. (3.134) can be can be integrated using the following two boundary conditions: (a) at A = 0; $G = G_B$, where G_B being the bulk Gibbs energy of the macroscopic liquid phase; and (b) at A=A; G = G. Integrating Eq. (3.134) at such boundary condition yields

$$G = G_b + A\sigma \tag{3.135}$$

This shows that the total Gibbs energy of a liquid phase consists of two terms; the bulk term and the surface term. This is because nature tends to minimize the Gibbs energy and hence the surface tension thereby surface area can attain only positive values. σ is minimized by adopting an equilibrium structure and equilibrium composition of the surface region of the liquid phase as well as function of p, T and n_i, Gibbs named later as surface excess (Kaptay, 2015). G_b is minimized by adopting the equilibrium volume and equilibrium bulk structure for the liquid phase as a function of p, T and n_i. Surface area is minimized by adopting an equilibrium shape for the liquid phase in the absence of gravity and other phases except the surrounding equilibrium vapour phase. At equilibrium, the liquid droplet acquires spherical shape as it provides the minimum surface area per unit volume among all other three dimensional structures.

Following Kaptay (2015), let the liquid solution phase consists of C components (C=2 for binary liquid alloys; present study) having n_i amount of matter of component i within it. The total amount of matter in the liquid solution phase then can be given as

$$n = \sum_i^C n_i \tag{3.136}$$

The liquid phase is embedded by the same C components vapour phase. As a result of partial pressures of the components, the vapour phase remains in equilibrium with that of the liquid solution phase. For a given p, T and n_i, the total integral absolute Gibbs energy (G) of the liquid solution attains minimum value referring to its equilibrium structure and hence equilibrium volume which when summed over n_i results into equilibrium volume of the phase. Eventually, the surface and total integral Gibbs energy of the phase are defined by Eqs. (3.134) and (3.135) respectively.

Each components i of the liquid phase is statistically distributed within this phase and its partial absolute Gibbs energy (G_i) in terms of standard partial absolute Gibbs energy (G_i^0) can be expressed as

$$G_i = G_i^0 + \Delta G_i \tag{3.137}$$

Here ΔG_i is the partial absolute mixing Gibbs energy of component i or the Gibbs energy change associated with the transfer of n_i amount of components from its standard pure liquid state to the liquid solution. ΔG_i carries the configurational entropy term and excess Gibbs energy term resulted from the attraction or repulsion between the components within the solution phase in compared to the attraction within the pure liquid phase (Lewis, 1907; Atkins, 2002; Lukas, Fries & Sundman, 2007; Kaptay, 2012−2015).

The integral absolute Gibbs energy (G) of the solution in terms of G_i can be given as

$$G = \sum_i^C G_i \tag{3.138}$$

Likewise, the integral absolute mixing Gibbs energy in terms of the partial absolute Gibbs energy of mixing can be expressed as

$$\Delta G = \sum_i^C \Delta G_i \tag{3.139a}$$

where ΔG is defined as

$$G = G^0 + \Delta G \tag{3.139b}$$

In the liquid surface, each atomic or molecular position is occupied by a different component and these atoms or molecules are statistically distributed. If A_i stands for the absolute partial surface area of i component, the total absolute surface area of the liquid solution phase can be given as

$$A = \sum_i^C A_i \tag{3.140}$$

For i component, Eq. (3.134) can be written of the form

$$\sigma_i \equiv \left(\frac{dG_i}{dA_i}\right)_{p,T,n_i} \tag{3.141}$$

Here σ_i is the partial surface tension of component i. Physically, it can be interpreted as when the shape of the liquid solution is transfigured slowly and gradually at constant p, T and n_i, the partial surface area of component i will gradually change resulting to gradual change in the partial Gibbs energy of the same component i; the ratio of former and later quantities gives the partial surface tension of the respective component. Similar to Eq. (3.134), Eq. (3.141) can be integrated using the boundary conditions: (a) at A_i=0, $G_i = G_{b,i}$; $G_{b,i}$ being the partial absolute bulk Gibbs energy of component i in the liquid solution and (b) at A_i=A_i, G_i= G_i. Therefore, the integrand of Eq. (3.141) takes the form

$$G_i = G_{b,i} + A_i\sigma_i \tag{3.142}$$

Using Eq. (3.142) in Eq. (3.138) yield

$$G = G_b + \sum_i^C A_i\sigma_i \tag{3.143}$$

where G_b can be expressed as

$$G_b = \sum_i^C G_{b,i} \tag{3.144}$$

Equating Eqs. (3.135) and (3.143), one obtains

$$A\sigma = \sum_i^C A_i\sigma_i \tag{3.145}$$

Now, combining Eq. (3.145) with Eq. (3.140) yields

$$\sum_i^C A_i(\sigma - \sigma_i) = 0 \tag{3.146}$$

In spite of infinite number of solutions, the most simplified solution of Eq. (3.146) can be given as

$$\sigma = \sigma_i \tag{3.147}$$

This shows that the partial surface tensions are equal to each other and also to the surface tension of the solution. For the considered C component liquid solution, there is C solutions of the type Eq. (3.147) obtained by putting i=1, 2, 3, ……, C. Therefore, the different atomic or molecular sites along the surface will have their own different partial surface tensions; one of them with a larger value and the other with a smaller value. It has been already mentioned that the nature tends to minimize the total Gibbs energy of the liquid solution thereby minimizing the partial surface tensions of all atomic or molecular sites which results in minimization of surface tension of the liquid solution. Kaptay (2015) developed Eq. (3.142) by extending the frame work of Gibbs thermodynamics irrespective of the structure of the bulk or surface of the liquid solution.

Using Eq. (3.137) in Eq. (3.141) yields

$$\sigma_i = \left[\frac{d\left(G_i^0+\Delta G_i\right)}{dA_i}\right]_{p,T,n_i} \tag{3.148}$$

Let us evaluate the first term on right hand side of Eq. (3.148) in form

$$\left(\frac{dG_i^0}{dA_i}\right)_{p,T,n_i} = \left(\frac{dG_i^0}{dA_i}\frac{dA_i^0}{dA_i^0}\frac{dn_{s,i}}{dn_{s,i}}\right)_{p,T,n_i} = \left(\frac{dG_i^0}{dA_i^0}\frac{dA_i^0}{dn_{s,i}}\frac{dn_{s,i}}{dA_i}\right)_{p,T,n_i} = \sigma_i^0\frac{\alpha_i^0}{\alpha_i} \tag{3.149}$$

where $n_{s,i}$ is the amount of component i in the surface region, α_i^0 is the molar surface area of component i in the pure liquid and α_i is the molar surface area of component i in the liquid mixture. The second term in the right hand side of Eq. (3.148) can be expressed as

$$\left(\frac{d\Delta G_i}{dA_i}\right)_{p,T,n_i} = \frac{\Delta G_{s,i}-\Delta G_{b,i}}{\alpha_i} \tag{3.150}$$

where $\Delta G_{s,i}$ is the partial molar Gibbs energy of mixing of component i in the surface region of the solution referring to the transfer of one mole of i atoms or molecules from the surface region of the pure i phase to the surface region of the solution. The term $\Delta G_{b,i}$ stands for the partial molar Gibbs energy of mixing of component i in the bulk of the

solution referring to the transfer of one mole of i atoms or molecules from the bulk of the pure i phase to the bulk of the solution. Following the thermodynamics of the solution (Lewis, 1907; Atkins, 2002; Lukas, Fries & Sundman, 2007; Kaptay, 2012, 2015), one can write

$$\Delta G_{b,i} = RT \ln x_i + \Delta G_{b,i}^{XS} = RT \ln a_i \tag{3.151}$$

where R is the universal gas constant, x_i is the bulk mole fraction or concentration of component i in the solution and $\Delta G_{b,i}^{XS}$ is the partial molar bulk excess Gibbs energy of mixing of the component i and a_i is the bulk activity of the component i. In the same manner, the partial molar Gibbs energy of mixing of the component i in the surface region can be written as

$$\Delta G_{s,i} = RT \ln x_{s,i} + \Delta G_{s,i}^{XS} = RT \ln a_{s,i} \tag{3.152}$$

where $x_{s,i}$ is the mole composition of component i in the surface region, $\Delta G_{s,i}^{XS}$ is the partial molar excess Gibbs energy of component i in the surface and $a_{s,i}$ is the activity of component i in the surface. According to the material balance phenomenon, we have

$$\sum_i^C x_{s,i} = 1 \tag{3.153}$$

Using Eqs. (3.149–3.152) in Eq. (3.148), following two forms of expression are obtained

$$\sigma_i = \sigma_i^0 \frac{\alpha_i^0}{\alpha_i} + \frac{RT}{\alpha_i} \ln\left(\frac{x_{s,i}}{x_i}\right) + \frac{\Delta G_{s,i}^{XS} - \Delta G_i^{XS}}{\alpha_i} \tag{3.154a}$$

$$\sigma_i = \sigma_i^0 \frac{\alpha_i^0}{\alpha_i} + \frac{RT}{\alpha_i} \ln\left(\frac{a_{s,i}}{a_i}\right) \tag{3.154b}$$

In case of two components (i, j) solution (binary liquid alloys, present study), Eq. (3.154) can be rewritten as

$$\sigma_i = \sigma_i^0 \frac{\alpha_i^0}{\alpha_i} + \frac{RT}{\alpha_i} \ln\left(\frac{x_{s,i}}{x_i}\right) + \frac{\Delta G_{s,i}^{XS} - \Delta G_i^{XS}}{\alpha_i} = \sigma_j^0 \frac{\alpha_j^0}{\alpha_j} + \frac{RT}{\alpha_j} \ln\left(\frac{x_{s,j}}{x_j}\right) + \frac{\Delta G_{s,j}^{XS} - \Delta G_j^{XS}}{\alpha_j} \quad (3.155)$$

The molar surface area of a pure component i in liquid state can be expressed as (Kaptay, 2016)

$$\alpha_i = f(V_i^0)^{2/3}(N_{Av})^{1/3} \quad (3.156a)$$

where N_{Av} (=6.023×10^{23} mol^{-1}) is the Avogadro's number, V_i^0 is the molar volume of pure component i at its melting temperature and f is the geometrical constant. The geometrical constant can be expressed as

$$f = \left(\frac{3f_b}{4}\right)^{2/3} \frac{\pi^{1/3}}{f_s} \quad (3.156b)$$

where f_b is the volume packing fraction and f_s is the surface packing fraction. Their values depend upon the type of crystal structure of the pure components of the liquid alloys.

CHAPTER 4

RESULTS AND DISCUSSION

4.1 Thermodynamic properties of binary liquid alloys

The fundamental and working expressions for the thermodynamic functions of binary liquid alloys on the basis of regular associated solution model have been presented in the former Chapter 3. The thermodynamic properties of binary liquid alloys, such as Bi−Tl, In−Bi, Al−Fe and Al−Mg have been studied at a temperature (near the melting point of the respective alloys) with the aid of aforementioned expressions. These properties have been presented in this chapter.

4.2 Existence of complex in binary liquid alloys

In regular associated solution model, the formation of complex in the initial melt of the alloy is assumed. As stated earlier, all the thermodynamic and microscopic structural properties of the binary liquid alloys are irreducible functions of the mole fractions of the complex in the preferred theoretical model. The existence of complex in the initial melt of the binary alloys can be explained by computing the mole fractions of the complex and unassociated atoms of constituents of the alloys.

The present work deals with the formation of three different types of complexes of binary liquid alloys, such as $A_\mu B_\nu$ (in which $\mu > 1$ and $\nu > 1$), $A_\mu B_\nu$ ($= A_\mu B$ in which $\mu > 1$ and $\nu = 1$) and $A_\mu B_\nu$ ($= AB$ in which $\mu = \nu = 1$). The essential theoretical modeling equations by the use of which the mole fractions of the complex and unassociated atoms are computed are presented in the Chapter 3.

4.3 Gibbs free energy of mixing (G_M) of binary liquid alloys

4.3.1 Effect of k and ω_{ij} on free energy of mixing

The free energy of mixing is inclusive function of the model parameters k and ω_{ij} (ω_{12}, ω_{13} and ω_{23}). The interpretation about the effect of these parameters on the free energy of mixing is associated with initial procedure of evaluating them by different theoretical modeling equations as mentioned in the Chapter 3. The value of k can be determined with the help of Eqs. (3.54) and (3.68). Strictly speaking, k can only be evaluated with the help of the determined values of ω_{ij} and the mole fraction of the complex $x_{A_\mu B_\nu}$. The interaction energy ω_{12} between unassociated atoms A and B is computed from the activity coefficient of species A at infinite dilution γ_1^0 and Eq. (3.52) or Eq. (3.81). Another input parameter $\ln k + \omega_{13}/\mathrm{RT}$ is determined from Eq. (3.54) or Eq. (3.83) with the knowledge of γ_1^0 and γ_2^0; later being the activity coefficient of free atom B at infinite dilution. The mole fractions of the complex and free species at equilibrium can be then computed from Eqs. (3.57) and (3.86) depending upon the types of complexes $x_{A_\mu B_\nu}$ and $x_{A_\mu B}$ assumed as stated earlier, along with activity data at one or other intermediate composition (a_1 and a_2) by iterative process. The values of ω_{13} and ω_{23} are determined from respective Eq. (3.55) or (3.84) and Eq. (3.56) or (3.85) depending on the nature of complex.

The above procedures of investigations need highly accurate activity data and precise values of γ_1^0 and γ_2^0. It has been observed that the accuracy in the values of γ_1^0 and γ_2^0 inherit highly reproducible values of ω_{13} and ω_{23} when investigated at several intermediate compositions. Inaccuracy in the available data is prone to irreproducibility of these parameters which have great reflections on the explanations of different thermodynamic as well as microscopic structural functions. In case the available data is less accurate, small adjustment can be made in the observed values of γ_1^0 and γ_2^0 in order to attain the constancy in the values of ω_{13} and ω_{23} (Lele & Ramchandrarao, 1981).

It has also been observed that the interaction energy parameters, k and mole fractions of complex and pure atoms A and B are interrelated to each other. They cannot be made independent of each other and determined irrespective of each other in regular associated solution model. Likewise, the free energy can only be determined with the knowledge of

abovementioned parameters. As a result, the procedure of computing free energy of mixing and its constituent parameters are comprehensive and hence need vigorous calculations. The prediction of the effect of any one these parameters on free energy of mixing are not so straightforward. In spite of these, it has been observed that the sign of ω_{ij} influence the compositional dependence curve of G_M. Increase in the negative values of ω_{ij} shift the value of G_M to a higher negative value whereas increase in the positive values of ω_{ij} shift its value to a lower negative value. Moreover, it has been observed that the slope of curve of compositional dependence of G_M is steeper for lower values of k and becomes flatten with the increase in value of k. The deviations from this behaviour may also occur due to the magnitudes and signs of ω_{ij} and activity data.

The basic concept of attractive or repulsive forces between the species A and B in the initial melt can also be understood in terms of sign and magnitude of ω_{ij}. Its negative value reveals the attraction between the corresponding species whereas its positive value reveals the repulsion between the corresponding species. For illustration, negative value of ω_{12} indicates that there appears attraction between the free monomers A and B whereas positive value of ω_{12} indicates that there appears repulsion between the free monomers A and B in the liquid mixture and so on.

4.4 Results for Bi−Tl, In−Bi, Al−Fe and Al−Mg liquid alloys

In the upcoming Sections of this Chapter, we present the computed values of free energy of mixing of Bi−Tl, In−Bi, Al−Fe and Al−Mg liquid alloys as a function of concentration. The procedures of evaluating the model parameters to compute compositional dependence of the free energy of mixing of above mentioned systems are also outlined.

4.4.1 Gibbs free energy of mixing (G_M) for Bi−Tl liquid alloys at 750 K

The alloys of bismuth (Bi) have low melting points due to which they are preferred over lead in solders as lead being toxic having hazardous impact on mankind and nature (Mc

Cormack et al., 1994; Suganuma, 2001; Gnecco et al., 2007; Plevachuk et al., 2011). The Bi−Tl liquid alloys have been studied by several researchers (Fruehan, 1971; Raychaudhari & Stafford, 1975; Zhang et. al, 2013; Yadav et al., 2015). The phase diagram of Bi−Tl alloys indicates the existence BiTl complex in the solid state (Hultgren *et al*., 1973). Accordingly, we have assumed the existence of complex of type $A_\mu B$ (where, A=Tl and B=Bi) with $\mu = 1$ and $\nu = 1$ in the liquid Bi−Tl alloy at 750 K. The compound forming concentration ($x_C = \mu/(\mu + \nu)$) in this alloy system is $x_1 = 0.5$, where 1 stands for Tl. The input parameters, such as mole fractions of the complex ($x_{A_\mu B} = x_{Bi-Tl}$) and unassociated atoms ($x_A = x_{Tl}$ and $x_B = x_{Bi}$), pairwise interaction energies (ω_{ij}) and equilibrium constant (k) are out most essential to compute free energy of mixing of the alloy. The methods of evaluating these parameters are mentioned as follows.

The values of the mole fraction of the complex ($x_{A_\mu B}$), the interaction energy parameter ω_{12}/RT and $\ln k + \omega_{13}/RT$ at equiatomic composition are obtained by simultaneously solving Eqs. (3.86), (3.92) and (3.95) by iterative procedure. The above procedure requires the activity coefficients of Tl and Bi at infinite dilution (γ_1^0 and γ_2^0) and activity coefficients (γ) at equiatomic composition ($x_1 = x_2 = 0.5$, where 1 and 2 stand for Tl and Bi respectively). The mole fraction of the complex has been then determined throughout the entire compositions $x_1 = 0.1$ to 0.9 with the help of Eq. (3.86) along with Eq. (3.63). Once the mole fraction of the complex is obtained, the mole fractions of unassociated species A (x_A) and B (x_B) are determined from Eq. (3.63). With the help of determined values of the complex and ω_{12}/RT, the values of other model parameters ω_{13}/RT, ω_{23}/RT and k have been then estimated respectively from Eqs. (3.84), (3.85) and (3.86). The values of interaction energy parameters and equilibrium constant so obtained have been slightly adjusted using the expression for free energy of mixing in order to explain the experimental values of free energy of mixing (Hultgren *et al*, 1973). The optimized values of the pairwise interaction energy parameters and equilibrium constant have been obtained with the aid of Microsoft Office Excel 2007 by goal seek method. The optimized values of above mentioned parameters for Bi−Tl liquid alloy at 750 K are found to be

ω_{12} =-6117.03 $Jmol^{-1}$, ω_{13} =-15089.90 $Jmol^{-1}$, ω_{23} =-1253.34 $Jmol^{-1}$ and $k = 0.3104$

All the interaction energy parameters are negative which indicate that both the unassociated species are attracted to each other as well to the complex in the initial melt. The computed values of mole fractions of the complex x_{Bi-Tl} and both the theoretical and experimental values of G_M/RT of $Bi - Tl$ liquid alloy at 750 K as a function of concentration of Tl (x_1) in the entire range from 0.1 to 0.9 are presented in Table 4.1. The plots of mole fractions x_{Bi-Tl}, x_{Bi} and x_{Tl} versus x_1(concentration of Tl) are as shown in Fig. 4.1(a). The plots of the theoretical and experimental values of G_M/RT versus x_1 are as shown in Fig. 4.1(b). All the graphs included in this work have been plotted by using the computer software Origin 6.1.

Table 4.1: x_{Bi-Tl} and G_M/RT for Bi–Tl liquid alloy at 750 K

Concentration of Tl (x_1)	Mole fraction of complex (x_{Bi-Tl})	Free energy of mixing (G_M/RT)	
		Theoretical	Experimental**
0.1	0.0578	-0.5079	-0.4860
0.2	0.1369	-0.8523	-0.8433
0.3	0.2177	-1.1128	-1.1249
0.4	0.2835	-1.3033	-1.3293
0.5*	0.3269	-1.4172	-1.4440
0.6	0.3347	-1.4364	-1.4533
0.7	0.3065	-1.3326	-1.3414
0.8	0.2169	-1.0768	-1.0853
0.9	0.0915	-0.6533	-0.6563

*Compound forming concentration
**Hultgren *et al*. (1973)

It can be observed from Fig. 4.1(a) that the compositional dependence of various species reveals that the maximum association occurs at 58 at. % of Tl where the compound forming composition is $x_1 = 0.5$. At this composition about 33.58 mol % of the liquid alloy is associated. The mole fraction of the complex declines slowly on either sides of $x_1 = 0.58$. The mole fraction of unassociated Tl (x_{Tl}) is grater at lower concentration of Bi and declines rapidly as the concentration of Bi increases. Similarly, the mole fraction of unassociated Bi (x_{Bi}) is greater at lower concentration of Tl and at first declines rapidly with the increase in the concentration of Tl whereas declines slowly when $x_1 \geq 0.8$. It

tends to zero when $x_1 > 0.96$ The plots of x_{Tl} and x_{Bi} intersects each other around the complex forming concentration which is at $x_1 = 0.5$.

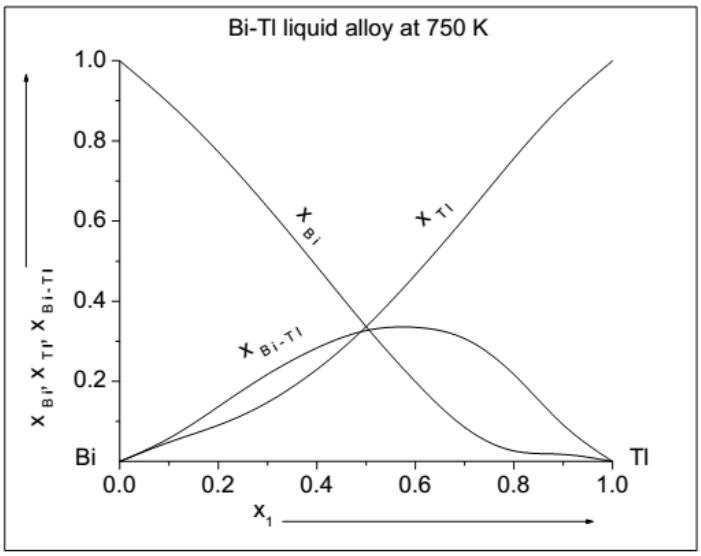

Figure 4.1(a): The mole fractions of Bi (x_{Bi}), Tl (x_{Tl}) and complex BiTl (x_{Bi-Tl}) versus concentration of Tl (x_1) of Bi−Tl liquid alloy at 750 K.

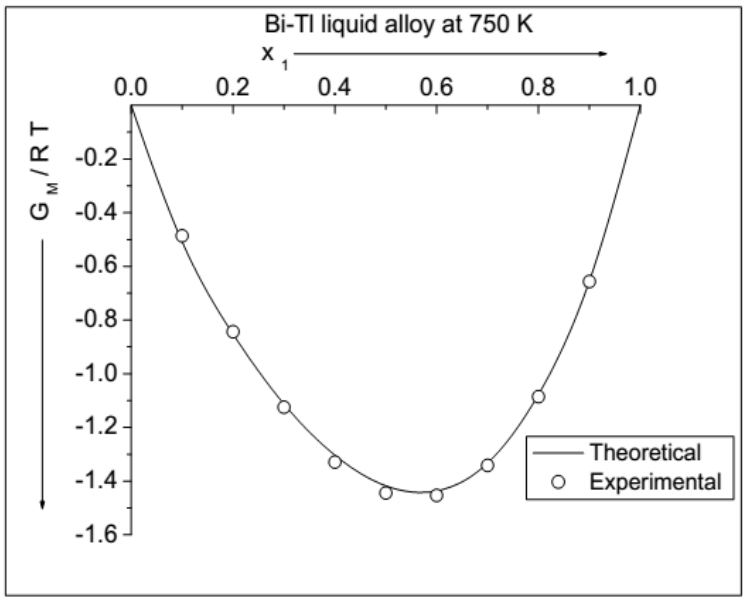

Figure 4.1(b): Free energy of mixing (G_M/RT) versus x_1 of Bi−Tl liquid alloy at 750 K.

Theoretically, it is found that the computed value G_M/RT is the minimum at $x_1 = 0.58$ and is -1.4419 for Bi−Tl liquid alloy at 750 K. Thus the alloy is asymmetric with respect to G_M. The minimum value of G_M^{XS}/RT (=-0.7471) for Bi−Tl system which indicates that

it is neither very strongly interacting nor very weakly interacting (see appendix A, Table a). As a result, the tendency of complex formation is also moderate. Fig. 4.1(b) shows that the computed and experimental values of free energy of mixing are in well agreement (Yadav et al., 2015). The asymmetry in free energy of mixing has been well explained by regular associated solution model.

4.4.2 Gibbs free energy of mixing (G_M) for In−Bi liquid alloys at 900 K

The physical applications of Bi−based alloys have been already mentioned in the Section 4.3.1. Additionally, the In−Bi alloy has crystalline structure and is used as a semiconductor and in photo−optic applications. It also possesses superconducting properties (Kirschner et al., 1974). As a result, this alloy system has been studied by several researchers (Kirschner et al., 1974; Xi et al., 2004; Mudry et al., 2007; Odusote et al., 2007; Yakymovych et al., 2008; Ohno & Tamaki, 2016; Yadav et al., 2015).

The phase diagram of In−Bi alloy (Hultgren et al., 1973) indicates the existence In_2Bi as one of the most stable intermetallic complex in the solid state. On this assumption, many researchers (Akenlade et al., 2001; Odusote et al., 2007; Yakymovych et al., 2008) have well explained the thermodynamic and structural properties of the alloy employing different theoretical models. Herein, we have also assumed the existence of the complex $A_\mu B$ ($= In_2Bi$), where $\mu = 2$ and $\nu = 1$ in the initial melt. Thus the compound formation concentration of the alloy is $x_1 = 0.66$ (where x_1 is the concentration of In). The basic ingredients essential for the computation of free energy of mixing have been determined by following the procedure outlined below.

The value of ω_{12}/RT has been determined from Eq. (3.81) with the aid of the activity coefficient of In (γ_1^0) at infinite dilution which is obtained by extrapolating from experiments on concentrations. The value of $\ln k + \omega_{13}/RT$ is determined using Eq. (3.83) with the aid of the activity coefficient Bi (γ_2^0) at infinite dilution in addition to γ_1^0 obtained by similar phenomenon. These values along with Eq. (3.63) have been used in Eq. (3.86) to determine the values of mole fraction of the complex $A_\mu B$ as a function of

concentration throughout the entire concentration range from $x_1 = 0.1$ to 0.9 by iterative procedure. For this purpose, the observed values of activities of pure species In (a_1) and Bi (a_2) have been used. Then the mole fractions of unassociated species A ($x_A = x_{In}$) and B ($x_B = x_{Bi}$) have been determined from Eqs. (3.63a) and (3.63b) respectively with the help of known values of $A_\mu B$. The values of ω_{13}/RT, ω_{23}/RT and k have been obtained from respective Eqs. (3.84), (3.85) and (3.68). The values so obtained have been slightly adjusted using Eq. (3.64) which is the expression for free energy of mixing in order to explain the experimental values of G_M. The optimized values of the above mentioned parameters have been obtained by the similar method (Section 4.4.1). The optimized values for the In−Bi liquid alloy at 900 K are found to be (Yadav et al., 2015)

ω_{12} =-5185.44 $Jmol^{-1}$, ω_{13} =-2950.39 $Jmol^{-1}$, ω_{23} =-4481.33 $Jmol^{-1}$ and $k = 0.9990$

The pairwise interaction energies are found to be negative which reveal that In and Bi atoms are attracted towards each other and also to the complex in the liquid mixture.

Table 4.2: x_{In-Bi} and G_M/RT for In−Bi liquid alloy at 900 K

Concentration of In (x_1)	Mole fraction of complex (x_{In-Bi})	Free energy of mixing (G_M/RT)	
		Theoretical	Experimental**
0.1	0.0066	-0.3912	-0.3916
0.2	0.0223	-0.6266	-0.6335
0.3	0.0408	-0.7907	-0.8016
0.4	0.0593	-0.8964	-0.9067
0.5	0.0727	-0.9452	-0.9491
0.6	0.0815	-0.9328	-0.9279
0.66*	0.0807	-0.8944	……..
0.7	0.0818	-0.8523	-0.8396
0.8	0.0818	-0.6926	-0.6765
0.9	0.0230	-0.4342	-0.4212

*Compound forming concentration
**Hultgren *et al*. (1973)

The computed values of the mole fraction of the complex (x_{In-Bi}) and theoretical as well as experimental values of free energy of mixing throughout the entire concentrations of In (x_1 =0.1 to 0.9) for In−Bi liquid alloy at 900 K are tabulated in Table 4.2. The compositional dependence of mole fractions x_{In-Bi}, x_{In} and x_{Bi} as a function of

concentration of In for In−Bi liquid alloy are plotted in Fig. 4.2(a). Both the theoretical and experimental values of G_M/RT as a function of concentration of In for the alloy are plotted in Fig. 4.2(b).

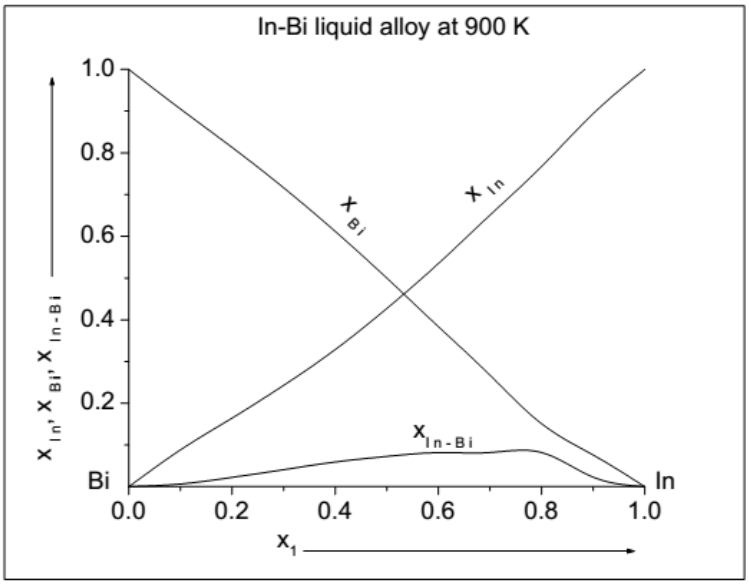

Figure 4.2 (a): Compositional dependence of mole fractions In (x_{In}), Bi (x_{Bi}) and In_2Bi (x_{In-Bi}) versus concentration of In (x_1) for In−Bi liquid alloy at 900 K.

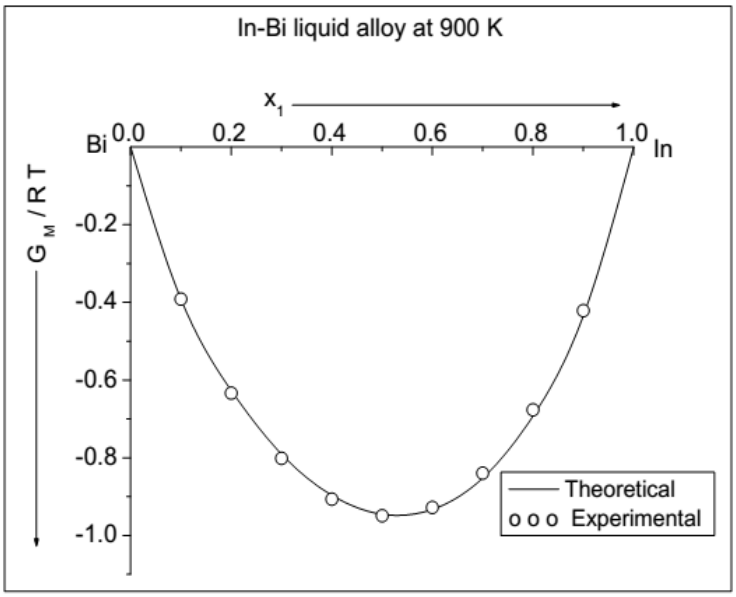

Figure 4.2(b): Gibbs free energy of mixing (G_M/RT) versus versus concentration of In (x_1) for In−Bi liquid alloy at 900 K.

Theoretically computed values of x_{In-Bi} as a function of concentration shows that the maximum association occurs at 76 at. % of In and at this composition about 8.7 mol % of the liquid alloy is associated. It can be observed from Fig. 4.2(a) that the plots do not have uniform variation. There are two peaks, the smaller at about x_1 =0.61 and the greater at about x_1 =0.76. In between the two peaks, there is a depression at compound forming concentration which is x_1 =0.66. The concentration of complex decreases rapidly beyond x_1 >0.76 but this decreament is quite slow from x_1 <0.76. As expected, the mole fraction of unassociated Bi (x_{Bi}) is maximum for lower concentration of In but decends rapidly with the increase in concentration of In. Likewise, the concentration of unassociated In atoms (x_{In}) is maximum for lower concentration of Bi but declines rapidly with the increase in concentration of Bi.

Theoretically it is determined that the minimum value of free energy of mixing (G_M) of the concerned alloy is -0.8944 RT at x_1 =0.66, which is the compound forming concentration. Also the computed value of excess free energy of mixing (G_M^{XS}/RT = -0.2484) at this concentration which is low and hence reveals that the concerned system is weakly interacting system (see appendix A, Table c). More precisely, there is weaker tendency of compound formation of the alloy in the liquid state. This assymetry in G_M has been well explained by regular associated solution model. Fig. 4.2(b) shows that both the theoretical and experimental values of G_M/RT are in a good agreement.

4.4.3 Gibbs free energy of mixing (G_M) for Al−Fe liquid alloys at 1873 K

Iron aluminides are used as high temperature structural and functional materials. They possess good oxidation resistance, weight reduction and good ductility and hence have numerous applications in present day technology (Cubero−Sesin & Horita, 2012). Among them, Al−Fe alloys can be combined with other metals (Mg, Si, Cu and Zn) by varying the composition and heat treatments to obtained different desirable physical properties (Taylor & Jones, 1958; Cubero-Sesin & Horita, 2012). Eventually, several theoreticians and experimentalists (Belton & Fruehan, 1969; Alven & Stoloff, 1997; Akinlade et al.,

2000; Morris & Munoz−Morris, 2005; Adhikari et al., 2014) have studied the physical properties of the concerned alloy.

The phase diagram of Al−Fe alloys (Hultgren *et al.*, 1973) shows the existence of Al_3Fe as one of the most stable intermetallic complex in the solid state. Akinlade et al. (2000) have studied the thermodynamics of liquid Al−Fe alloys assuming the complex Al_3Fe employing complex formation model. We, therefore, have also assumed the existence of Al_3Fe phase in the initial liquid mixture. As a result, the compound forming concentration of the alloy is $x_1 = 0.75$, where 1 is for Al. The basic input parameters, such as mole fractions x_{Al-Fe} (complex), x_{Al} (free monomer Al), x_{Fe} (free monomer Fe), interaction energies (ω_{12}/RT, ω_{13}/RT and ω_{23}/RT) and k to compute free energy of mixing of the alloy are determined by following the procedure mentioned in the Section 4.3.2. The optimized values of the interaction energy parameters and equilibrium constant for Al−Fe liquid alloy at 1873 K so obtained are found to be (Adhikari et al., 2014)

ω_{12} =-45143.60 $Jmol^{-1}$, ω_{13} =-39911.30 $Jmol^{-1}$, ω_{23} =-90427.30 J mol^{-1} and k =0.8816

All the interaction energy parameters are negative which indicates that there appears attraction between the unassociated atoms of Al and Fe. They are also attracted towards the complex.

The computed values of mole fractions x_{Al}, x_{Fe} and x_{Al-Fe} as a function of concentration of Al (x_1) for Al−Fe liquid alloy are furnished in Table 4.3. Also the theoretical and experimental values of free energy of mixing (G_M/RT) as a function of concentration of the alloy are furnished in Table 4.3. The values of mole fractions x_{Al}, x_{Fe} and x_{Al-Fe} versus concentration of Al (x_1) are plotted in Fig. 4.3(a). Both the theoretical and experimental values of G_M/RT versus x_1 are plotted in Fig. 4.3(b).

Theoretically determined result of compositional dependence of mole fraction of the complex shows that the maximum association occurs at 86 at. % of Al. About 6 mol % of

the liquid alloy is associated at this composition. Though the value of x_{Al-Fe} descends rapidly beyond x_1 >0.86, this decrement is rather slow in the range x_1 <0.86. Fig. 4.3(a) shows that the curve of x_{Al-Fe} is almost flattened near about the complex formation concentration in the range x_1 =0.74 to 0.78, where the complex formation concentration is x_1 =0.75. The concentration of mole fraction of Fe is the maximum at lower concentration Al whereas it declines rapidly as the concentration of Al increases. In the same manner, the concentration of mole fraction of Al is the maximum at lower concentration of Fe but decreases rapidly with the increase in the concentration of Fe.

Table 4.3: x_{Al-Fe} and G_M/RT for Al−Fe liquid alloy at 1873 K

Concentration of Al (x_1)	Mole fraction of complex (x_{Al-Fe})	Free energy of mixing (G_M/RT)	
		Theoretical	Experimental**
0.1	0.0020	-0.5828	-0.5897
0.2	0.0070	-0.9634	-0.9768
0.3	0.0110	-1.2326	-1.2388
0.4	0.0200	-1.4031	-1.4121
0.5	0.0300	-1.4798	-1.4764
0.6	0.0410	-1.4579	-1.4436
0.7	0.0510	-1.3252	-1.3048
0.75*	0.0522	-1.2102	……..
0.8	0.0540	-1.0621	-1.0463
0.9	0.0540	-0.6433	-0.6494

*Compound forming concentration
**Hultgren *et al*. (1973)

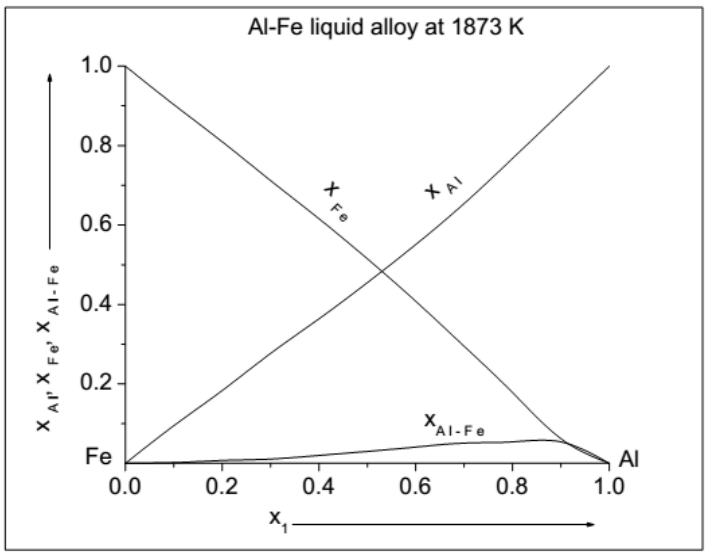

Figure 4.3(a): Plot of mole fractions of free monomers (x_{Al} and x_{Fe}) and the complex (x_{Al-Fe}) versus concentration of Al (x_1) of Al−Fe liquid alloy at 1873 K.

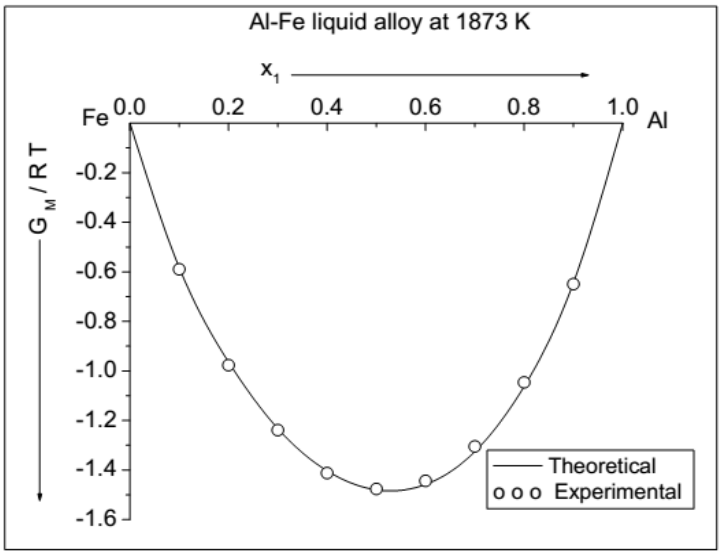

Figure 4.3(b): Plot of G_M/RT versus x_1 of Al−Fe liquid alloy at 1873 K.

Theoretical investigations shows that the minimum value of G_M/RT is found to be -1.4835 and is at $x_1 = 0.52$ which is close to equiatomic composition of the concerned alloy. Thus Al−Fe liquid alloy is symmetric in G_M. The computed value excess free energy of mixing (G_M^{XS}/RT = -0.7615) is low which corresponds that the concerned system is moderately interacting (see appendix A, Table e). Therefore, the strength of compound formation is moderate in this system. Fig. 4.3(b) shows that both the computed and experimental values of G_M/RT are in well agreement. Regular associated solution model is fruitful in explaining the free energy of mixing of the concerned liquid alloy.

4.4.4 Gibbs free energy of mixing (G_M) for Al−Mg liquid alloys at 1073 K

The Al−Mg alloys are excellent corrosion resistance having high toughness, weldability, strain hardenable, low density, moderate strength and low cost maintenance. Hence are profoundly used in building and constructions, automotive, cryogenic, marine applications, chemical plants, etc. (Holtyn, 1966; Allan, 1997; Tang et al., 2008). These desirable properties attributed the consent of several researchers (Tiwari, 1987; Agarwal & Sommer, 1991; Zuo & Chang, 1993; Zhong et al. 2005) in metallurgical science and engineering to investigate the phase diagram and properties of the alloy.

The phase diagram of Al–Mg (Hultgren *et al.*, 1973) indicates the existence of complex Al_3Mg_2 as one of the most stable compounds in solid state. This stable complex has been mentioned in many other research works (Zou & Chang, 1993). Based on this fact, thermodynamic properties of Al–Mg melt have been studied by both theoreticians and experimentalists (Tiwari, 1987; Agarwal & Sommer, 1991; Zhog et al., 2005). Eventually, we have also assumed the presence of complex Al_3Mg_2 in the initial melt of Al–Mg at 1073 K. The compound forming concentration of the alloy is x_1 =0.6, where 1 is for Al. The methods for evaluating the input parameters to compute free energy of mixing for the complex of the type $A_\mu B_\nu$ (=Al_3Mg_2), where both μ and ν are greater than one are mentioned below.

The value of ω_{12}/RT is determined from Eq. (3.52) with help the knowledge of activity coefficient of Al (γ_1^0) at infinite dilution which is obtained by extrapolation of experiments on concentrations. The value of k exp (ω_{13}/RT) is determined from Eq. (3.54) with aid of known values of γ_1^0 and γ_2^0 later being the activity coefficient of Mg at infinite dilution. It is also obtained by employing the similar method as for γ_1^0. The mole fraction of the complex x_{Al-Mg} ($A_\mu B_\nu$) is then obtained from Eq. (3.57) with help of above determined parameters along with the activities of Al (a_1) and Mg (a_2) and Eqs. (3.5) and (3.6) by following iterative procedure. The mole fractions of the left over atoms of A (=Al) and B (=Mg) are then calculated from Eqs. (3.5) and (3.6) respectively throughout the entire concentration range from x_1= 0.1 to 0.9. The values of activities have been slightly adjusted only to calculate the mole fraction of the complex (Lele & Ramchandrarao, 1981). The values of interaction energy parameters and equilibrium constant so obtained are slightly accommodated using the expression for free energy of mixing (Eq. (3.18)) and the experimental values of free energy of mixing. The optimized values of these model parameters are determined by the above mentioned procedure (Section 4.4.1). The optimized values of the parameters for Al–Mg liquid alloy at 1073 K are found to be

ω_{12}= -6253.57 Jmol^{-1}, ω_{13}= 30687.97 Jmol^{-1}, ω_{23}= 16682.12 J mol^{-1} and k = 0055

The interaction energy ω_{12} is negative which indicates that there appears attraction between free monomers Al and Mg. Whereas the values of ω_{13} and ω_{23} are positive which indicate that there appear repulsion between the free monomers and the complex Al_3Mg_2 in the liquid mixture.

The computed values of mole fraction of complex x_{Al-Mg} as a function of concentration of Al–Mg liquid alloy at 1873 K are tabulated in Table 4.4. Also the theoretically computed values of G_M/RT along with the experimental values as a function of concentration are presented in Table 4.4. The compositional dependence of mole fractions x_{Al}, x_{Mg} and x_{Al-Mg} of the alloy are plotted in Fig. 4.4(a). Both the theoretical and experimental values of G_M/RT versus x_1 of the alloy are imaged in Fig. 4.4(b).

Table 4.4: x_{Al-Mg} and G_M/RT for Al–Mg liquid alloy at 1073 K

Concentration of Al (x_1)	Mole fraction of complex (x_{Al-Mg})	Free energy of mixing (G_M/RT)	
		Theoretical	Experimental**
0.1	0.0031	-0.3911	-0.3894
0.2	0.0148	-0.6305	-0.6288
0.3	0.0362	-0.8040	-0.7998
0.4	0.0707	-0.9233	-0.9132
0.5	0.1532	-0.9877	-0.9709
0.6*	0.1644	-0.9621	-0.9676
0.7	0.0553	-0.8344	-0.8940
0.8	0.0247	-0.6515	-0.7375
0.9	0.0104	-0.4001	-0.4714

*Compound forming concentration
**Hultgren *et al*. (1973)

The plot of compositional dependence of mole fractions of various species show that the maximum association occurs at 57 at. % of Al which is close to the compound formation concentration which is at x_1 = 0.6. At this composition about 18 mol % of the liquid alloy is associated. Fig. 4.4(a) shows that the concentration of mole fraction of the complex decreases rapidly on either sides of the peak value. As expected, the concentration of unassociated atoms of Mg is maximum at lower concentration of Al whereas decreases rapidly with the increase in the concentration of Al. Likewise, the concentration of unassociated atoms of Al is maximum at lower concentration of Mg and declines rapidly at higher concentrations of Mg.

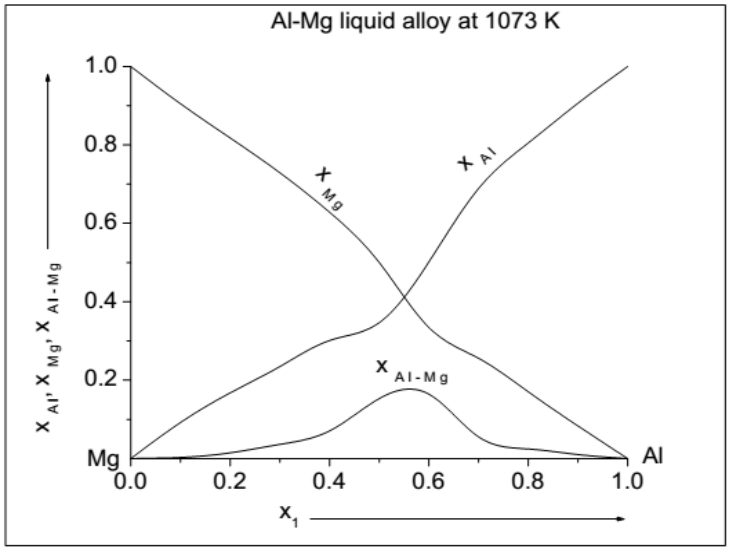

Figure 4.4(a): Plot of mole fractions of free monomers (x_{Al} and x_{Mg}) and the complex (x_{Al-Mg}) versus concentration of Al (x_1) of Al–Mg liquid alloy at 1073 K.

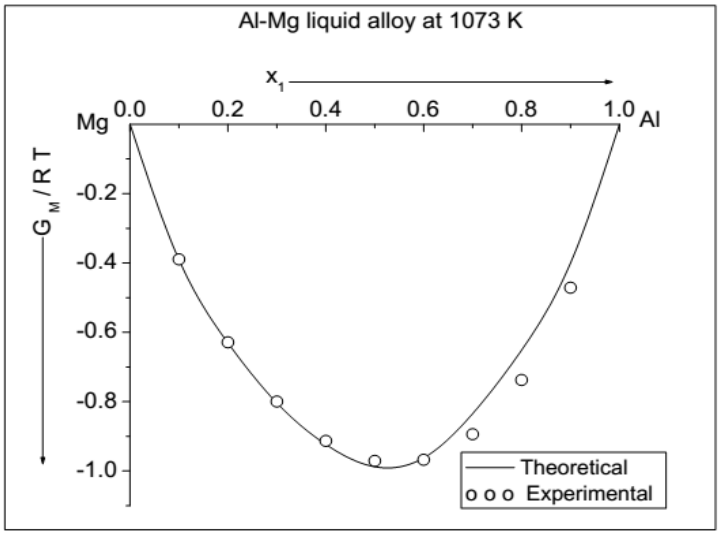

Figure 4.4(b): Plot of G_M/RT versus concentration of Al (x_1) of Al–Mg liquid alloy at 1073 K.

Theoretical investigations show that the minimum value of free energy of mixing is -0.9709 RT at x_1= 0.5 of the preferred alloy at 1073 K. This reveals that the system is symmetric in G_M. Moreover, the computed values of G_M^{XS} (= -0.2778 RT) at this concentration and temperature which corresponds that the preferred system is moderately interacting and hence the affinity towards the compound formation is moderate. It can be

observed from Fig. 4.4(b) that the theoretical and experimental values of free energy of mixing are in good agreement. The symmetricity in G_M is well explained by regular associated solution model.

4.5 Activity of binary liquid alloys

Activity is an important thermodynamic quantity and any deviation of the liquid alloy can be incorporated into it. The interaction among the constituent species of the liquid alloy, which in turn determine the bond energies can be interpreted on the fundamentals of magnitudes of activities. The details of theory containing basic formulations and working expressions for activity have been already presented in the Sections 3.2.1.4 and 3.3.1.4 of the Chapter 3. In this section, we present the procedures to estimate the activities and results so obtained along with discussion for some binary liquid alloys on the basis of regular associated solution model. The activities of Bi−Tl, In−Bi, Al−Fe and Al−Mg liquid alloys have been computed by employing the preferred model.

4.6 Results for Bi−Tl, In−Bi, Al−Fe and Al−Mg liquid alloys

The theoretically computed values of activities of the constituent species of Bi−Tl, In−Bi, Al−Fe and Al−Mg liquid alloys as a function of concentration have been presented in the following sections.

4.6.1 Activities of Bi (a_{Bi}) and Tl (a_{Tl}) for Bi-Tl liquid alloy at 750 K

The activities of constituent species which are Bi (a_{Bi}) and Tl (a_{Tl}) of the preferred system have been computed from Eqs. (3.71a) and (3.71b) respectively. The input parameters to compute the activity are the mole fractions of complex (x_{Bi-Tl}) and free monomers Bi (x_{Bi}) and Tl (x_{Tl}) along with the pairwise interaction energies. To maintain consistency, we have used the same values of above mentioned parameters as used to compute free energy of mixing in the Section 4.4.1. Theoretically computed values of activities of Bi and Tl along with their experimental values in the entire range as a

function of concentration of Tl (x_1) are presented in Table 4.5. The theoretical and experimental values of activities of Bi and Tl as a function of concentration for Bi–Tl liquid alloy are imaged in Fig. 4.5.

Table 4.5: Activities of Bi (a_{Bi}) and Tl (a_{Tl}) of Bi–Tl liquid alloy at 750 K

Concentration of Tl (x_1)	Activity of Tl (a_{Tl})		Activity of Bi (a_{Bi})	
	Theoretical	Experimental**	Theoretical	Experimental**
0.1	0.0184	0.018	0.8947	0.911
0.2	0.0343	0.034	0.7754	0.811
0.3	0.0570	0.058	0.6404	0.677
0.4	0.0965	0.1	0.4928	0.505
0.5*	0.1635	0.17	0.3378	0.326
0.6	0.2762	0.283	0.1909	0.175
0.7	0.4423	0.447	0.0735	0.075
0.8	0.6625	0.669	0.0183	0.022
0.9	0.8682	0.87	0.0090	0.005

*Compound forming concentration
**Hultgren *et al*. (1973)

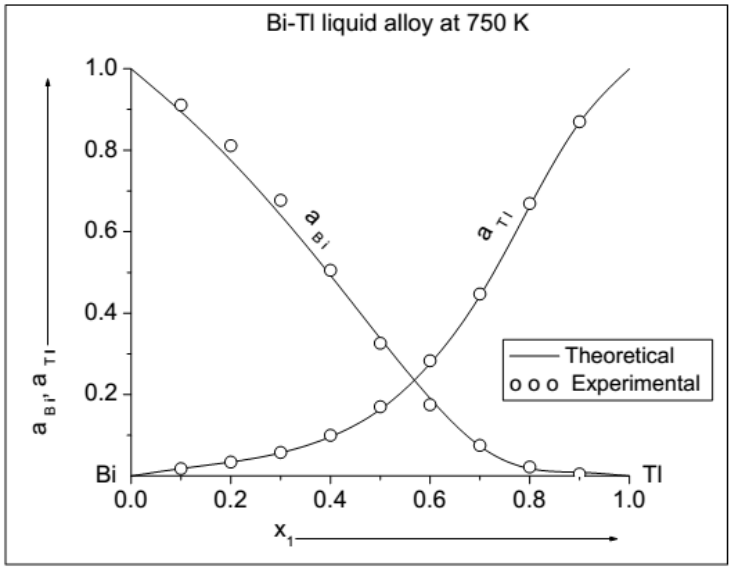

Figure 4.5: Activities of Bi (a_{Bi}) and Tl (a_{Tl}) versus of concentration of Tl (x_1) of Bi–Tl liquid alloy at 750 K.

Both the theoretical and experimental values of activities of unassociated species (Bi and Tl) are in well agreement throughout the entire concentration (Figure 4.5). The activity of Tl has quite lower values in the concentration range $x_1 \leq 0.4$ but increases rapidly in rest of the concentration i.e., $x_1 \geq 0.4$. The activity of Bi also remains quite small in the

concentration range $x_1 \geq 0.8$ but increases rapidly in the concentration range $x_1 \leq 0.7$. As expected, the activity of Bi has small values at lower concentration of Bi and increases with the increase in the concentration of Bi. Similarly, the activity of Tl has small values at lower concentration of Tl and increases with increase in concentration of Tl.

4.6.2 Activities of In (a_{In}) and Bi (a_{Bi}) for In−Bi liquid alloy at 900 K

The activities of unassociated species In and Bi of In−Bi liquid alloy are calculated from Eqs. (3.71a) and (3.71b) respectively. The essential input parameters, such as mole fraction of the complex and free monomers, and interaction energies required to compute the activity are taken from Table 4.2 and the Section 4.4.2 respectively. The mole fractions of Tl and Bi are evaluated using Eqs. (3.63a) and (3.63b). To maintain consistency, the same input ingredients were taken to compute activity as those for free energy of mixing. The computed and observed values of a_{In} and a_{Bi} as a function of concentration is depicted in Table 4.6 and are portrayed in Fig. 4.6.

Table 4.6: Activities of In (a_{In}) and Bi (a_{Bi}) of In−Bi liquid alloy at 900 K

Concentration of In (x_1)	Activity of In (a_{In})		Activity of Bi (a_{Bi})	
	Theoretical	Experimental**	Theoretical	Experimental**
0.1	0.0498	0.05	0.8999	0.903
0.2	0.1030	0.105	0.7954	0.794
0.3	0.1677	0.173	0.6809	0.674
0.4	0.2489	0.259	0.5567	0.542
0.5	0.3523	0.366	0.4271	0.409
0.6	0.4743	0.490	0.3014	0.286
0.66*	0.5555	…….	0.2328	…….
0.7	0.6113	0.626	0.1892	0.181
0.8	0.7488	0.764	0.0945	0.099
0.9	0.8891	0.891	0.0426	0.041

*Compound forming concentration
**Hultgren *et al*. (1973)

The theoretical and experimental values of activities of both the monomers In and Bi are in excellent agreement (Fig. 4.6). As expected, the activity of In as a function of concentration is small at lower concentration of In, however, increases with the increase in concentration of In. Likewise, the activity of Bi has small values as lower concentration of Bi but increases as the concentration of Bi increases. It can be thus

concluded that the model parameters of regular associated solution model have well reproduced the activity of In−Bi liquid alloy.

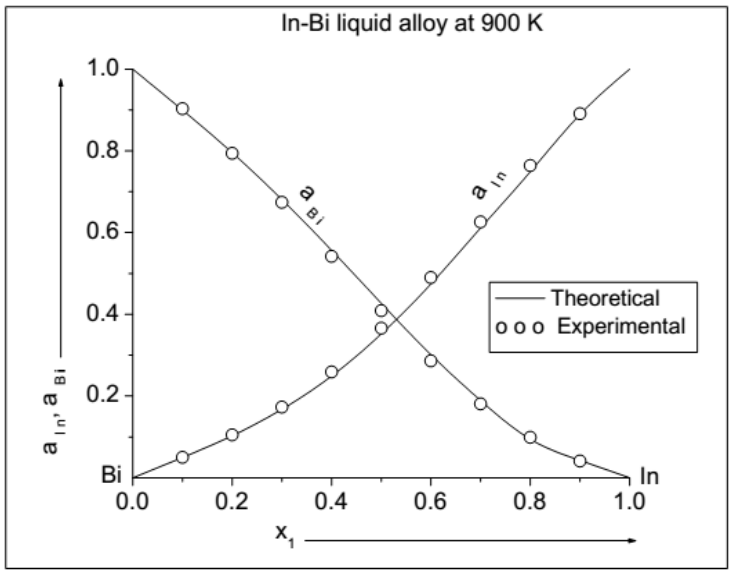

Figure 4.6: Activities of unassociated species In (a_{In}) and Bi (a_{Bi}) versus concentration of In (x_1) of In−Bi liquid alloy at 900 K.

4.6.3 Activities of Al (a_{Al}) and Fe (a_{Fe}) for Al−Fe liquid alloy at 1873 K

The activities of Al and Fe of Al−Fe liquid alloy have been evaluated using Eqs. (3.71a) and (3.71b) with the aid of determined values of model parameters in Table 4.3 and the Section 4.4.3. The mole fractions of Al and Fe are estimated following the similar procedure as mentioned in the Section 4.6.2. The computed as well as the experimental values of activities of Al and Fe as a function of concentration for the concerned system are tabulated in Table 4.7. The plots of compositional dependence of the theoretical and experimental values of a_{Al} and a_{Fe} are portrayed in Fig. 4.7.

There is excellent agreement between the computed and experimental values of activities of both species Al and Fe of the concerned system (Fig. 4.7). The activity of Al has quite small value in the concentration range $x_1 \leq 0.2$ but it increases rapidly in the concentration range $x_1 \geq 0.3$. Also the activity of Fe has quite small value in the

concentration range $x_1 \geq 0.8$, however, it increases rapidly in the concentration range $x_1 \leq 0.7$. The activities of both the species have smaller values at their low concentrations and increases with increase in their respective concentration.

Table 4.7: Activities of Al (a_{Al}) and Fe (a_{Fe}) of Al−Fe liquid alloy at 1873 K

Concentration of Al (x_1)	Activity of Al (a_{Al})		Activity of Fe (a_{Fe})	
	Theoretical	Experimental**	Theoretical	Experimental**
0.1	0.0089	0.009	0.8792	0.877
0.2	0.0274	0.028	0.7288	0.719
0.3	0.0638	0.064	0.5592	0.550
0.4	0.1216	0.122	0.4003	0.388
0.5	0.2115	0.209	0.2585	0.250
0.6	0.3403	0.331	0.1460	0.142
0.7	0.5076	0.488	0.0685	0.069
0.75*	0.6017	……..	0.0428	……..
0.8	0.6971	0.673	0.0246	0.026
0.9	0.8684	0.859	0.0047	0.006

*Compound forming concentration
**Hultgren *et al*. (1973)

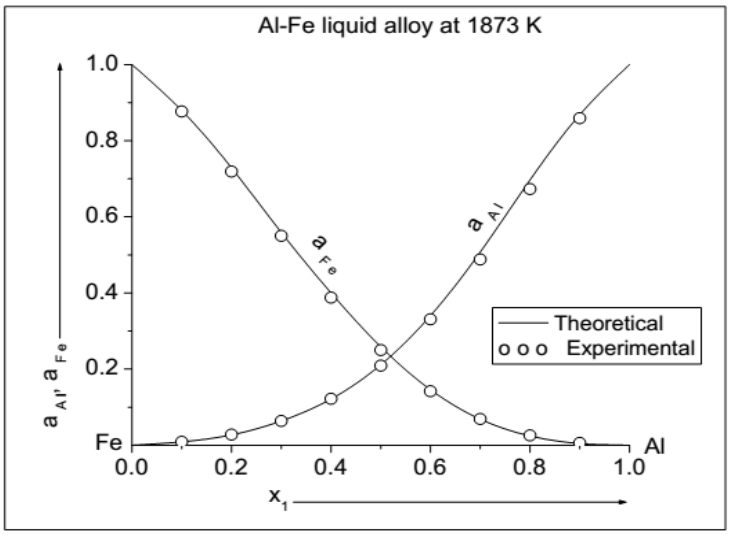

Figure 4.7: Activities of unassociated species Al (a_{Al}) and Fe (a_{Fe}) versus concentration of Al (x_1) of Al−Fe liquid alloy at 1873 K.

4.6.4 Activities of Al (a_{Al}) and Fe (a_{Mg}) for Al−Mg liquid alloy at 1073 K

The activities of unassociated atoms of Al and Mg in Al−Mg liquid alloy as a function of concentration have been computed from Eqs. (3.36) and (3.38) respectively. For such

purpose, the values of mole fraction of complex x_{Al-Mg} (Al_3Mg_2) and interaction energies have been inherited from Table 4.4 and Section 4.4.4. The mole fractions of Al and Mg have been computed from Eqs. (3.5) and (3.6), respectively. The computed values of activity of Al and Mg as function of concentration of Al–Mg system are presented in Table 8.8. The plots of compositional dependence of a_{Al} and a_{Mg} of the concerned system are imaged in Fig. 4.8.

Table 4.8: Activities of Al (a_{Al}) and Mg (a_{Mg}) of Al–Mg liquid alloy at 1073 K

Concentration of Al (x_1)	Activity of Al (a_{Al})		Activity of Mg (a_{Mg})	
	Theoretical	Experimental**	Theoretical	Experimental**
0.1	0.0520	0.052	0.8990	0.9
0.2	0.1060	0.106	0.7976	0.798
0.3	0.1663	0.166	0.6896	0.687
0.4	0.2414	0.239	0.5671	0.565
0.5	0.3372	0.329	0.4256	0.435
0.6*	0.5336	0.439	0.2445	0.305
0.7	0.6733	0.572	0.1691	0.187
0.8	0.7933	0.72	0.1035	0.093
0.9	0.9043	0.874	0.0451	0.03

*Compound forming concentration
**Hultgren *et al*. (1973)

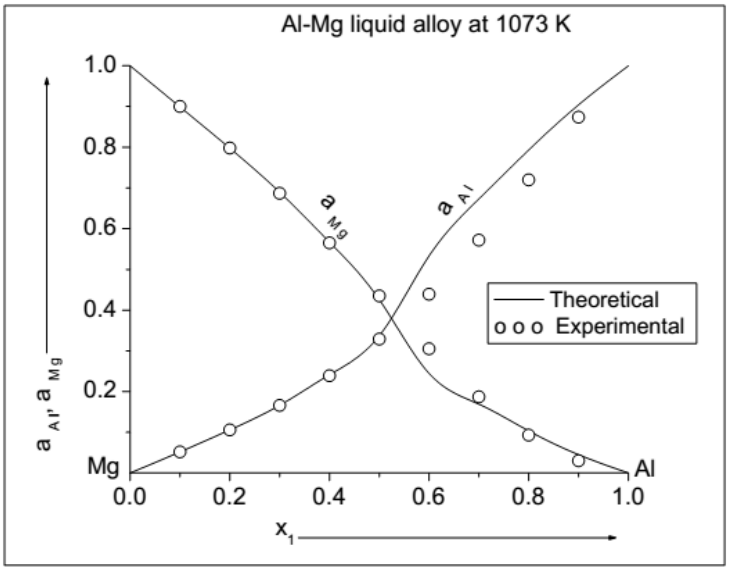

Figure 4.8: Activities of unassociated species Al (a_{Al}) and Mg (a_{Mg}) versus concentration of Al (x_1) of Al–Mg liquid alloy at 1073 K.

Fig. 4.8 shows that there is slight deviation between the compositional dependence of computed and the experimental values of the activity of Mg at the concentration $x_1 = 0.6$, where 1 is for Al. In the rest of the concentration range, both the theoretical and experimental values of the activity of Mg as a function of concentration are in well agreement. Moreover, there is slight disagreement between compositional dependence of the computed and observed values of the activity of Al in the concentration range $0.6 \leq x_1 \leq 0.9$. However, both of these values are in well agreement in the rest of the concentration range. As one aspect, the activity of Al has small values at lower concentration of Al and increases with increase in concentration of Al. Similar variation is also observed for the activity of Mg.

4.7 Heat of mixing of binary liquid alloys

It has been already mentioned that the heat of mixing is important thermodynamic function to understand the nature and extent of bonding between the constituents atoms of liquid alloys. The knowledge of the heat of mixing plays significant role in materials processing, design and characterization to obtained the desired characteristics. The details of fundamentals expressions and methodology to obtain the working expression for the heat of mixing of binary liquid alloys in reference frame of regular associated solution model have been mentioned in the Sections 3.2.1.5 and 3.3.1.5 of the former Chapter 3. In the former portion of this section, we highlight few efforts made by several researchers to study the heat of mixing of binary alloys. In the later portion, we present the computed results of the heat of mixing for Bi−Tl, In−Bi, Al−Fe and Al−Mg liquid alloys and compare it with the experimental values. Additionally, we have also computed and presented the results of the compositional contributions of the heat associated with the formation of complexes and the heat of mixing of the monomers to the net enthalpy change of the corresponding liquid alloys.

Several researchers in the field of material science and engineering have been working since decades to contrive a simple theory to compute the compositional dependence of the heat of mixing of binary alloys. Much advancement has been made in recent years due to evolution of computer−assisted techniques to compute the thermodynamics of binary as

well as multicomponent systems. Among them, Miedema's theory (Miedema et al., 1980; Miedema et al., 1981; Ouyang, et al., 1996; Bakker, 1998) has been employed to compute the heat of mixing of the most of the binary alloys. The compositional dependence of the integral heat of mixing of liquid alloys can be contemptly computed using Hoch–Arpshofen model (Hoch & Arpshofen, 1984). Hafner (1977) and Singh (1984) computed the heat of mixing of binary liquid alloys employing pseudopotential theory. Later association model was devised by Sommer (1982) and is suitable for a large number of liquid alloys. The enthalpy of mixing of several binary liquid alloys has been computed on the basis of the molecular interaction volume model (Yang et al., 2008). In this work, we intend to apply regular associated solution model to compute the heat of mixing of some binary liquid alloys.

4.7.1 Computation of input parameters

From Eqs. (3.41) and (3.73), it can be observed that the essential input parameters in order to compute the heat of mixing are mole fractions of components of liquid mixture (x_A, x_B and $x_{A_\mu B_\nu}$), pairwise interaction energies (ω_{12}, ω_{13} and ω_{23}), temperature derivative terms of pairwise interaction energies ($\partial\omega_{12}/\partial T$, $\partial\omega_{13}/\partial T$ and $\partial\omega_{23}/\partial T$) and the heat of dissociation ($RT^2 d\ln k/dT$). As stated earlier, we have used the same values of mole fractions and interaction energy parameters as used to compute free energy of mixing and activity to maintain consistency. The temperature derivative terms of interaction energy parameters and the heat of dissociation are evaluated using Eqs. (3.41) and (3.73) depending upon the type of complex formed in the corresponding alloys with the aid of determined values of mole fractions and interaction energies. The optimized values of model parameters so obtained to explain free energy of mixing and activity must also explain the heat of mixing of the liquid alloys.

4.8 Results for Bi–Tl, In–Bi, Al–Fe and Al–Mg liquid alloys

Now we present the computed results of the heat of mixing (H_M) for Bi–Tl, In–Bi, Al–Fe and Al–Mg liquid alloys**.** The theoretical values have been compared with their respective

experimental values to test the validity of the preferred statistical model. Additionally, the computed results of the compositional contributions of the heat associated with the formation of the complex and the heat of mixing of the monomers to the net enthalpy change of the concerned liquid alloys have also been presented in this section.

4.8.1 Heat of mixing (H_M) for Bi–Tl liquid alloy at 750 K

The compositional dependence of heat of mixing for Bi–Tl liquid alloy at 750 K has been computed using Eq. (3.73). Among the required essential input parameters, the equilibrium values of mole fraction of the complex and interaction energies as a function of concentration has been inherited from the Table 4.1 and Section 4.4.1 respectively. The mole fractions of free monomers Bi and Tl as a function of concentration are then estimated from Eqs. (3.63) with the knowledge of mole fraction of the complex (Table 4.1). The other input parameters, such as temperature derivative terms of pairwise interaction energies and the heat of dissociation are determined by using the expression for the heat of mixing form Eq. (3.73) with the assistance of experimental values of the heat of mixing, and the mole fractions of different species and interaction energies. For this purpose, we have employed the procedure of successive approximation from the programming in Microsoft Office Excel 2007. The optimized values of the temperature derivative terms of interaction energies and the heat of dissociation for the concerned system are found to be (Yadav et al., 2015)

$\frac{\partial \omega_{12}}{\partial T} = +7.64$ J mol^{-1}K^{-1}, $\frac{\partial \omega_{13}}{\partial T} = -0.890$ J mol^{-1}K^{-1}, $\frac{\partial \omega_{23}}{\partial T} = +1.01$ J mol^{-1}K^{-1} and

$RT^2 \frac{d \ln K}{dT} = 8050 \pm 950$ J mol^{-1}

All the temperature derivative terms of interaction energy parameters have finite values. It can be concluded that the pairwise interaction energy ω_{12} which represents the interaction between the unassociated atoms of Tl and Bi in the initial melt depends considerably on temperature. Moreover, ω_{13} representing the interaction between the unassociated atoms of Tl and the complex BiTl in the liquid mixture also considerably

depends upon temperature. Likewise, ω_{23} representing the interaction between the unassociated atoms of Bi and the complex also considerably depends upon temperature.

The theoretical value of H_M/RT obtained from Eq. (3.73) and its experimental values as a function of concentration are tabulated in Table 4.9. Both the theoretical and the experimental values of H_M/RT as a function of concentration are plotted in Fig. 4.9(a). Additionally, we have also computed the compositional contributions of the heat associated with the formation of complex and the heat of mixing of the species Tl, Bi and the complex BiTl to the net enthalpy change of the system (Osamura & Predel, 1977; Lele and Ramchandrarao, 1981; Yadav et al. 2016). The plot of contributions as function of concentration is portrayed in the Fig. 4.9(b).

Table 4.9: H_M/RT for Bi−Tl liquid alloy at 750 K

Concentration of Tl (x_{Tl})	H_M/RT	
	Theoretical	Experimental**
0.1	-0.1778	-0.1823
0.2	-0.3439	-0.3426
0.3	-0.4689	-0.4693
0.4	-0.5692	-0.5758
0.5*	-0.6731	-0.6844
0.6	-0.7283	-0.7327
0.7	-0.6904	-0.6925
0.8	-0.5534	-0.5564
0.9	-0.3202	-0.3204

*Compound forming concentration
**Hultgren *et al*. (1973)

The theoretical and the experimental values of H_M/RT as a function of concentration for Bi−Tl liquid alloy are in excellent agreement (Fig. 4.9(a)). The heat of mixing of the concerned alloy is found to have negative values at all concentrations. The minimum values of both of the heat of mixing H_M are found to be at x_1= 0.6, where the theoretical value is -0.7283 RT and the experimental value is -0.7327 RT (Hultgren *et al*., 1973). Thus the Bi−Tl liquid alloy is asymmetric in H_M and this behaviour has been well explained by regular associated solution model. Further, the contribution from the complex formation term is the maximum at 59.32 at. % of Tl and the mixing of species Tl, Bi and BiTl contributes the maximum at 64.41 at. % of Tl. As a result of which the net enthalpy change shows absolute maximum at 61.02 at. % of Tl, Fig. 4.9(b).

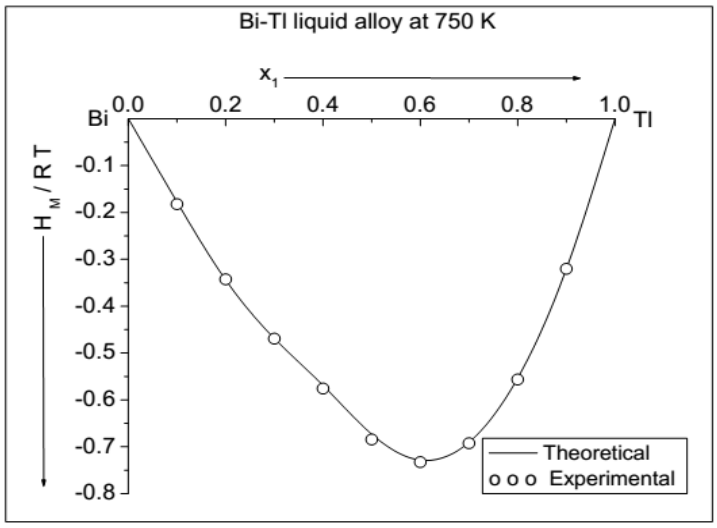

Figure 4.9(a): Heat of mixing (H_M/RT) versus concentration of Tl (x_1) of Bi−Tl liquid alloy at 750 K.

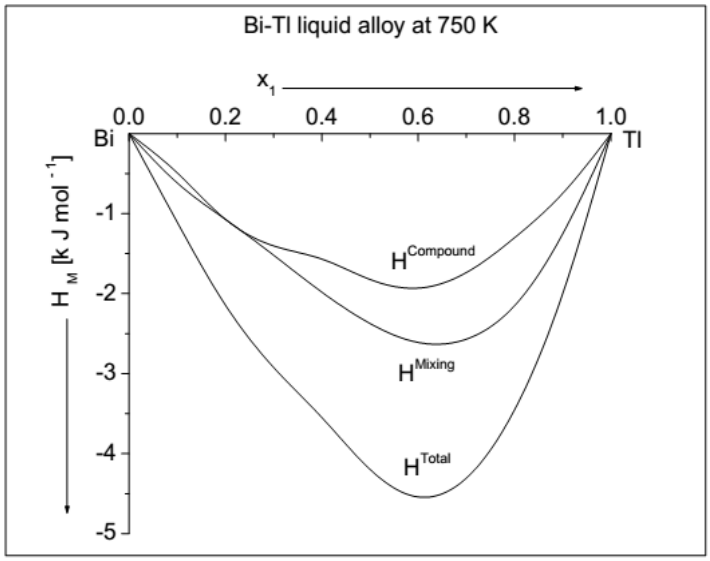

Figure 4.9(b): Compositional contributions of the heat associated with formation of complex and the mixing of species to the net enthalpy change versus x_1 of Bi−Tl liquid alloy at 750 K**.**

4.8.2 Heat of mixing (H_M) for In−Bi liquid alloy at 900 K

The heat of mixing for In−Bi liquid alloy at 900 K as a function of concentration has been computed using Eq. (3.73). The compositional dependence of mole fraction of In_2Bi

complex and interaction energy parameters required to compute H_M have been taken from the Table 4.2 and the Section 4.4.2 respectively. The mole fractions of the free species In and Bi have been evaluated using Eq. (3.62). The temperature terms of interaction energy parameters are then estimated using the expression for H_M (Eq. (3.73)) and the observed values of H_M (Hultgren *et al.*, 1973) following the procedure as mentioned in the Section 4.8.1.

Table 4.10: H_M/RT for In−Bi liquid alloy at 900 K

Concentration of In (x_{In})	H_M/RT	
	Theoretical	Experimental**
0.1	-0.0740	-0.0726
0.2	-0.1349	-0.1330
0.3	-0.1841	-0.1816
0.4	-0.2202	-0.2207
0.5	-0.2422	-0.2441
0.6	-0.2431	-0.2452
0.66*	-0.2327	……
0.7	-0.2188	-0.2134
0.8	-0.1608	-0.1575
0.9	-0.0890	-0.0832

*Compound forming concentration
**Hultgren *et al*. (1973)

The optimized values of temperature derivative terms of interaction energy parameters for the concerned system so obtained are found to be (Yadav et al., 2015)

$\frac{\partial \omega_{12}}{\partial T} = +1.10$ J mol^{-1}K^{-1}, $\frac{\partial \omega_{13}}{\partial T} = +3.10$ J mol^{-1}K^{-1}, $\frac{\partial \omega_{23}}{\partial T} = +0.910$ J mol^{-1}K^{-1} and

$RT^2 \frac{d \ln K}{dT} = 5000 \pm 650$ J mol^{-1}

Theoretical investigations thus clarify that these temperature derivative terms of interaction energy parameters considerably depend upon temperature of the preferred alloy. The computed and the observed values of H_M/RT as a function of concentration are tabulated in Table 4.10. The plots of the theoretical and the experimental values of H_M/RT as a function of concentration for the In−Bi liquid alloy at 900 K are portrayed in Fig. 4.10(a). We have also computed the compositional contributions of the heat associated with formation of In_2Bi complex and the heat of mixing of species In, Bi and

the complex In_2Bi to the total enthalpy change for the concerned system. The above mentioned values as a function of concentration are plotted in Fig. 4.10(b).

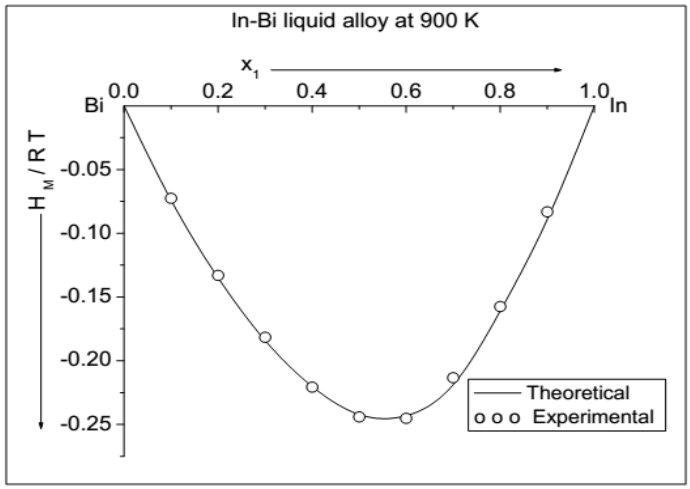

Figure 4.10(a): Heat of mixing (H_M/RT) versus concentration of In (x_1)for In−Bi liquid alloy at 900 K.

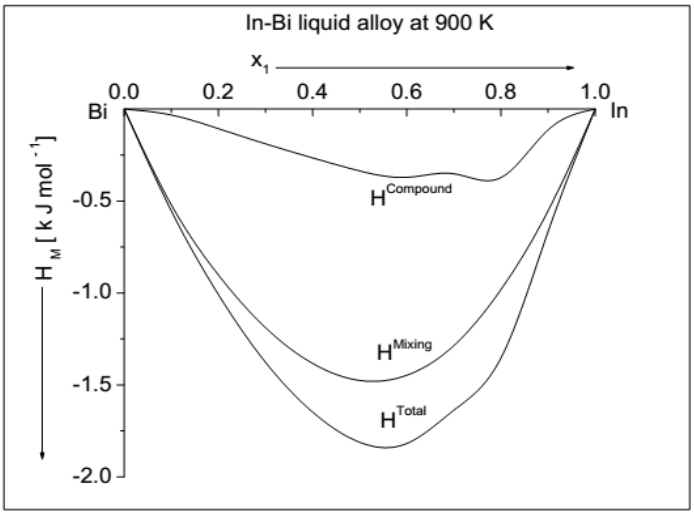

Figure 4.10(b): The compositional contribution from the heat associated with formation of complex and the heat of mixing of species to the net enthalpy change versus concentration of In (x_1) for In−Bi liquid alloy at 900 K.

The computed and the experimental values of H_M/RT as a function of concentration have the minimum values at x_1= 0.6, where the theoretical value of H_M/RT is found to be -0.2454 RT and the experimental value of H_M/RT is found to be -0.2484 RT. Fig. 4.10(a) shows that both the theoretical and the experimental values of H_M/RT as a function of

concentration are in excellent agreement throughout the entire concentration. This asymmetry in the heat of mixing of In−Bi liquid alloy at 900 K has been well explained by regular associated solution model. From Fig. 4.10(b), it can be observed that the contribution from the complex formation term is the maximum at 76.27 at. % of In and the mixing of species In, Bi and In_2Bi terms contributes the maximum at 52.54 at. % of In. As a result, the net enthalpy change shows the absolute maximum at 55.90 at. % In in the In−Bi liquid alloy at 900 K.

4.8.3 Heat of mixing (H_M) for Al−Fe liquid alloy at 1873 K

Eq. (3.73) has been used to compute compositional heat of mixing of the concerned alloy in liquid stated at stipulated temperature as a function of concentration. The essential ingredients, such as mole fraction of Al_3Fe complex and interaction energy parameters have been inherited from the Table 4.3 and the Section 4.4.3 respectively. The mole fraction of unassociated species Al and Fe as a function of concentration have been computed from Eq. (3.63). The temperature derivative of the interaction energy parameters are then estimated using Eq. (3.73) in order to explain the experimental value of the heat of mixing following the same methodology as stated in the Section 4.8.2. The optimized values of these parameters so obtained for Al−Fe liquid alloy at 1873 K are found to be (Adhikari et al., 2014)

$$\frac{\partial\omega_{12}}{\partial T} = +11.70 \text{ J mol}^{-1}\text{K}^{-1},\ \frac{\partial\omega_{13}}{\partial T} = -21.00 \text{ J mol}^{-1}\text{K}^{-1},\ \frac{\partial\omega_{23}}{\partial T} = +21.70 \text{ J mol}^{-1}\text{K}^{-1} \text{ and}$$

$$RT^2\frac{d\ln K}{dT} = 106900 \pm 3000 \text{ J mol}^{-1}$$

This shows that all the temperature derivative terms of interaction energies have finite values and hence the interaction energy parameters considerably depend on temperature of the concerned liquid alloy.

Theoretically computed values of H_M/RT along with the experimental values as a function of concentration are presented in Table 4.11. The plots both of these values are

portrayed in Fig. 4.11(a). We have also computed the compositional contributions of the heat associated with the formation of Al_3Fe and the heat associated with mixing of species Al, Fe and the complex Al_3Fe to the net enthalpy change of the concerned alloy at stipulated temperature. These values so obtained versus concentration of Al (x_1) are plotted in Fig. 4.11(b).

Table 4.11: H_M/RT for Al–Fe liquid alloy at 1873 K

Concentration of Al (x_{Al})	H_M/RT	
	Theoretical	Experimental**
0.1	-0.3946	-0.3872
0.2	-0.7196	-0.7170
0.3	-0.9590	-0.9803
0.4	-1.1385	-1.1672
0.5	-1.2345	-1.2474
0.6	-1.2390	-1.2677
0.7	-1.1349	-1.1557
0.75*	-1.0310	……..
0.8	-0.8976	-0.9177
0.9	-0.5396	-0.5390

*Compound forming concentration
**Hultgren *et al*. (1973)

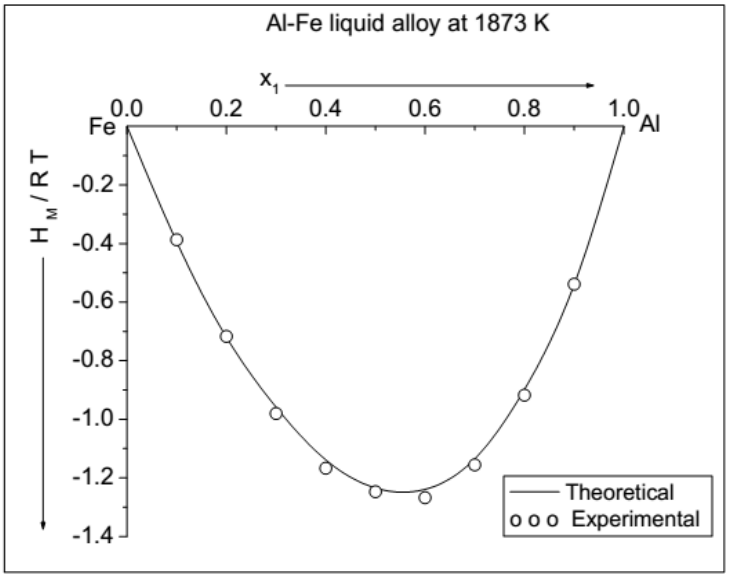

Figure 4.11(a): Heat of mixing (H_M/RT) versus concentration of Al (x_1) for Al–Fe liquid alloy at 1873 K.

It can be observed from Fig. 4.11(a) that both the theoretical and the experimental values of H_M/RT are in well agreement. Theoretical investigations shows that the computed

value of H_M/RT as a function of concentration has minimum value (= -1.2489 RT) at x_1= 0.56 which is in accordance with the experimental value (= -1.2707 RT) (Hultgren *et al.*, 1973). Thus it can be stated that the model fitting parameters of regular associated solution model obtained theoretically have not only explained free energy of mixing and the activity of the concerned system but also have successfully yielded the heat of mixing. The preferred theoretical model is fruitful in explaining the heat of mixing of Al–Fe liquid alloy at 1873 K. Additionally, Fig. 4.11(b) shows that the contribution from the complex formation term is the maximum at 84.75 at. % of Al and the heat of mixing of species Al, Fe and Al_3Fe term contribute the maximum at 49.15 at. % of Al. As the consequence of which the net enthalpy change shows the absolute maximum at about 55.93 at. % of Al in the concerned system.

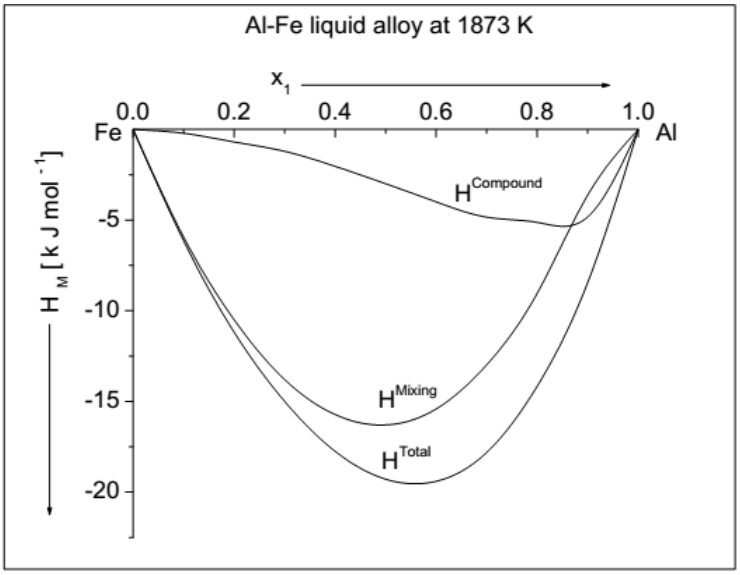

Figure 4.11(b): The compositional contribution from the heat associated with formation of complex and the heat of mixing of species to the net enthalpy change versus x_1 for Al–Fe liquid alloy at 1873 K.

4.8.4 Heat of mixing (H_M) for Al–Mg liquid alloy at 1073 K

In Al–Mg liquid alloy, we have assumed the formation of the complex Al_3Mg_2 of the type $A_\mu B_\nu$. Therefore, the heat of mixing of the alloy is computed using Eq. (3.41) with

the aid of mole fraction of the complex and interaction energy parameters taken respectively from the Table 4.4 and the Section 4.4.4. The temperature derivative terms of interaction energy parameters are estimated from Eq. (3.41) with the help of experimental value of the heat of mixing by successive approximation employing the procedure mentioned in the Section 4.8.1. The optimized values of the temperature derivative terms of interaction energies for the concerned alloy at stipulated temperature are found to be

$\frac{\partial\omega_{12}}{\partial T} = +5.44$ J mol^{-1}K^{-1}, $\frac{\partial\omega_{13}}{\partial T} = +23.0$ J mol^{-1}K^{-1}, $\frac{\partial\omega_{23}}{\partial T} = +9.67$ J mol^{-1}K^{-1} and

$RT^2 \frac{d \ln K}{dT} = 30000 \pm 1850$ J mol^{-1}

The aforementioned values of temperature derivative terms of pairwise interaction energy parameters clarify that they are strongly temperature dependent.

Theoretically computed values of H_M/RT as a function of concentration along with the experimental values are furnished in Table 4.12. The compositional dependence of the theoretical and the experimental values of H_M/RT versus the concentration of Al (x_1) are plotted in Fig. 4.12(a). The computed values of the compositional contributions from the heat associated with the formation of Al_3Mg_2 complex and the heat associated with the mixing of species Al, Mg and Al_3Mg_2 to the net enthalpy change as a function of concentration for the alloy are plotted in Fig. 4.12(b).

Table 4.12: H_M/RT for Al–Mg liquid alloy at 1073 K

Concentration of Al (x_{Al})	H_M/RT	
	Theoretical	Experimental**
0.1	-0.1192	-0.1078
0.2	-0.2126	-0.2057
0.3	-0.2913	-0.2877
0.4	-0.3557	-0.3467
0.5	-0.3988	-0.3777
0.6*	-0.3914	-0.3763
0.7	-0.3237	-0.3369
0.8	-0.2349	-0.2601
0.9	-0.1274	-0.1462

*Compound forming concentration

**Hultgren *et al*. (1973)

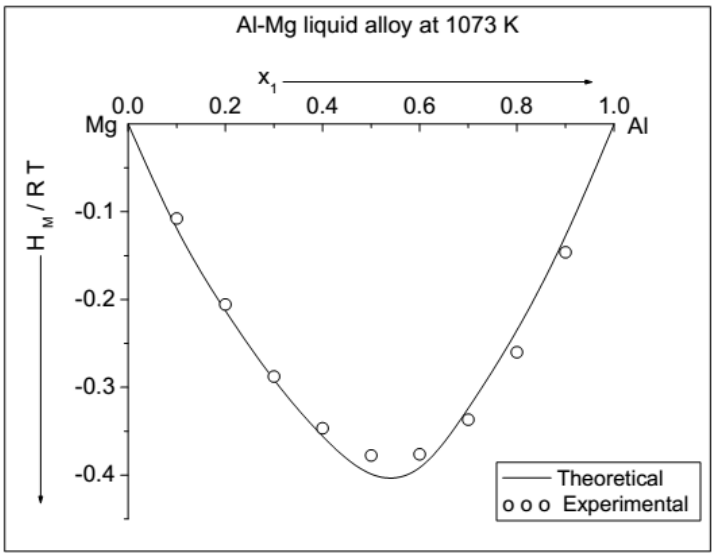

Figure 4.12(a): Heat of mixing (H_M/RT) versus concentration of Al (x_1) for Al–Mg liquid alloy at 1073 K.

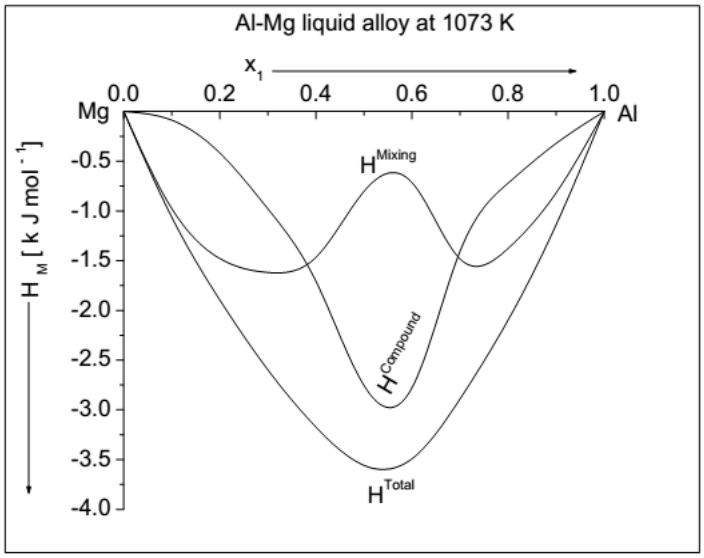

Figure 4.12(b): The compositional contribution from the heat associated with formation of complex and the heat of mixing of species to the net enthalpy change versus x_1 for Al–Mg liquid alloy at 1073 K.

Fig. 4.12(a) shows that both the theoretical and the experimental values of the heat of mixing are in good agreement except at or about equiatomic concentration, where there is slight disagreement between them. Both the theoretical and the experimental values of

H_M/RT are minimum at x_1= 0.54, where 1 is for Al. At this concentration, the theoretical value of H_M/RT is -0.4035 RT and the corresponding experimental value is -0.3814 RT (Hultgren *et al.*, 1973). This low negative value of H_M/RT suggests that the bonding between the species Al and Mg to form the complex Al_3Mg_2 is quite weak. Thus the heat of mixing of the concerned alloy has been well explained by preferred theoretical model. Theoretical investigations also indicate that the compositional contribution from heat associated with the formation of Al_3Mg_2 complex is the maximum at 55.93 at. % of Al. The contribution from the heat associated with the mixing of Al, Mg and the complex Al_3Mg_2 the maximum at 32.20 at. % of Al. As a result, the net enthalpy change shows the absolute maximum at about 54.24 at. % of Al in the Al−Mg liquid alloy at 1073 K, Fig. 4.12(b).

4.9 Entropy of mixing of binary liquid alloys

The study of the entropy of mixing of the binary liquid alloys provides various structural information and helps to analyze the equilibrium state. It has been already mentioned that the entropy are difficult to determine from the experiments and hence the necessity of the theoretical models for its investigations are outmost essential (Saboungi et al., 1990). Eventually, several models so far have been proposed to compute the entropy of binary liquid alloys (Hoshino, 1980; Hoshino & Young, 1980; Khanna & Singh, 1982; Singh & Khanna, 1984; Bhuiyan et al., 2009; Vora, 2010). In this work, we intend to apply the regular associated solution model to study and explain the entropy of mixing of some binary liquid alloys, such as Bi−Tl, In−Bi, Al−Fe and Al−Mg at their respective melting temperatures. The basic expressions required to compute the entropy of mixing of aforementioned systems are derived and presented in Chapter 3.

4.10 Results for Bi−Tl, In−Bi, Al−Fe and Al−Mg liquid alloys

The results for computed values of entropy of mixing as a function of concentration of the concerned systems have been presented in this section. These values are also compared with the experimental values to test the validity of the preferred model.

4.10.1 Entropy of mixing (S_M) for Bi−Tl liquid alloy at 750 K

The entropy of mixing as a function of concentration for Bi−Tl liquid has been computed using Eq. (3.74). For this purpose, we require the model fitting parameters, such as equilibrium values of mole fractions of various species, pairwise interaction energies, equilibrium constant, temperature derivative terms of pairwise interaction energies and the heat of dissociation. The equilibrium values of mole fraction x_{Bi-Tl} of the complex x_{Bi-Tl} are taken from the Table 4.1 and the values of equilibrium constant and pairwise interaction energies are taken from the Section 4.4.1. The mole fractions x_{Bi} and $x_{Tl}$of free monomers are then computed from Eq. (3.63). The values of temperature derivative terms $\partial\omega_{12}/\partial T$, $\partial\omega_{13}/\partial T$ and $\partial\omega_{23}/\partial T$; and the heat of dissociation are taken from the Section 4.8.1. Theoretically computed values of S_M/R along with the experimental values as a function of concentration are tabulated in Table 4.13. The plot of the theoretical and the experimental values of S_M/R versus concentration of Tl (x_1) is portrayed in Fig. 4.13.

Table 4.13: S_M/R for Bi−Tl liquid alloy at 750 K

Concentration of Tl (x_1)	S_M/R	
	Theoretical	Experimental**
0.1	0.3302	0.3037
0.2	0.5084	0.5003
0.3	0.6497	0.6551
0.4	0.7341	0.7531
0.5*	0.7441	0.7592
0.6	0.7081	0.7230
0.7	0.6422	0.6491
0.8	0.5234	0.5284
0.9	0.3331	0.3348

*Compound forming concentration
**Hultgren *et al*. (1973)

The computed values of S_M/R as a function of concentration are in well agreement with the experimental values throughout the entire concentration. Both the theoretical and the experimental values are positive at all compositions. Thus it can be concluded that the Bi−Tl liquid alloy at 750 K is more ordered at lower and higher concentration of Tl. The entropy of mixing of Bi−Tl liquid alloy at 750 K is well explained by the regular associated solution model.

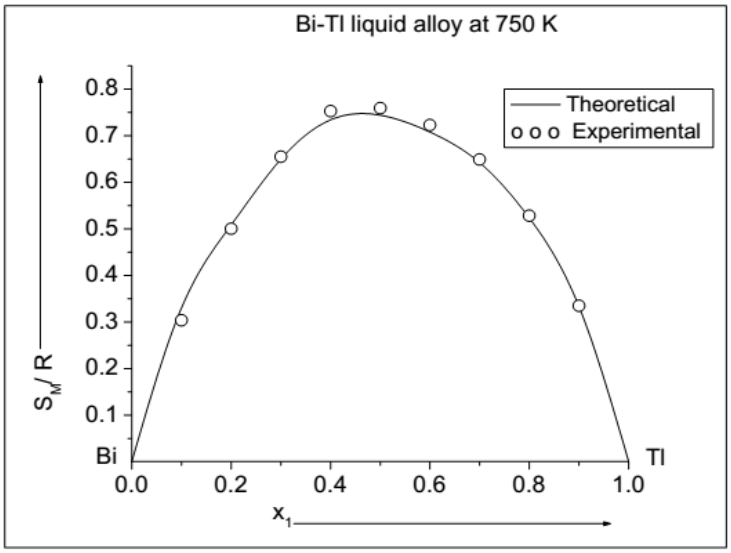

Figure 4.13: Plot of S_M/R versus concentration of Tl (x_1) of Bi−Tl liquid alloy at 750 K.

4.10.2 Entropy of mixing (S_M) for In−Bi liquid alloy at 900 K

Eq. (3.74) has been used to compute the entropy of mixing for the concerned system as a function of concentration. For such computations, the equilibrium values mole fraction of In_2Bi complex are taken from the Table 4.2 and the values of equilibrium constant and pairwise interaction energy parameters are taken from the Section 4.4.2. The mole fractions of unassociated species In and Bi are then obtained from Eq. (3.63). Further, the values of temperature derivative term of interaction energies and the heat of dissociation are inherited from the Section 4.8.2. The computed and the experimental values of S_M/R as a function of concentration are presented in Table 4.14. The plot of the theoretical and experimental values of S_M/R versus concentration of In (x_1) is as shown in Fig. 4.14.

Fig. 4.14 shows that both the computed and the experimental values of S_M/R as a function of concentration are in well agreement at all compositions of the concerned system. Additionally, both of these values are positive at all concentrations of In. Theoretical findings thus indicates that preferred alloy is more ordered at lower and higher concentrations of In. The entropy of mixing of In−Bi liquid alloy at 900 K is well explained by the preferred theoretical model.

Table 4.14: S_M/R for In−Bi liquid alloy at 900 K

Concentration of In (x_1)	S_M/R	
	Theoretical	Experimental**
0.1	0.3173	0.3193
0.2	0.4918	0.5008
0.3	0.6066	0.6199
0.4	0.6762	0.6858
0.5	0.7030	0.7049
0.6	0.6897	0.6828
0.66*	0.6612	……..
0.7	0.6334	0.6259
0.8	0.5318	0.5194
0.9	0.3453	0.3404

*Compound forming concentration
**Hultgren *et al*. (1973)

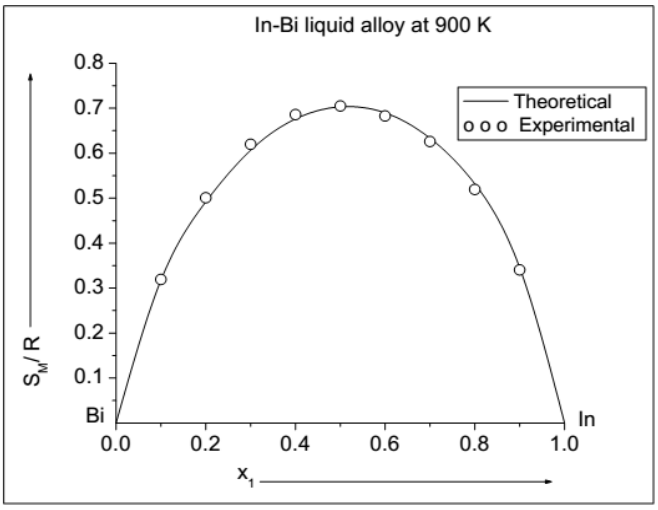

Figure 4.14: Plot of S_M/R versus concentration of In (x_1) of In−Bi liquid alloy at 900 K.

4.10.3 Entropy of mixing (S_M) for Al−Fe liquid alloy at 1873 K

The compositional dependence of the entropy of mixing for Al−Fe liquid at chosen temperature has been computed using Eq. (3.74). Herein required equilibrium values of mole fraction of Al_3Fe are taken from Table 4.3 and values of equilibrium constant and interaction energy parameters are taken from the Section 4.4.3. The mole fractions of unassociated species are determined using Eq. (3.63). The other required model parameters, such as temperature derivative terms of interaction energies and the heat of dissociation are taken from the Section 4.8.3. Theoretically computed values of S_M/R

along with the experimental values as a function of concentration are furnished in Table 4.15. The plot of the theoretical as well the experimental values of S_M/R versus concentration of Al (x_1) is shown in Fig. 4.15.

From Fig. 4.15, it can be observed that the computed values of S_M/R as a function of concentration are in good agreement at lower and higher concentrations of Al. But there is considerable disagreement between them in intermediate concentrations of Al. Both of these values are found to be positive at all concentration. It can be also stated that the Al–Fe liquid alloy at 1873 K is more ordered at lower and higher concentrations of Al.

Table 4.15: S_M/R for Al–Fe liquid alloy at 1873 K

Concentration of Al (x_1)	S_M/R	
	Theoretical	Experimental**
0.1	0.1820	0.2026
0.2	0.2439	0.2598
0.3	0.2736	0.2649
0.4	0.2646	0.2481
0.5	0.2454	0.2086
0.6	0.2189	0.1762
0.7	0.1903	0.1492
0.75*	0.1791	……..
0.8	0.1646	0.1286
0.9	0.1037	0.1046

*Compound forming concentration
**Hultgren *et al*. (1973)

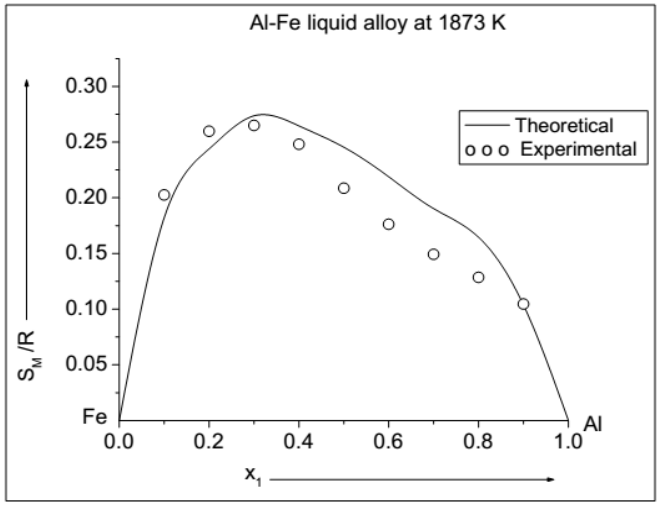

Figure 4.15: Plot of S_M/R versus concentration of Al (x_1) of Al–Fe liquid alloy at 1873 K.

4.10.4 Entropy of mixing (S_M) for Al–Mg liquid alloy at 1073 K

We have assumed the existence of complex $A_\mu B_\nu$ (=Al_3Mg_2) in Al–Mg liquid alloy at 1073 K. Therefore, the entropy of mixing for this system as a function of concentration has been computed from Eq. (3.43). For this purpose, the equilibrium value of the mole fraction x_{Al-Mg} of the complex has been taken from Table 4.4. Also the values of equilibrium constant and pairwise interaction energy parameters have been taken from the Section 4.4.4. The mole fractions of the unassociated atoms of Al (x_{Al}) and Mg (x_{Mg}) are then determined from Eqs. (3.5) and (3.6) respectively. The temperature derivative terms of interaction energy parameters and the heat of dissociation required to compute the compositional dependence of S_M are taken from the Section 4.8.4. Table 4.16 contains the computed and the experimental values of S_M/R as a function of concentration. Both of these values versus concentration of Al (x_1) are plotted in Fig. 4.16.

Table 4.16: S_M/R for Al–Mg liquid alloy at 1073 K

Concentration of Al (x_{Al})	S_M/R	
	Theoretical	Experimental**
0.1	0.2718	0.2816
0.2	0.4180	0.4228
0.3	0.5127	0.5116
0.4	0.5677	0.5666
0.5	0.5890	0.5933
0.6*	0.5708	0.5913
0.7	0.5107	0.5571
0.8	0.4166	0.4771
0.9	0.2727	0.3253

*Compound forming concentration
**Hultgren *et al*. (1973)

Theoretically computed values of S_M/R for Al–Mg liquid alloy at 1073 K as a function of concentration are in good agreement with the experimental values at lower concentration of Al in the range $x_1 \leq 0.56$. But there is slight deviation or there is fair agreement between these values at higher concentration of Al in the concentration range $x_1 \geq 0.6$. Both of the theoretical and experimental values of S_M/R are positive at all concentrations, Fig. 4.16. The theoretical findings also reveal that the alloy under consideration is more

ordered at lower and higher concentrations of Al. Thus the regular associated solution model thus successfully explains the entropy of mixing of the concerned system.

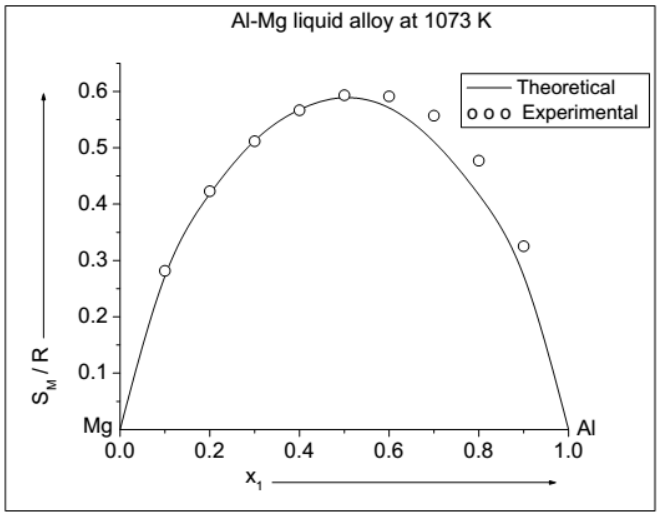

Figure 4.16: Plot of S_M/R versus the concentration of Al (x_1) of Al−Mg liquid alloy at 1073 K.

4.11 Thermodynamic properties of binary liquid alloys at different temperatures

In this section, we have presented the extensions made in the regular associated solution model to predict the thermodynamic properties of liquid binary alloys, such as Bi−Tl, In−Bi, Al−Fe and Al−Mg at different temperatures (above the melting temperatures of the respective alloys). Such predictions have been made by developing theoretical modeling equations in the frame work of regular associated solution model which are presented in the upcoming sections of this Chapter. We have also presented the results and discussion related to these thermodynamic properties of liquid alloys at different temperatures in the present section.

4.12 Theoretical modeling equations

The theoretical modeling equations have been developed by considering the temperature derivative terms of interaction energies ($\partial\omega_{12}/\partial T$, $\partial\omega_{13}/\partial T$ and $\partial\omega_{23}/\partial T$), the equilibrium constant (K) and the mole fractions of unassociated atoms (x_A and x_B) as

well as complex (x_{A-B}) to be constant with the change in temperature of the liquid alloys. With the help of these equations, the interaction energy parameters of the alloys at different temperatures have been computed which in turn are employed to compute the activity coefficients of unassociated components of the alloys. Once the activity coefficients are obtained, the activities and partial excess free energies of components of the alloys can be determined which in turn can be used to compute and predict the free energy of the liquid alloys at different temperatures.

Since in regular associated solution model only interaction energy parameters (ω_{12}, ω_{13} and ω_{23}) are temperature dependent, they can be related with the temperature derivative terms of interaction energy parameters by following expression (Yadav et al., 2016)

$$d\left[\omega_{i,j}(T)\right]_x = \frac{\partial \omega_{i,j}}{\partial T} dT \tag{4.1}$$

where $i, j = 1, 2$ and 3 for $i \neq j$; x is the mole fractions and $dT = T - T_K$ is the change in temperature. Herein, the term T stands for the melting temperature of the concerned liquid alloy and T_K is for the temperature of interest at which the thermodynamic properties are to be computed.

The activity coefficients of free monomers A and B (γ_A and γ_B) of the liquid alloys can then be computed using Eqs. (3.24) and (3.65) depending upon the existence of types of complexes in the liquid mixtures with the help of determined values of pairwise interaction energy parameters at different temperatures. The gross activity coefficients (γ_1 and γ_2) of free monomers are obtained from Eqs. (3.34), (3.37), (3.69) and (3.70). The activities of A (a_A) and B (a_B) can then be computed from Eqs. (3.36), (3.38), (3.71) at the temperatures of interests.

The partial excess free energy (G_q^{XS}; q=A or B) of components of the liquid alloy can be related to the activity coefficients (γ_A or γ_B) as (Yadav et al., 2016)

$$G_q^{XS} = RT \sum \ln \gamma_q \tag{4.2}$$

where the terms have their usual meanings. The excess free energy of mixing (G_M^{XS}) of the liquid alloy in terms of partial excess free energy ($G_{A,B}^{XS}$) can be expressed as

$$G_M^{XS} = \sum x_l \, G_q^{XS} \tag{4.3}$$

where x_l $(l = 1, 2)$ is the gross mole fractions of components A and B in the liquid mixture, such that $\sum x_l = 1$.

The free energy of mixing (G_M) of the liquid alloy then can be computed at temperatures of interests by the following expression

$$G_M = G_M^{XS} + RT(\sum x_l \ln x_l) \tag{4.4}$$

4.13 Prediction of activities at different temperatures

The present section deals with the procedures to compute and predict the activities of components of abovementioned binary liquid alloys at different temperatures. The results and discussion for the activities are highlighted in this section. Additionally, the mathematical prediction equations for the activity coefficients of the components of liquid alloys obtained by polynomial fitting of different orders are also presented in the following sub−sections.

4.13.1 Prediction of activities (a_{Tl} and a_{Bi}) for Bi−Tl liquid alloy at different temperatures

The mechanisms to determine the activities of binary liquid alloys are mentioned in the Section 4.12 of this Chapter. The activities of Tl (a_{Tl}) and Bi (a_{Bi}) are computed at temperatures T_k =750 K, 850 K, 950 K and 1050 K among which T=750 K is the

melting temperature of the concerned liquid alloy. At first, the interaction energy parameters (ω_{12}, ω_{13} and ω_{23}) are computed at above mentioned temperatures from Eq. (4.1) with the knowledge of determined values of the temperature derivative terms of interaction energy parameters ($\partial\omega_{12}/\partial T$, $\partial\omega_{13}/\partial T$ and $\partial\omega_{23}/\partial T$). The values of $\partial\omega_{12}/\partial T$, $\partial\omega_{13}/\partial T$ and $\partial\omega_{23}/\partial T$ are taken from the Section 4.8.1. The computed values of ω_{12}, ω_{13} and ω_{23} at different temperatures for Bi−Tl liquid alloy are depicted in Table 4.17.

Table 4.17: Interaction energies of Bi−Tl liquid alloy at different temperatures

Temperature (K)	Interaction energy parameters (J mol^{-1})		
	ω_{12}	ω_{13}	ω_{23}
750	-6117.03	-15089.90	-1253.34
850	-5353.03	-15178.90	-1152.34
950	-4589.03	-15267.90	-1051.34
1050	-3825.03	-15356.90	-950.34

It has been already mentioned that the interaction energy parameters indicate the strength of attraction between the constituent atoms (ω_{12}) and also between the constituent atoms and the complex (ω_{13} and ω_{23}). It can be observed that the increase in temperature of Bi−Tl liquid alloy results in decrease in the negative values of interaction energy parameters. This reveals that the attraction between the constituent atoms (Tl and Bi) as well as between the complex (TlBi) and constituent atoms decreases with increase in temperature of the alloy beyond its melting temperature. Moreover, theoretical predictions indicate that the tendency of complex formation decreases at elevated temperatures.

The activity coefficients of Tl (γ_{Tl}) and Bi (γ_{Bi}) are then computed at stipulated temperatures from Eqs. (3.69) and (3.70) respectively. For this process, we have taken the values of mole fractions from Table 4.1 and interaction energies from Table 4.17. The mathematical prediction equations (obtained from polynomial fitting of fourth order) along with the values of essential parameters to predict γ_{Tl} and γ_{Bi} at different temperatures are depicted in Table 4.18.

The activities of Tl (a_{Tl}) and Bi (a_{Bi}) for Bi−Tl liquid alloy at different temperatures are then computed from Eqs. (3.71a) and (3.71b), respectively. Theoretically computed values of a_{Tl} and a_{Bi} at above mentioned temperatures as a function of concentration are tabulated in Table 4.19. The computed values of a_{Tl} and a_{Bi} as a function of concentration at above mentioned temperatures are portrayed in Figs. 4.17 (a−b).

Table 4.18: Prediction equations for activity coefficients of Tl (γ_{Tl}) and Bi (γ_{Bi}) at different temperatures for Bi−Tl liquid alloy; $x_l = 0.1 - 0.9$

Physical quantity	Prediction equation	Temperature (K)	Values of parameters (L_Z)				
			L_0	L_1	L_2	L_3	L_4
γ_{Tl}	$\sum_{Z=0}^{4} L_Z x_l^Z$	750	0.0116	2.1744	-9.4050	16.8881	-8.6728
		850	0.0173	2.4630	-10.1555	17.6075	-8.9388
		950	0.0223	2.7645	-11.0567	18.5942	-9.3333
		1050	0.0269	3.0543	-11.9577	19.6047	-9.7395
γ_{Bi}	$\sum_{Z=0}^{4} L_Z x_l^Z$	750	1.0980	-1.6419	8.0733	-18.7826	11.6163
		850	1.1184	-1.9493	9.4549	-20.7844	12.5498
		950	1.1352	-2.1998	10.5742	-22.3998	13.3036
		1050	1.1488	-2.4048	11.4908	-23.7228	13.9234

Table 4.19: Activity (a_{Tl} and a_{Bi}) for Bi−Tl liquid alloys at different temperatures

Concentration of Tl (x_1)	T = 750K		T = 850K		T = 950K		T = 1050K	
	a_{Tl}	a_{Bi}	a_{Tl}	a_{Bi}	a_{Tl}	a_{Bi}	a_{Tl}	a_{Bi}
0.1	0.0184	0.8947	0.0226	0.8952	0.0265	0.8956	0.0302	0.8960
0.2	0.0343	0.7753	0.0414	0.7772	0.0480	0.7787	0.0541	0.7800
0.3	0.0570	0.6404	0.0673	0.6444	0.0770	0.6477	0.0853	0.6503
0.4	0.0965	0.4928	0.1108	0.4998	0.1235	0.5055	0.1349	0.5101
0.5*	0.1635	0.3378	0.1816	0.3475	0.1973	0.3553	0.2109	0.3618
0.6	0.2762	0.1909	0.2962	0.2009	0.3130	0.2092	0.3272	0.2162
0.7	0.4423	0.0735	0.4599	0.0799	0.4744	0.0854	0.4864	0.0901
0.8	0.6624	0.0183	0.6728	0.0209	0.6812	0.0231	0.6880	0.0250
0.9	0.8683	0.0090	0.8709	0.0107	0.8731	0.0123	0.8748	0.0138

*Compound forming concentration

The perusal of Figs. 4.17 (a−b) corresponds that the activities of components of the preferred liquid alloy increases with the increase in temperature of the alloy beyond its melting temperature. This phenomenon reveals that the tendency of leaving the respective atoms from the liquid mixture increases at elevated temperatures which eventually results

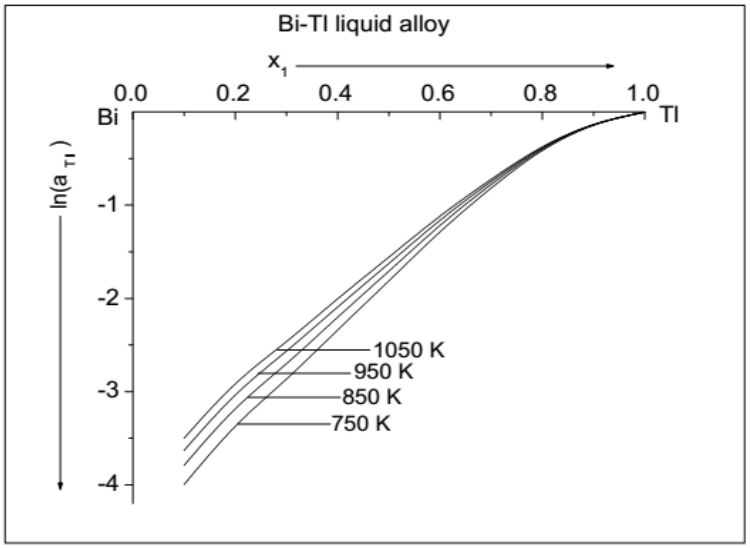

Figure 4.17(a): Plot of activity of Tl (a_{Tl}) versus the concentration of Tl (x_1) for Bi–Tl liquid alloy at different temperatures.

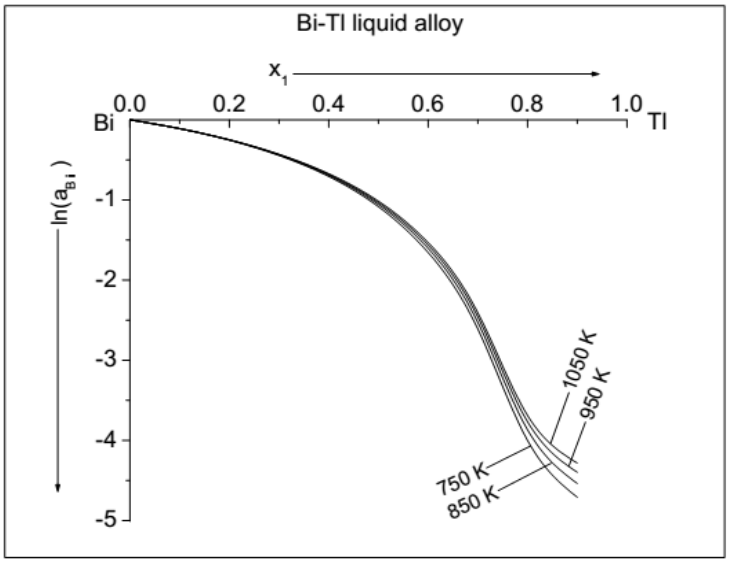

Figure 4.17(b): Plot of activity of Bi (a_{Bi}) versus the concentration of Tl (x_1) of Bi–Tl liquid alloy at different temperatures.

in weaker tendency towards complex formation. At the complex formation concentration ($x_{CC} = x_1 = 0.5$), the activity of Tl (a_{Tl}) are 0.1635, 0.1816, 0.1973 and 0.2109 at 750 K, 850 K, 950 K and 1050 K respectively (Table 4.19). The activity of Tl is the minimum at 750 K which is the melting temperature of the alloy and the maximum at 1050 K. Similarly, the activity of Bi (a_{Bi}) at the complex formation concentration is the maximum at 1050 K ($a_{Bi} = 0.3618$), followed by 950 K ($a_{Bi} = 0.3553$), 850 K ($a_{Bi} = 0.3475$) and

the minimum at 750 K ($a_{Bi} = 0.3378$) (Table 4.19). These theoretical investigations are in accordance with results obtained by other researchers employing different techniques for different alloys (Rais et al,, 1982; Alquasmi & Egan, 1983; Saboungi & Carbin, 1984; Awe et al., 2011; Wang et al., 2013; Yadav et al., 2016).

4.13.2 Prediction of activities (a_{In} and a_{Bi}) for In−Bi liquid alloy at different temperatures

Following the same procedure as mentioned in the Section 4.13.1, the activity of In (a_{In}) and Bi (a_{Bi}) for the In−Bi liquid alloys have been computed at temperatures T_k =900 K, 1000 K, 1100 K and 1200 K; where T=900 K is the melting temperature of the alloy. The interaction energy parameters (ω_{12}, ω_{13} and ω_{23}) are computed at above mentioned temperatures from Eq. (4.1) with the knowledge of determined values of the temperature derivative terms of interaction energy parameters ($\partial\omega_{12}/\partial T$, $\partial\omega_{13}/\partial T$ and $\partial\omega_{23}/\partial T$). For this purpose, the values of $\partial\omega_{12}/\partial T$, $\partial\omega_{13}/\partial T$ and $\partial\omega_{23}/\partial T$ are taken from the Section 4.8.2. The computed values of ω_{12}, ω_{13} and ω_{23} at different temperatures for In−Bi liquid alloy are depicted in Table 4.20.

Table 4.20: Interaction energies of In−Bi liquid alloy at different temperatures

Temperature (K)	Interaction energy parameters (J mol^{-1})		
	ω_{12}	ω_{13}	ω_{23}
900	-5185.44	-2950.39	-4481.33
1000	-5075.44	-2640.39	-4390.33
1100	-4965.44	-2330.39	-4299.33
1200	-4855.44	-2020.39	-4208.33

All the interaction energy parameters of the concerned liquid alloy decreases with the increase in its temperature, however, the increment or decrement of these parameters entirely depends upon the positivity or negativity of their temperature derivative terms. These theoretical findings predict that the attraction between the constituent atoms of the liquid alloy and also between these atoms and the complex decreases with the increase in its temperature. The values of these interaction energy parameters are greatest at the melting temperature of the alloy (900 K) and least at 1200 K. Therefore, it can be

predicted that the tendency of associated between the constituent atoms of the liquid mixture is the maximum at 900 K and the minimum at 1200 K. Moreover, the strength of attraction among above mentioned species is greater at 1000 K than that of 1100 K.

Table 4.21: Prediction equations for activity coefficients of In (γ_{In}) and Bi (γ_{Bi}) at different temperatures for In−Bi liquid alloy; $x_l = 0.1 - 0.9$

Physical quantity	Prediction equation	Temperature (K)	Values of parameters (L_Z)				
			L_0	L_1	L_2	L_3	L_4
γ_{In}	$\sum_{Z=0}^{4} L_Z x_l^Z$	900	0.5227	-0.4553	2.3172	-1.3345	-0.0460
		1000	0.5657	-0.5522	2.5364	-1.6846	0.1410
		1100	0.6031	-0.6353	2.7104	-1.9561	0.2858
		1200	0.6362	-0.7117	2.8690	-2.1982	0.4143
γ_{Bi}	$\sum_{Z=0}^{4} L_Z x_l^Z$	900	1.0644	-1.0088	4.9561	-10.4807	5.9289
		1000	1.0685	-1.0679	5.2604	-10.8227	6.0530
		1100	1.0716	-1.1133	5.4991	-11.0859	6.1477
		1200	1.0744	-1.1521	5.6957	-11.2948	6.2206

Table 4.22: Activities (a_{In} and a_{Bi}) for In−Bi liquid alloys at different temperatures

Concentration of In (x_1)	T = 900K		T = 1000K		T = 1100K		T = 1200K	
	a_{In}	a_{Bi}	a_{In}	a_{Bi}	a_{In}	a_{Bi}	a_{In}	a_{Bi}
0.1	0.0498	0.8999	0.0534	0.9005	0.0564	0.9010	0.0591	0.9014
0.2	0.1030	0.7954	0.1090	0.7974	0.1141	0.7991	0.1186	0.8005
0.3	0.1677	0.6809	0.1754	0.6848	0.1820	0.6880	0.1877	0.6907
0.4	0.2489	0.5567	0.2576	0.5626	0.2650	0.5676	0.2712	0.5717
0.5	0.3523	0.4271	0.3609	0.4348	0.3682	0.4412	0.3743	0.4466
0.6	0.4743	0.3014	0.4817	0.3098	0.4878	0.3168	0.4930	0.3228
0.66*	0.5555	0.2328	0.5561	0.2379	0.5621	0.2448	0.5668	0.2507
0.7	0.6113	0.1892	0.6164	0.1968	0.6206	0.2033	0.6241	0.2089
0.8	0.7488	0.0945	0.7514	0.0997	0.7535	0.1042	0.7553	0.1081
0.9	0.8891	0.0426	0.8898	0.0456	0.8903	0.0483	0.8908	0.0505

*Compound forming concentration

The activity coefficients of the free monomers In (γ_{In}) and Bi (γ_{Bi}) for In−Bi liquid alloys at temperature of interests are computed using Eqs. (3.69) and (3.70) respectively with the help of values from Table 4.20 and Table 4.2. The mathematical prediction equations obtained from polynomial fitting of fourth order to determine γ_{In} and γ_{Bi} at different temperatures are presented in Table 4.21. The activities of In (a_{In}) and Bi (a_{Bi}) at temperatures of interests are then computed from Eqs. (3.71a) and (3.71b) respectively

with the help of above determined values of activity coefficients. The values so obtained are tabulated in Table 4.22 and portrayed in Figs. 4.18(a−b).

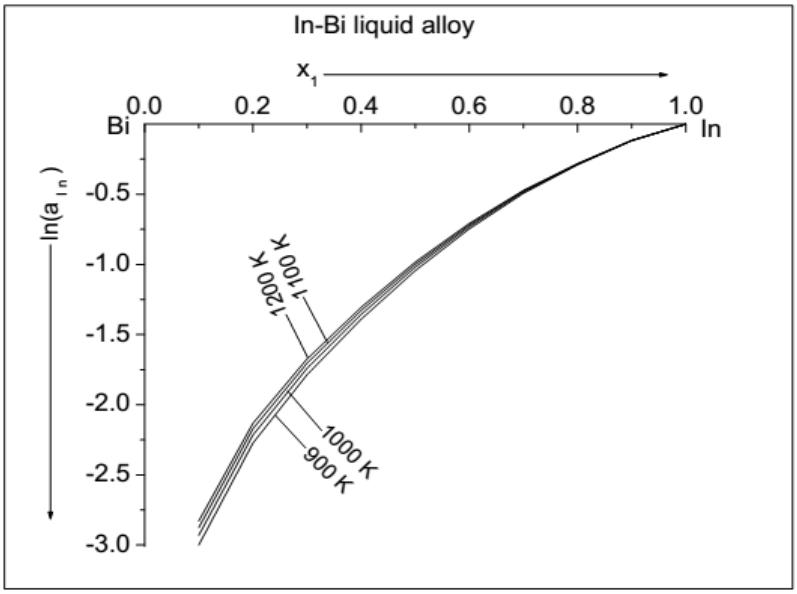

Figure 4.18 (a): Activity of In (a_{In}) versus concentration of In (x_1) for In−Bi liquid alloy at different temperatures.

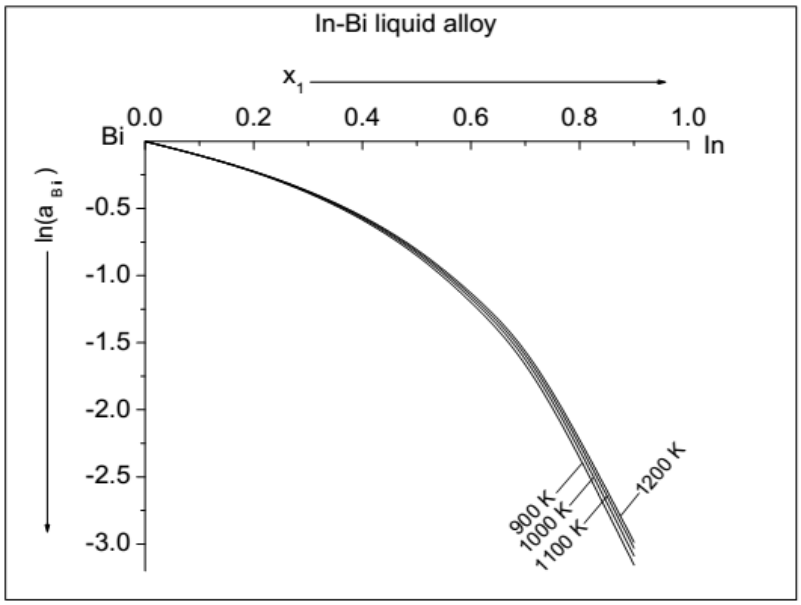

Figure 4.18 (b): Activity of Bi (a_{Bi}) versus concentration of In (x_1) for In−Bi liquid alloy at different temperatures.

It can be observed that the activities of the unassociated atoms of the alloy increases with increase in its temperature beyond melting temperature (Fig. 4.18). At the complex

forming concentration ($x_{CC} = x_1 = 0.66$), the activities of In are 0.5555, 0.5561, 0.5621 and 0.5668 at temperatures 900 K, 1000 K, 1100 K and 1200 K respectively. Similarly, the activities of Bi at this concentration are 0.2328, 0.2379, 0.2448 and 0.2507 at temperatures 900 K, 1000 K, 1100 K and 1200 K respectively. The minimum values of activities of both of the components are at 900 K and the maximum at 1200 K indicating that the tendency of leaving the complex of the respective components is the maximum at 1200 K and the minimum at 900 K which is the melting temperature of the alloy.

4.13.3 Prediction of activities (a_{Al} and a_{Fe}) for Al–Fe liquid alloy at different temperatures

Following the procedure as mentioned in the Section 4.13.1, the interaction energy parameters for Al–Fe liquid alloy at different temperatures (T_K=1873 K, 1973 K, 2073 K and 2173 K, where T=1873 K is the melting temperature of the alloy) are estimated using Eq. (4.1). The values of temperature derivative terms of interaction energy parameters required for this process are taken from the Section 4.8.3. The values so computed are furnished in Table 4.23.

Table 4.23: Interaction energies of Al–Fe liquid alloy at different temperatures

Temperature (K)	Interaction energy parameters (J mol^{-1})		
	ω_{12}	ω_{13}	ω_{23}
1873	-45143.60	-39911.30	-90427.30
1973	-43973.60	-42011.30	-88257.30
2073	-42803.60	-44111.30	-86087.30
2173	-41633.60	-46211.30	-83917.30

It can be observed that the values of interaction energies ω_{12} and ω_{23} decreases with increase in temperature of the alloy beyond its melting temperature which indicates that the attraction between the unassociated atoms (Al and Fe) as well as between the complex (Al_3Fe) and the unassociated atoms decreases at elevated temperatures. However, the value of interaction energies ω_{13} increases at such temperatures which may be due to the negative value of its temperature derivative term ($\partial\omega_{13}/\partial T$).

The methodology of evaluating the activity coefficients (γ_{Al} and γ_{Fe}) of the constituent atoms of the alloy is as mentioned in the Section 4.13.2. The essential ingredients to compute these coefficients at abovementioned temperatures are inherited from the Tables 4.3 and 4.23. The mathematical equations (obtained by polynomial fitting of fourth order) to predict the activity coefficients at different temperatures are tabulated in Table 4.24. The activities (a_{Al} and a_{Fe}) of the components of the liquid alloy are then computed from Eq.(3.71) with knowledge of above determined values of activity coefficients. Theoretically obtained values of a_{Al} and a_{Fe} at above mentioned temperatures are presented in Table 4.25. The compositional and temperature dependence of a_{Al} and a_{Fe} are portrayed in Figs. 4.19(a–b).

Table 4.24: Prediction equations for activity coefficients of Al (γ_{Al}) and Fe (γ_{Fe}) at different temperatures for Al–Fe liquid alloy; $x_l = 0.1 - 0.9$

Physical quantity	Prediction equation	Temperature (K)	Values of parameters (L_Z)				
			L_0	L_1	L_2	L_3	L_4
γ_{Al}	$\sum_{Z=0}^{4} L_Z x_l^Z$	1873	0.0234	0.7838	-1.9727	5.8892	-3.7459
		1973	0.0397	0.7635	-1.6302	5.1318	-3.3246
		2073	0.0569	0.7567	-1.3712	4.5043	-2.9639
		2173	0.0753	0.7506	-1.1459	3.9365	-2.6305
γ_{Fe}	$\sum_{Z=0}^{4} L_Z x_l^Z$	1873	0.9862	0.2458	-3.6552	2.6763	-0.2279
		1973	0.9899	0.1823	-3.0987	1.8594	0.0903
		2073	0.9935	0.1235	-2.6031	1.1726	0.3345
		2173	0.9963	0.0771	-2.1928	0.6443	0.4933

Table 4.25: Activities (a_{Al} and a_{Fe}) for Al–Fe liquid alloys at different temperatures

Concentration of Al (x_1)	T = 1873K		T = 1973K		T = 2073K		T = 2173K	
	a_{Al}	a_{Fe}	a_{Al}	a_{Fe}	a_{Al}	a_{Fe}	a_{Al}	a_{Fe}
0.1	0.0089	0.8792	0.0106	0.8811	0.0125	0.8827	0.0144	0.8842
0.2	0.0274	0.7288	0.0316	0.7347	0.0359	0.7402	0.0404	0.7452
0.3	0.0638	0.5592	0.0712	0.5698	0.0785	0.5795	0.0859	0.5885
0.4	0.1216	0.4003	0.1317	0.4140	0.1416	0.4268	0.1513	0.4388
0.5	0.2115	0.2585	0.2234	0.2730	0.2348	0.2867	0.2455	0.2998
0.6	0.3403	0.1460	0.3517	0.1584	0.3623	0.1705	0.3722	0.1823
0.7	0.5076	0.0685	0.5157	0.0769	0.5232	0.0854	0.5300	0.0939
0.75*	0.6017	0.0428	0.6093	0.0513	0.6143	0.0575	0.6190	0.0641
0.8	0.6971	0.0246	0.7005	0.0288	0.7037	0.0332	0.7065	0.0377
0.9	0.8684	0.0047	0.8686	0.0058	0.8687	0.0070	0.8688	0.0082

*Compound forming concentration

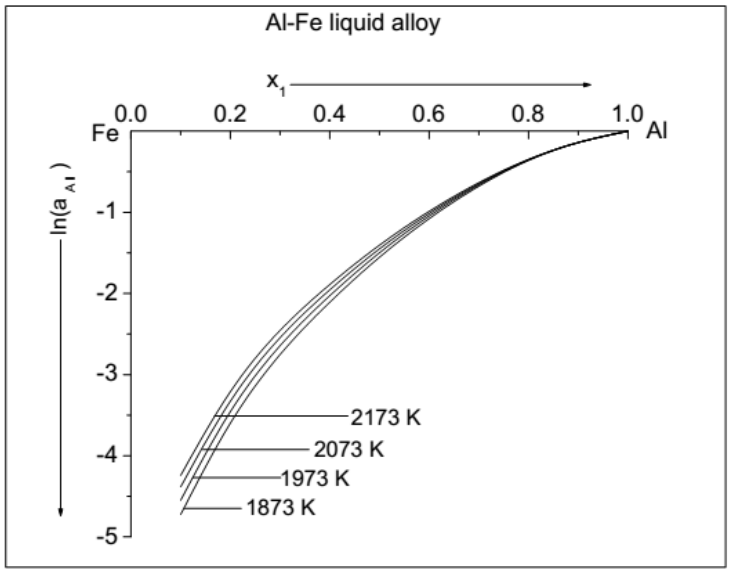

Figure 4.19 (a): Activity of Al (a_{Al}) versus concentration of Al (x_1) for Al–Fe liquid alloy at different temperatures.

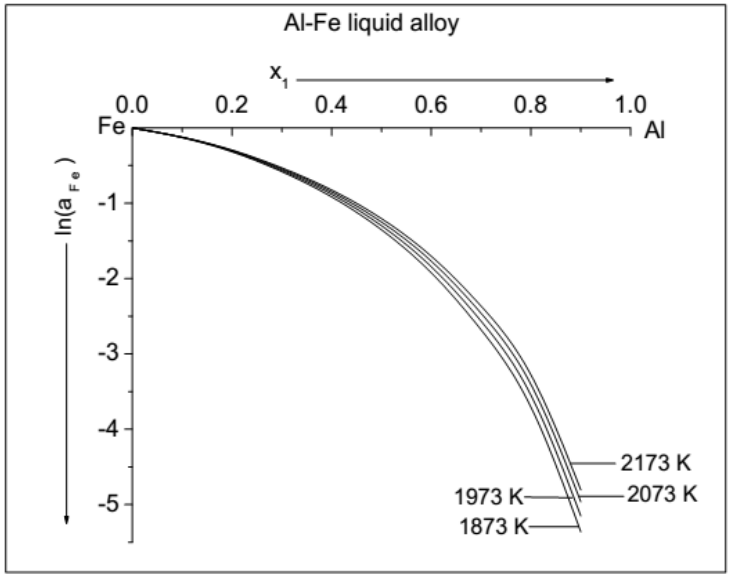

Figure 4.19 (b): Activity of Fe (a_{Fe}) versus concentration of Al (x_1) for Al–Fe liquid alloy at different temperatures.

The perusal of the above Table and Figs. 4.19 (a–b) indicates that the activities of the both components of the concerned alloy increases with increase in its temperature. Theoretically computed values of a_{Al} are 0.6017, 0.6093, 0.6143 and 0.6190 at 1873 K, 1973 K, 2073 K and 2173 K, respectively at complex formation concentration ($x_{CC} = x_1$=0.75). Likewise, the values of a_{Fe} at this concentration are 0.0428, 0.0513, 0.0575 and

0.0641 at 1873 K, 1973 K, 2073 K and 2173 K respectively. Thus it can be stated that the tendency towards complex formation in the initial melt of the liquid mixture is the maximum at its melting temperature (1873 K) and the minimum at 2173 K. Moreover, the tendency towards complex formation is greater at 1973 K than that of 2073 K.

4.13.4 Prediction of activities (a_{Al} and a_{Mg}) for Al-Mg liquid alloy at different temperatures

Following the similar procedures as in the Section 4.13.1, the interaction energy parameters of Al−Mg liquid alloy are computed at temperatures (T_K) 1173 K, 1273 K and 1373 K using Eq. (4.1), the melting temperature of the alloy being 1073 K. The temperature derivative terms of the interaction energy parameters required for this phenomenon are taken from the Section 4.8.4. Table 4.26 contains the computed values of the interaction energy action energy parameters for the concerned systems at different temperatures as mentioned above.

Table 4.26: Interaction energies of Al−Mg liquid alloy at different temperatures

Temperature (K)	Interaction energy parameters (J mol^{-1})		
	ω_{12}	ω_{13}	ω_{23}
1073	-6253.57	30687.97	16682.12
1173	-5709.57	32987.97	17649.12
1273	-5165.57	35287.97	18616.12
1373	-4621.57	37587.97	19583.12

The negative value of interaction energy ω_{12} which is the indicative of the strength of attraction between the unassociated atoms Al and Mg of the concerned liquid mixture decreases with the increases in its temperature. This predicts that the strength of association between Al and Mg in the initial melt decreases gradually with increases in temperature. However, the positive values of the interaction energies ω_{13} and ω_{23} increases with increase in temperature of the liquid mixture. These values predicts that the interaction between free atoms of Al and the complex (Al_3Mg_2), and also between free atoms of Mg and Al_3Mg_2 decreases with increase in temperature. It can thus be

stated that the strength of attraction among the free atoms of liquid mixture and the complex gradually decreases with increase in temperature beyond its melting temperature.

The activity coefficients (γ_{Al} and γ_{Mg}) for the preferred liquid alloy are computed from Eqs. (3.34) and (3.37) with the aid of above determined values of interaction energy parameters and the values of mole fractions are taken from Table 4.4. The mathematical prediction equations to determine the activity coefficients at above mentioned temperatures are presented in Table 4.27. The activities (a_{Al} and a_{Mg}) of the unassociated atoms of Al and Mg for the concerned system at different temperatures are then computed from Eq. (3.36) and (3.38) with knowledge of above computed values of essential ingredients. The values so obtained are depicted in Table 4.28. The compositional and temperature dependence of the computed activities for Al–Mg liquid alloys at different temperatures are shown in Figs. 4.20 (a–b).

Table 4.27: Prediction equations for activity coefficients of Al (γ_{Al}) and Mg (γ_{Mg}) at different temperatures for Al–Mg liquid alloy; $x_l = 0.1 - 0.9$

Physical quantity	Prediction equation	Temp. (K)	Values of parameters (L_Z)					
			L_0	L_1	L_2	L_3	L_4	L_5
γ_{Al}	$\sum_{Z=0}^{5} L_Z x_l^Z$	1073	0.2179	5.5332	-33.0471	84.4548	-90.0165	33.9776
		1173	0.2876	5.2797	-32.1269	82.5344	-88.2765	33.4231
		1273	0.3537	5.0203	-31.1765	80.5461	-86.4387	32.8173
		1373	0.4130	4.8087	-30.4870	79.1882	-85.2630	32.4647
γ_{Mg}	$\sum_{Z=0}^{5} L_Z x_l^Z$	1073	1.3874	-7.3153	45.1750	-117.5322	128.910	-50.5224
		1173	1.3860	-7.3255	45.5157	-118.6588	130.589	-51.3686
		1273	1.3913	-7.4106	46.1444	-120.3398	132.760	-52.3750
		1373	1.3938	-7.4629	46.6108	-121.6725	134.560	-53.2276

It can be observed that the activities of both of the components of the liquid alloy increases with increase in its temperature beyond melting temperature which is 1073 K (Fig. 4.20). The values of a_{Al} at the compound forming concentration (x_{CC}=x_1=0.6) are 0.5336, 0.5433, 0.5515 and 0.5587 whereas that of a_{Mg} are 0.2445, 0.2536, 0.2616 and 0.2686 respectively at 1073 K, 1173 K, 1273 K and 1373 K . These values eventually predict that the tendency towards association in the liquid melt decreases with increase in its temperature and is the maximum at its melting temperature.

Table 4.28: Activities (a_{Al} and a_{Mg}) for Al−Mg liquid alloys at different temperatures

Concentration of Al (x_1)	T = 1073K		T = 1173K		T = 1273K		T = 1373K	
	a_{Al}	a_{Mg}	a_{Al}	a_{Mg}	a_{Al}	a_{Mg}	a_{Al}	a_{Mg}
0.1	0.0520	0.8990	0.0572	0.9000	0.0620	0.9007	0.0663	0.9013
0.2	0.1060	0.7976	0.1148	0.8004	0.1226	0.8027	0.1298	0.8048
0.3	0.1663	0.6896	0.1774	0.6945	0.1873	0.6988	0.1962	0.7025
0.4	0.2414	0.5671	0.2539	0.5742	0.2650	0.5804	0.2748	0.5856
0.5	0.3372	0.4256	0.3498	0.4335	0.3608	0.4403	0.3704	0.4462
0.6*	0.5336	0.2445	0.5433	0.2536	0.5515	0.2616	0.5587	0.2686
0.7	0.6733	0.1691	0.6793	0.1794	0.6845	0.1885	0.6890	0.1967
0.8	0.7933	0.1035	0.7964	0.1118	0.7990	0.1193	0.8011	0.1261
0.9	0.9043	0.0451	0.9037	0.0505	0.9044	0.0547	0.9050	0.0586

*Compound forming concentration

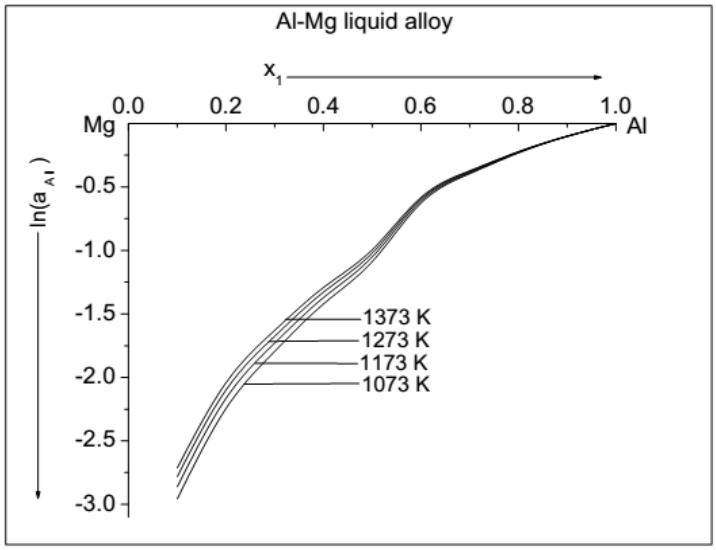

Figure 4.20 (a): The plot of a_{Al} versus x_1 for Al−Mg liquid alloy at different temperatures.

4.14 Prediction of free energy of mixing (G_M) at different temperatures

The methodology amended to compute and predict the free energy of mixing of some binary liquid alloys, such as Bi−Tl, In−Bi, Al−Fe and Al−Mg at different temperatures are highlighted in the present section. Herein, the results and discussion related to above predictions are also amended. The mathematical prediction equations obtained by polynomial fitting of different orders to predict the partial excess free energy of the components of these melts are also included in the following sub−sections.

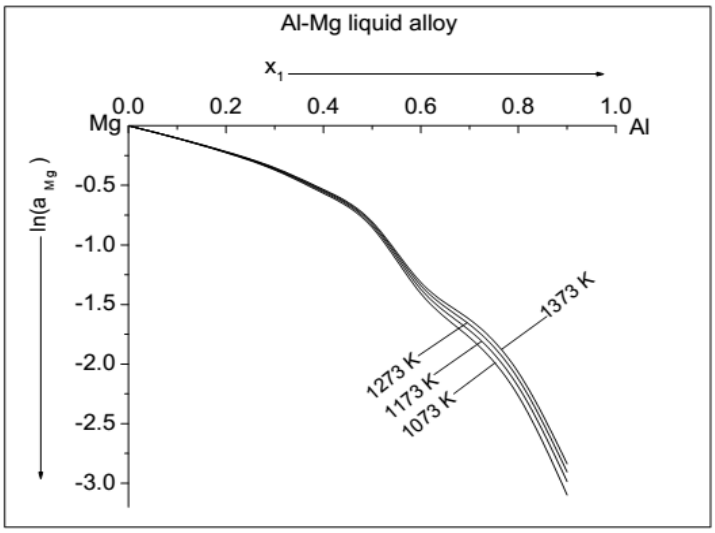

Figure 4.20 (b): The plot of a_{Mg} versus x_1 for Al–Mg liquid alloy at different temperatures.

4.14.1 Prediction of free energy of mixing for Bi–Tl liquid alloy at different temperatures

On the floor of the present theoretical modeling, the knowledge of partial excess free energies of the components of the liquid alloys at different temperatures is outmost essential to predict the free energy of mixing of the corresponding liquid alloys. Therefore, the partial excess free energies of Tl (q=Tl) and Bi (q=Bi) of Bi–Tl liquid alloys at different temperatures are first determined from Eq. (4.2) with the aid of computed values of activity coefficients of the respective components from the prediction equations in Table 4.18 in the Section 4.13.1. The temperatures of interests for the concerned liquid alloy are 750 K, 850 K, 950 K and 1050 K, where 750 K is its melting temperature. The mathematical equations obtained by polynomial fittings of fourth order to predict the partial excess free energy of Tl (G_{Tl}^{XS}/RT) and Bi (G_{Bi}^{XS}/RT) at different temperatures are presented in Table 4.29 (see Appendix A, Table b and Fig. a). These prediction equations are obtained from the computer software Origin Lab 6.1 by the method of interpolation/extrapolation. These findings are in accordance with the other researchers (Saboungi & Carbin, 1984; Ali, et al., 2004; Awe et al., 2011).

Once the partial excess free energies of Tl (G_{Tl}^{XS}) and Bi (G_{Bi}^{XS}) are computed, the excess free energy of mixing (G_M^{XS}/RT) for the concerned liquid alloy at above mentioned temperatures are obtained by using Eq. (4.3) with the help of predicted values of partial excess free energies from Table 4.29. The free energy of mixing (G_M/RT) of the liquid alloy is then computed with the knowledge of the determined values of excess free energies of mixing from Eq. (4.4). The values of G_M/RT so computed at different temperatures are tabulated in Table 4.30. The free energy of mixing for Bi−Tl liquid alloy at different temperatures as a function of concentration is plotted in Fig. 4.21.

Table 4.29: Prediction equations for partial excess free energy of Tl (G_{Tl}^{XS}/RT) and Bi (G_{Bi}^{XS}/RT) at different temperatures for Bi−Tl liquid alloy; $x_l = 0.1 - 0.9$

Physical quantity	Prediction equation	Temperature (K)	Values of parameters (L_Z)				
			L_0	L_1	L_2	L_3	L_4
G_{Tl}^{XS}/RT	$\sum_{Z=0}^{4} L_Z x_l^Z$	750	-1.3640	-4.9004	17.2653	-14.2938	3.3234
		850	-1.1808	-4.3692	13.7909	-9.2538	1.0015
		950	-1.0145	-4.4027	13.5313	-9.4218	1.3051
		1050	-0.8795	-4.4348	13.3398	-9.5840	1.5632
G_{Bi}^{XS}/RT	$\sum_{Z=0}^{4} L_Z x_l^Z$	750	0.8478	-13.0065	58.4751	-100.5667	52.3252
		850	0.8409	-12.8912	57.9478	-99.4692	51.8791
		950	0.8355	-12.8007	57.5325	-98.6029	51.5268
		1050	0.8310	-12.7270	57.1929	-97.8954	51.2381

Table 4.30: Free energy of mixing (G_M/RT) for Bi−Tl liquid alloy at different temperatures

Concentration of Tl (x_1)	Free energy of mixing (G_M/RT)			
	T = 750 K	T = 850 K	T = 950 K	T = 1050 K
0.1	-0.5079	-0.4788	-0.4623	-0.4489
0.2	-0.8523	-0.8386	-0.8076	-0.7825
0.3	-1.1128	-1.1003	-1.0745	-1.0398
0.4	-1.3033	-1.2962	-1.2460	-1.2053
0.5*	-1.4172	-1.3815	-1.3290	-1.2865
0.6	-1.4364	-1.3721	-1.3228	-1.2829
0.7	-1.3326	-1.3017	-1.2601	-1.2264
0.8	-1.0768	-1.0811	-1.0611	-1.0367
0.9	-0.6533	-0.5780	-0.5619	-0.5488

*Compound forming concentration

Theoretical predictions show that the values of excess free energy of mixing (G_M^{XS}/RT) for the liquid alloy decreases with increase in its temperature beyond melting temperature

(appendix A, Table a). These findings indicate that the strength of bonding between atoms of the complex decreases with increase in temperature of the alloy. As a result, the tendency towards complex formation decreases at elevated temperatures. At the complex formation concentration (x_{CC}= x_1=0.5, where 1 is for Tl), the value of G_M/RT is the maximum at 750 K where it is -1.4172 and the minimum at 1050 K where it is -1.2865. The liquid mixture thus shows greater tendency toward the complex formation at 750 K than that of at 1050 K. Also the value of G_M/RT at the complex formation concentration is greater at 850 K where it is -1.3815 than that of 950 K where it is -1.3290. The tendency towards the compound formation is thus greater at 850 K than that of 950 K.

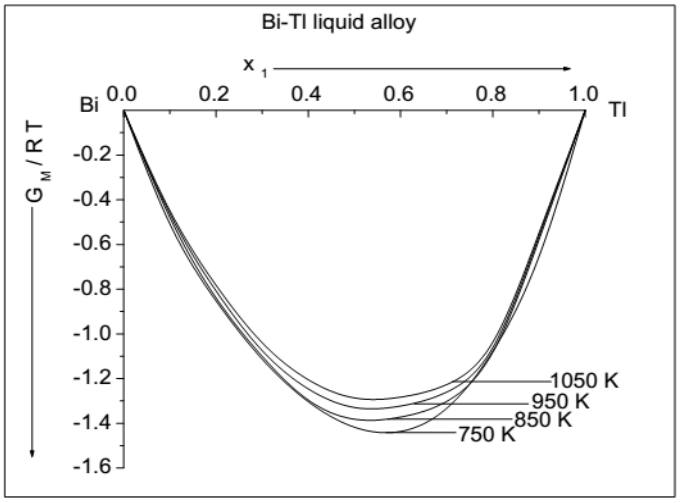

Figure 4.21: The plot of G_M/RT versus x_1 for Bi–Tl liquid alloy at different temperatures.

4.14.2 Prediction of free energy of mixing for In–Bi liquid alloy at different temperatures

Following the similar procedure as mentioned in the Section 4.14.1, the partial excess free energy of the components In (G_{In}^{XS}) and Bi (G_{Bi}^{XS}) of In–Bi liquid alloys are determined at temperatures , 900 K, 1000 K, 1100 K and 1200 K, where the melting temperature of the alloy is 900 K. These values are determined with the help of Eq. (4.2) and the predicted values of activity coefficients from Table 4.21 in the Section 4.13.2. The mathematical prediction equations (obtained from polynomial fitting of fourth order) for

G_{In}^{XS}/RT and G_{Bi}^{XS}/RT at different temperatures are depicted in Table 4.31 (see Appendix, Table d and Fig. b). The procedure of obtaining the prediction equations is as mentioned in the Section 4.14.1.

Table 4.31: Prediction equations for partial excess free energy of In (G_{In}^{XS}/RT) and Bi (G_{Bi}^{XS}/RT) at different temperatures for In−Bi liquid alloy; $x_l = 0.1 - 0.9$

Physical quantity	Prediction equation	Temperature (K)	Values of parameters (L_Z)				
			L_0	L_1	L_2	L_3	L_4
$\frac{G_{In}^{XS}}{RT}$	$\sum_{Z=0}^{4} L_Z x_l^Z$	900	-0.6458	-1.0026	5.6010	-5.7228	1.7832
		1000	-0.5661	-1.1191	5.5944	-5.6960	1.8013
		1100	-0.5005	-1.2176	5.6013	-5.6929	1.8255
		1200	-0.4459	-1.2995	5.6013	-5.6813	1.8400
$\frac{G_{Bi}^{XS}}{RT}$	$\sum_{Z=0}^{4} L_Z x_l^Z$	900	0.1404	-2.1492	9.9248	-18.2714	9.4627
		1000	0.1384	-2.1140	9.8083	-17.9354	9.2920
		1100	0.1366	-2.0847	9.7125	-17.6619	9.1539
		1200	0..1355	-2.0652	9.6516	-17.4613	9.0519

Table 4.32: Free energy of mixing (G_M/RT) for In−Bi liquid alloy at different temperatures

Concentration of In (X_{In})	Free energy of mixing (G_M/RT)			
	T = 900 K	T = 1000 K	T = 1100 K	T = 1200 K
0.1	-0.3912	-0.3874	-0.3813	-0.3762
0.2	-0.6266	-0.6244	-0.6136	-0.6045
0.3	-0.7907	-0.7873	-0.7729	-0.7610
0.4	-0.8964	-0.8876	-0.8711	-0.8574
0.5	-0.9452	-0.9260	-0.9087	-0.8944
0.6	-0.9328	-0.9070	-0.8904	-0.8766
0.66*	-0.8944	-0.8727	-0.8572	-0.8443
0.7	-0.8523	-0.8264	-0.8119	-0.7998
0.8	-0.6926	-0.6898	-0.6787	-0.6694
0.9	-0.4342	-0.4138	-0.4077	-0.4026

*Compound forming concentration

The excess free energy of mixing (G_M^{XS}/RT) of the concerned system at above mentioned temperatures is then determined from Eq. (4.3) with the help of predicted values of partial excess free energies of In and Bi (Table 4.31) throughout the entire concentration. This computation eventually yields the free energy of mixing (G_M/RT) of the concerned alloy at different temperatures from Eq. (4.4) at all concentrations. Theoretically predicted values of G_M/RT at different temperatures as a function of concentration are presented in

Table 4.32. The plots of G_M/RT as a function of concentration at different temperatures are as portrayed in Fig. 4.22.

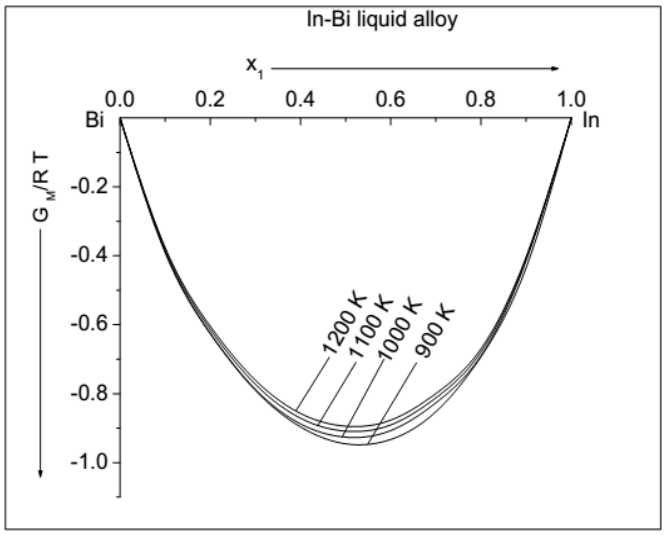

Figure 4.22: The free energy of mixing (G_M/RT) versus concentration of In (x_1) for In−Bi liquid alloy at different temperatures.

The theoretically obtained values of excess free energy of mixing (G_M^{XS}/RT) of the alloy gradually decreases at elevated temperatures (see appendix, Table c). Moreover, the perusal of Fig. (4.22) corresponds that the free energy of mixing of the preferred liquid alloy decreases with the increase in its temperature beyond melting temperature. Theoretically computed values of G_M/RT thus predicts that the strength of bonding between the atoms of the complex gradually decreases with increase in temperature. The values of G_M/RT at the complex formation concentration (x_{CC}= x_1= 0.66) are -0.8944, -0.8727, -0.8572 and -0.8443 at temperatures 900 K, 1000 K, 1100 K and 1200 K respectively. It can thus be forecasted that the tendency towards the complex formation is the greatest at 900 K and the least at 1200 K. Moreover, this tendency is greater at 1000 K than that of at 1100 K.

4.14.3 Prediction of free energy of mixing (G_M/RT) for Al−Fe liquid alloy at different temperatures

At first, the partial excess free energy of Al (G_{Al}^{XS}) and Fe (G_{Fe}^{XS}) are determined at different temperatures from Eq. (4.2) with the aid of the predicted values of corresponding activity coefficients in Table 4.24 at temperatures 1873 K, 1973 K, 2073 K and 2173 K, where 1873 K is the melting temperature of the alloy. The prediction equations related with the computations of G_{Al}^{XS}/RT and G_{Fe}^{XS}/RT at above mentioned temperatures are tabulated in Table 4.33 (also see appendix A, Table f; Fig. c). The procedure of yielding the prediction equations are as mentioned in the Section 4.14.1.

The excess free energy of mixing (G_M^{XS}/RT) of the alloy at above mentioned temperatures are then computed with the knowledge of the predicted values of partial excess free energies from Table 4.33 from Eq. (4.3). Finally, the free energy of mixing (G_M/RT) are computed by Eq. (4.4) with the computed values of essential input parameters at all concentrations. Theoretically computed values of G_M/RT at different temperatures as a function of concentration are presented in Table 4.34. The plots of compositional dependence of G_M/RT at different temperatures are portrayed in Fig. 4.23.

Table 4.33: Prediction equations for partial excess free energy of Al (G_{Al}^{XS}/RT) and Fe (G_{Fe}^{XS}/RT) at different temperatures for Al−Fe liquid alloy; $x_i = 0.1 - 0.9$

Physical quantity	Prediction equation	Temperature (K)	Values of parameters (L_Z)				
			L_0	L_1	L_2	L_3	L_4
$\frac{G_{Al}^{XS}}{RT}$	$\sum_{Z=0}^{4} L_Z x_i^Z$	1873	-2.9255	5.2820	-2.9516	2.0825	-1.5087
		1973	-2.7081	4.8665	-2.7457	1.9811	-1.4114
		2073	-2.5115	4.4880	-2.5468	1.8713	-1.3150
		2173	-2.3335	4.1503	-2.3905	1.8072	-1.2448
$\frac{G_{Fe}^{XS}}{RT}$	$\sum_{Z=0}^{4} L_Z x_i^Z$	1873	-0.0799	1.2819	-8.5545	11.5899	-8.5912
		1973	-0.0829	1.3315	-8.5910	12.0150	-8.7733
		2073	-0.0855	1.3745	-8.6155	12.3842	-8.9295
		2173	-0.0882	1.4178	-8.6566	12.7501	-9.0874

The values of excess free energy of mixing (G_M^{XS}/RT) computed from the modeling equations gradually decreases at elevated temperatures (appendix A, Table e). Fig. 4.23 shows that the free energy of mixing for the concerned liquid alloy gradually decreases with increase in its temperature beyond melting temperature which is 1873 K. The computed values of G_M/RT from theoretical modeling equations in the frame of regular

associated solution model predicts that the tendency towards the compound formation decreases at elevated temperatures beyond melting temperature of the liquid alloy. The computed value of free energy of mixing at the compound forming concentration (x_{CC}= x_1=0.75) is the maximum at 1873 K (G_M/RT = -1.2102) followed by 1973 K (G_M/RT = -1.1240), 2073 K (G_M/RT = -1.0871) and the minimum at 2173 K (G_M/RT = -1.0534). It can thus be predicted that the tendency towards the compound formation in the liquid alloy is the maximum at 1873 K (melting temperature) and the least at 2173 K. Also the tendency towards compound formation is greater at 1973 K than that of at 2073 K.

Table 4.34: Free energy of mixing (G_M/RT) for Al–Fe liquid alloy at different temperatures

Concentration of Al (x_{Al})	Free energy of mixing (G_M/RT)			
	T = 1873 K	T = 1973 K	T = 2073 K	T = 2173 K
0.1	-0.5828	-0.5685	-0.5508	-0.5347
0.2	-0.9634	-0.9375	-0.9059	-0.8773
0.3	-1.2326	-1.1865	-1.1451	-1.1075
0.4	-1.4031	-1.3400	-1.2927	-1.2497
0.5	-1.4798	-1.3985	-1.3493	-1.3046
0.6	-1.4579	-1.3640	-1.3168	-1.2738
0.7	-1.3252	-1.2332	-1.1917	-1.1541
0.75*	-1.2102	-1.1240	-1.0871	-1.0534
0.8	-1.0621	-0.9941	-0.9623	-0.9333
0.9	-0.6433	-0.6418	-0.6233	-0.6066

*Compound forming concentration

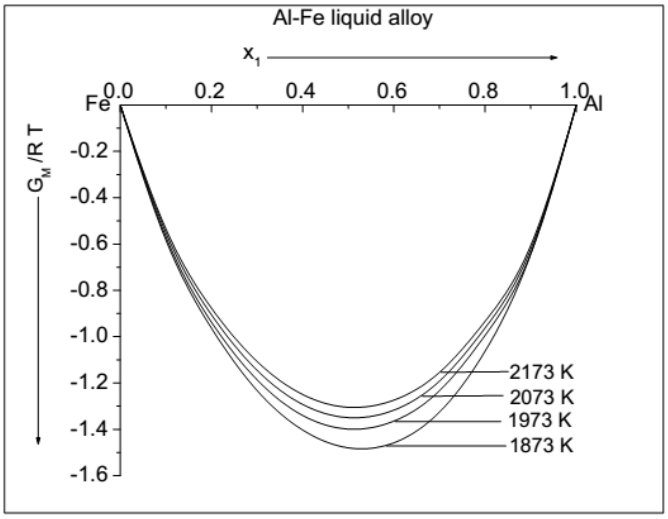

Figure 4.23: The Gibbs free energy of mixing (G_M/RT) versus concentration of Al (x_1) for Al–Fe liquid alloy at different temperatures.

4.14.4 Prediction of Gibbs free energy of mixing (G_M/RT) for Al–Mg liquid alloy at different temperatures

The partial excess free energies (G_{Al}^{XS} and G_{Mg}^{XS}) of the components of Al–Mg liquid alloy at temperatures 1073 K, 1173 K, 1273 K and 1373 K, among which 1073 K is its melting temperature are determined from Eq. (4.2) with help of computed values of activity coefficients of corresponding atoms in Table 4.27 of the Section 4.13.4. The mathematical equations to predict G_{Al}^{XS}/RT and G_{Mg}^{XS}/RT at the temperatures of interests are tabulated in Table 4.35 (see appendix A, Table h; Fig. d). These equations along with the values of essential parameters are obtained following the methodology as mentioned in the Section 4.14.1. The excess free energy of mixing (G_M^{XS}) of the liquid alloy is then computed using Eq. (4.3) and determined values of partial excess free energies from Table 4.35 throughout the entire range of concentration. The free energy of mixing (G_M/RT) of the liquid alloy at different temperatures is then computed from Eq. (4.4) with the help of computed values of excess free energy of mixing. Theoretically predicted values of G_M/RT as a function of concentration of Al at above mentioned temperatures are presented in Table 4.36. The plot of G_M/RT for the concerned liquid alloy as a function of concentration at different temperatures is plotted in Fig. 4.24.

Table 4.35: Prediction equations for partial excess free energy of Al (G_{Al}^{XS}/RT) and Mg (G_{Fe}^{XS}/RT) at different temperatures for Al–Mg liquid alloy; $x_l = 0.1 - 0.9$

Physical quant.	Prediction equation	Temp. (K)	Values of parameters (L_Z)					
			L_0	L_1	L_2	L_3	L_4	L_5
$\frac{G_{Al}^{XS}}{RT}$	$\sum_{Z=0}^{5} L_Z x_l^Z$	1073	-1.0251	6.8328	-41.3425	108.8995	-119.2402	46.0801
		1173	-0.8938	6.2981	-39.1406	103.5105	-113.4168	43.8365
		1273	-0.7834	5.8530	-37.3203	99.0647	-108.6221	41.9936
		1373	-0.6884	5.4641	-35.7216	95.1687	-104.4261	40.3814
$\frac{G_{Mg}^{XS}}{RT}$	$\sum_{Z=0}^{5} L_Z x_l^Z$	1073	0.5361	-10.0238	61.0496	-156.2169	169.1734	-65.8013
		1173	0.5271	-9.8702	60.4113	-155.1090	168.8636	-66.0064
		1273	0.5180	-9.7272	59.8287	-154.1125	168.5661	-66.1731
		1373	0.5093	-9.5805	59.1781	-152.8826	167.9140	-66.1667

Theoretically predicted values of excess free energy of mixing (G_M^{XS}/RT) of the preferred alloy descends at elevated temperatures (see appendix A, Table g). Further, the perusal of

Fig. 4.24 shows that the free energy of mixing of the concerned liquid alloy decreases with increase in temperature beyond its melting temperature. As a result, it can be predicted that the strength of bonding and hence the tendency of compound formation in the liquid alloy decreases with increase in temperature above its melting temperature. The value of G_M/RT is the maximum at 1073 K which is its melting temperature and the least at 1373 K predicting that the most stable complex is formed at former temperature than the later. Also the value of G_M/RT is greater at 1172 K than that of 1273 K which predicts that the stability of the complex in the liquid state of this alloy is greater at the former temperature than that of the later.

Table 4.36: Free energy of mixing (G_M/RT) for Al–Mg liquid alloy at different temperatures

Concentration of Al (X_{Al})	Free energy of mixing (G_M/RT)			
	T = 1073 K	T = 1173 K	T = 1273 K	T = 1373 K
0.1	-0.3911	-0.3811	-0.3723	-0.3648
0.2	-0.6305	-0.6111	-0.5955	-0.5821
0.3	-0.8040	-0.7739	-0.7533	-0.7358
0.4	-0.9233	-0.8811	-0.8577	-0.8377
0.5	-0.9877	-0.9431	-0.9199	-0.9000
0.6*	-0.9621	-0.9148	-0.8934	-0.8751
0.7	-0.8344	-0.7861	-0.7659	-0.7486
0.8	-0.6515	-0.6204	-0.6049	-0.5916
0.9	-0.4001	-0.3897	-0.3810	-0.3735

*Compound forming concentration

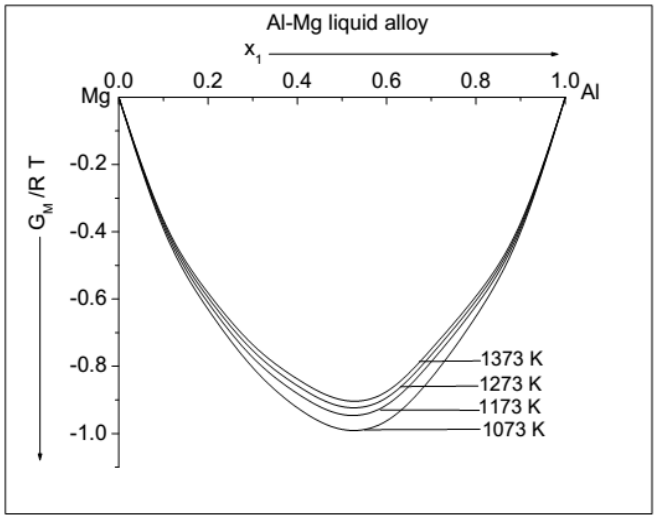

Figure 4.24: The free energy of mixing (G_M/RT) versus concentration of Al (x_1) for Al–Mg liquid alloy at different temperatures.

4.15 Structural properties of binary liquid alloys

Though the alloys have profound uses in the solid state; they are grown from liquid state near to their melting temperatures. The liquid states are termed as disordered states having only short range interactions among the constituent atoms in the nearest neighbourhoods. The information about the various structural properties at microscopic level can be obtained and discussed with the aid of the Bhatia−Thornton partial structure factors of individual pairs of the liquid mixtures. These structural factures serves as fundamental quantity to relate the structural properties with the thermodynamic function (Bhatia & Thornton, 1970). The concentration fluctuation in long wavelength limit has been evolved as powerful tool to understand and visualize the nature of structure of the liquid mixtures at microscopic level (Bhatia & Thornton, 1970; Bhatia & Hargrove, 1974; Bhatia & Singh, 1984; Singh, 1987; Prasad & Singh 1990; Singh et al., 1991; Singh &Sommer, 1997; Alkinlade et al., 2000; Passerone et al., 2009; Novakovic et al., 2011; Adhikari et al., 2010; Adhikari, 2011; Yadav et al., 2015, 2016). Further, the functions for chemical short range order parameter, ratio of diffusion coefficients and excess stability can also be correlated with the structure factures (Darken & Gurry, 1953; Yih & Thompson, 1982; Waseda, 1980; Chieux & Ruppersberg, 1980; Saboungi et al., 1990).

In this lime light, we have computed the microscopic structural properties, such as concentration fluctuation in long wavelength limit ($S_{CC}(0)$), chemical short range order parameter (α_1) and ratio of mutual to intrinsic diffusion coefficients (D_M/D_{id}) for Bi−Tl, In−Bi, Al−Fe and Al−Mg liquid alloys at temperatures 750 K, 900 K, 1873 K and 1073 K respectively in this work. These structural properties have been computed in the frame work of regular associated solution model. The results and discussion of the structural properties are presented in the upcoming sub−sections of this Chapter.

4.16 Results for Bi−Tl, In−Bi, Al−Fe and Al−Mg liquid alloys

In this section, we present the results for the structural properties of some binary liquid alloys, such as Bi−Tl, In−Bi, Al−Fe and Al−Mg at 750 K, 900 K, 1873 K and 1073 K

respectively in the frame work of preferred theoretical model. The structural properties of above mentioned liquid alloys have been investigated by computing concentration fluctuation in long wavelength limit ($S_{CC}(0)$), chemical short range order parameter (α_1) and ratio of diffusion coefficients (D_M/D_{id}) at stipulated temperatures.

4.16.1 $S_{CC}(0)$, α_1 and D_M/D_{id} for Bi−Tl liquid alloy at 750 K

Theoretical value of $S_{CC}(0)$ for Bi−Tl liquid alloy at 750 K is computed from Eq. (3.122) with the help of essential input ingredients which are mole fractions of free monomers and complex, interaction energy parameters and derivative terms of mole fractions with respect to concentration. The mole fractions of free monomers x_A and x_B (where A=Tl and B=Bi), and that of complex TlBi (x_{Tl-Bi}) are inherited from Table 4.1 whereas the values of pairwise interaction energies are taken from the Section 4.4.1. The values of derivative terms of the mole fraction of the complex ($X'_{A_\mu B};\ \mu = 1$) with respect to concentration are determined from Eq. (3.123). With the knowledge of these determined values, the derivative terms of mole fraction of free monomers (X'_A and X'_B) with respect to concentration are obtained from Eq. (3.124). The value of $S^{id}_{CC}(0)$ is computed from Eq. (3.113) and the experimental value of $S_{CC}(0)$ is computed from Eq. (3.111) with the help of experimental data of activities of Tl (a_{Tl}) and Bi a_{Bi} (Hultgren *et al*., 1973) throughout the entire concentration. The values of α_1 and D_M/D_{id} as a function of concentration are computed from Eqs. (3.128) and (3.133) respectively. To compute D_M/D_{id}, we have taken Z = 10. The computed values of $S_{CC}(0)$ and α_1 and D_M/D_{id} as a function of concentration are tabulated in Table 4.37 and are plotted in Figs. 4.25(a−c).

To maintain homogeneity, we have used the same input parameters that were used for the computation of free energy of mixing of the concerned liquid alloy. Strictly speaking, none of the parameters have been adjusted for the computation of $S_{CC}(0)$. The perusal of Fig. 4.25(a) shows that the theoretically and experimentally computed values of $S_{CC}(0)$ are less than the ideal values at all concentrations. These findings reveal that the concerned system is complete ordering in nature and hence the association of the type A−B (hetero−coordinating) is favoured in the initial melt. Further, both the theoretical and

the experimental values of $S_{CC}(0)$ are in good agreement at all concentrations except at $x_1 = 0.2$ where there is slight disagreement between them.

Table 4.37: The computed values of $S_{CC}(0)$, α_1 and D_M/D_{id} as a function of concentration for Bi−Tl liquid alloy at 750 K

Concentration of Tl (x_1)	$S_{CC}(0)$			α_1	D_M/D_{id}
	Theoretical	Experimental**	Ideal		
0.1	0.0805	0.0882	0.09	-0.0117	1.1185
0.2	0.1225	0.1484	0.16	-0.0298	1.3066
0.3	0.1336	0.1279	0.21	-0.0541	1.5717
0.4	0.1244	0.1134	0.24	-0.0850	1.9289
0.5*	0.1037	0. 0944	0.25	-0.1237	2.4117
0.6	0.0814	0. 0870	0.24	-0.1631	2.9494
0.7	0.0635	0. 0643	0.21	-0.1875	3.3079
0.8	0.0580	0. 0577	0.16	-0.1495	2.7572
0.9	0.0532	0. 0508	0.09	-0.0648	1.6929

*Compound forming concentration
**Hultgren *et al*. (1973)

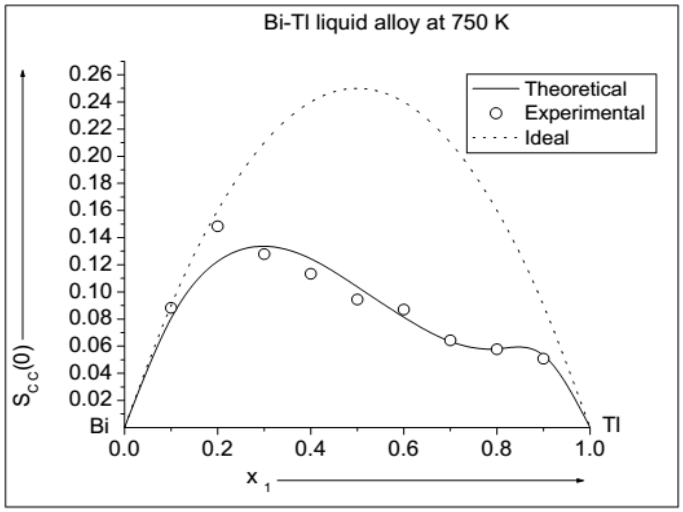

Figure 4.25(a): Concentration fluctuation in long wavelength limit ($S_{CC}(0)$ versus concentration of Tl (x_1) for Bi−Tl liquid alloy at 750 K.

Fig. 4.25(b) shows that the value of α_1 is negative throughout the entire concentration. It also indicates that the preferred association in the liquid mixture of the concerned alloy is between A and B in the nearest neighbours. Fig 4.25(c) indicates that the computed values of D_M/D_{id} is positive and greater than one at all concentrations which also

clarifies the hetero−coordinating behaviour of the liquid alloy. These results of α_1 and D_M/D_{id} stand in favour of that predicted by $S_{CC}(0)$ for Bi−Tl liquid alloy at 750 K.

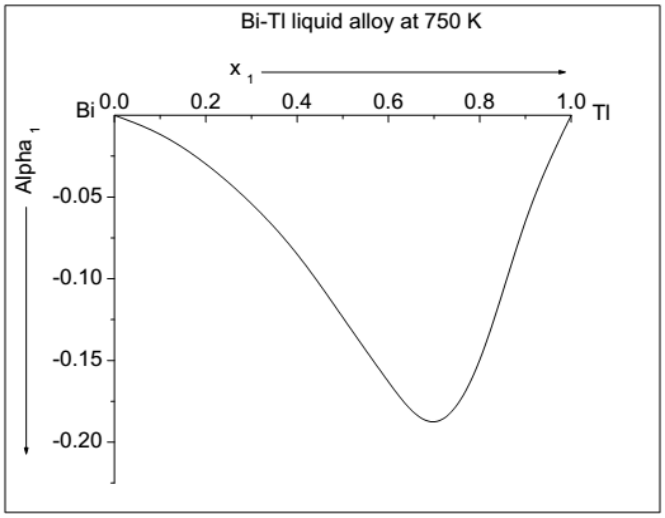

Figure 4.25(b): Chemical short range parameter (α_1) versus concentration of Tl (x_1) for Bi−Tl liquid alloy at 750 K.

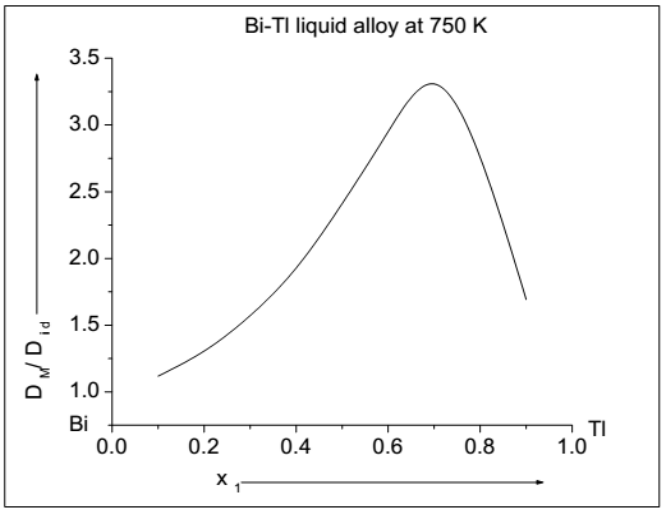

Figure 4.25(c): Ratio of diffusion coefficients (D_M/D_{id}) versus concentration of Tl (x_1) for Bi−Tl liquid alloy at 750 K.

4.16.2 $S_{CC}(0)$, α_1 and D_M/D_{id} for In−Bi liquid alloy at 900 K

Theoretical values of $S_{CC}(0)$ for In−Bi liquid alloy at 900 K have been computed from Eq. (3.122). For this purpose, the values of mole fractions of the complex and free monomers are taken from the Table 4.2 and that of pairwise interaction energy

parameters are taken from the Section 4.4.2. The remaining input ingredients x'_A, x'_B and $x'_{A_\mu B}$ are determined using Eqs. (3.124) and (3.123) following the similar procedure as mentioned in the Section 4.16.1. The experimental and the ideal values of $S_{CC}(0)$ are evaluated from Eqs. (3.111) and (3.113) respectively. The values of α_1 and D_M/D_{id} are then obtained respectively from Eqs. (3.128) and (3.133) with aid of above determined values of $S_{CC}(0)$ and $S_{CC}^{id}(0)$ throughout the entire concentrations. The values so computed as a function of concentration are depicted in Table 4.38 and are portrayed in Figs. 4.26 (a-c).

Table 4.38: The computed values of $S_{CC}(0)$, α_1 and D_M/D_{id} as a function of concentration for In−Bi liquid alloy at 900 K

Concentration of In (x_1)	$S_{CC}(0)$			α_1	D_M/D_{id}
	Theoretical	Experimental**	Ideal		
0.1	0. 0888	0. 0884	0.09	-0.0014	1.0141
0.2	0. 1471	0. 1388	0.16	-0.0087	1.0877
0.3	0. 1735	0. 1595	0.21	-0.0206	1.2103
0.4	0. 1767	0. 1601	0.24	-0.0346	1.3585
0.5	0. 1662	0. 1579	0.25	-0.0480	1.5040
0.6	0. 1490	0. 1491	0.24	-0.0576	1.6107
0.66*	0.1377	……..	…….	-0.0609	1.6469
0.7	0. 1290	0. 1345	0.21	-0.0591	1.6277
0.8	0. 1019	0. 1133	0.16	-0.0540	1.5709
0.9	0. 0732	0. 0751	0.09	-0.0225	1.2297

*Compound forming concentration

**Hulgren *et al*. (1973)

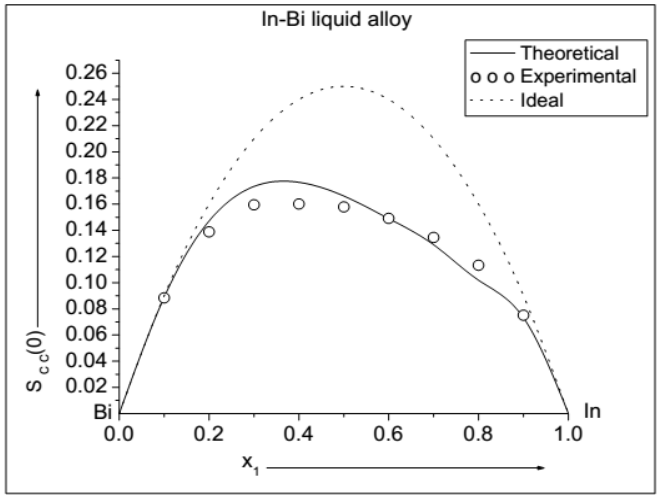

Figure 4.26(a): Concentration fluctuation in ling wavelength limit ($S_{CC}(0)$) versus concentration of In (x_1) for In−Bi liquid alloy at 900 K.

It can be observed from Fig. 4.26 (a) that the computed as well as experimental values of $S_{CC}(0)$ are in reasonable agreements. Both of these values are less than the ideal values at all concentrations which suggest that the preferred liquid alloy is ordering in nature and hence the mixing of atoms of the alloy takes place in the initial melt.

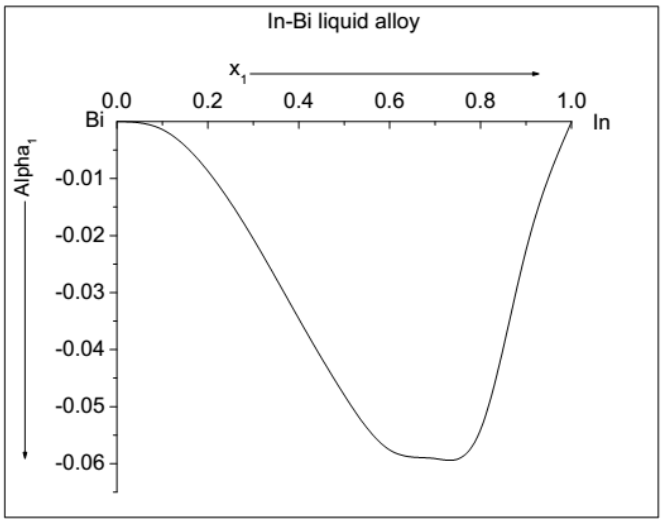

Figure 4.26(b): Chemical short range parameter (α_1) versus concentration of In (x_1) for In−Bi liquid alloy at 900 K.

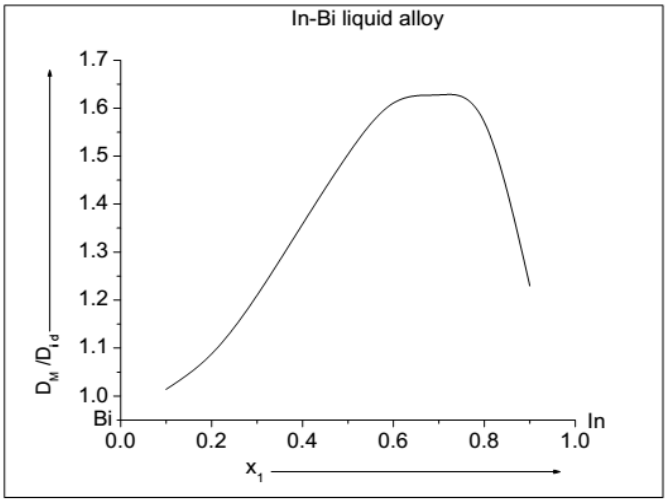

Figure 4.26(c): Ratio of diffusion coefficients (D_M/D_{id}) versus concentration of In (x_1) for In−Bi liquid alloy at 900 K.

Fig. 4.26(b) shows that the computed values of α_1 are negative at all concentrations. The concerned liquid alloy is thus compound forming with preferable association between In (=A) and Bi (=B) in the liquid state near to the melting temperature of the alloy. There is

depression in the flattened part of the curve of α_1 at about compound forming concentration which is 0.66. The asymmetry in the value of α_1 is clearly observed. It can also be depicted from the perusal of Fig. 4.26(c) that the theoretically computed values of D_M/D_{id} are positive and greater than one at all concentrations which also verifies the earlier findings from the computation of $S_{CC}(0)$ and α_1.

4.16.3 $S_{CC}(0)$, α_1 and D_M/D_{id} for Al−Fe liquid alloy at 1873 K

Following the similar procedure as mentioned in the former section, the theoretical, experimental and ideal values of $S_{CC}(0)$ are computed for Al−Fe liquid alloy at 1873 K. The essential ingredients required for this purpose, such as mole fractions of the complex and free monomers are taken from the Table 4.3 and the pairwise interaction energy parameters are taken from the Section 4.4.3. Additionally, the derivative terms of the mole fractions of free monomers (x'_A and x'_B) and the complex ($x'_{A_\mu B}$) are determined from Eqs. (3.124) and (3.123) respectively. Theoretical values of α_1 and D_M/D_{id} for the concerned liquid alloys are computed from Eqs. (3.128) and (3.133) respectively with the knowledge of determined values of $S_{CC}(0)$. All the computed values as a function of concentration are presented in Table 4.39. The plots of $S_{CC}(0)$, α_1 and D_M/D_{id} as a function of concentration are portrayed in Figs. 4.27(a−c).

Table 4.39: The computed values of $S_{CC}(0)$, α_1 and D_M/D_{id} as a function of concentration for Al−Fe liquid alloy at 1873 K

Concentration of Al (x_1)	$S_{CC}(0)$			α_1	D_M/D_{id}
	Theoretical	Experimental*	Ideal		
0.1	0. 0670	0. 0640	0.09	-0.0332	1.3436
0.2	0. 0989	0. 0835	0.16	-0.0582	1.6177
0.3	0. 1074	0. 0979	0.21	-0.0872	1.9550
0.4	0. 1075	0. 1031	0.24	-0.1097	2.2316
0.5	0.0990	0. 1006	0.25	-0.1324	2.5262
0.6	0. 0876	0. 0953	0.24	-0.1481	2.7386
0.7	0. 0780	0. 0842	0.21	-0.1448	2.6937
0.75**	0.0754	……	…….	-0.0847	1.9254
0.8	0. 0705	0. 0702	0.16	-0.1128	2.2709
0.9	0. 0528	0. 0497	0.09	-0.0658	1.7039

*Compound forming concentration

**Hulrgren *et al*. (1973)

Fig. 4.27 (a) shows that the computed as well as the experimental values of $S_{CC}(0)$ are less than the ideal values throughout the entire concentration indicating that the concerned liquid alloy is ordering in nature at its melting temperature. The deviation between the ideal and theoretical values of $S_{CC}(0)$ is maximum near about the compound forming concentration which is $x_{CC} = x_1 = 0.75$, where 1 for Al. Both the theoretical and the experimental values of $S_{CC}(0)$ are in good agreement.

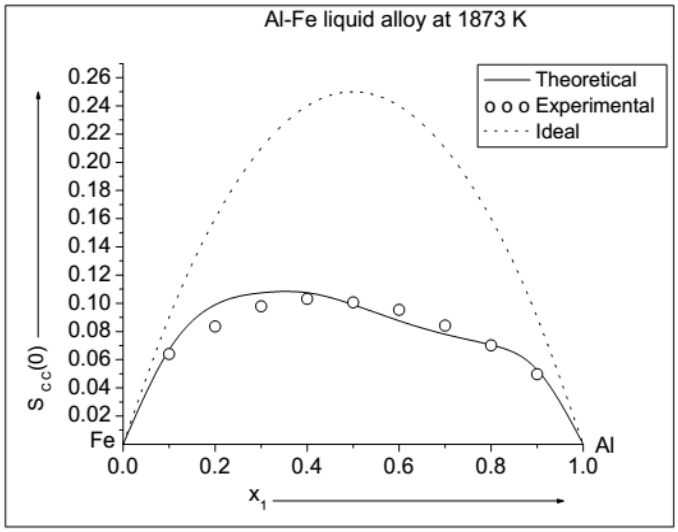

Figure 4.27(a): Concentration fluctuation in ling wavelength limit ($S_{CC}(0)$) versus concentration of Al (x_1) for Al−Fe liquid alloy at 1873 K.

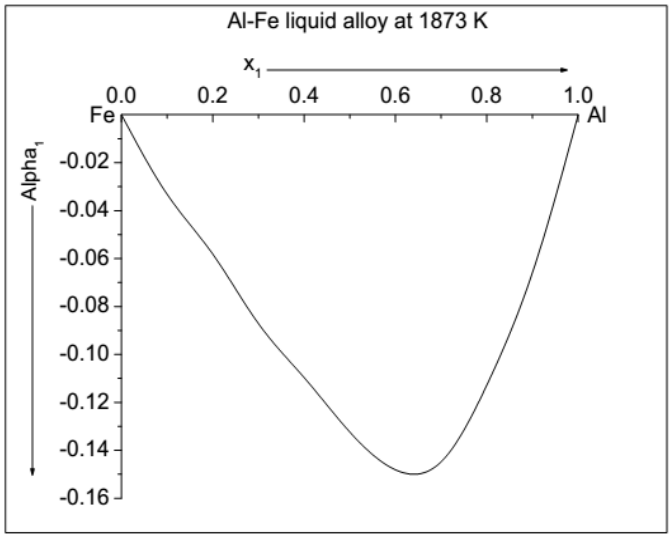

Figure 4.27(b): Chemical short range parameter (α_1) versus concentration of Al (x_1) for Al−Fe liquid alloy at 1873 K.

The perusal of Fig. 4.27 (b) notifies that theoretically computed values of α_1 are negative at all concentrations which also verifies the nature of liquid alloy described by $S_{CC}(0)$. Further, there is asymmetry in the behaviour of α_1. The computed values of D_M/D_{id} is positive and greater than one at all concentrations, Fig. 4.27 (c). These values also verify the earlier findings about the structural behaviour of the liquid alloy. With no doubt, it can thus be stated that Al−Fe liquid alloy at 1873 K shows hetero−coordinating tendency in which the association of the type A−B (A=Al and B=Fe) is favoured.

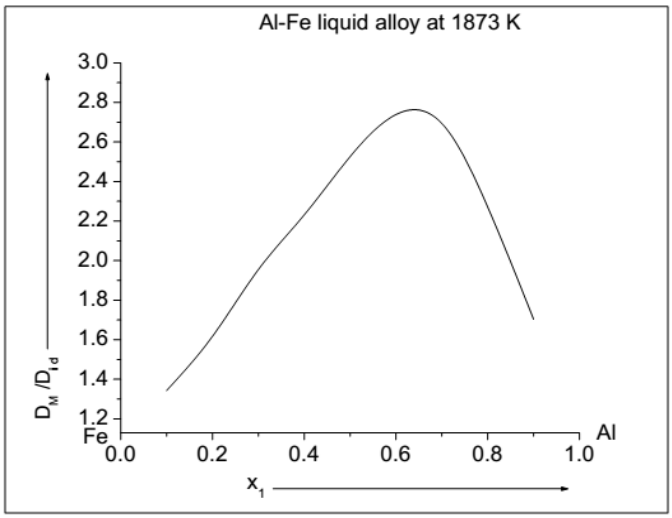

Figure 4.27(c): Ratio of diffusion coefficients (D_M/D_{id}) versus concentration of Al (x_1) for Al−Fe liquid alloy at 1873 K.

4.16.4 $S_{CC}(0)$, α_1 and D_M/D_{id} for Al−Mg liquid alloy at 1073 K

In Al−Mg liquid alloy, we have assumed the existence of the complex of the type $A_\mu B_\nu$ (=Al_3Mg_2) at 1073 K. The theoretical value of $S_{CC}(0)$ for this system is computed using Eq. (3.128) with the knowledge of essential input parameters. For this purpose, the values of mole fractions of the complex and free species are taken from Table 4.4 and that of pairwise interaction energies are taken from the Section 4.4.4. The values of x'_A, and x'_B are obtained from Eq. (3.24) while that of $x'_{A_\mu B}$ are obtained from Eq. (3.118) at all concentrations. The ideal and the experimental values of $S_{CC}(0)$ are calculated from Eqs. (3.113) and (3.111) respectively. The values of α_1 and D_M/D_{id} are calculated from Eqs. (3.128) and (3.133) respectively with the help of determined values of $S_{CC}(0)$. It has been

already mentioned that the values of essential input parameters required for these methodologies are the same as used to compute the free energy of mixing. The computed values of $S_{CC}(0)$, α_1 and D_M/D_{id} as a function of concentration for Al–Mg liquid alloy at 1073 K are tabulated in Table 4.40. The compositional dependence of $S_{CC}(0)$, α_1 and D_M/D_{id} are plotted in Figs. 4.28(a–c).

Table 4.40: The computed values of $S_{CC}(0)$, α_1 and D_M/D_{id} as a function of concentration for Al–Mg liquid alloy at 1073 K

Concentration of Al (x_1)	$S_{CC}(0)$			α_1	D_M/D_{id}
	Theoretical	Experimental**	Ideal		
0.1	0.0899	0.0890	0.09	-0.0001	1.0011
0.2	0.1574	0.1526	0.16	-0.0016	1.0163
0.3	0.1856	0.1767	0.21	-0.0130	1.1313
0.4	0.1737	0.1770	0.24	-0.0368	1.3856
0.5	0.1324	0.1669	0.25	-0.0815	1.8878
0.6*	0.1247	0.1431	0.24	-0.0847	1.9254
0.7	0.1542	0.1202	0.21	-0.0349	1.3620
0.8	0.1418	0.0944	0.16	-0.0127	1.1281
0.9	0.0829	0.0592	0.09	-0.0085	1.0857

*Compound forming concentration
**Hultgren *et al*. (1973)

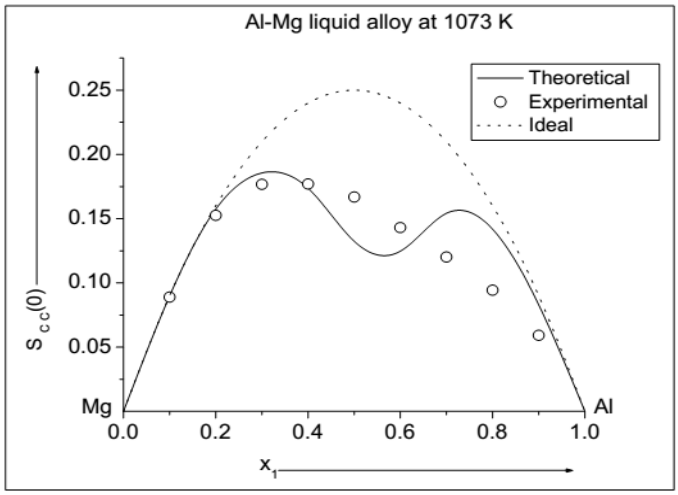

Figure 4.28(a): Concentration fluctuation in ling wavelength limit ($S_{CC}(0)$) versus concentration of Al (x_1) for Al–Mg liquid alloy at 1073 K.

It can be observed that the theoretical and the experimental values of $S_{CC}(0)$ are less than that of ideal values throughout the entire concentration range, Fig. 4.28(a). It can be thus stated that the concerned system is ordering in nature in which there is preferred

association between the atoms of Al and Mg in the liquid melt. The perusal of the Fig. 4.28(a) also notifies that there is a sharp depression in the values of $S_{CC}(0)$ at about $x_1 = 0.61$, which is close to the complex forming concentration ($x_1 = 0.60$, 1 stands for Al). Both the theoretical and the experimental values of $S_{CC}(0)$ are in reasonable agreement.

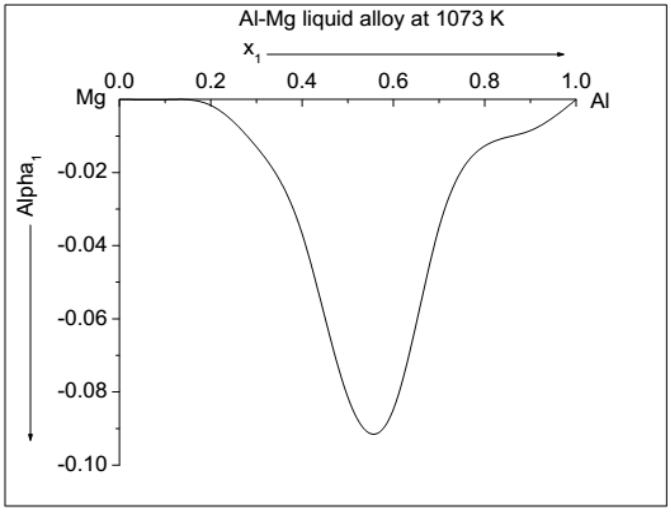

Figure 4.28(b): Chemical short range parameter (α_1) versus concentration of Al (x_1) for Al−Mg liquid alloy at 1073 K.

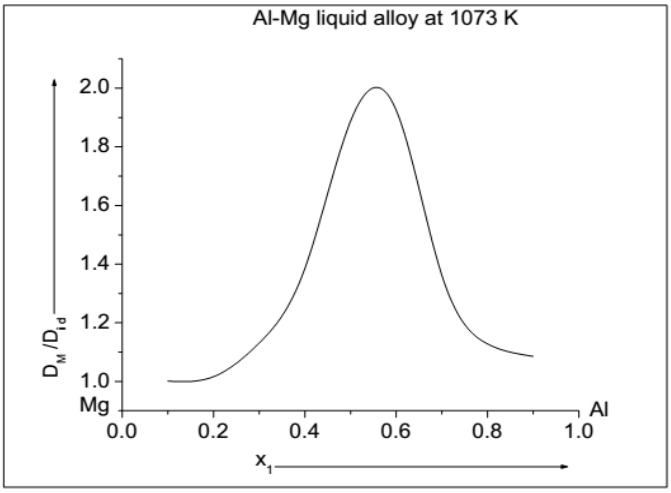

Figure 4.28(c): Ratio of diffusion coefficients (D_M/D_{id}) versus concentration of Al (x_1) for Al−Mg liquid alloy at 1073 K.

Fig. 4.28(b) shows that the theoretically obtained value α_1 is negative and at all concentrations. This negative value strengthens our earlier finding about the

hetero−coordinating nature of the initial melt. There is sharp peak in the value of α_1 at about $x_1 = 0.56$ which is much closure to the compound forming concentration of the alloy. It can be observed from the Fig. 4.28(c) that the computed value of D_M/D_{id} is found to be positive and greater than one at all concentration which is also indicative for the mixing behaviour of the liquid mixture. The compositional dependence of the computed values of $S_{CC}(0)$, α_1 and D_M/D_{id} stand in favour of the ordering nature of Al−Mg liquid alloy at 1073 K.

4.17 Structural properties of binary liquid alloys at different temperatures

In this section, we present the procedures to predict the structural properties of some binary liquid alloys at different temperatures by extending regular associated solution model. The structural properties, such as concentration fluctuation in long wavelength limit ($S_{CC}(0)$), chemical short range order parameter (α_1) and ratio of mutual to intrinsic diffusion coefficients (D_M/D_{id}) have been predicted for Bi−Tl, In−Bi, Al−Fe and Al−Mg liquid alloys at different temperatures. To predict the structural properties of preferred liquid alloys, we have used the same set of interaction energy parameters those were used for the prediction of thermodynamic properties at different temperatures (Section 4.13) to maintain consistency. As stated, the further assumptions for this purpose are as described in the Section 4.13. The results and discussion of these properties for the corresponding liquid alloys are also included in the following sections.

4.18 Structural properties of Bi−Tl liquid alloy at different temperatures

The structural properties of Bi−Tl liquid have been predicted by computing $S_{CC}(0)$, α_1 and D_M/D_{id} with help of theoretical modeling equations at temperatures 750 K, 850 K, 950 K and 1050 K, among which 750 K is its melting temperature. Additionally, the mathematical prediction equations to predict $S_{CC}(0)$ at different temperatures are also included in this section.

4.18.1 Prediction of $S_{CC}(0)$ for Bi−Tl liquid alloy at different temperatures

Theoretical values of $S_{CC}(0)$ are computed from Eq. (3.122) with the help of necessary input ingredients. Herein, it is assumed that the mole fractions of the complex and unassociated monomers are only concentration dependent and hence these values are inherited from Table 4.2. The pairwise interaction energy parameters at different temperatures are taken from the Table 4.17 of the Section 4.13.1. The derivative terms of mole fractions of the complex ($x'_{A_\mu B}$) and the unassociated species (x'_A and x'_B) are determined from Eqs. (3.123) and (3.124) respectively. The ideal values of $S_{CC}(0)$ are obtained from Eq. (3.113) and remains the same at temperatures as depends only upon the concentrations of the free species. The mathematical prediction equations to predict $S_{CC}(0)$ of the system at different temperatures along with the values of the parameters are tabulated in Table 4.41. These prediction equations are obtained from the polynomial fitting equations of fifth order using the computer Software Origin Lab 6.1. Theoretically computed values of $S_{CC}(0)$ as a function of concentration at different temperatures are presented in Table 4.42 and are plotted in Fig. 4.29.

Table 4.41: Prediction equations for $S_{CC}(0)$ at different temperatures for Bi−Tl liquid alloy; $x_l = 0.1 - 0.9$

Physical quantity	Prediction equation	Temp. (K)	Values of parameters (L_Z)					
			L_0	L_1	L_2	L_3	L_4	L_5
$S_{CC}(0)$	$\sum_{Z=0}^{5} L_Z {x_l}^Z$	750	0.00078	0.9060	-1.0449	-3.3920	7.1226	-3.5914
		850	0.00084	0.8829	-0.6132	-4.8365	8.8666	-4.2997
		950	0.00090	0.8761	-0.4648	-5.2375	9.2734	-4.4471
		1050	0.00095	0.8681	-0.3263	-5.5982	9.6301	-4.5737

It is to be noted that $S_{CC}(0) < S_{CC}^{id}(0)$ corresponds to unlike atoms pairing at nearest neighbours and $S_{CC}(0) > S_{CC}^{id}(0)$ is indicative of like atoms pairing at nearest neighbours. It can be observed from Fig. 4.29 that the concentration fluctuation in long wavelength limit ($S_{CC}(0)$) of Bi−Tl liquid alloy increases with increases in temperature beyond its melting temperature. At the compound forming concentration ($x_{CC} = x_1 = 0.5$, 1 is for Tl), the computed values of $S_{CC}(0)$ are 0.1037, 0.1064, 0.1110 and 0.1151 at temperatures 750 K, 850 K, 950 K and 1050 K respectively, where its ideal value is 0.25. The computed values of $S_{CC}(0)$ get closure to the ideal values at corresponding

concentration with increase in the temperature of the liquid alloy. Eventually, it can be forecasted that the concerned liquid alloy shows ideal behaviour at elevated temperatures. More strictly, the present investigations forecast that the mixing properties of the liquid alloy decreases with increase in its temperature. From the perusal of Fig. 4.29, it is observed that at compound forming concentration, the deviation of the computed $S_{CC}(0)$ from the computed $S_{CC}^{id}(0)$ is the highest at temperature 750 K (the deviation = 0.1463) and the lowest at 1050 K (the deviation = 0.1349). These values predicts that the concerned liquid alloy exhibit the strongest tendency for compound formation and hence is most interacting at 750 K whereas is least interacting at 1050 K. Similarly, the values of deviations are 0.1439 and 0.1390 temperatures 850 K and 950 K, respectively forecasting that the alloy is comparatively more interacting at former temperature than the later. These investigations are accordance with the results forecasted by the values of thermodynamic properties. Similar tendency for different liquid alloys are predicted by researchers by employing different techniques (Lee et al, 2004; Awe et al., 2011; Kaptay, 2012; Yadav et al., 2016).

Table 4.42: Predicted values of $S_{CC}(0)$ for Bi−Tl liquid alloys as a function of concentration at different temperatures

Concentration of Tl (x_1)	$S_{CC}(0)$				$S_{CC}^{id}(0)$
	T = 750 K	T = 850 K	T = 950 K	T = 1050 K	
0.1	0.0805	0.0816	0.0823	0.0828	0.09
0.2	0.1225	0.1257	0.1276	0.1291	0.16
0.3	0.1336	0.1391	0.1424	0.1452	0.21
0.4	0.1244	0.1297	0.1342	0.1381	0.24
0.5*	0.1037	0.1064	0.1110	0.1151	0.25
0.6	0.0814	0.0815	0.0855	0.0890	0.24
0.7	0.0635	0.0630	0.0662	0.0690	0.21
0.8	0.0580	0.0594	0.0621	0.0645	0.16
0.9	0.0532	0.0545	0.0562	0.0576	0.09

*Compound forming concentration

4.18.2 Prediction of α_1 and D_M/D_{id} for Bi−Tl liquid alloy at different temperatures

The theoretical values of chemical short range order parameter (α_1) and the ratio of diffusion coefficients (D_M/D_{id}) for Bi−Tl liquid alloy at above mentioned temperatures

are computed from Eqs. (3.128) and (3.133) respectively with the help of predicted values of $S_{CC}(0)$ in Table 4.42. The values of α_1 and D_M/D_{id} so computed at different temperatures as a function of concentration are depicted in Table 4.43. The compositional dependence of α_1 and D_M/D_{id} at different temperatures are plotted in Figs. 4.30(a–b).

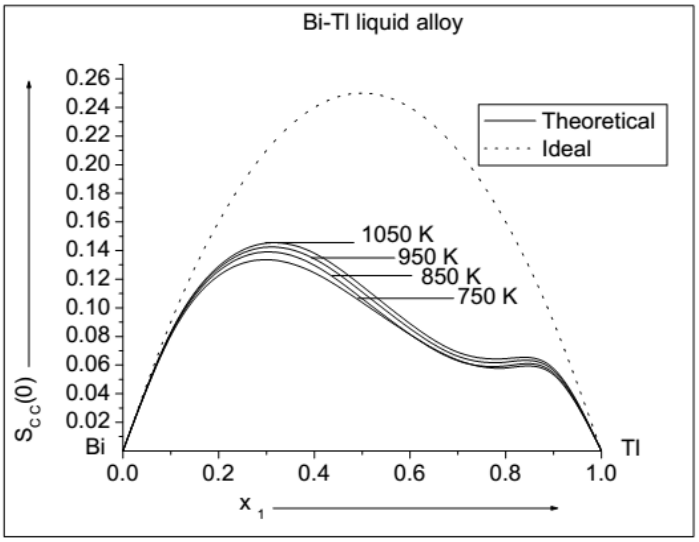

Figure 4.29: Concentration fluctuation in long wavelength limit ($S_{CC}(0)$) versus concentration of Tl (x_1) for Bi–Tl liquid alloy at different temperatures.

Table 4.43: The computed values of α_1 and D_M/D_{id} as a function of concentration for Bi–Tl liquid alloy at different temperatures

Conc. of Tl (x_1)	T = 750 K		T = 850 K		T = 950 K		T = 1050 K	
	α_1	D_M/D_{id}	α_1	D_M/D_{id}	α_1	D_M/D_{id}	α_1	D_M/D_{id}
0.1	-0.0117	1.1185	-0.0103	1.1035	-0.0093	1.0940	-0.0086	1.0864
0.2	-0.0298	1.3066	-0.0265	1.2727	-0.0248	1.2541	-0.0234	1.2392
0.3	-0.0541	1.5717	-0.0485	1.5099	-0.0453	1.4744	-0.0427	1.4459
0.4	-0.0850	1.9289	-0.0784	1.8508	-0.0731	1.7881	-0.0687	1.7373
0.5*	-0.1237	2.4117	-0.1189	2.3500	-0.1112	2.2514	-0.1049	2.1713
0.6	-0.1631	2.9494	-0.1602	2.9449	-0.1531	2.8075	-0.1450	2.6956
0.7	-0.1875	3.3079	-0.1830	3.2316	-0.1784	3.1716	-0.1696	3.0416
0.8	-0.1495	2.7572	-0.1450	2.6959	-0.1363	2.5776	-0.1291	2.4819
0.9	-0.0648	1.6929	-0.0611	1.6510	-0.0568	1.6025	-0.0533	1.5633

*Compound forming concentration

It has been already stated that the computation of α_1 helps to understand the nature of atomic arrangements in the liquid alloy. More precisely, it should be noted that $\alpha_1 < 0$ is indicative of hetero–atomic arrangement, $\alpha_1 > 0$ corresponds to homo–atomic

arrangements and $\alpha_1 = 0$ corresponds to random distribution of atoms in the nearest neighbours of liquid mixture. The perusal of Fig. 4.30(a) reveals that the $\alpha_1 < 0$ at all concentrations and preferred temperatures. However, the plots of α_1 as a function of concentration become shallow with the increase of temperature of the liquid alloy beyond its melting temperature predicting a lower degree of association or compound formation with increase in temperature. At the compound forming concentration ($x_{CC} = 0.5$), the values of α_1 are -0.1237, -0.1189, -0.1112 and -0.1049 at temperatures 750 K, 850 K, 950 K and 1050 K respectively. These values predict that the liquid alloy shows the strongest tendency towards chemical ordering at 750 K (its melting temperature) and gradually this tendency decreases at elevated temperatures. These findings are accordance with the nature predicted by the thermodynamic properties and $S_{CC}(0)$ (Awe et al., 2011).

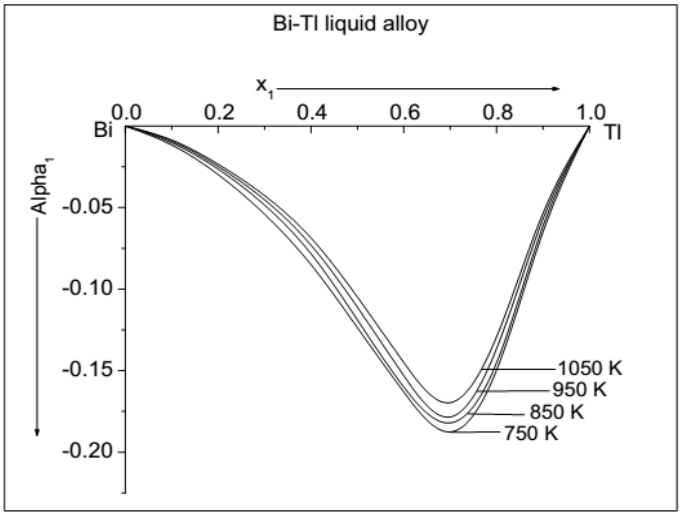

Figure 4.30(a): Chemical short range order parameter (α_1) versus concentration of Tl (x_1) for Bi−Tl liquid alloy at different temperatures.

To further strengthen our findings about the nature of local arrangement of atoms in the initial melt of the concerned alloy, we have also computed the ratio of diffusion coefficients (D_M/D_{id}) at different temperatures. Once again recalling that $\frac{D_M}{D_{id}} > 1$ corresponds to chemical ordering, $\frac{D_M}{D_{id}} < 1$ indicates segregation leading to phase separation and $\frac{D_M}{D_{id}} = 1$ refers to random or ideal mixing in the liquid alloy. It can be

observed from Fig. 4.30 (b) that the computed values of D_M/D_{id} are greater than one at all concentration and preferred temperatures of the liquid alloy indicating the presence of chemical ordering. However, the values of D_M/D_{id} gradually decreases and move towards one with increase in temperature beyond the melting temperature of the liquid alloy. It can be predicted that the liquid alloy shows ideal behaviour at higher temperatures. At the compound forming concentration, the value of D_M/D_{id} is the maximum (=2.4117) at its melting temperature (750 K) and the minimum (=2.1713) at 1050 K predicting that the tendency towards chemical ordering is strongest at former temperature that the later. Moreover, this alloy is more ordered at 850 K than that of 950 K where respective values of D_M/D_{id} are 2.3500 and 2.2514.

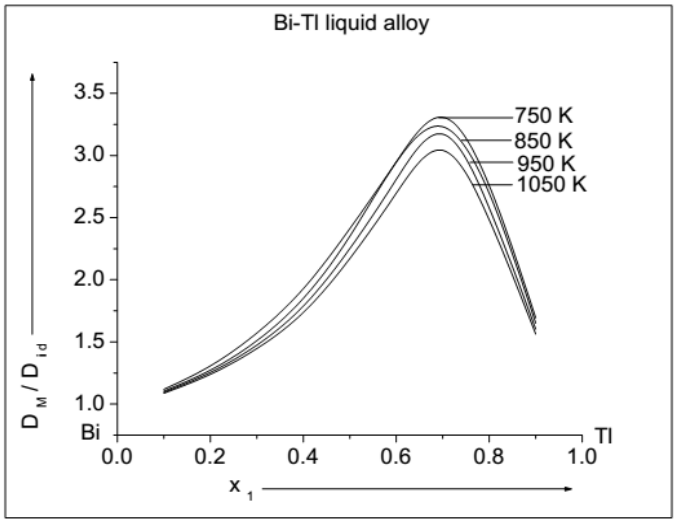

Figure 4.30(b): Ratio of diffusion coefficients (D_M/D_{id}) versus concentration of Tl (x_1) for Bi−Tl liquid alloy at different temperatures.

4.19 Structural properties of In−Bi liquid alloy at different temperatures

In structural properties, we have computed $S_{CC}(0)$, α_1 and D_M/D_{id} for In−Bi liquid alloy at temperatures 900 K, 1000 K, 1100 K and 1200 K, among which 900 K is its melting temperature. In the following sub−sections, the methodologies to obtain such properties and results and discussion related with them are outlined.

4.19.1 Prediction of $S_{CC}(0)$ for In−Bi liquid alloy at different temperatures

The values of $S_{CC}(0)$ for the concerned alloy are computed at temperatures of interests using Eq. (3.122) with the knowledge of necessary input parameters. The mole fractions of the complex and free monomers are inherited from Table 4.2 and the pairwise interaction energies are taken from the Section 4.4.2. The values of x'_A, x'_B and $x'_{A_\mu B}$ are obtained from Eqs. (3.124) and (3.123) following the similar trends as mentioned in the Section 4.18.1. The values of $S^{id}_{CC}(0)$ are computed from Eqs. (3.111) and (3.113) respectively at above mentioned temperatures. The mathematical equations to predict $S_{CC}(0)$ at different temperatures along with the values of essential parameters are presented in Table 4.44. The values $S_{CC}(0)$ as a function of concentration for In−Bi liquid alloy at different temperatures are tabulated in Table 4.45. The plots of $S_{CC}(0)$ so obtained as a function of concentration are portrayed in Fig. 4.31.

Table 4.44: Prediction equations for $S_{CC}(0)$ at different temperatures for In−Bi liquid alloy; $x_l = 0.1 - 0.9$

Physical quantity	Prediction equation	Temp. (K)	Values of parameters (L_Z)					
			L_0 (10^{-5})	L_1	L_2	L_3	L_4	L_5
$S_{CC}(0)$	$\sum_{Z=0}^{5} L_Z x_l^Z$	900	6.7134	1.0272	-1.2363	-2.0292	4.6428	-2.4039
		1000	5.0874	1.0330	-1.1840	-2.1597	4.7295	-2.4183
		1100	2.6923	1.0381	-1.1459	-2.2435	4.7653	-2.4135
		1200	2.7797	1.0439	-1.1190	-2.3092	4.7968	-2.4119

Table 4.45: Predicted values of $S_{CC}(0)$ for In−Bi liquid alloys as a function of concentration at different temperatures

Concentration of In (x_1)	$S_{CC}(0)$				$S^{id}_{CC}(0)$
	T = 900 K	T = 1000 K	T = 1100 K	T = 1200 K	
0.1	0.0888	0.0897	0.0904	0.0912	0.09
0.2	0.1471	0.1495	0.1515	0.1532	0.16
0.3	0.1735	0.1771	0.1801	0.1828	0.21
0.4	0.1767	0.1810	0.1847	0.1879	0.24
0.5	0.1661	0.1708	0.1747	0.1781	0.25
0.6	0.1490	0.1532	0.1569	0.1600	0.24
0.66*	0.1377	0.1414	0.1447	0.1475	……
0.7	0.1290	0.1324	0.1354	0.1379	0.21
0.8	0.1019	0.1040	0.1057	0.1073	0.16
0.9	0.0732	0.0741	0.0748	0.0754	0.09

*Compound forming concentration

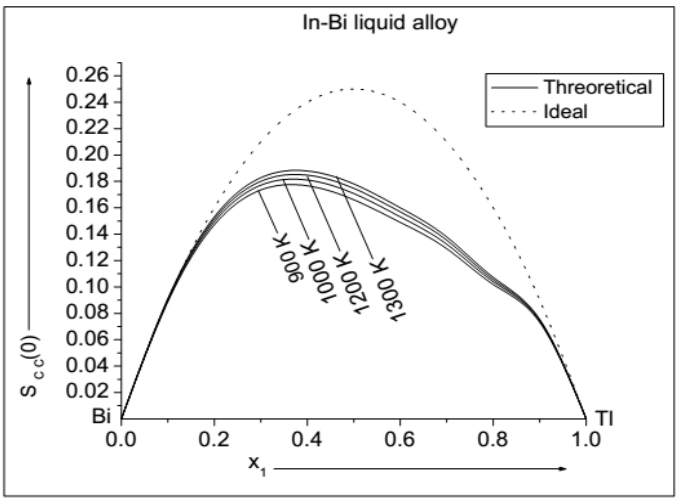

Figure 4.31: Concentration fluctuation in long wavelength limit ($S_{CC}(0)$) versus concentration of In (x_1) for In−Bi liquid alloy at different temperatures.

Fig. 4.31 shows that variation of $S_{CC}(0)$ with temperature follows the similar trend as that of free energy of mixing (Section 4.14.2). The predicted values of $S_{CC}(0)$ are greater than the ideal values in the concentration range $x_1 < 0.16$ at temperatures above 1100 K indicating the transformation from ordering to segregating nature. Whereas the computed values of $S_{CC}(0)$ are less than the ideal values at rest of the concentrations at all preferred temperatures indicating the hetero−coordinating behaviour is favoured in the liquid alloy at these concentrations and temperatures. However, the computed values of $S_{CC}(0)$ gets closure to the ideal values with increase in its temperature which refers to weaker tendency towards compound formation. The deviation between the computed and ideal values of $S_{CC}(0)$ at compound formation concentration ($x_{CC} = x_1 = 0.66$) is greatest at 900 K (deviation = 0.0867) and the least at 1200 K (deviation = 0.0769) revealing the greatest tendency towards compound formation at former temperature than the later. Similarly, the deviation (= 0.083) is greater at 1000 K than that of 1100 K (deviation = 0.0797) indicating the liquid alloy is more ordered at former temperature than the later.

4.19.2 Prediction of α_1 and D_M/D_{id} for In−Bi liquid alloy at different temperatures

Theoretical values of α_1 and D_M/D_{id} are computed at above mentioned temperatures for In-Bi liquid alloy from Eqs. (3.128) and (3.133) with the help of determined values of

$S_{CC}(0)$ in Table 4.45. The values so computed at different temperatures as a function of concentrations is tabulated in Table 4.46 are plotted in Figs. 4.32(a–b).

Table 4.46: The computed values of α_1 and D_M/D_{id} as a function of concentration for In–Bi liquid alloy at different temperature

Conc. of In (x_1)	T = 900 K		T = 1000 K		T = 1100 K		T = 1200 K	
	α_1	D_M/D_{id}	α_1	D_M/D_{id}	α_1	D_M/D_{id}	α_1	D_M/D_{id}
0.1	-0.0014	1.0141	-0.0003	1.0034	0.0005	0.9946	0.0013	0.9873
0.2	-0.0087	1.0877	-0.0070	1.0704	-0.0056	1.0560	-0.0044	1.0442
0.3	-0.0206	1.2103	-0.0182	1.1858	-0.0163	1.1654	-0.0147	1.1489
0.4	-0.0346	1.3585	-0.0316	1.3261	-0.0291	1.2992	-0.0270	1.2773
0.5	-0.0480	1.5040	-0.0443	1.4639	-0.0413	1.4308	-0.0388	1.4038
0.6	-0.0576	1.6107	-0.0536	1.5663	-0.0503	1.5298	-0.0476	1.4997
0.66*	-0.0609	1.6469	-0.0569	1.6029	-0.0538	1.5669	-0.0511	1.5371
0.7	-0.0591	1.6277	-0.0553	1.5856	-0.0523	1.5514	-0.0497	1.5228
0.8	-0.0540	1.5709	-0.0511	1.5390	-0.0488	1.5132	-0.0468	1.4911
0.9	-0.0225	1.2297	-0.0211	1.2151	-0.0199	1.2034	-0.0190	1.1933

*Compound forming concentration

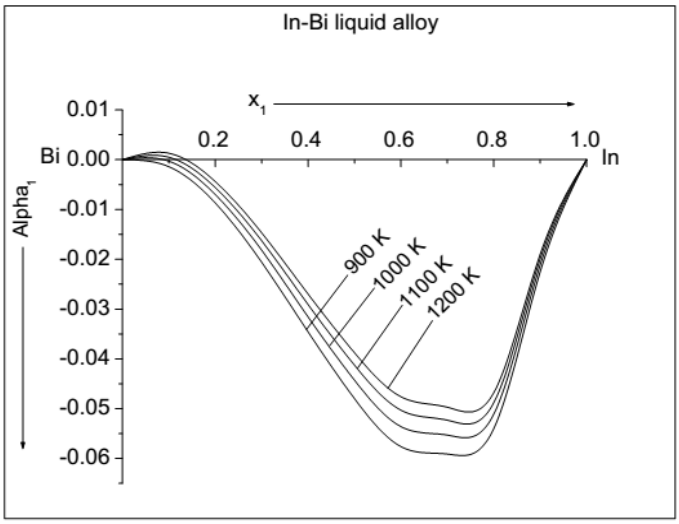

Figure 4.32(a): Chemical short range order parameter (α_1) versus concentration of In (x_1) for In–Bi liquid alloy at different temperatures.

The perusal of Fig. 4.32(a) shows that the computed values α_1 as a function of concentration becomes shallow with the increase of temperature which is indicative of a lower degree of association or compound formation with increase in temperature of the liquid alloy beyond its melting temperature. The computed values of α_1 are positive in the

concentration range $x_1 < 0.16$ at temperatures 1100 K and 1200 K which predicts the transformation from ordering to segregation and is in favour of nature predicted by $S_{CC}(0)$. Also at complex forming concentration ($x_{CC} = x_1 = 0.66$), the computed values of α_1 are -0.0609, -0.0569, -0.0538 and -0.0511 at temperatures 900 K, 1000 K, 1100 K and 1200 K. These values also suggest that the tendency towards compound formation gradually decreases with increase in temperature of the liquid alloy. The peaks of all the plots of α_1 as a function of concentration lie at about compound forming concentration.

Fig. 4.32(b) shows that the compositional dependence of D_M/D_{id} decreases with increase in temperature forecasting the decrease in tendency of chemical ordering in the liquid alloy at higher temperatures. The values of D_M/D_{id} are found to be less than one in the concentration range $x_1 < 0.16$ at temperatures 1100 K and 1200 K and these results also support the transformation from chemical ordering to segregation as predicted by α_1. The peaks of D_M/D_{id} at all preferred temperatures lie at about the compound formation concentration ($x_1 = 0.66$). At this concentration the values of D_M/D_{id} is the maximum (=1.6469) at 900 K and the minimum (=1.5371) at 1200 K which indicates that the alloy is the most interacting at former temperature than the later. Similarly, the value of D_M/D_{id} at this concentration is greater at 1000 K than that of 1100 K predicting that the alloy is more interacting at former than the later temperature.

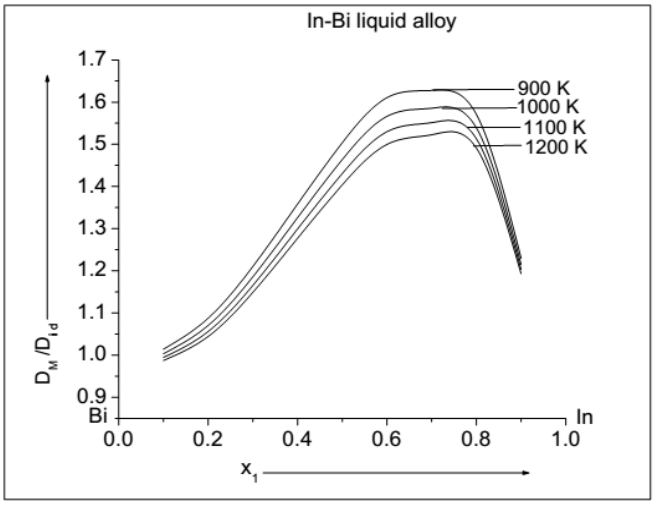

Figure 4.32(b): Ratio of diffusion coefficients (D_M/D_{id}) versus concentration of In (x_1) for In−Bi liquid alloy at different temperatures.

4.20 Structural properties of Al−Fe liquid alloy at different temperatures

The structural properties, such as $S_{CC}(0)$, α_1 and D_M/D_{id} of Al−Fe liquid have been computed at temperatures 1873 K, 1973 K, 2073 K and 2173 K; 1873 K being its melting temperature. The methodology to compute along with the results and discussion associated with such findings are amended in the following sections.

4.20.1 Prediction of $S_{CC}(0)$ for Al−Fe liquid alloy at different temperatures

The theoretical and the ideal values of $S_{CC}(0)$ for the concerned system are computed at above mentioned temperatures using Eqs. (3.122) and (3.113) respectively. The essential ingredients required for this purpose, namely mole fractions of complex and free monomers are inherited from Table 4.3 and pairwise interaction energies are taken from the Section 4.4.3. x'_A, x'_B and $x'_{A_\mu B}$ are estimated using corresponding Eqs. (3.124) and (3.123). The mathematical equations to predict $S_{CC}(0)$ as a function of concentration at different temperatures along with the values of essential parameters are depicted in Table 4.47. The procedures of obtaining the prediction equations and above included parameters are as mentioned in the Section 4.18.1. The computed values of $S_{CC}(0)$ and $S_{CC}^{id}(0)$ as a function of concentration at different temperatures are depicted in Table 4.48. The plots of $S_{CC}(0)$ and $S_{CC}^{id}(0)$ as a function of concentration at different temperatures are portrayed in Fig. 4.33.

Table 4.47: Prediction equations for $S_{CC}(0)$ at different temperatures for Al−Fe liquid alloy; $x_l = 0.1 - 0.9$

Physical quantity	Prediction equation	Temp. (K)	Values of parameters (L_Z)					
			L_0 (10^{-4})	L_1	L_2	L_3	L_4	L_5
$S_{CC}(0)$	$\sum_{Z=0}^{5} L_Z {x_l}^Z$	1873	5.7273	0.8224	-1.8218	0.5813	1.7579	-1.3397
		1973	5.0331	0.8422	-1.8286	0.5774	1.7023	-1.2933
		2073	4.8164	0.8605	-1.8269	0.5509	1.6736	-1.2580
		2173	4.4808	0.8783	-1.8282	0.5448	1.6118	-1.2067

Table 4.48: The computed values of $S_{CC}(0)$ as a function of concentration at different temperatures for Al–Fe liquid alloy

Concentration of Al (x_1)	$S_{CC}(0)$				$S_{CC}^{id}(0)$
	T = 1873 K	T = 1973 K	T = 2073 K	T = 2173 K	
0.1	0.0670	0.0687	0.0703	0.0719	0.09
0.2	0.0989	0.1026	0.1062	0.1097	0.16
0.3	0.1074	0.1122	0.1170	0.1216	0.21
0.4	0.1075	0.1131	0.1185	0.1240	0.24
0.5	0.0990	0.1045	0.1100	0.1155	0.25
0.6	0.0876	0.0926	0.0974	0.1022	0.24
0.7	0.0780	0.0816	0.0852	0.0888	0.21
0.75*	0.0754	0.0782	0.0810	0.0837	……
0.8	0.0705	0.0725	0.0745	0.0764	0.16
0.9	0.0528	0.0531	0.0534	0.0536	0.09

*Compound forming concentration

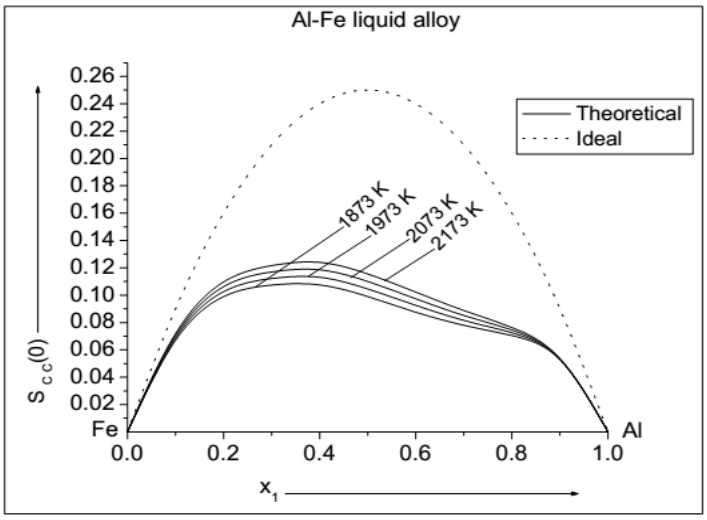

Figure 4.33: Concentration fluctuation in long wavelength limit ($S_{CC}(0)$) versus concentration of Al (x_1) for Al–Fe liquid alloy at different temperatures.

Fig. 4.33 shows that the computed values of $S_{CC}(0)$ gradually increases and get closure to ideal values with increase in temperature of the liquid alloy above its melting temperature. The theoretical investigations thus forecast that the tendency to form complex decreases with increase in temperature and hence the liquid alloy shows ideal behaviour. These findings are accordance with the predictions made by analyzing the thermodynamic properties at different temperatures. At complex formation concentration ($x_{CC} = x_1 = 0.75$), the deviation between the ideal and computed values of $S_{CC}(0)$ are

0.1121, 0.1093, 0.1065 and 0.1038 at temperatures 1873 K, 1973 K, 2073 K and 2173 K respectively predicting that the concerned system to be the most interacting at 1873 K (melting temperature) and the least at 2173 K.

4.20.2 Prediction of α_1 and D_M/D_{id} for Al-Fe liquid alloy at different temperatures

Theoretical values of α_1 and D_M/D_{id} at temperatures of interests for the concerned system are obtained using Eqs. (3.128) and (3.133) respectively with the aid of determined values of $S_{CC}(0)$ in Table 4.48. The values so computed are tabulated in Table 4.49. Figs. 4.34(a–b) display the plots of compositional dependence of α_1 and D_M/D_{id} at different temperatures.

Table 4.49: The computed values of α_1 and D_M/D_{id} as a function of concentration for Al–Fe liquid alloy at different temperatures

Conc. of Al (x_1)	T = 1873 K		T = 1973 K		T = 2073 K		T = 2173 K	
	α_1	D_M/D_{id}	α_1	D_M/D_{id}	α_1	D_M/D_{id}	α_1	D_M/D_{id}
0.1	-0.0332	1.3436	-0.0301	1.3100	-0.0272	1.2797	-0.0246	1.2520
0.2	-0.0582	1.6177	-0.0530	1.5595	-0.0482	1.5068	-0.0439	1.4589
0.3	-0.0872	1.9550	-0.0801	1.8710	-0.0737	1.7953	-0.0677	1.7266
0.4	-0.1097	2.2316	-0.1009	2.1225	-0.0929	2.0246	-0.0856	1.9362
0.5	-0.1324	2.5262	-0.1222	2.3922	-0.1129	2.2727	-0.1044	2.1655
0.6	-0.1481	2.7386	-0.1374	2.5933	-0.1277	2.4638	-0.1188	2.3477
0.7	-0.1448	2.6937	-0.1359	2.5730	-0.1277	2.4638	-0.1201	2.3646
0.75*	-0.1298	2.4905	-0.1228	2.3995	-0.1164	2.3153	-0.1103	2.2386
0.8	-0.1128	2.2709	-0.1077	2.2076	-0.1030	2.1487	-0.0986	2.0940
0.9	-0.0658	1.7039	-0.0650	1.6947	-0.0640	1.6860	-0.0635	1.6777

*Compound forming concentration

It can be observed from Fig. 4.34(a) that plots of α_1 shallows with increased in temperature of the liquid alloy indicating the decrease in ordering or compound forming behaviour at higher temperatures. At the compound forming concentration, the values of α_1 are computed to be -0.1298, -0.1228, -0.1164 and -0.1103 at temperatures 1873 K, 1973 K, 2073 K and 2173 K respectively forecasting the similar results as by $S_{CC}(0)$ in the former section. The perusal of Fig. 4.34(b) indicates that the values of D_M/D_{id} decreases with increase in temperature of the liquid alloy which reveals that the strength of chemical ordering in the melt decreases at higher temperatures. However, the values of

D_M/D_{id} are greater than one at all preferred temperatures throughout the entire concentration range indicating that the chemical ordering still prevails in the melt. The nature predicted by D_M/D_{id} is similar to that by α_1 and $S_{CC}(0)$ at higher temperatures.

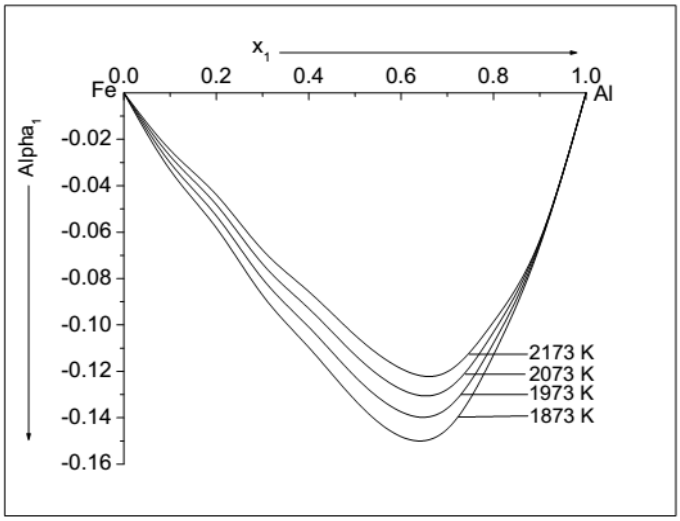

Figure 4.34(a): Chemical short range order parameter (α_1) versus concentration of Al (x_1) for Al−Fe liquid alloy at different temperatures.

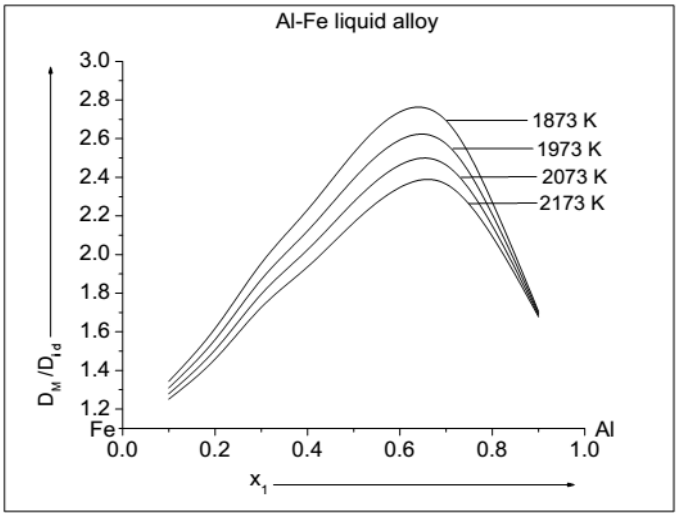

Figure 4.34(b): Ratio of diffusion coefficients (D_M/D_{id}) versus concentration of Al (x_1) for Al−Fe liquid alloy at different temperatures.

4.21 Structural properties of Al−Mg liquid alloy at different temperatures

The structural properties of Al−Mg liquid alloy have been analyzed by computing $S_{CC}(0)$, α_1 and D_M/D_{id} at temperatures 1073 K, 1173 K, 1273 K and 1373 K, among which 1073

K is its melting temperature. In the following sub−sections, we present the methodologies amended to compute the above mentioned parameters along with results and discussion related to them.

4.21.1 Prediction of $S_{CC}(0)$ for Al−Mg liquid alloy at different temperatures

Theoretical values of $S_{CC}(0)$ have been predicted at above mentioned temperatures with the help of modeling Eq. (3.117) within the constraints of the preferred model. For this purpose, the values of mole fractions of complex and unassociated atoms are taken from Table 4.4 and the values of pairwise interaction energy parameters are taken from the Section 4.4.4. The values of x'_A, x'_B and $x'_{A_\mu B_\nu}$ are determined from the corresponding Eqs. (3.119) and (3.118) following the similar trends as mentioned in the Section 4.18.1. The values of temperature independent quantity $S^{id}_{CC}(0)$ are computed using Eq. (3.113). The mathematical equations (obtained by polynomial fitting of eighth order) to predict $S_{CC}(0)$ at different temperatures along with the values of essential parameters are tabulated in Table 4.50. The values so computed as a function of concentration at different temperatures are depicted in Table 4.51. Fig. 4.35 displays the plots of $S_{CC}(0)$ as a function of concentration for the concerned system at different temperatures.

Table 4.50: Prediction equations for $S_{CC}(0)$ at different temperatures for Al−Mg liquid alloy; $x_l = 0.1 - 0.9$

Physical quantity	Prediction equation	Parameters L_Z	Values of L_Z			
			T = 1073 K	T = 1173 K	T = 1273 K	T = 1373 K
$S_{CC}(0)$	$\sum_{Z=0}^{8} L_Z x_l^Z$	L_0 (10^{-4})	-0.9560	-1.0144	-1.0704	-1.0817
		L_1	1.8625	1.9448	1.9867	1.9606
		L_2	-20.1561	-21.4074	-22.1120	-21.3253
		L_3	157.1877	166.5118	172.7208	166.7305
		L_4	-629.2269	-664.6362	-690.806	-668.3289
		L_5	1321.8578	1394.7637	1452.4785	1405.7000
		L_6	-1494.2325	-1576.6566	-1645.2883	-1590.3616
		L_7	862.5823	910.6590	952.3552	918.2921
		L_8	-199.8747	-211.1790	-221.3346	-212.6671

Fig. 4.35 shows that the computed values of $S_{CC}(0)$ increases with increase in temperature notifying weaker tendency towards compound formation in the melt. It is

observed that $S_{CC}(0) > S_{CC}^{id}(0)$ in the concentration range $x_1 < 0.24$ at temperatures greater than its melting temperature which indicates that the ordering nature transforms into segregating nature in the above mentioned conditions. However, the segregation to ordering transformations takes place in the concentration range $x_1 > 0.24$ at temperatures 1173 K, 1273 K and 1373 K. The deviation between the computed and ideal values of $S_{CC}(0)$ is the maximum (=0.1153) at1073 K and the minimum (=0.1067) at 1373 K revealing the liquid alloy to be the most interacting at former temperature and the least interacting at the later temperature. Likewise, the deviation is more at 1173 K (where the deviation is 0.1126) than that of 1273 K (where the deviation is 0.1097) indicating that the liquid alloy is more interacting at former than the later temperature. These predictions forecasted by the present analysis are similar to that made by the thermodynamic properties.

Table 4.51: The computed values of $S_{CC}(0)$ as a function of concentration for Al–Mg liquid alloy at different temperatures

Concentration of Al (x_1)	$S_{CC}(0)$				$S_{CC}^{id}(0)$
	T = 1073 K	T = 1173 K	T = 1273 K	T = 1373 K	
0.1	0.0899	0.0920	0.0932	0.0943	0.09
0.2	0.1574	0.1605	0.1632	0.1656	0.16
0.3	0.1856	0.1893	0.1926	0.1956	0.21
0.4	0.1737	0.1769	0.1799	0.1827	0.24
0.5	0.1324	0.1355	0.1384	0.1431	0.25
0.6*	0.1247	0.1274	0.1303	0.1333	0.24
0.7	0.1542	0.1595	0.1644	0.1688	0.21
0.8	0.1418	0.1455	0.1487	0.1516	0.16
0.9	0.0829	0.0842	0.0853	0.0863	0.09

*Compound forming concentration

4.21.2 Prediction of α_1 and D_M/D_{id} for Al–Mg liquid alloy at different temperatures

The values of α_1 and D_M/D_{id} for the concerned system are computed at above mentioned temperatures using Eqs. (3.128) and (3.133), respectively with the knowledge of above determined values of $S_{CC}(0)$ in Table 4.51 of the former section. The values so computed for Al–Mg liquid alloy at different temperatures for entire range of concentration are presented in Table 4.52. These values are portrayed in Figs. 4.36(a–b).

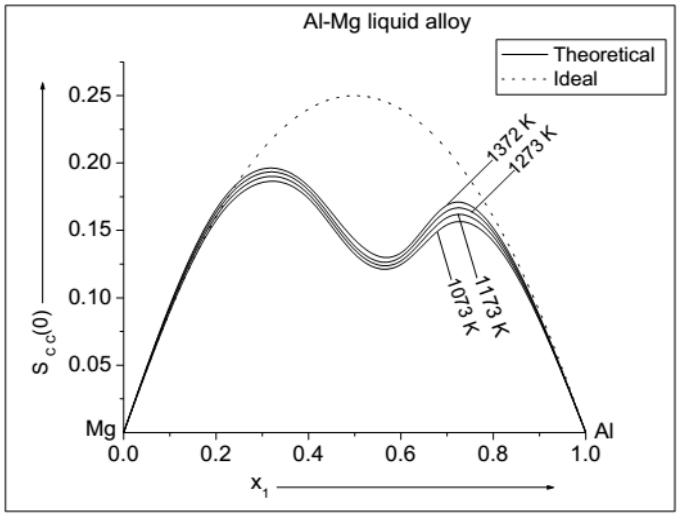

Figure 4.35: Concentration fluctuation in long wavelength limit ($S_{CC}(0)$) versus concentration of Al (x_1) for Al−Mg liquid alloy at different temperatures.

Table 4.52: The computed values of α_1 and D_M/D_{id} as a function of concentration for Al−Mg liquid alloy at different temperatures

x_1	T = 1073 K		T = 1173 K		T = 1273 K		T = 1373 K	
	α_1	D_M/D_{id}	α_1	D_M/D_{id}	α_1	D_M/D_{id}	α_1	D_M/D_{id}
0.1	-0.0001	1.0011	0.0022	0.9779	0.0035	0.9655	0.0045	0.9549
0.2	-0.0016	1.0163	0.0003	0.9971	0.0019	0.9807	0.0034	0.9664
0.3	-0.0130	1.1313	-0.0108	1.1094	-0.0090	1.0903	-0.0073	1.0735
0.4	-0.0368	1.3816	-0.0344	1.3565	-0.0323	1.3338	-0.0304	1.3133
0.5	-0.0815	1.8878	-0.0779	1.8450	-0.0746	1.8064	-0.0695	1.7465
0.6*	-0.0847	1.9254	-0.0813	1.8846	-0.0776	1.8417	-0.0741	1.8004
0.7	-0.0349	1.3620	-0.0307	1.3164	-0.0270	1.2777	-0.0239	1.2444
0.8	-0.0127	1.1281	-0.0099	1.0998	-0.0075	1.0758	-0.0055	1.0551
0.9	-0.0085	1.0857	-0.0068	1.0689	-0.0055	1.0551	-0.0043	1.0429

*Compound forming concentration

The perusal of Fig. 4.36(a) shows that the negative values of α_1 decreases with increase in the temperature of the liquid alloy above 1073 K which is indicative of the decreased tendency towards ordering nature, however, the peaks of plots of α_1 are found be at compound forming concentration which is at $x_1 = 0.6$. The computed values of α_1 are positive in the concentration range $x_1 < 0.24$ above 1073 K predicting the segregating (homo−coordinating) tendency in the initial melt. The trend of segregation to ordering transformation at elevated temperature is similar to that forecasted by $S_{CC}(0)$.

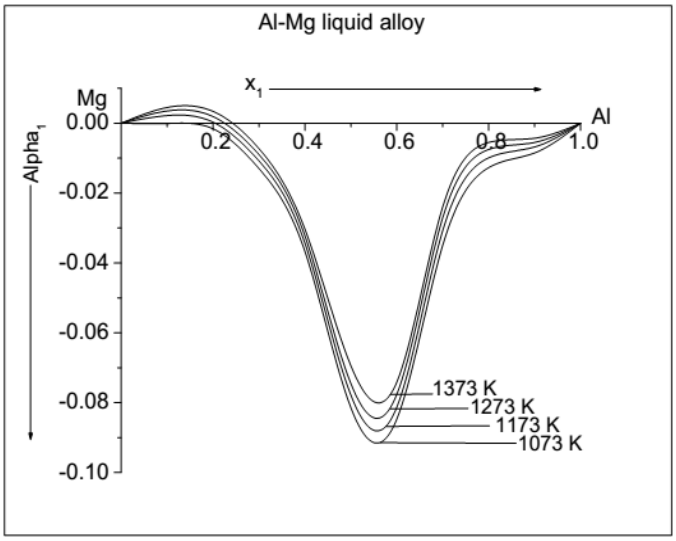

Figure 4.36(a): α_1 versus x_1 for Al−Mg liquid alloy at different temperatures.

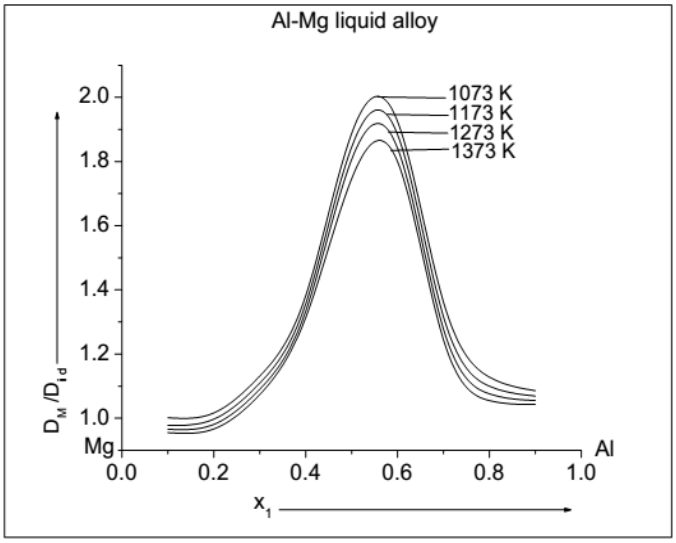

Figure 4.36(b): D_M/D_{id} versus x_1 for Al−Mg liquid alloy at different temperatures.

It can be observed from Fig. 4.36(b) that the values of D_M/D_{id} decreases with increase in temperature which reveals the decrease in tendency towards chemical ordering in the mixture. These values get closure to ideal values at higher temperature predicting that the liquid alloy shows ideal behaviour at higher temperatures. However, the peak value of this physical quantity is maintained at the compound forming concentration at all temperatures. The values of D_M/D_{id} are less than one in the concentration range $x_1 < 0.24$ at temperatures above its melting temperature (1073 K). Considering the behaviour forecasted by $S_{CC}(0)$ and α_1 for this system, these values are as expected.

4.22 Surface properties of binary liquid alloys

A number of physical properties, such as kinetics of phase transformation, catalytic activities of alloy catalysts, wettability and other mechanical behaviours of liquid alloys can be explained and forecasted with the assistance of surface phenomena. In this limelight, modeling surface properties of liquid alloys is ingoing problem in the accountability of the researchers and engineers in the field of surface science. Since decades both theoreticians (Gibbs, 1875-1878; Langmuir, 1917; Butler, 1932; Guggenheim , 1945; McLean 1957; William & Nason, 1974; Overbury et al., 1975; Burton & Machlin, 1976; Kerker et al., 1977; Prasad & Singh, 1991; Picha et al., 2004; Rusanov, 2007, 2014; March & Alonso, 2008; Mekler & Kaptay, 2008, 2016; Novakovic, 2010; Gasior et al., 2012; Kaptay, 2015; Yadav et al., 2016) and experimentalists (Harris 1968; Sachter & Planck, 1969; Sinfelt et al., 1972; Brongersma & Buck, 1975; Sakurai et al., 1985; Gasior et al., 2001; Koo et al., 2013; Sandor, et al., 2013; Weltsch et al., 2013) have been working to explain the physical properties of liquid as well as solid alloys taking epicenter to be the surface properties. In this work, therefore, we intend to study the surface properties, such as surface tension and surface segregation of some binary liquid alloys in the frame work of Renovated Butler model (Kaptay, 2015) in the former sections of this Chapter. In the later sections, we have correlated the thermodynamic properties of the liquid alloys (obtained by extending regular associated solution model) with the Renovated Butler model to predict their surface properties at different temperatures. The expressions to compute the surface properties of the preferred binary liquid alloys are mentioned in the Chapter 3.

4.23 Surface properties for Bi−Tl, In−Bi, Al−Fe and Al−Mg liquid alloys

In this section, we present the procedures that have been followed to compute the surface properties (surface tension, σ and surface segregation, x_i^S and x_j^S) for some liquid alloys such as Bi−Tl at 750 K, In−Bi at 900 K, Al−Fe at 1873 K and Al−Mg at 1073 K in the frame work of Renovated Butler model. The results so obtained along with discussion are also amended in the following sub−sections.

4.23.1 Surface properties for Bi−Tl liquid alloy at 750 K

The surface tension for Bi−Tl liquid alloy at T (=750 K) has been computed using Eq. (3.155). The molar surface areas of the components of the liquid alloy (α_i; i =A and B; A = Tl and B = Bi) required for this purpose are estimated from Eq. (3.156) by substituting f = 1.06 (Mekler & Kaptay, 2008; Yadav et al., 2016). The molar volume of the pure component (V_i^0) is computed from the ratio of its atomic mass to density (m/ρ). The densities and surface tensions (σ_i^0) of the pure components of the liquid mixtures are taken from Table 4.53.

The surface partial excess free energy ($\Delta G_{s,i}^{XS}$) of a monomer is obtained using the relation

$$\Delta G_{s,i}^{XS} = \beta(\Delta G_i^{XS}) \tag{4.5}$$

where β is the ratio of surface partial excess free energy to the bulk partial excess free energy (ΔG_i^{XS}). Herein, the theoretical values of bulk partial excess free energy are taken from Table 4.29 and the value of β is taken to be 0.8181 (Kaptay 2016).

Table 4.53: Densities and surface tensions of pure metals (Brandes & Brook,1992)

Metal	Melting temperature T_0 (K)	Density ρ (kg m^{-3})	Surface tension σ_i^0 (N m^{-1})
Al	933	$2385-0.280x\,(T-T_0)$	$0.914-0.35x10^{-3}\,x\,(T-T_0)$
Bi	544	$10068-1.33x\,(T-T_0)$	$0.378-0.70x10^{-4}\,x\,(T-T_0)$
Fe	1809	$7015-0.883\,x\,(T-T_0)$	$1.872-0.49\,x10^{-3}\,x\,(T-T_0)$
In	429.6	$7023-0.6798\,x\,(T-T_0)$	$0.556-0.90\,x10^{-4}\,x\,(T-T_0)$
Mg	924	$1590-0.2647\,x\,(T-T_0)$	$0.559-0.35\,x10^{-3}\,x\,(T-T_0)$
Tl	575	$11280-1.43\,x\,(T-T_0)$	$0.464-0.80\,x10^{-4}\,x\,(T-T_0)$

With the help of above calculated input parameters, the surface tension of the liquid alloy is computed by solving the left hand side and the right hand side of Eq. (3.155) to get the surface mole concentrations (x_i^s) of the components at all bulk concentrations. The compositional dependence surface tension (σ) and surface mole concentrations of Tl (x_{Tl}^s)

and Bi (x_{Bi}^{s}) for the Bi−Tl liquid alloy at 750 K are tabulated in Table 4.54.; and are plotted in Figs. 4.37(a−b).

Table 4.54: The computed values of σ, x_{Tl}^{s} and x_{Bi}^{s} for Bi−Tl liquid alloy at 750 K

Conc. of Tl (x_1)	σ (N m^{-1})		x_{Tl}^{s}	x_{Bi}^{s}
	Theoretical	Ideal		
0.1	0.3700	0.3722	0.0327	0.9673
0.2	0.3771	0.3809	0.0696	0.9304
0.3	0.3853	0.3895	0.1162	0.8838
0.4	0.3949	0.3982	0.1786	0.8214
0.5	0.4057	0.4068	0.2634	0.7366
0.6	0.4173	0.4154	0.3770	0.6231
0.7	0.4288	0.4241	0.5214	0.4786
0.8	0.4389	0.4327	0.6928	0.3072
0.9	0.4457	0.4414	0.8566	0.1434

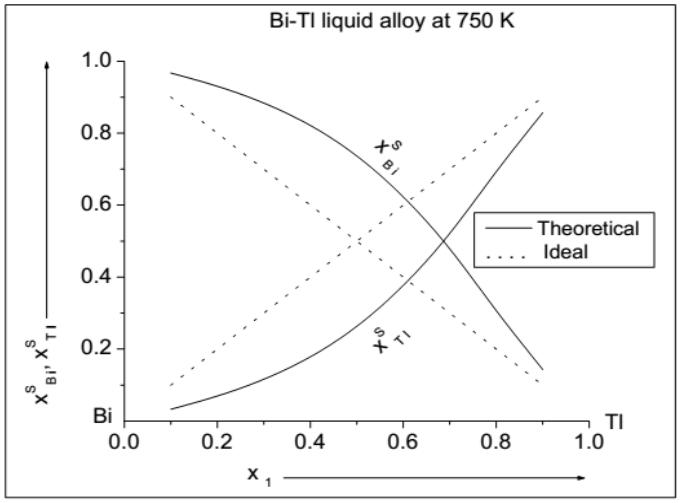

Figure 4.37(a): Surface concentration of Tl (x_{Tl}^{s}) and Bi (x_{Bi}^{s}) versus concentration of Tl (x_1) for Bi−Tl liquid alloy at 750 K.

Fig. 4.37(a) shows that the surface mole concentration of Tl is less than the ideal value but that of Bi is more than the ideal values at all bulk concentrations corresponding to the segregation of Bi atoms on the surface while the Tl atoms remains in the bulk in the liquid alloy at 750 K. It can be observed from Fig. 4.37(b) that the surface tension of the system is less than the ideal values in the bulk concentration range $x_1 < 0.6$ whereas exceeds the ideal values at rest of the bulk concentrations. The surface tension of the system increases with increase in the bulk concentration of Tl.

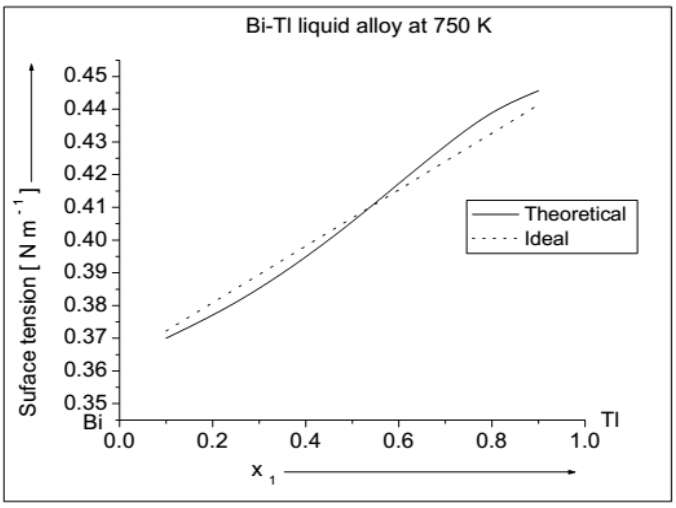

Figure 4.37(b): Surface tension versus concentration of Tl (x_1) for Bi−Tl liquid alloy at 750 K.

4.23.2 Surface properties for In−Bi liquid alloy at 900 K

The surface tension (σ) and surface concentrations of In (x_{In}^s) and Bi (x_{Bi}^s) for In−Bi liquid alloy at T (=900 K) are computed following the similar procedure as mentioned in the former section. The theoretical values of bulk partial excess free energies (A=In and B=Bi) are inherited from Table 4.31 and the values of densities and surface tensions of monomers of the liquid alloy are taken from Table 4.53. The values so computed as a function of concentration are depicted in Table 4.55 and are plotted in Figs. 4.38(a−b).

Table 4.55: The computed values of σ, x_{In}^s and x_{Bi}^s for In−Bi liquid alloy at 900 K

Conc. of In (x_1)	σ (N m^{-1})		x_{In}^s	x_{Bi}^s
	Theoretical	Ideal		
0.1	0.3617	0.3691	0.0263	0.9737
0.2	0.3713	0.3852	0.0574	0.9426
0.3	0.3821	0.4013	0.0954	0.9046
0.4	0.3943	0.4173	0.1431	0.8569
0.5	0.4083	0.4334	0.2044	0.7956
0.6	0.4239	0.4494	0.2834	0.7166
0.7	0.4418	0.4655	0.3873	0.6127
0.8	0.4620	0.4816	0.5262	0.4738
0.9	0.4854	0.4976	0.7175	0.2825

Fig. 4.38(a) shows that the surface concentration of In is less than its ideal value whereas

that of Bi is greater than its ideal values at all bulk concentrations indicating that the In atoms remains in the bulk but the Bi atoms segregate on the surface of the liquid mixture at its melting temperature, 900 K. The perusal of Fig. 4.38(b) communicates that the computed values of surface tension of the liquid alloy is less than corresponding ideal values at all bulk concentrations.

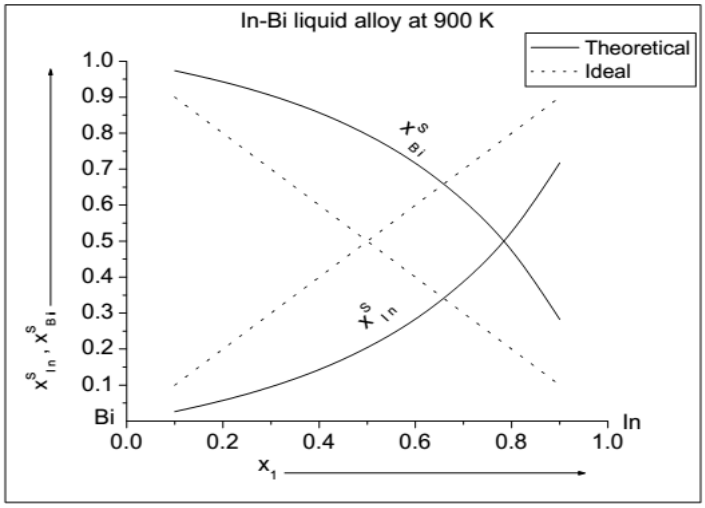

Figure 4.38(a): Surface concentrations of In (x^s_{In}) and Bi (x^s_{Bi}) versus concentration of In (x_{In}) for In−Bi liquid alloy at 900 K.

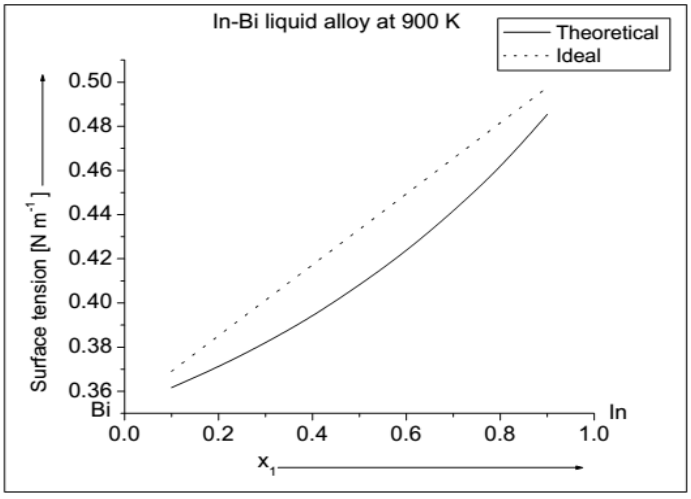

Figure 4.38(b): Surface tension versus concentration of In (x_{In}) of In−Bi liquid alloy at 900 K.

4.23.3 Surface properties for Al−Fe liquid alloy at 1873 K

The surface tension (σ) and surface mole concentrations of Al (x_{Al}^s) and Fe (x_{Fe}^s) for the preferred system at T (=1873 K) are computed by the similar process as mentioned in the Section 4.23.1 throughout all bulk concentration. Herein, the theoretical values of bulk partial excess free energy of Al (=Al) and Fe (=B) are taken from Table 4.33. The densities of pure atoms of A and B and their surface tensions are obtained from Table 4.53. The values of σ, x_{Al}^s and x_{Fe}^s so computed as a function of bulk concentration are presented in Table 4.56 and are portrayed in Figs. 4.39(a–b).

Table 4.56: The computed values of σ, x_{Al}^s and x_{Fe}^s for Al–Fe liquid alloy at 1873 K

Conc. of Al (x_1)	σ (N m^{-1})		x_{Al}^s	x_{Fe}^s
	Theoretical	Ideal		
0.1	1.3548	1.7151	0.7190	0.2810
0.2	1.1590	1.5895	0.8457	0.1543
0.3	1.0272	1.4640	0.9038	0.0962
0.4	0.9261	1.3384	0.9375	0.0625
0.5	0.8437	1.2128	0.9592	0.0409
0.6	0.7743	1.0873	0.9740	0.0260
0.7	0.7148	0.9617	0.9844	0.0156
0.8	0.6636	0.8361	0.9917	0.0083
0.9	0.6203	0.7106	0.9967	0.0033

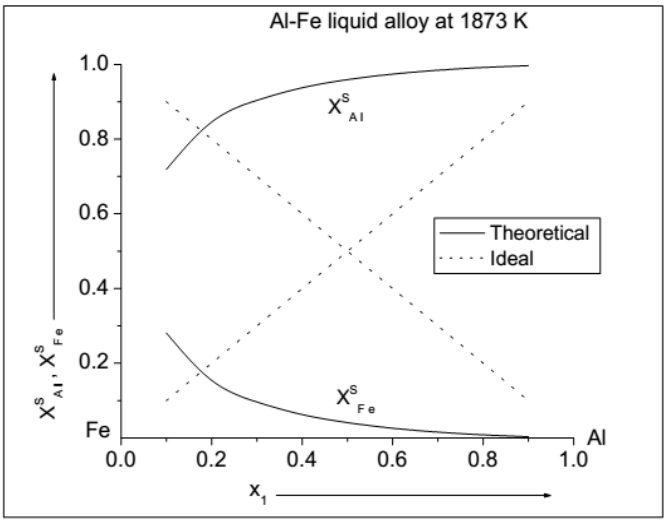

Figure 4.39(a): Surface concentrations of Al (x_{Al}^s) and Fe (x_{Fe}^s) versus concentration of Al (x_1) for Al–Fe liquid alloy 1873 K.

The perusal of Fig. 4.39(a) shows that the surface concentrations of Al is greater whereas that of Fe is less than their corresponding ideal values at all bulk concentrations.

Therefore, theoretical investigations reveal that Al atoms segretate to the surface whereas Fe atoms remain in the bulk of liquid mixture at its melting tempearture. Fig. 4.39(b) shows that the surface tension of the concerned system is less than the corresponding ideal value at all bulk concentrations, however, it decreases with increase of bulk concentration of Al.

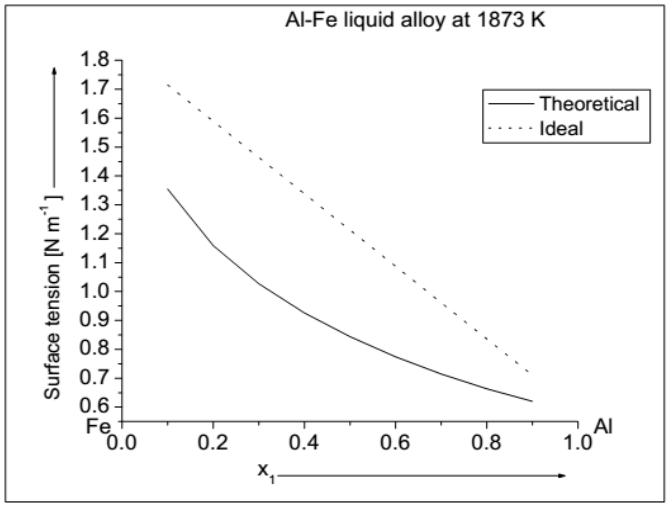

Figure 4.39(b): Surface tension versus concentration of Al (x_1) for Al−Fe liquid alloy at 1873 K.

4.23.4 Surface properties for Al−Mg liquid alloy at 1073 K

The methodology amended to compute the surface tension (σ) and surface concentrations of Al (x^s_{Al}) and Mg (x^s_{Mg}) for the preferred system at T (=1073 K) is similar to that mentioned in the Section 4.23.1. The values of bulk partial excess free energies of A (=Al) and B (=Mg) required for the process are taken from Table 4.35 and their corresponding densities and surface tensions are calculated from Table 4.53. The computed values of σ, x^s_{Al} and x^s_{Mg} as a function of concentration are furnished in Table 4.57 and are plotted in Figs. 4.40(a−b).

The surface concentration of Al is less than ideal value whereas that of Mg atoms is greater than ideal values indicating that the former atoms remain in the bulk whereas the later segregate on the surface of the liquid mixture at melting temperature, Fig. 4.40(a).

Fig. 4.40(b) communicates that the surface tension of the preferred liquid alloy is found to be less than ideal value throughout the entire bulk concentration at 1073 K.

Table 4.57: The computed values of σ, $x^s_{Al}$and x^s_{Mg} for Al−Mg liquid alloy at 1073 K

Conc. of Al (x_1)	σ (N m^{-1})		x^s_{Al}	x^s_{Mg}
	Thoretical	Ideal		
0.1	0.5212	0.5427	0.0153	0.9847
0.2	0.5369	0.5785	0.0333	0.9667
0.3	0.5551	0.6143	0.0553	0.9447
0.4	0.5761	0.6501	0.0832	0.9168
0.5	0.6008	0.6859	0.1200	0.8800
0.6	0.6306	0.7217	0.1710	0.8290
0.7	0.6673	0.7576	0.2455	0.7545
0.8	0.7136	0.7934	0.3619	0.6381
0.9	0.7752	0.8292	0.5657	0.4343

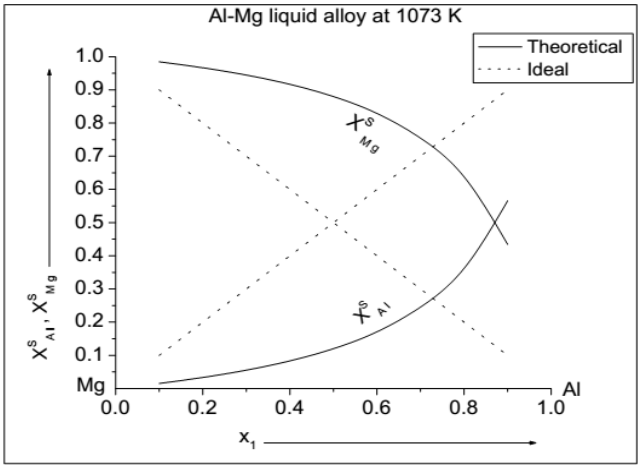

Figure 4.40(a): Surface concentrations of Al (x^s_{Al}) and Mg (x^s_{Mg}) versus concentration of Al (x_1) for Al−Mg liquid alloy at 1073 K.

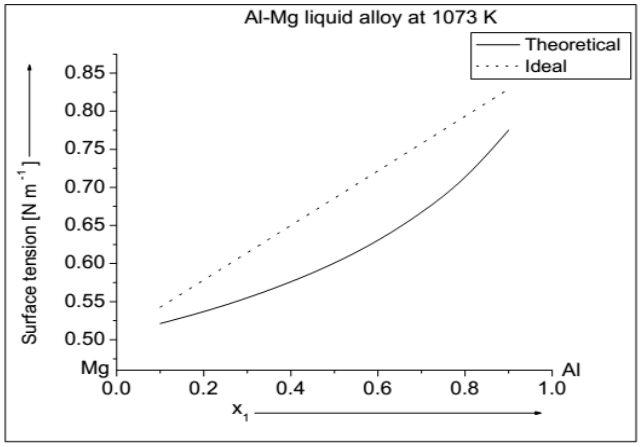

Figure 4.40(b): Surface tension versus concentration of Al (x_1) for Al−Mg liquid alloy at1073 K.

4.24 Prediction of surface properties of binary liquid alloys at different temperatures

In the present work, we have correlated extended regular associated solution model with Renovated Butler model to predict the surface properties of few binary liquid alloy at different temperatures. For this purpose, the predicted values of the bulk partial excess free energies of the components of the liquid alloys have been used to compute their surface properties at different temperatures. The results of the investigations along with necessary discussion are included in the upcoming sections.

4.24.1 Surface properties of Bi−Tl liquid alloy at different temperatures

In surface properties, we have predicted the surface tensions and surface concentrations (x^s_{Tl} and x^s_{Bi}) of Bi−Tl liquid alloy at temperatures T = 750 K, 850 K, 950 K and 1050 K using models as described above. The values of σ, x^s_{Tl} and x^s_{Bi} are computed at different temperatures using Eq. 3.155 following the similar procedures as stated in the Section 4.23.1. The values of densities and surface tension of the pure components Tl (=A) and Bi (=B) required for this purpose are determined from Table 4.53. Also the values of bulk partial excess free energies of Tl and Bi at corresponding temperatures are taken from the Table 4.29. The mathematical equations to predict the surface concentrations and surface tensions as a function of bulk concentration along with the values of parameters at above mentioned temperatures are given in Tables 4.58. These prediction equations are obtained from the polynomial fitting equations of different orders using the computer Software Origin Lab 6.1. The computed values of x^s_{Tl} and x^s_{Bi} as a function of concentration at different temperatures are presented in Tables 4.59 and that of σ are depicted in Table 4.60. The computed values of σ, x^s_{Tl} and x^s_{Bi} as a function of concentration at different temperatures are plotted in Figs. 4.41(a –b).

The perusal of Fig. 4.41(a) corresponds that the surface concentrations of Tl gradually increases whereas that of Bi gradually decreases with increase in temperature of the alloy beyond its melting temperature. As a result, it can be predicted that the Tl atoms tend to

move from bulk to the surface and the Bi atoms tend to move from surface to bulk at higher temperatures. Additionally, both of these values (x_{Tl}^{s} and x_{Bi}^{s}) move towards their respective ideal values at higher temperatures and hence the alloy also shows ideal behaviour with respect to surface properties (Kaptay, 2012). The surface tensions of the preferred liquid alloy decreases with increase in its temperatures, Fig. 4.41(b) (Aqra et al., 2011; Gancarz & Gasior, 2016; Gancarz 2017). One of the reasons behind this behaviour of the liquid alloy may be result of decrease in its cohesive force at elevated temperatures as predicted from the computations of thermodynamic and structural properties.

Table 4.58: Prediction equations for x_{Tl}^{s} and x_{Bi}^{s} for Bi−Tl liquid alloy at different temperatures; $x_l = 0.1 - 0.9$

Physical quantity	Prediction equation	Parameter (L_Z)	Values of parameters			
			T = 750 K	T = 850 K	T = 950 K	T = 1050 K
x_{Tl}^{s}	$\sum_{Z=0}^{2} L^Z x_l^Z$	L_0	0.0377	0.0275	0.0211	0.0162
		L_1	-0.0991	0.0317	0.1278	0.2081
		L_2	1.1281	1.0032	0.9156	0.0841
x_{Bi}^{s}	$\sum_{Z=0}^{2} L^Z x_l^Z$	L_0	0.9623	0.9725	0.9789	0.9838
		L_1	0.0993	-0.0316	-0.1278	-0.2081
		L_2	-1.1282	-1.0033	-0.9156	-0.8412
σ	$\sum_{Z=0}^{4} L^Z x_l^Z$	L_0 (N m^{-1})	0.3632	0.3515	0.3444	0.3375
		L_1 (N m^{-1})	0.0701	0.1446	0.1479	0.1494
		L_2 (N m^{-1})	-0.0399	-0.3272	-0.3281	-0.3254
		L_3 (N m^{-1})	0.2255	0.6581	0.6568	0.6509
		L_4 (N m^{-1})	-0.1716	-0.3954	-0.3977	-0.3977

Table 4.59: The computed values of X_{Tl}^{S} and X_{Bi}^{S} for Bi−Tl liquid alloy at different temperatures

Conc. of Tl (x_1)	T = 750 K		T = 850 K		T = 950 K		T = 1050 K	
	X_{Tl}^{S}	X_{Bi}^{S}	X_{Tl}^{S}	X_{Bi}^{S}	X_{Tl}^{S}	X_{Bi}^{S}	X_{Tl}^{S}	X_{Bi}^{S}
0.1	0.0327	0.9673	0.0378	0.9622	0.0421	0.9579	0.0459	0.9541
0.2	0.0696	0.9304	0.0798	0.9202	0.0883	0.9117	0.0957	0.9043
0.3	0.1162	0.8838	0.1314	0.8686	0.1440	0.8560	0.1550	0.8450
0.4	0.1786	0.8214	0.1979	0.8021	0.2147	0.7853	0.2290	0.7710
0.5	0.2634	0.7366	0.2849	0.7151	0.3049	0.6951	0.3217	0.6783
0.6	0.3770	0.6231	0.3989	0.6011	0.4204	0.5796	0.4381	0.5619
0.7	0.5214	0.4786	0.5470	0.4531	0.5669	0.4331	0.5830	0.4170
0.8	0.6928	0.3072	0.7179	0.2821	0.7323	0.2677	0.7437	0.2563
0.9	0.8566	0.1434	0.8535	0.1465	0.8614	0.1386	0.8675	0.1325

Table 4.60: The computed values of σ for Bi−Tl liquid alloy at different temperatures

Conc. of Tl (x_1)	σ [N m^{-1}]			
	T = 750 K	T = 850 K	T = 950 K	T = 1050 K
0.1	0.3700	0.3635	0.3567	0.3500
0.2	0.3771	0.3714	0.3649	0.3583
0.3	0.3853	0.3801	0.3738	0.3675
0.4	0.3949	0.3895	0.3834	0.3772
0.5	0.4057	0.3997	0.3937	0.3875
0.6	0.4173	0.4107	0.4046	0.3983
0.7	0.4288	0.4230	0.4167	0.4102
0.8	0.4389	0.4334	0.4267	0.4198
0.9	0.4457	0.4367	0.4293	0.4217

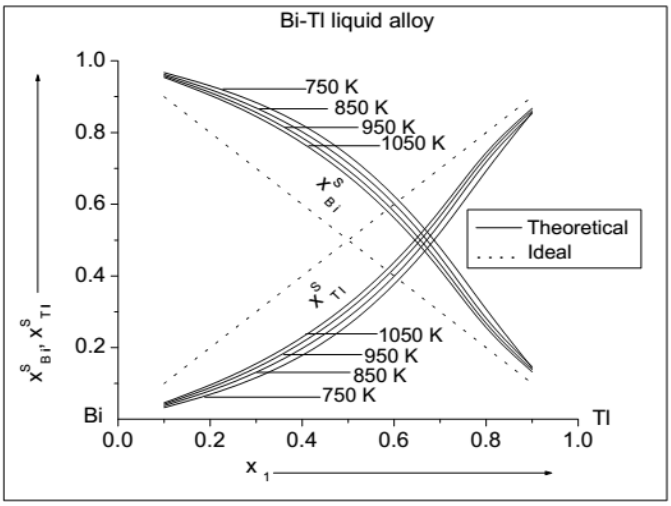

Figure 4.41(a): Plots of x^s_{Tl} and x^s_{Bi} versus concentration of Tl (x_1) for Bi−Tl liquid alloy at different temperatures.

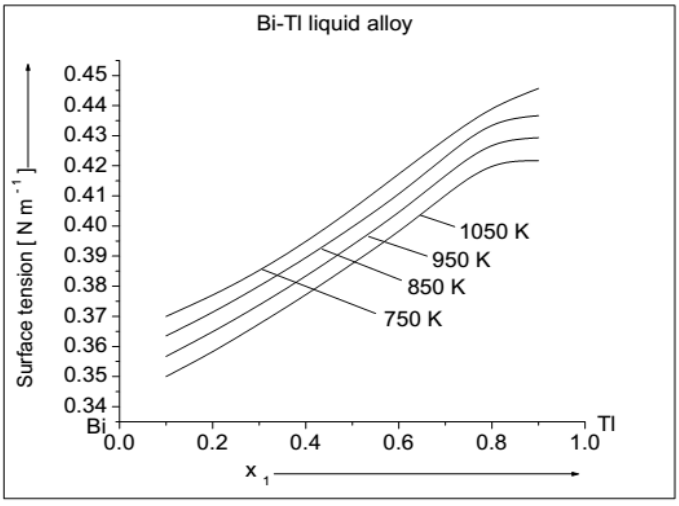

Figure 4.41(b): Plots of surface tensions versus concentration of Tl (x_1) for Bi−Tl liquid alloy at different temperatures.

4.24.2 Surface properties of In−Bi liquid alloy at different temperatures

The surface tension (σ) and surface mole concentrations of In (=A; x_{In}^{s}) and Bi (=B; x_{Bi}^{s}) for In−Bi liquid alloy are computed at temperatures T = 900 K, 1000 K, 1100 K and 1200 K using Eq. (3.155) and employing the methodology stated in the former section. Herein, the required essential bulk partial excess free energies of the pure components of the liquid alloy are inherited from Table 4.31. The densities and surface tensions of the respective pure components are taken from Table 4.53. The mathematical equations to predict σ, x_{In}^{s} and x_{Bi}^{s} as a function of bulk concentration along with the values of parameters at temperatures mentioned above are depicted in Table 4.61. The methods of obtaining these equations are similar to mentioned in the Section 4.23.1. The computed values of compositional dependence x_{In}^{s} and x_{Bi}^{s} at different temperatures are depicted in Table 4.62 and that of σ are depicted in Table 4.63. The plots of values so computed are portrayed in Figs. 4.42(a–b).

Table 4.61: Prediction equations for x_{In}^{s} and x_{Bi}^{s} for In−Bi liquid alloy at different temperatures; $x_l = 0.1 - 0.9$

Physical quantity	Prediction equation	Parameter (L_Z)	Values of parameters			
			T = 900 K	T = 1000 K	T = 1100 K	T = 1200 K
x_{In}^{s}	$\sum_{Z=0}^{2} L^Z x_l^Z$	L_0	0.0560	0.0517	0.0462	0.0412
		L_1	-0.2351	-0.1642	-0.0852	-0.0129
		L_2	1.0510	1.0062	0.9552	0.9047
x_{Bi}^{s}	$\sum_{Z=0}^{2} L^Z x_l^Z$	L_0	0.9440	0.9483	0.9538	0.9588
		L_1	0.2351	0.1642	0.0852	0.0129
		L_2	-1.0510	-1.0062	-0.9552	-0.9047
σ	$\sum_{Z=0}^{4} L^Z x_l^Z$	L_0 (N m^{-1})	0.3535	0.3450	0.3378	0.3309
		L_1 (N m^{-1})	0.0756	0.1007	0.1076	0.1080
		L_2 (N m^{-1})	0.0676	-0.0406	-0.0597	-0.0527
		L_3 (N m^{-1})	-0.0148	0.1561	0.1884	0.1788
		L_4 (N m^{-1})	0.0303	-0.0597	-0.0816	-0.0813

Fig. 4.42(a) corresponds that the values of x_{In}^{s} increases whereas that of x_{Bi}^{s} decreases with increase in temperature of the alloy beyond its melting temperature (900 K). These investigations forecast that the atoms of In will gradually move from the bulk region to

the surface and the atoms of Bi will gradually move from surface region to the bulk at higher temperatures. Strictly speaking, both of these values get closure to their respective ideal values. The perusal of Fig. 4.42(b) communicates that the surface tension of the concerned liquid alloy decreases with increase in its temperature and these forecasting are as generalized expectations. One of the prominent causes of this behaviour may be due to the decrease in cohesive force of the liquid mixture at higher temperatures and is accordance with earlier predictions from thermodynamic and structural properties.

Table 4.62: The computed values of x_{In}^{S} and x_{Bi}^{S} for In−Bi liquid alloy at different temperatures

Conc. of In (x_1)	T = 900 K		T = 1000 K		T = 1100 K		T = 1200 K	
	X_{In}^{S}	X_{Bi}^{S}	X_{In}^{S}	X_{Bi}^{S}	X_{In}^{S}	X_{Bi}^{S}	X_{In}^{S}	X_{Bi}^{S}
0.1	0.0263	0.9737	0.0303	0.9697	0.0341	0.9659	0.0375	0.9625
0.2	0.0574	0.9426	0.0653	0.9347	0.0729	0.9271	0.0799	0.9201
0.3	0.0954	0.9046	0.1071	0.8929	0.1189	0.8811	0.1295	0.8705
0.4	0.1431	0.8569	0.1586	0.8414	0.1747	0.8253	0.1891	0.8109
0.5	0.2044	0.7956	0.2234	0.7766	0.2439	0.7561	0.2619	0.7381
0.6	0.2834	0.7166	0.3058	0.6942	0.3303	0.6697	0.3515	0.6485
0.7	0.3873	0.6127	0.4125	0.5875	0.4398	0.5602	0.4629	0.5371
0.8	0.5262	0.4738	0.5548	0.4452	0.5821	0.4179	0.6045	0.3955
0.9	0.7175	0.2825	0.7367	0.2633	0.7578	0.2422	0.7745	0.2255

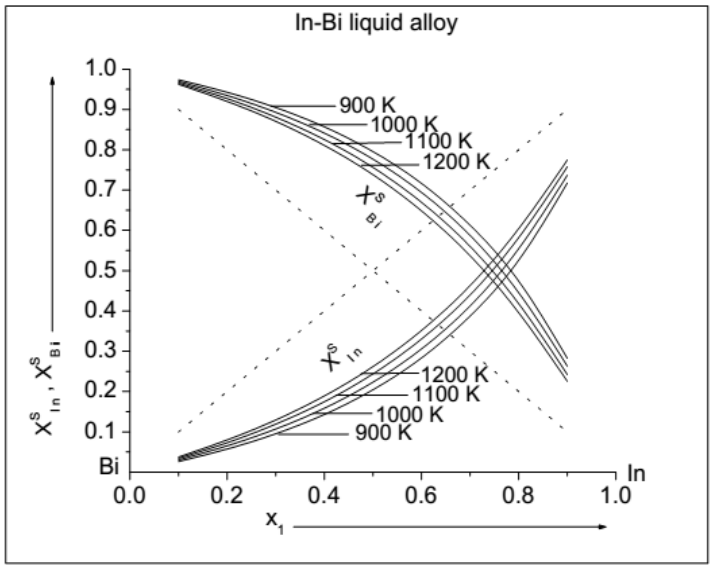

Figure 4.42(a): The computed values of x_{In}^{S}, x_{Bi}^{S} versus concentration of In (x_1) for In−Bi liquid alloy at different temperatures.

Table 4.63: The computed values of σ for In−Bi liquid alloy at different temperatures

Conc. of In (x_1)	σ [N m^{-1}]			
	T = 900 K	T = 1000 K	T = 1100 K	T = 1200 K
0.1	0.3617	0.3549	0.3482	0.3414
0.2	0.3713	0.3645	0.3581	0.3515
0.3	0.3821	0.3753	0.3691	0.3627
0.4	0.3943	0.3874	0.3814	0.3752
0.5	0.4083	0.4011	0.3952	0.3891
0.6	0.4239	0.4166	0.4108	0.4047
0.7	0.4418	0.4345	0.4285	0.4221
0.8	0.4620	0.4554	0.4491	0.4423
0.9	0.4854	0.4772	0.4699	0.4623

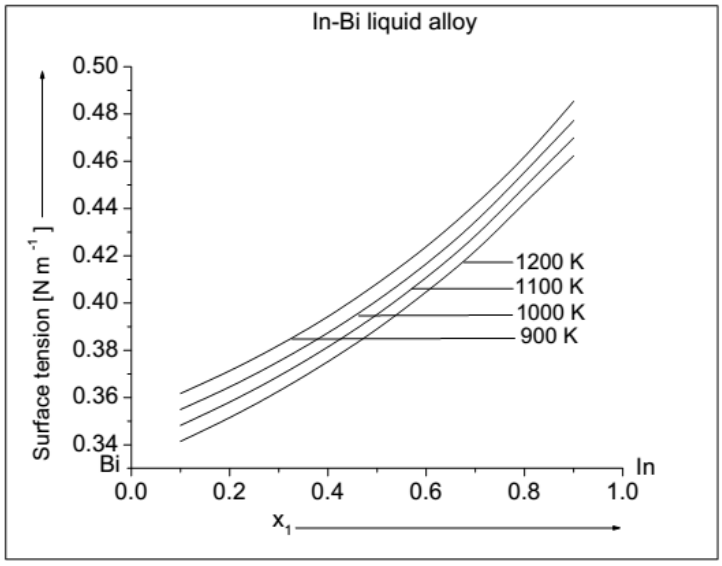

Figure 4.42(b): The computed values of surface tensions versus concentration of In (x_1) for In−Bi liquid alloy at different temperatures.

4.24.3 Surface properties of Al−Fe liquid alloy at different temperatures

The surface tensions (σ) and surface concentrations of components Al (=A; x_{Al}^{s}) and Fe (=B; x_{Fe}^{s}) of the concerned system are computed at temperatures T = 1873 K, 1973 K, 2073 K and 2173 K employing the similar procedures as mentioned in the Section 4.23.1. For this purpose, the values of bulk partial excess free energies, densities and surface tensions of the pure components of the alloy are taken from corresponding Tables 4.33 and 4.53. The mathematical equations to predict σ, x_{Al}^{s} and x_{Fe}^{s} at different temperatures (obtained from the procedure mentioned in the Section 4.23.1) along with the values of

input parameters are given in Table 4.64. The computed values of σ, x_{Al}^{s} and x_{Fe}^{s} at different temperatures are presented in Tables 4.65 and 4.66. These values as a function of concentration and temperature are plotted in Figs. 4.43(a–b).

Table 4.64: Prediction equations for x_{Al}^{s} and x_{Fe}^{s} for Al–Fe for liquid alloy at different temperatures; $x_l = 0.1 - 0.9$

Physical quantity	Prediction equation	Parameter (L_Z)	Values of parameters			
			T = 1873 K	T = 1973 K	T = 2073 K	T = 2173 K
x_{Al}^{s}	$\sum_{Z=0}^{4} L^Z x_l^Z$	L_0	0.5166	0.4717	0.4301	0.3916
		L_1	2.5680	2.7380	2.8892	3.0160
		L_2	-5.8906	-6.1924	-6.4566	-6.6575
		L_3	6.3045	6.5822	6.8248	6.9977
		L_4	-2.5254	-2.6268	-2.7153	-2.7759
x_{Fe}^{s}	$\sum_{Z=0}^{4} L^Z x_l^Z$	L_0	0.4835	0.5283	0.5702	0.6070
		L_1	-2.5696	-2.7375	-2.8917	-2.9930
		L_2	5.8974	6.1896	6.4641	6.5677
		L_3	-6.3150	-6.5766	-6.8342	-6.8695
		L_4	2.5306	2.6233	2.7194	2.7147
σ	$\sum_{Z=0}^{4} L^Z x_l^Z$	L_0 (N m^{-1})	1.6246	1.5983	1.5689	1.5374
		L_1 (N m^{-1})	-3.1978	-3.1807	-3.1565	-3.1277
		L_2 (N m^{-1})	5.3991	5.3182	5.2184	5.1180
		L_3 (N m^{-1})	-5.2766	-5.2098	-5.0816	-4.9614
		L_4 (N m^{-1})	2.0542	2.0443	1.9851	1.9324

Table 4.65: The computed values of X_{Al}^{S} and X_{Fe}^{S} for Al–Fe liquid alloy at different temperatures

Conc. of Al (x_1)	T = 1873 K		T = 1973 K		T = 2073 K		T = 2173 K	
	X_{Al}^{S}	X_{Fe}^{S}	X_{Al}^{S}	X_{Fe}^{S}	X_{Al}^{S}	X_{Fe}^{S}	X_{Al}^{S}	X_{Fe}^{S}
0.1	0.7190	0.2810	0.6883	0.3117	0.6594	0.3407	0.6318	0.3682
0.2	0.8457	0.1543	0.8246	0.1754	0.8045	0.1955	0.7847	0.2163
0.3	0.9038	0.0962	0.8896	0.1104	0.8754	0.1246	0.8611	0.1389
0.4	0.9375	0.0625	0.9272	0.0728	0.9171	0.0829	0.9067	0.0933
0.5	0.9592	0.0409	0.9521	0.0479	0.9448	0.0552	0.9374	0.0626
0.6	0.9740	0.0260	0.9693	0.0308	0.9643	0.0357	0.9591	0.0409
0.7	0.9844	0.0156	0.9815	0.0185	0.9783	0.0217	0.9749	0.0251
0.8	0.9917	0.0083	0.9901	0.0100	0.9883	0.0117	0.9864	0.0136
0.9	0.9967	0.0033	0.9962	0.0038	0.9955	0.0045	0.9947	0.0053

It can be observed from Fig. 4.43(a) that the surface mole concentrations of Al decrease whereas that of Fe increases with increase in temperature of the concerned liquid alloy beyond its melting temperatures. These results forecast that Al atoms gradually move

Table 4.66: The computed values σ for Al−Fe liquid alloy at different temperatures

Conc. of Al (x_1)	σ [N m^{-1}]			
	T = 1873 K	T = 1973 K	T = 2073 K	T = 2173 K
0.1	1.3548	1.3292	1.3013	1.2718
0.2	1.1590	1.1341	1.1066	1.0779
0.3	1.0272	0.9996	0.9714	0.9423
0.4	0.9261	0.8977	0.8686	0.8389
0.5	0.8437	0.8136	0.7837	0.7533
0.6	0.7743	0.7423	0.7116	0.6805
0.7	0.7148	0.6812	0.6496	0.6177
0.8	0.6636	0.6291	0.5965	0.5637
0.9	0.6203	0.5860	0.5522	0.5184

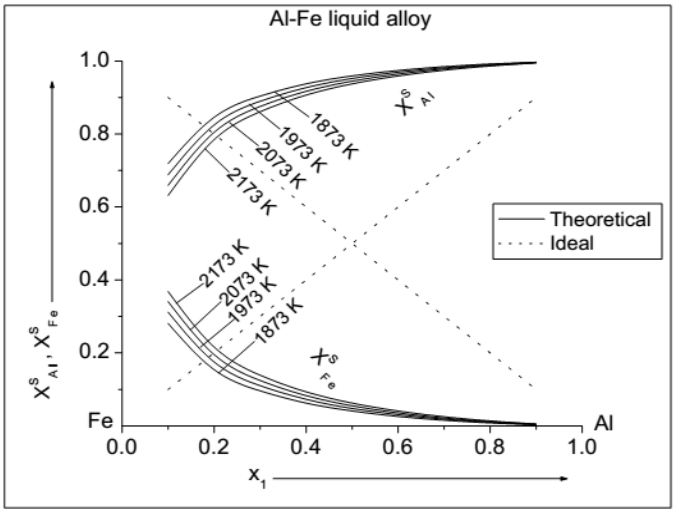

Figure 4.43(a): The computed values of x^s_{Al}, x^s_{Fe} versus concentrations of Al (x_1) for Al−Fe liquid alloy at different temperatures.

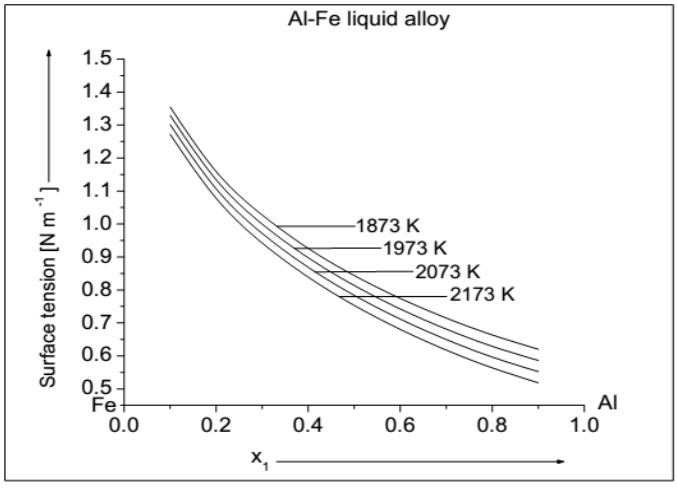

Figure 4.43(b): The computed values of surface tensions versus concentrations of Al (x_1) for Al−Fe liquid alloy at different temperatures.

from the surface to the bulk region whereas Fe atoms move from bulk to the surface region with the gradual increase in the temperatures of the liquid alloy beyond its melting temperature. However, both of these values move towards their respective ideal values at higher temperatures. As expected, the surface tension of the liquid alloy decreases at higher temperatures, Fig. 4.43(b). These theoretical forecasting are in agreement with that of thermodynamic and structural properties of the liquid alloy at different temperatures predicting the decrease in interactions between its components at higher temperatures.

4.24.4 Surface properties of Al−Mg liquid alloy at different temperatures

The surface tensions (σ) and surface mole concentrations of pure components Al (=A, x_{Al}^{s}) and Mg (=B, x_{Mg}^{s}) for Al−Mg liquid alloy are computed at temperatures T= 1073 K, 1173 K, 1273 K and 1373 K by the similar procedure as mentioned in the Section 4.23.1. For this purpose, the values of bulk partial excess free energies of pure components are taken from Table 4.35 and the values of their densities and surface tensions are taken from Table 4.53 at corresponding temperatures. The mathematical equations (along with the values of input parameters) to predict the values of σ, x_{Al}^{s} and x_{Mg}^{s} at above mentioned temperatures as a function of bulk concentrations are presented in Table 4.67. The methodologies to obtain these prediction equations are as mentioned in the Section 4.23.1. The computed values of x_{Al}^{s} and x_{Mg}^{s} are depicted in Table 4.68 and that of σ are depicted in Table 4.69 and portrayed in Figs. 4.44(a−b).

The perusal of Fig. 4.44(a) communicates that the Al (x_{Al}^{s}) gradually increases whereas that of Mg (x_{Mg}^{s}) gradually decreases with increase in the temperature of the liquid alloy above its melting temperature. Both of these values gradually move towards their respective ideal values at elevated temperatures. Further, there is movement of atoms of Al from the bulk region to the surface region due to the factor induced by increase in the temperature of the initial melt to maintain equilibrium. Similarly, the equilibrium state in the liquid mixture is achieved by the movement of Mg atoms from the surface to the bulk region at elevated temperatures. As expected, the surface tension of the liquid alloy gradually decreases at elevated temperatures which are due to the decrease in the

intermolecular force of attraction between the atoms of the liquid mixture (Pstrus′ et al., 2011; Gancarz & Gasior, 2016). These findings further strengthen the results predicted of the thermodynamic properties of the system at elevated temperatures earlier.

Table 4.67: Prediction equations for x_{Al}^{S} and x_{Mg}^{S} for Al–Mg for liquid alloy at different temperatures; $x_l = 0.1 - 0.9$

Physical quantity	Prediction equation	Parameter (L_Z)	Values of parameters			
			T = 1073 K	T = 1173 K	T = 1273 K	T = 1373 K
x_{Al}^{S}	$\sum_{Z=0}^{4} L^Z x_l^Z$	L_0	0.0259	0.0275	0.0205	0.0190
		L_1	-0.2756	-0.2670	-0.1160	-0.0681
		L_2	2.1568	2.1757	1.4979	1.3764
		L_3	-3.8713	-3.7121	-2.3542	-2.0907
		L_4	2.8374	2.6536	1.8252	1.6547
x_{Mg}^{S}	$\sum_{Z=0}^{4} L^Z x_l^Z$	L_0	0.9741	0.9780	0.9798	0.9809
		L_1	0.2756	0.1679	0.1135	0.0686
		L_2	-2.1568	-1.6365	-1.4904	-1.3792
		L_3	3.8713	2.6564	2.3449	2.0960
		L_4	-2.8374	-2.0157	-1.8211	-1.6579
σ	$\sum_{Z=0}^{4} L^Z x_l^Z$	L_0 (N m^{-1})	0.5098	0.4790	0.4441	0.4095
		L_1 (N m^{-1})	0.0892	0.0424	0.0461	0.0461
		L_2 (N m^{-1})	0.2867	0.4681	0.4743	0.4961
		L_3 (N m^{-1})	-0.3727	-0.5514	-0.5497	-0.5770
		L_4 (N m^{-1})	0.3421	0.3709	0.3616	0.3692

Table 4.68: The values of x_{Al}^{S} and x_{Mg}^{S} for Al–Mg liquid alloy at different temperatures

Conc. of Al (x_1)	T = 1073 K		T = 1173 K		T = 1273 K		T = 1373 K	
	X_{Al}^{S}	X_{Mg}^{S}	X_{Al}^{S}	X_{Mg}^{S}	X_{Al}^{S}	X_{Mg}^{S}	X_{Al}^{S}	X_{Mg}^{S}
0.1	0.0153	0.9847	0.0179	0.9821	0.0205	0.9796	0.0229	0.9771
0.2	0.0333	0.9667	0.0388	0.9612	0.0440	0.9560	0.0490	0.9510
0.3	0.0553	0.9447	0.0639	0.9362	0.0721	0.9279	0.0798	0.9202
0.4	0.0832	0.9168	0.0955	0.9045	0.1071	0.8929	0.1180	0.8820
0.5	0.1200	0.8800	0.1376	0.8624	0.1531	0.8469	0.1675	0.8325
0.6	0.1710	0.8290	0.2035	0.7965	0.2239	0.7761	0.2423	0.7577
0.7	0.2455	0.7545	0.2617	0.7183	0.3062	0.6938	0.3280	0.6721
0.8	0.3619	0.6381	0.3949	0.6051	0.4231	0.5769	0.4476	0.5524
0.9	0.5657	0.4343	0.5844	0.4156	0.6125	0.3875	0.6360	0.3640

Table 4.69: The values of σ for Al−Mg liquid alloy at different temperatures

Conc. of Al (x_1)	σ [N m^{-1}]			
	T = 1073 K	T = 1173 K	T = 1273 K	T = 1373 K
0.1	0.5212	0.4869	0.4525	0.4180
0.2	0.5369	0.5034	0.4696	0.4356
0.3	0.5551	0.5221	0.4889	0.4555
0.4	0.5761	0.5438	0.5113	0.4785
0.5	0.6008	0.5701	0.5383	0.5062
0.6	0.6306	0.6045	0.5734	0.5417
0.7	0.6673	0.6381	0.6071	0.5755
0.8	0.7136	0.6804	0.6496	0.6181
0.9	0.7752	0.7383	0.7069	0.6750

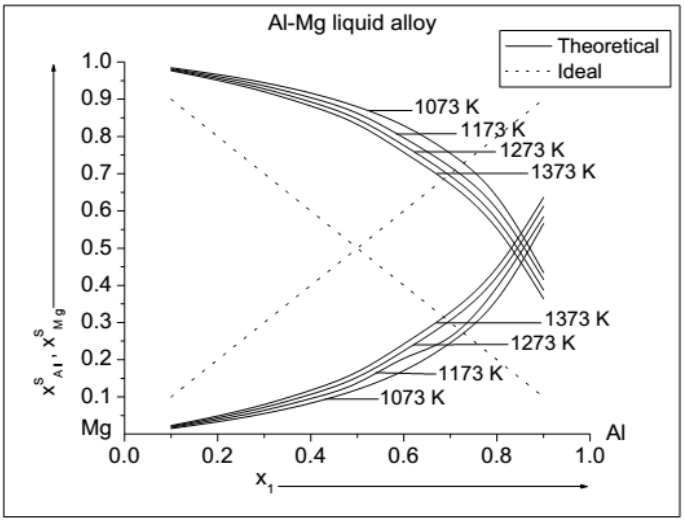

Figure 4.44(a): x^S_{Al} and x^S_{Mg} versus x_1 at for Al−Mg liquid alloy at different temperatures.

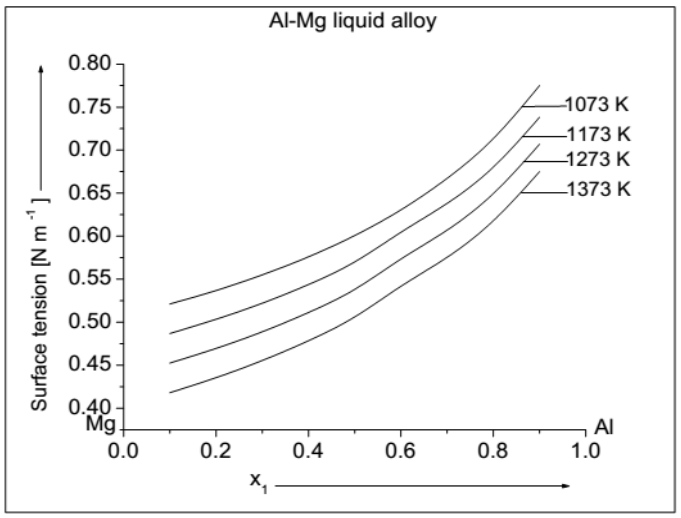

Figure 4.44(b): Surface tensions versus x_1 for Al−Mg liquid alloy at different temperatures.

4.25 Discussion

4.25.1 Discussion about the thermodynamic properties of binary liquid alloys

The thermodynamics of the initial melt of the binary alloys plays vital role in various metallurgical processes, characterization and design. To obtain the materials with predetermined characteristics, the knowledge of the energetic of mixing is of outmost essential. In this Chapter, therefore, we have explained the thermodynamic properties, such as free energy of mixing, activity, enthalpy of mixing and entropy of mixing of some compound forming binary liquid alloys employing regular associated solution model. This model has been applied to study and explain the above mentioned thermodynamic properties Bi−Tl, In−Bi, Al−Fe and Al−Mg liquid alloys at temperatures 750 K, 900 K, 1873 K and 1073 K respectively.

One of the most essential ingredients to compute free energy of mixing of the alloys is mole fractions of complex and free monomers. In these alloy systems, three different types of complexes, such as $A_\mu B_\nu$ ($\mu > 1$ and $\nu > 1$), $A_\mu B_\nu$ (=$A_\mu B$ in which $\mu > 1$ and $\nu = 1$) and $A_\mu B_\nu$ (= AB in which both $\mu = \nu = 1$) are assumed to exist in liquid mixtures near to their respective melting temperatures. The terms A and B in $A_\mu B_\nu$ represent the constitutional atoms of the liquid mixture, and μ and ν are small indices whose values are obtained from the phase diagrams at compound forming concentration in the solid state. We have assumed the presence of complexes BiTl, In_2Bi, Al_3Fe and Al_3Mg_2 as the most stable intermetallic compounds in the respective Bi−Tl, In−Bi, Al−Fe and Al−Mg liquid alloys on the fundamental of respective phase diagrams of solid states (Hultgren *et al.*, 1973). Theoretical investigations shows that the maximum values of mole fractions of complexes in the liquid alloys are at or quite close to the compound forming concentrations. The extent of compound formation tendency among the Bi−Tl, In−Bi, Al−Fe and Al−Mg liquid alloys have been analyzed by plotting mole fractions ($A_\mu B_\nu$) of the respective alloys as a function of concentration as shown in Fig. 4.45(a). The tendency of compound formation is the greatest for Bi−Tl alloy and the least for Al−Fe alloy among the above mentioned alloys. The extent of compound formation tendency

among them can be ordered as $x_{Bi-Tl} > x_{Al-Mg} > x_{In-Bi} > x_{Al-Fe}$. However, the natures of variation of mole fraction of the complex as a function of concentrations are similar for Bi−Tl and Al−Mg liquid alloys. These variations are also similar for In−Bi and Al−Fe liquid alloys.

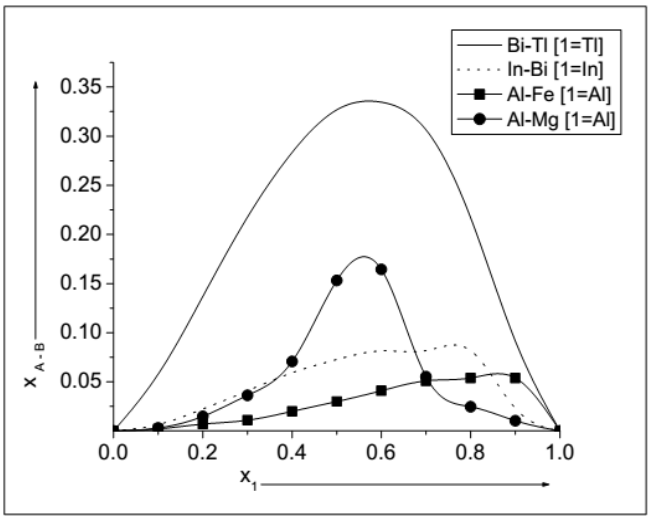

Figure 4.45(a): Mole fraction of complex (x_{A-B}) as a function of concentration of different liquid alloys.

The free energies of mixing as a function of concentration for preferred liquid alloys are plotted in Fig. 4.45(b). The computed values G_M/RT are almost the same for Bi−Tl and Al−Fe system at concentration greater than 0.6, however, there is slight variations at concentration less than 0.6. Additionally, the values of G_M/RT are almost the same for In−Bi and Al−Mg systems in spite of small deviation at about equiatomic concentration. But on the basis of theoretical computation, G_M/RT is the maximum for Al−Fe system followed by Bi−Tl, Al−Mg and the least for In−Bi. Contrarily, the mole fraction of the complex is the maximum for Bi−Tl followed by Al−Mg, In−Bi and the least for Al−Fe. Therefore, the degree of interaction in binary liquid alloys should not be considered on the values of mole fractions of the complex alone. The asymmetry in G_M/RT as a function of concentration has been well explained on the basis of regular associated solution model. Theoretical and experimental values of G_M/RT are in well agreements for all the concerned systems.

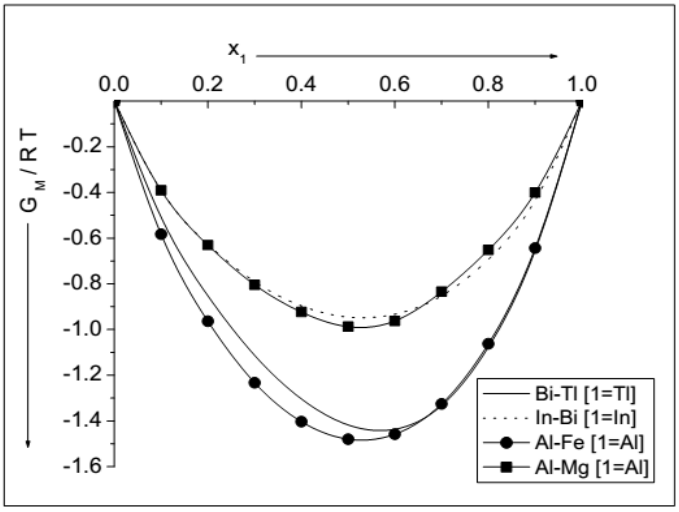

Figure 4.45(b): Free energy of mixing as a function of concentration for different alloys.

It has been already mentioned that the activity is the fundamental thermodynamic quantity in terms of which other thermodynamic functions can be expressed. It is directly obtained from the experiments. The discrepancy between the observed and computed values of activity has great reflection on thermodynamic as well as structural properties of liquid alloys. The deviation from the ideal behavoiur of the alloy can thus be incorporated into the activity. In the framework of regular associated solution model, the activity is irreducible functions of mole fractions of the complex ($A_\mu B_\nu$) and free monomers (A and B) along with interaction energy parameters (ω_{12}, ω_{13} and ω_{23}). Any observed fit between computed and observed free energy of mixing for a given set of mole fractions and interaction energy parameters becomes irrelevant if the same set of parameters is incapable to explain the other thermodynamic functions, such as activity, enthalpy of mixing and entropy of mixing. For consistency, we, therefore, have used the same values of the above mentioned input parameters to compute activity which were used for the computation of free energy of mixing.

Theoretical computations of the activities of components of the concerned alloy systems reveal that the activities of the components of strongly interacting systems have smaller values in compared to that of weakly interacting systems at their corresponding lower concentrations. The interacting nature of the alloys can also be interpreted on the basis of

values of activities. Accordingly, Al–Fe seems to be most interacting among the concerned systems followed by Bi–Tl, Al–Mg and the least interacting being In–Bi system. This disclosure is in accordance to that made from the computation of free energy of mixing stand point. Theoretically it is found that the computed values of activities of both components are in excellent agreement with their corresponding experimental values for Bi–Tl, In–Bi and Al–Fe liquid alloys among the preferred systems. There is slight disagreement between computed and experimental values of activities of Al in the concentration range $0.6 \leq x_1 \leq 0.9$ for Al–Mg liquid alloy, however, are in well agreement at rest of the concentrations (Fig. 4.8).

In the preferred model, the pairwise interaction energy parameters are considered to be temperature dependent. If not so, then $\frac{\partial \omega_{ij}}{\partial T} = 0$, where i, j = 1, 2, 3 and i≠j. On this assumption, the expression for the heat of mixing for the liquid alloys having the complex of the type $x_{A_\mu B_\nu}$ becomes

$$H_M = \frac{1}{[1+(\mu+\nu-1)x_{A_\mu B_\nu}]}\left[\left(x_A x_B \omega_{12} + x_A x_{A_\mu B_\nu} \omega_{13} + x_B x_{A_\mu B_\nu} \omega_{23}\right) - x_{A_\mu B_\nu} RT^2 \frac{d \ln K}{dT}\right]$$

and for the liquid alloys having the complex of the type $x_{A_\mu B}$ becomes

$$H_M = \frac{1}{(1+\mu x_{A_\mu B})}\left[\left(x_A x_B \omega_{12} + x_A x_{A_\mu B} \omega_{13} + x_B x_{A_\mu B} \omega_{23}\right) - x_{A_\mu B} RT^2 \frac{d \ln K}{dT}\right]$$

Then the heat of mixing of the concerned liquid alloys can be obtained with the aid of the mole fractions of the complex and free species and pairwise interaction energies. The values of H_M so obtained vary greatly with corresponding experimental values. By considering the temperature derivative terms of pairwise interaction energies in account, the theoretical and the experimental values of H_M are in good agreement. This clarifies the accountability of temperature derivative terms of pairwise interaction energies as the necessary input parameter in order to compute the heat of mixing of the binary liquid alloys on the basis of the preferred theoretical model.

We have determined the temperature derivative terms of interaction energies and the term related to the heat of dissociation $RT^2 \frac{d \ln K}{dT}$ by following the method of successive approximation as mentioned in the former sections. The term related to the heat of dissociation is more prone to errors. Any observed fit between the computed and the experimental values of free energy of mixing and activity for a given set of interaction energies, equilibrium values of mole fractions of various species and equilibrium constant, therefore, cannot be taken as sufficient unless the same set explains the heat of mixing of the alloys. For consistency, we have thus taken the same set of these aforementioned parameters to obtain the optimized values of temperature dependent energy parameters and the heat of dissociation. The best fit values of these model parameters vary considerably with the type of liquid alloys taken into account. The computed and the experimental values of the heat of mixing as a function of concentration of the concerned liquid systems are found to be in well agreement, except that for Al–Mg liquid alloy only at or about equiatomic compositions. Thus the asymmetry in the heat of mixing of the concerned liquid alloys has been well explained by regular associated solution model. This simply clarifies the fruitfulness of the preferred model in explaining the heat of mixing of the concerned binary liquid alloys at their corresponding melting temperatures.

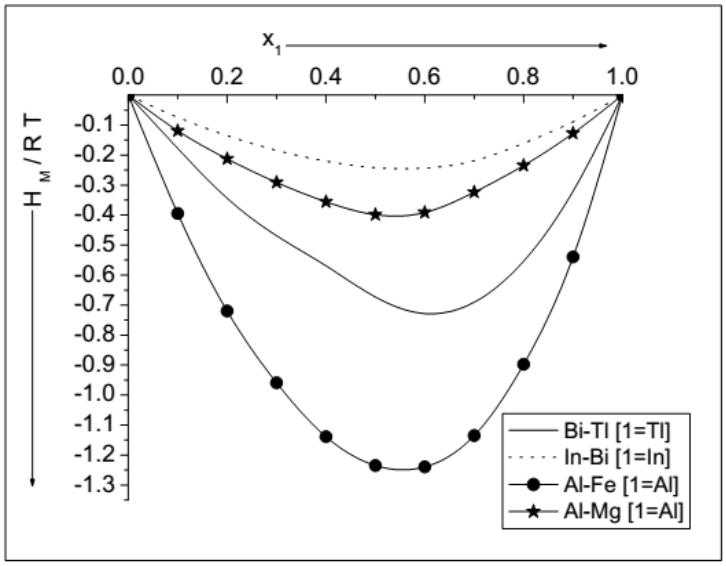

Figure 4.46: Heat of mixing of different systems as a function of concentration.

We have also computed the compositional contributions of the heat associated with the formation of the complexes and the heats of mixing of the monomers to the net enthalpy changes of the concerned systems. Theoretical investigations reveal that the compositional contribution from the term associated with the heat of formation of the complex to the net enthalpy change is at or quite close to the complex formation concentration of the respective alloy. But the compositional contribution from the heat of mixing of species to the net enthalpy change is not rigidly confined to any specific concentration.

The study of the heat of mixing gives the strength of bonding between the corresponding atoms of the alloy in the liquid mixture. In order to study the extent of bonding between the constituent atoms of the alloys under consideration, we have plotted the computed values of the heat of mixing of concerned liquid alloys as a function of concentration and are as shown in Fig. 4.46. Our theoretical findings reveal that the heat of mixing is the maximum for Al−Fe followed by Bi−Tl, Al−Mg and the least for In−Bi liquid alloys. This result is in accordance with that obtained from the comparative study of free energy of mixing and activity. But the minimum in the value of the heat of mixing is different for different liquid system.

The entropy of mixing can attain both positive and negative values depending upon the liquid alloy taken for investigation (Hultgren *et al.*, 1973). The negative values of S_M, in general is attributed to hetero−coordinating behaviour of the liquid alloy. The study of S_M thus gives the knowledge about the ordering tendency of the concerned liquid alloy. Theoretically computed and the experimental values of S_M/R as a function of concentration for the binary liquid alloys considered in this work are found to have positive values at all concentrations. Herein, we have used the same model fitting parameters, such as the equilibrium values of mole fractions of species of liquid mixture, equilibrium constant, interaction energy parameters, temperature derivative terms of interaction energy parameters and heat of dissociation those were taken to compute free energy of mixing and enthalpy of mixing. Both the theoretical and the experimental values of S_M/R are in excellent agreement for Bi−Tl and In−Bi liquid alloys but are in

fairly good agreement for Al−Fe and Al−Mg liquid alloys. The computed values of S_M/R indicates that Al−Fe liquid alloy is the most ordered followed by Al−Mg, In−Bi and the least ordered is Bi−Tl, whereas the values of S_M/R are comparable at most of concentration in In−Bi and Bi−Tl liquid alloys.

It has been already mentioned that in this work, theoretical modeling equations have been developed by extending regular associated solution model to predict the thermodynamic properties (activities and free energy of mixing) of some binary liquid alloys at different temperatures. The activities and free energy of mixing for Bi−Tl liquid alloy are computed at temperatures 750 K, 850 K, 950 K and 1050 K, among which 750 K is its melting temperature. The predicted values of these activities increase with increase in temperature of this alloy beyond its melting temperature. But the free energy of mixing of the alloy decreases with increase in its temperature. The theoretical findings thus predict that the tendency of free components in leaving the complex increases with increase in its temperature. As a result, the bonding between these components decreases with increase in temperature beyond its melting temperature. Therefore, the assumed complex of the liquid alloy is the most stable at its melting temperature (750 K) and the stability gradually decreases at elevated temperature. The activities and free energy of mixing for In−Bi liquid alloy are computed at temperatures 900 K, 1000 K, 1100 K and 1200 K, 900 K being its melting temperature. It can thus be predicted that the activity of the alloy increases with increase in its temperature thereby decreasing the stability of the alloy. But the values of G_M/RT decreases with increase in temperature of the liquid alloy beyond its melting temperature. As a result, it can be forecasted that the bonding between the atoms of the assumed complex of the liquid mixture decreases with increase in its temperature.

The activities and free energy of mixing for Al−Fe liquid alloy are computed at temperatures 1873 K, 1973 K, 2073 K and 2173 K, among which 1873 K is its melting temperature. The theoretical values obtained from the modeling equations predict that the activities of the components of the alloy increase whereas G_M/RT decrease with increase in temperature the alloy beyond its melting temperature. Eventually, the theoretical finding forecasts that the tendency towards complex formation the greatest at its melting

temperature (1873 K) among preferred temperatures. This behaviour of the liquid alloy gradually decreases with increase in its temperature. The activities of unassociated atoms Al and Mg, and G_M/RT for Al−Mg liquid alloy are computed at temperatures 1073 K, 1173 K, 1273 K and 1373 K, among which 1073 K is its melting temperature. The similar result is obtained for Al−Mg as stated for former preferred liquid alloys.

The present analysis thus forecasts that the activities of the considered binary liquid alloys increases whereas their free energy of mixing and excess free energy of mixing decreases with increase in temperatures beyond their respective melting temperatures. As a result, the tendency of the components of the alloy in leaving the complexes increases at elevated temperatures and hence the strength of the complex decreases at elevated temperatures. Thus the preferred liquid alloys are found to be the most interacting at their melting temperatures among the concerned temperatures of interests. The interacting nature of the liquid alloys thus decreases with increase in their temperatures beyond melting temperatures. Strictly speaking, the liquid alloys considered under study in this work shows ideal behaviour at higher temperatures. The results obtained in this work are in accordance with that of the other researchers for different systems employing different techniques (Rais et al,, 1982; Alquasmi & Egan, 1983; Saboungi & Carbin, 1984; Ali et al., 2004; Awe et al., 2011; Wang et al., 2013).

4.25.2 Discussion about the structural properties of binary liquid alloys

It has been already mentioned that the study and investigation of structural properties, such as $S_{CC}(0)$, α_1 and D_M/D_{id} helps to better understand the nature of local arrangement of atoms at microscopic level as well as the tendency towards compound formation in the liquid binary alloys. The prediction of these properties at different temperatures usually higher than the melting temperature of the respective liquid alloys helps to forecast the prevailing tendencies of the liquid alloys towards ordering (hetero−coordinating) or segregation (homo−coordinating) at elevated temperatures. At a concerned composition and temperature, $S_{CC}(0) < S_{CC}^{id}(0)$ refers to ordering nature for which $\alpha_1 < 0$ and $\frac{D_M}{D_{id}} > 1$

whereas $S_{CC}(0) > S_{CC}^{id}(0)$ corresponds to tendency towards segregation for which $\alpha_1 > 0$ and $\frac{D_M}{D_{id}} < 1$. In the case of ideal mixing, $S_{CC}(0) \rightarrow S_{CC}^{id}(0)$ and hence $\alpha_1 \rightarrow 0$ and $\frac{D_M}{D_{id}} \rightarrow 1$. In the present study, we have found that the computed as well as the experimental values (computed from modeling equation) of $S_{CC}(0)$ are less than the corresponding ideal values at all concentrations for the preferred liquid alloys at their respective melting temperatures. Eventually, the computed values of α_1 are negative and D_M/D_{id} are positive and greater than one at all concentrations for all considered systems. The theoretical investigations thus reveal that all the liquid alloys taken under study in this work are complete ordering in nature at their melting temperatures and shows tendency towards chemical ordering or compound formation. Further, it has been observed that the binary liquid alloys exhibit asymmetric behaviour around the equiatomic composition. The deviation between the ideal and computed values of $S_{CC}(0)$ is distinctly noticeable in the concerned systems; however, the maximum deviation does not exactly correspond to the compound forming concentration in all cases as expected.

According to the statistical thermodynamics, $S_{CC}(0)$ can be expressed in terms of thermodynamic functions specially activity and free energy of mixing; Eqs. (3.117) and (3.122). As the thermodynamic functions are greatly influenced by the selections of μ, ν, K and ω_{ij} thereby overruling the position of minima in $S_{CC}(0)$. The tendency towards the compound formation can also be analyzed by evaluating the Darken's excess stability (ES) which in turn can be expressed in terms of $S_{CC}(0)$ as (Darken, 1967; Saboungi et al., 1990)

$$ES = \frac{\partial^2 G_M^{XS}}{\partial x_1^2} = \frac{RT}{x_2}\left[\frac{\partial \ln a_i}{\partial x_1} - \frac{1}{x_1}\right] = RT\left[\frac{1}{S_{CC}(0)} - \frac{1}{x_1 x_2}\right] \tag{4.6}$$

where the terms have their usual meanings.

The excess stability functions of the preferred liquid alloys have been computed using Eq. (4.6) and the experimental values of $S_{CC}(0)$. The computed values of the compositional

dependence of excess stability for the liquid alloys preferred in this work are portrayed in Fig. 4.47.

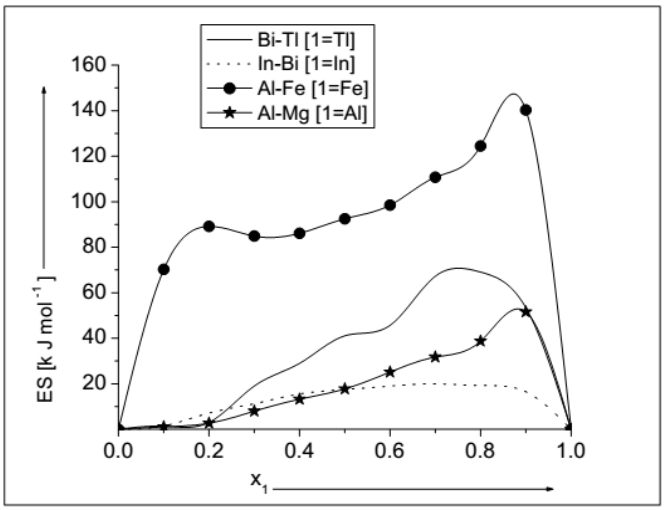

Figure 4.47: The compositional dependence of experimental values of excess stability (ES) for different liquid alloys.

The perusal of Fig. 4.47 communicates that the observed values of excess stability are positive throughout the entire concentration for all the preferred binary liquid alloys at their respective melting temperatures. These findings further clarify the compound forming tendencies or ordering natures of the liquid alloys at stated temperatures.

However, the predicted values of $S_{CC}(0)$ increases whereas that of α_1 and D_M/D_{id} decreases with increase in temperatures of the considered systems above their respective melting temperatures. Therefore, the present study forecasts that the ordering or compound formation tendency of the liquid alloys decreases with increase in temperatures. More specifically, the liquid alloys show ideal behaviour at higher temperatures. The computed values of $S_{CC}(0)$ are found to be less than the ideal values for Bi−Tl and Al−Fe liquid alloys at all concentrations and temperatures which indicates that the ordering tendency still prevail in these alloys within these range of temperatures. But in case of In−Bi and Al−Mg liquid alloys, the computed values of $S_{CC}(0)$ exceeds corresponding ideal values within the concentration ranges $x_1 < 0.16$ and $x_1 < 0.24$

respectively above their respective melting temperatures indicating the tendency towards segregation. Above these constrained concentration ranges, both of the alloys show segregating (homo−coordinating) to ordering (hetero−coordinating) transformations. Theoretical predictions made by the computations of α_1 and D_M/D_{id} for the preferred liquid alloys at different temperatures follows the similar trends as that of $S_{CC}(0)$. Moreover, these forecasts are also accordance with the results predicted by the computations of thermodynamic functions at different temperatures. The theoretical findings thus reveal that the liquid alloys tend towards ideal mixtures at higher temperatures.

4.25.3 Discussion about the surface properties of binary liquid alloys

The study of surface phenomena help to understand the kinetics of phase transformations, catalytic activities of alloys catalysts, wettability and various other mechanical behaviour of the liquid alloys. The accurate experimental procedure to determine the surface tension of clean metal and alloy surfaces (due to contamination with oxides) is difficult and hence very few reliable data are available. Due to this inadequacy, devising statistical approaches for the determination of surface tensions and surface concentrations of liquid alloys have fundamental importance. The surface properties, such as surface tension and surface segregation of two Bi−based, such as Bi−Tl at 750 K and In−Bi at 900 K and two Al−based binary liquid alloys, such as, Al−Fe at 1873 K and Al−Mg at 1073 K have been studied on the basis of Renovated Butler model.

Theoretically computed values of surface tension (σ) for Bi−Tl liquid alloy at 750 K is less than its ideal values in the bulk concentration range $x_1 < 0.6$ (1 is for Tl) and exceeds ideal value at rest of the concentrations. The value of σ of the system increases with the increase in the bulk concentrations of Tl. Moreover, the computed value of the surface concentration of Tl (x_{Tl}^S) atoms is less whereas that of Bi (x_{Bi}^S) atoms is greater than their corresponding ideal values throughout the bulk concentrations. It can be, therefore, concluded that Tl atoms remains in the bulk whereas Bi atoms segregates on

the surface of the liquid mixture at 750 K. The computed value of σ for In−Bi liquid alloy at 900 K is less that its ideal value at all bulk concentrations of In. σ of this system increases with the increase in the concentrations of In. The computed value x_{In}^{S} of is less but that of x_{Bi}^{S} is greater than that their respective ideal values and hence the former remains in the bulk and the later segregates on the surface. The comparative study of the two Bi−based liquid alloys shows that the extent of segregation of Bi atoms in the surface region is greater in In−Bi melt than that of Bi−Tl melt at their respective melting temperatures.

.

Theoretically obtained value of σ for Al−Fe liquid alloy at 1873 K is less than its ideal value in the entire bulk concentrations of Al but its value decreases with increase in the bulk concentrations of Al. The determined value of x_{Al}^{S} is greater than its ideal value, therefore, it segregates on the surface whereas that of x_{Fe}^{S} is less than its ideal value and hence it remains in the bulk in the binary solution at 1873 K. Likewise, the computed value of σ for Al−Mg liquid alloy at 1073 K is also less than its ideal value at all bulk concentrations of Al and its value increases with the increase in bulk concentrations. As the computed value of x_{Al}^{S} is less whereas that of x_{Mg}^{S} is greater than their corresponding ideal values, the former atoms remains in the bulk whereas the later segregates on the surface of the liquid mixture at 1073 K throughout the entire bulk concentrations. The results of two Al−based liquid alloys show that the Al atoms segregate in the surface region in Al−Fe melt whereas they remain in the bulk region in Al−Mg melt at their respective melting temperatures.

As stated earlier, we have also predicted the surface properties of the concerned systems at different temperatures by correlating the thermodynamic properties predicted on the basis of extended regular associated solution model with Renovated Butler model. The surface properties of Bi−Tl liquid alloy have been predicted at temperatures 750 K, 850 K, 950 K and 1050 K. The predicted values of the surface tensions of the system gradually decrease with the gradual increase in temperatures above its melting temperature. The computes value of x_{Tl}^{S} increases whereas that of x_{Bi}^{S} decreases with the

increase in temperature of the alloy. Both of these values get closure to their respective ideal values which may be due to the decrease in the cohesive force between the liquid layers at higher temperatures as predicted by the thermodynamic properties. Likewise, the surface properties of In−Bi liquid alloy have been predicted at temperatures 900 K, 1000 K, 1100 K and 1200 K. The computed values of σ for this system decreases with increase in its temperatures as expected. The surface concentrations of In increases whereas that of Bi decreases with increases with increase in the temperatures of the system beyond its melting temperature following the similar trends as that of earlier system. The surface properties of Al−Fe alloy have been forecasted at temperatures 1873 K, 1973 K, 2073 K and 2173 K. Herein the computed values of σ at different temperatures shows the similar trend as earlier systems. Theoretically determined value of surface concentrations of Al gradually decreases whereas that of Fe increases with the increase in the temperature of this liquid alloy and hence Al atoms move from the surface to the bulk region whereas the Fe atoms move from the bulk to the surface to attain equilibrium. The surface properties of Al−Mg liquid alloys have been computed at temperatures 1073 K, 1173 K, 1273 K and 1373 K. The computed values of σ at higher temperatures show the similar trends as by the systems mentioned above. With the increase in temperature of the alloy x_{Al}^{S} gradually increases but x_{Mg}^{S} decreases, however, they get closure to their ideal values. The results obtained in this work follow the similar trends as obtained and defined by earlier researchers (Hoar & Melford, 1957; Gasior et al. 2001, 2011; Aqra et al., 2011; Pstrus′ et al., 2011; Kaptay, 2012, 2015; Gancarz & Gasior, 2016; Gancarz, 2017) for different systems employing different techniques.

CHAPTER 5

CONCLUSION AND RECOMMENDATIONS

5.1 Conclusion

The presented work is basically confined to study the mixing behaviour of some binary liquid alloys, such as Bi−Tl, In−Bi, Al−Fe and Al−Mg. The work is clearly partitioned into two sections. In the former section, the work is focused to study and to explain the thermodynamic properties, such as free energy of mixing (G_M), activity (a), heat of mixing (H_M) and entropy of mixing (S_M); and microscopic structural properties, such as concentration fluctuation in long wavelength limit ($s_{CC}(0)$), chemical short range order parameter (α_1) and ratio of diffusion coefficients (D_M/D_{id}) of above mentioned liquid alloys in the frame work of regular associated solution model. The modeling expressions for these thermodynamic and structural functions have also been derived assuming the complex of the type $A_\mu B_\nu$ both for $\mu > 1$ and $\nu > 1$; and $\mu > 1$ and $\nu = 1$. Herein, μ and ν are small indices whose values depends upon the stiochiometric composition at which the most intermetallic compound is formed and are determined from the knowledge of the phase diagram of the respective alloy in the solid state. The validity of the preferred statistical model has been established by comparing the computed values the thermodynamic and structural properties with the experimental values. The surface properties, such as surface tensions (σ) and surface segregations (x_A^s and x_B^s) have been computed and analyzed by employing Renovated Butler model. In the later section, regular associated solution model has been extended to predict and to explain the thermodynamic and structural properties of the liquid alloys at different temperatures. The work has been then correlated with the Renovated Butler model to predict the surface properties of these liquid alloys at different temperatures.

The liquid alloys selected for the study in this work covers a wide spectrum of mixing behaviour from symmetric to asymmetric in thermodynamic properties whereas most of

them show asymmetric in the structural properties. Moreover, these alloys have numerous applications in the modern day technological advancements (details of applications are mentioned in Chapter 3). Eventually, the study and explanation of the anomalies in the mixing properties of these alloys have fundamental importance in the field of metallurgical processing, characterization and design. Moreover, the prediction of the thermodynamic and structural properties for the concerned systems at different temperatures will provide the database in case of unavailability of the experimental data as the experimental techniques are being cumbersome and difficult to handle at different higher temperatures. The experimental determination of the surface properties of liquid alloys are more prone to errors as the metallic surfaces have high probability of being contaminated with oxides (Hoar & Melford, 1957; Tanaka et al., 1966). In this limelight, the determination of the surface properties of binary systems and hence forecasting these properties on the basis of modeling equations at higher temperatures will definitely initialize a pavement in the field of surface science.

The anomalies or asymmetric trends in the mixing behaviour of the liquid alloys have been reported by many researchers (Hultgren *et al*., 1973; Takeuchi et al., 1973; McAlister & Crozier, 1974; Hoshino & Young, 1986). These observed phenomena might be due to the presence of strong interactions between the ingredient atoms of the liquid mixtures resulting in the presence of intermetallic compounds at one or more stoichiometric compositions in the solid state (Sommer, 1990; Young, 1992). Eventually, many researchers believed in the existence of the atomic ordering or chemical complexes in the initial melt of the liquid mixtures and devised different statistical approaches to explain the energetic of different liquid alloys (Jordan, 1970; Bhatia & Hargrove, 1974; Lele & Ramchandrarao, 1981; Hoshino, 1983; Bhatia & Singh, 1984; Singh & Sommer, 1992; Godbole et al., 2004; Adhikari 2013). Likewise, the thermodynamic and structural functions in regular associated solution model are derived on the basis of the existence of chemical complex of the type $A_\mu B_\nu$ in the initial melt of binary alloys. We, therefore, have assumed the presence of complexes TlBi, In_2Bi, Al_3Fe and Al_3Mg_2 in the respective Bi−Tl, In−Bi, Al−Fe and Al−Mg liquid alloys and explained their mixing properties in the frame work of preferred model.

Following Hume−Rothery and Powell (1935), the size mismatch and difference in the electronegativity of the alloying metals also overrule the thermodynamic and structural behaviour of the initial melt corresponding to the anomalies in these properties. The compound forming alloys are generally characterized by large electronegativity differences. For the alloy of the type A−B, the size factor can be obtained from the expression $\Omega_{A-B} = \Omega_A/\Omega_B$; Ω being the atomic volume at the melting temperature of the alloy and the electronegativity difference can be obtained as $E_{A-B} = E_A - E_B$; E_A and E_B are the electronegativity of components A and B respectively for $E_A > E_B$. The computed values of Ω_{A-B}; E_{A-B} and ionic character (IC) are found to be 0.87, 0.82, 1.50, 0.73; 0.40, 0.24, 0.22, 0.30 and 0.0392, 0.0010, 0.0120, 0.0223 respectively for Bi−Tl, In−Bi, Al−Fe and Al−Mg liquid alloys. The computed values of the size factors, the difference in the electronegativity and IC for the concerned liquid alloys are small enough leading to the compound formation tendency and asymmetric tendency in the mixing behaviours. Even though, the phase diagrams of these liquid alloys clearly indicate the existence of intermetallic compounds at one or more stiochiometric compositions (Hultgren *et al.*, 1973). It can be thus interpreted that the compound formation tendency of the concerned systems cannot be explained on the basis of their size factors and electronegativity differences.

Some of the important conclusions of the work carried out in this thesis can be summarized as follows:

A. Model parameters

(i) The model fit parameters, such as pairwise interaction energies (ω_{12}, ω_{13} and ω_{23}) and the equilibrium constant (k) have been computed for all the preferred binary liquid alloys with the aid of observed values of the activity coefficients of the constituent atoms at infinite dilutions and free energy of mixing. The compositional dependence of mole fractions of the complex (x_{A-B}) and unassociated atoms (x_A and x_B) have been then computed for all the systems

with the help of modeling equations in the frame work of regular associated solution model.

(ii) All the interaction energy parameters are assumed to be temperature dependent in the preferred model. The temperature derivative terms of the pairwise interaction energy parameters ($\partial\omega_{12}/\partial$T, $\partial\omega_{13}/\partial$T and $\partial\omega_{23}/\partial$T) have been obtained from the modeling equations with assistance of the observed values of heat of mixing for the respective liquid alloys.

(iii) The mole fractions of the complexes, free monomers, equilibrium constants and temperature derivative terms of interaction energy parameters are assumed to be constant at higher temperatures. The values of interaction energy parameters are computed from the modeling equations at higher temperatures for each of the above mentioned systems. These modeling equations are obtained by extending regular associated solution model under curtained constraints.

B. Free energy of mixing (G_M)

(i) The theoretical and the experimental values of G_M/RT are in well or good agreement for all the considered liquid alloys at their respective melting temperatures. The asymmetric and the symmetric in G_M of the systems are well explained by regular associated solution model.

(ii) The computed values of G_M^{XS}/RT gradually decreases at elevated temperatures indicating the decrease in the compound forming tendency of the liquid alloys. The liquid alloys are found to be the most interacting at their respective melting temperatures and this nature declines at higher temperatures.

(iii) On the floor of the comparative study of the free energy of mixing of preferred binary liquid alloys at their respective melting temperatures, their interaction tendencies can be ordered as Al−Fe > Bi−Tl > Al−Mg > In−Bi.

C. Activity (a)

(i) The activities of the preferred liquid alloys have been computed using the same model parameters that have been used for the estimations of free energy of mixing.

(ii) The compositional dependence of the computed values of activities for the considered liquid alloys is in good agreement with their corresponding experimental values at their respective melting temperatures.

(iii) The modeling equations have been used to compute the activities of the systems at different temperatures. The predicted values of the activities gradually increases with increase in temperatures of the systems revealing the similar tendency towards compound formation as forecasted by free energy of mixing at different temperatures.

D. Heat of mixing (H_M)

(i) To compute the compositional dependence of H_M/RT of the liquid alloys considered for study in this thesis, we have used the same set of model parameters that have been used for the computations of other thermodynamic parameters.

(ii) The compositional dependence of the computed and the experimental values of H_M/RT for all the preferred liquid alloys are in well agreement. Hence, the regular associated solution model has well explained the asymmetry in H_M of considered systems.

(iii) The comparative study of the heat of mixing of the liquid alloys preferred in this work shows that Al−Fe is the most interacting system followed by Bi−Tl,

Al–Mg and In–Bi being the least interacting system. The similar trend has been predicted by the comparative study of free energy of mixing.

E. Entropy of mixing (S_M)

(i) For consistency, we have used the same set of model parameters that has been used for the estimation of above mentioned thermodynamic properties to compute the entropy of mixing of the liquid alloys taken under study in this work.

(ii) The computed as well as the experimental values of S_M/R as a function of concentration are in well agreement for Bi–Tl, In–Bi and Al–Fe whereas in reasonable agreement for Al–Mg at their respective melting temperatures. They are found to have positive values throughout the entire concentration range. Theoretically, it is found that the concerned systems are more ordered at lower and higher concentrations of x_1.

F. Structural properties

(i) We have used the same set of model parameters to determine the structural properties that were used to compute thermodynamic properties.

(ii) The compositional dependence of the computed values of $S_{CC}(0) < S_{CC}^{id}(0)$, $\alpha_1 < 0$ and $D_M/D_{id} > 1$ for all the preferred systems revealing the systems to be completely ordering in nature at their respective melting temperatures.

(iii) The computed values of $S_{CC}(0)$ gradually increases and get close to corresponding ideal values with increase in temperatures of the liquid alloys beyond their melting temperatures. Furthermore, the deviation between the ideal and computed values of $S_{CC}(0)$ gradually decreases at elevated

temperatures. It can be thus predicted that the systems are found to be the most interacting at their melting temperature and this tendency, however, decreases at elevated temperatures. More precisely, the liquid alloys show ideal behaviours at higher temperatures. These predictions are further verified by the decrease in negative values of α_1 and decrease in positive values of D_M/D_{id} as a function of concentration at higher temperatures. However, In−Bi and Al−Mg liquid alloys show the transformation from ordering to segregating tendency at or above 1100 K in the concentration range $x_1 < 0.16$ and at or above 1173 K in the concentration range $x_1 < 0.24$ respectively.

G. Surface properties

(i) The surface properties of the liquid alloys have been computed in the frame work Renovated Butler model. Additionally, theoretically computed partial excess free energies of the components of the preferred liquid alloys at different temperatures (obtained by extending regular associated solution model) have been correlated with the Renovated Butler model to explain their surface behaviours at different temperatures.

(ii) The computed value of $\sigma < \sigma^{id}$ for the liquid alloys except Bi−Tl in which $\sigma < \sigma^{id}$ in the bulk concentration range $x_1 < 0.6$ and exceeds ideal value at rest of the concentrations. Theoretical investigations confirm the segregation of the alloy component having a lower surface tension, i. e. the extent of segregation of Bi−atoms at the surface layer, which is more pronounced in In−Bi melts with respect to that of liquid Bi−Tl alloys. Moreover, in case of two Al−based melt, the Al−atoms segregate on the Al−Fe surface phase whereas they remain in the bulk region of Al−Mg.

(iii) The computed values of σ as a function of bulk concentration gradually decreases at elevated temperatures. The surface concentrations of the individual atoms of the liquid alloys gradually get closure to their respective

ideal values at higher temperatures. The atoms of the surface phase move towards region and vice-versa at elevated temperatures to maintain the equilibrium in the liquid mixture.

5.2 Recommendations

i. The validity of the theoretical models are first established by explaining the explaining the thermodynamic properties of the liquid alloys. This procedure further yields the best fit values of the model parameters. In case of unavailability of the observed thermodynamic databases the theoretical model cannot be devised. Therefore, more techniques should be tooled for the experimental measurements with high accuracy.

ii. In this work, we have explained the mixing behaviours of few binary liquid alloys. Moreover, we have predicted the thermodynamic, structural and surface properties of the liquid alloys at different temperatures by extending the theoretical models. The further extensive work is required to predict and explain the transport properties of the liquid alloys at different temperatures.

iii. The predicted values of the mixing properties of the liquid alloys could not be compared with the experimental values due to unavailability of such database. The experiments should be, therefore, devised on the floor of theoretical database for the design and characterization of new materials.

iv. Due to the complexities in the expressions for the mixing behaviours, the regular associated solution model could not be employed to study and explain the mixing properties of ternary liquid alloys. Therefore, further modifications in the model are required to explain and predict such properties of ternary liquid alloys.

CHAPTER 6

SUMMARY

The mixing behaviours of few compound forming binary liquid alloys, such as Bi−Tl at 750 K, In−Bi at 900 K, Al−Fe at 1873 K and Al−Mg at 1073 K have been studied and explained in this work on the basis of modeling equations. The thermodynamic and structural properties of the alloy systems have been analyzed in the framework of regular associated solution model. The surface properties of these alloys have been explained in the framework of Renovated Butler model. Further, regular associated solution model have been extended to compute and predict the mixing behaviours of above mentioned alloys at different temperatures. These thermodynamic properties have been correlated with Renovated Butler model to forecast the surface properties of these systems at different temperatures.

The main features of this work can be summarized as follows:

1. The thermodynamic properties, such as free energy of mixing (G_M), activity (a), heat of mixing (H_M) and entropy of mixing (S_M) of the above mentioned liquid alloys have been well explained by regular associated solution model. Consequently, the model fit parameters so obtained have well reproduced the structural properties, such as concentration fluctuation in long wavelength limit ($S_{CC}(0)$), chemical short range order parameter (α_1) and the ratio of diffusion coefficients (D_M/D_{id}).

2. The model fit parameters of the regular associated solution model are determined from the experimental values of the activity coefficients of the unassociated atoms of the melt at infinite dilution and activity data irrespective of other theoretical model. This unique feature has been utilized to extend the preferred model to predict the thermodynamic and structural properties of above mentioned liquid alloys at different temperatures.

3. The predicted excess free energy of mixing of the liquid alloys gradually decreases with increase in their temperatures above respective melting temperatures. Consequently, the activity of the components of the liquid alloys gradually increases at elevated temperatures. These theoretical investigations predict that the compound forming tendencies of the liquid alloys gradually declines at elevated temperatures and are the systems are found to be most interacting at their respective melting temperatures.

4. The predicted values of $S_{CC}(0)$ gradually increases and get closure to the ideal values at elevated temperatures. These findings also communicate that the tendency towards compound formation in the liquid alloys decreases at higher temperatures. Moreover, the liquid alloys show ideal behaviour at higher temperatures. These theoretical forecasting's are further clarified by the computations of α_1 and D_M/D_{id} at different temperatures.

5. The surface properties, surface tension (σ) and surface segregations (x_A^S and x_B^S) of the components of the liquid alloys of the type A−B have been computed in the framework of Renovated Butler model.

6. The surface properties of the preferred liquid alloys have been predicted at different temperatures by associating Renovated Butler model with the extended regular associated solution model. The surface tensions of the alloy systems gradually decrease at elevated temperatures which is due to decrease in the strength of bonding between the atoms to form the complex as predicted by the thermodynamic and structural properties. Additionally, there are movements of atoms from the surface region to the bulk region and vice−versa in the liquid mixture at elevated temperatures to nullify the change in surface tension gradient induced by high temperatures.

7. More precisely, the preferred liquid alloys show ordering tendency at least at or closed to their melting temperatures, however, there is transformation from ordering to segregating nature at elevated temperatures. These thermodynamic and surface databases at different temperatures obtained by theoretical modeling will provide reference to devise experimental procedures for the fabrications of new materials.

REFERENCES

Adebayo, G. A., & Anusionwu, B. C. (2006). Dynamical properties of Ag−Cu binary alloy from molecular dynamics simulation. *The European Physical Journal B −Condensed Matter and Complex System*, 54, 423−427.

Adhikari, D. (2011). Disorder in liquid Cu−Pd alloys. *Phase Transitions,* 84, 308−314.

Adhikari, D. (2011). Inhomogeneity in structure of Mg−Pb liquid alloy. *Physica B,* 406, 445−448.

Adhikari, D. (2013). *Regular associated solution model for the properties of binary liquid alloys* (Unpublished doctoral dissertation). T. M. Bhagalpur University, Bhagalpur, India.

Adhikari, D., Jha, I. S., & Singh, B. P. (2010). Structural asymmetry in liquid Fe−Si alloys. *Philosophical Magazine,* 90, 2687−2694.

Adhikari, D., Jha, I. S., & Singh, B. P. (2012). Transport and surface properties of Al−Mn alloy. *Advanced Materials Letters,* 3, 226−230.

Adhikari, D., Singh, B. P., & Jha, I. S. (2010). Structural and energetic asymmetry in liquid Ag−Al alloys. *Physics and Chemistry of Liquids,* 48, 787−796.

Adhikari, D., Singh, B. P., & Jha, I. S. (2010). Thermodynamic properties and microscopic structure of liquid Cd−Na alloys by estimating complex concentration in a regular associated solution. *Journal of Molecular Liquids,* 156, 115−119.

Adhikari, D., Singh, B. P., & Jha, I. S. (2012). Energetics of Cd−based binary liquid alloys. *Journal of Non-Crystalline Solids,* 358, 1362−1367.

Adhikari, D., Yadav, S. K. & Jha, L. N. (2014). Thermo−physical properties of Al−Fe melt. *Journal of Chinese Advanced Material Society,* 2, 149−153.

Aditya, M. V. (2010). Study of thermodynamic properties of liquid binary alloys by a pseudo−potential method. *Journal of Engineering Physics and Thermophysics,* 83, 1070−1079.

Agarwal, R. & Sommer, F. (1991). Calorimetric measurements of liquid Al−Mg alloys. *Zeitschrift für Metallkunde*, 82, 118−120.

Akinlade, O. (1994). Thermodynamics of molten K−Te alloys. *Journal of Physics F: Metal Physics*, 6, 4615−4624.

Akinlade, O., Ali, I. & Singh, R.N. (2001). Correlation between bulk and surface phenomena in Ga (−Bi, In) and In−Bi liquid alloys. *International Journal of Modern Physics B,* 15, 30−39.

Akinlade, O.A., Singh, R.N., & Sommer, F. (2000). Thermodynamics of liquid Al−Fe alloys. *Journal of Alloys and Compounds*, 299, 163−168.

Akinlade, O., & Singh, R. N. (2001). Surface segregation and surface tension in liquid Fe−Cu alloys. *Zeitschrift für Metallkunde*, 92, 1111−1113.

Akinlade, O., Singh, R. N., & Sommer, F. (2000). Thermodynamics if liquid Al−Fe alloys. *Journal of Alloys and Compound,* 299, 163−168.

Alblas, B. P. (1983). *Order and disorder in liquid alloys* (Doctoral dissertation). University of Groningen, The Netherlands.

Ali, I., Osman, S.M. & Singh, R.N. (1999). Ordering and structural properties of Al−Ge alloys. *Journal of Non-Crystalline Materials,* 321, 250−252.

Ali, I., Osman, S.M., Sulaiman, N. & Singh, R.N. (2004). Thermodynamic properties of He−H_2 fluid mixtures over wide range of temperatures and pressures. *Physical Review E*, 69, 1−11.

Alkins, P., & De Paula, J. (2002). *Physical Chemistry*. United Kingdom: Oxford University Press.

Allan, R. G. (1997). Applications for Aluminium alloys in marine industry a current perspective. *Proceedings of Alumitech,* 97, 292.

Allen, M. P., & Tildesley, D. J. (1987). *Computer simulation of liquids*. Oxford: Clarendon Press.

Alonso, J. A., Lopez, J. M., & March, N. H. (1982). Concentration fluctuations in simple liquid alloys with atomic size mismatch. *Journal of Physique−LETTERS,* 43, 441−445.

Alonso, J.A. & March, N.H. (1982). Concentration fluctuations in simple metallic liquid alloys. *Physica B+C,* 114, 67−70.

Alqasmi, R., & Egan, J. J. (1983). Thermodynamic of liquid sodium−tin alloys using calcium fluoride solid electrolytes. *Berichte Der Bunsen−Gesellschaft fur Physikalische Chemie,* 87, 815−817.

Alven, D. & Stoloff, M. (1997). The influence of composition on the environmental embattlement of Fe3Al alloys. *Materials Science and Engineering A,* 239*,* 362−368.

Anusionwu, B.C. (2006). Thermodynamic and surface properties of Sb−Sn and In−Sn liquid alloys. *Pramana: Journal of Physics,* 67, 319−330.

Anusionwu, B.C., Adebayo, G.A. & Madu, C.A. (2009). Thermodynamic and surface properties of liquid Al−Ga and Al−Ge alloys. *Applied Physics A,* 97, 533−541.

Anusionwu, B. C., & Echendu, O. K. (2010). Thermodynamic studies of the surface and transport properties in Ag−In and Ag−Sb liquid alloys. *Physics and Chemistry of Liquids,* 48, 127−114.

Aqra, F., Ayyad, Ah. & Takrori, F. (2011). Model calculation of the surface tension of liquid Ga−Bi alloy. *Applied Surface Science,* 257, 3577−3580.

Arzpeyma, G., Gheribi, A. E., & Medrij, M. (2013). On the prediction of Gibbs free energy of mixing of binary liquid alloys. *Jounal of Chemical Thermodynamics,* 57, 82−91.

Ashcroft, N. W., & Langreth, D. C. (1967). Structure of binary liquid mixtures. *Physical Review,* 156, 685−692.

Awe, O. E., Akinlade, O., & Hussain, L. A. (2003). Thermodynamic properties of liquid Te–Ga and Te–Tl alloys. *Journal of Alloys and Compounds,* 36, 227−233.

Awe, O.E., Odusote, Y.A. & Hussain, L.A. (2008). Thermodynamic properties of some gallium based binary alloys. *Physica B,* 403, 2629−2633.

Awe, O. E., Odusote, Y. A., Hussain, L. A., & Akinlade, O. (2011). Temperature dependence of thermodynamic properties of Si−Ti binary liquid alloys. *Thermochimica Acta,* 519, 1−5.

Awe, O.E. & Olawole, O. (2012). Correlation between bulk and surface properties in Cd−X (X= Hg, Mg) liquid alloys. *Journal of Non−Crystalline Solids,* 358, 1491−1496.

Bangwei, Z. (1983). Application of Miedema's coordinates to the formation of binary amorphous alloys. *Physica B+C,* 121, 405−408.

Bangwei, Z., Liao, S., Shu, X., Xie, H., & Yuan, X. (2013). Theoretical calculation of the mixing enthalpies of 21 III B−IV B, III B−V B and IV B−V B binary alloy systems. *Physics Metals and Metallogr,* 114, 457−468.

Basu, J., Murty, B. S., & Ranganathan, S. (2008). Glass forming ability: Miedema approach to (Zr, Ti, Hf) − (Cu, Ni) binary and ternary alloys. *Journal of Alloys and Compounds,* 465, 163−172.

Bekker, H. (1998). *Enthalpies in alloys: Miedema's semi−emperical model.* Switzerland: Trans Tech Publication Limited.

Belton, G.R. & Fruehan, R.J. (1969). Mass spectrometric determination of the activities in Fe−Al and Ag−Al liquid alloys. *Transactions of the Metallurgical Society of AIME*, 245, 113−117.

Belton, J. W., & Evans, M. G. (1945). Studies in the molecular and surface forces. *Transactions of the Faraday Society,* 41, 1−12.

Bhatia, A. B., & Hargrove, W. H. (1974). Concentration fluctuations and thermodynamic properties of some compound forming binary molten systems. *Physical Review B,* 10, 3186−3196.

Bhatia, A. B., Hargrove, W. H., & Thornton, D. E. (1974). Concentration fluctuations and partial structure factors of compound−forming binary molten alloys. *Physical Review B,* 9, 435−444.

Bhatia, A. B., & March, N. H. (1975). Size effects, peaks in concentration fluctuations and liquidus curves of Na−Cs. *Journal of Physics F: Metal Physics,* 5, 1100−1106.

Bhatia, A. B., & Singh, R. N. (1980). Volume of mixing of compound forming molten alloys. *Physics Letters A,* 78, 460−462.

Bhatia, A. B., & Singh, R. N. (1984). A quasi-lattice theory for compound forming molten alloys. *Physics Chemistry Liquids,* 13, 177−190.

Bhatia, A. B., & Thornton, D. E. (1970). Structural aspects of the electrical resistivity of binary alloys. *Pysical Review B,* 2, 3004-3012.

Bhuiyan, G. M., Alam, M. S., Ahmed, A. Z., Syed, I. M., & Rashid, R. I. (2009). Entropy for Ag_xIn_{1-x} liquid binary alloys. *Journal of Chemical Physics,* 131, 034502−034508.

Blagoveshchenskii, N.M., Lisichkin, Yu.V., Morozov, V.A., Novikov, A.G., Savostin, V.V., & Shimkevich, A.L. (2002). Structure and possible cluster formation in liquid lead−potassium alloys. *Applied Physics A*,74, 1107−1118.

Brandes, E. A., & Brook, G. B. (1992). *Smithells Metals Reference Book*. Jordanhill, Oxford: Butterwarth−Heinemann.

Brewer, L. (1965). *Prediction of high temperature metallic phase diagrams*. New York: John Wiley.

Brewer, L. (1967). *Phase stability in metals and alloys*. New York: McGraw−Hill.

Brewer, L., & Lamoreanx, R. H. (1980). Molybdenum: Physicochemical properties of its compounds and alloys .I. Thermochemical properties. *Atomic Energy Review*, 11, 11-191.

Brongersma, H. H., & Buck, T. M. (1975). Selected topics in low−energy iron scattering: surface segregation in Cu/Ni alloys and iron neutralization. *Surface Science,* 53, 649−658.

Burton, J. J., & Machlin, E. S. (1976). Prediction of segregation to alloy surface from bulk phase diagrams. *Physical Review Letters,* 37, 1433−1436.

Busch, G., & Gunthe-Rodt, H. J. (1974). *Solid State Physics* (H. Ehrenreich, F. Seitz & D. Turnball Eds. Vol. 29). New work: Academic Press.

Butler, J. A. V. (1932). The thermodynamics of the surface of solutions. *Proceedings of the Royal Society of London A,* 135, 348−375.

Calaway, W.F. & Saboungi, M.L. (1983). Electrical resistivity of the Na−Pb system: measurements and interpretation. *Journal of Physics F: Metal Physics,* 13, 1213−1224.

Chieux, P., & Ruppesberg, H. (1980). Atomic structure the observation of chemical short range order in liquid and amorphous systems by diffraction methods. *Journal of Physique Colloques,* C8 41, 145−152.

Chushak Ya., & Baumketner A. (1999). Theoretical and computer simulation study of density fluctuations in liquid binary alloys. *The European Physical Journal B*, 7, 129−136.

Cowley, J. M. (1950). An approximate theory of order in alloys. *Physical Review,* 77, 667−675.

Cubero-Sesin, J. M., & Horita, Z. (2012). Mechanical properties and microstructures of Al−Fe alloy processed by hig−-pressure torsion. *Metallurgical Materials Transactions A,* 43, 5182−5192.

Darken, L. S. (1948). Diffusion, mobility and their interrelation through free energy in binary metallic system. *Transactions AIME,* 157, 184−201.

Darken, L. S. (1967). Thermodynamics of binary metallic solutions. *Transitions Metallurgical Society, AIME,* 239, 80−89.

Darken, L. S., & Gurry, R. W. (1953). *Physical chemistry of metals*. New York: Mc Graw-Hill Book Corporation.

De Boer, F. R., Boom, R., Mattens, W. C. M., & Miedema, A. R. (1989). *Cohesion in Metals*. Amesterdam: North Holland Physics Publishing.

Desai, P. D. (1987). Thermodynamic properties of selected binary aluminum alloy systems. *Journal of Physics and Chemistry Reference Data,* 16, 109−124.

Dooley, D. E., Olson, D. L., Edwards, G. R., & Gibbs, F. E. (2001). Development of an electronic phase diagram and the predictions of plutonium alloy phase stability using electronic properties. *Journal of Physics: Condensed Matter,* 13, 8677−8696.

Faber, T. E., & Ziman, J. M. (1965). A theory of the electrical properties of liquid metals. *Philosophical Magazine,* 11, 153−173.

Faber, T. F. (1972). *An introduction to the theory of liquid metals and alloys*. London: Cambridge University Press.

Flory, P. J. (1942). Thermodynamics of high polymers solutions. *Journal of Chemical Physics,* 10, 51−61.

Gancarz, T. (2017). Density, surface tension and viscosity of Ga−Sn alloys. *Journal of Molecular Liquids,* 241, 231−236.

Gancarz, T. & Gasior, W. (2016). The effect of Na addition on the density, surface tension and viscosity of liquid Sn−Zn alloys. *Fluid Phase Equilibria,* 418, 57−61.

Garzel, G., Janezak-Rusch, T., & Zabdyr, L. (2012). Reassessment of the Ag−Cu phase diagram for nanosystems including particle size and shape effects. *Calphad,* 36, 52−56.

Gasior, W., Fima, P., & Moser, Z. (2012). Modeling of the thermodynamic properties of liquid Fe−Ni and Fe−Co alloys from the surface tension data. *Archives of Metallurgy and Materials,* 56, 13−23.

Gasior, W., Moser, Z., & Pstrus, J. (2001). Density and surface tension of the Pb−Sn liquid alloys. *Journal of Phase Equilibria,* 22, 20−25.

Gerling, U., Pool, M. J., & Predel, B. (1983). A Contribution to the associate model for binary liquid alloys. *Zeitschrift für Metallkunde,* 74, 616−619.

Gibbs, J. W. (1878). On the equilibrium of heterogeneous substances. *Transactions of the Connecticut Academy of Arts and Science,* 111, 108−248, 343−524.

Gnecco, F., Ricci, E., Amore, S., Giuranno, D., Borzone, G., Zonicchi, G., & Novakovic, R. (2007). Wetting behaviour and reactivity of lead free Au−In−Sn and Bi−In−Sn alloys on copper substrates. *International Journal of Adhesion and Adhesives,* 27, 409−416.

Godbole, R. P., Jha, S. A., Milanarun, M., & Mishra, A. K. (2004). Thermodynamics of liquid Cu-Mg alloys. *Journal of Alloys Compounds,* 363, 187-193.

Goel, R.P., Kellogg, H.H., & Larrain, J. (1980). Mathematical description of the thermodynamic properties of the systems Fe−O and Fe−O−SiO2. *Metallurgical Transactions B,* 11, 107−112.

Guggenheim, E. A. (1945). Statistical thermodynamics of the surface of regular solutions. *Transactions of the Faraday Society,* 41, 150−156.

Guggenheim, E. A. (1952). *Mixtures.* Oxford: Oxford University Press.

Guiner, A. (1963). *X-ray Diffraction.* San Francisco and London: W. H. Freemen and Company.

Hafner, J. (1977). Structure and thermodynamics of liquid metals and alloys. *Physical Review A,* 16, 351−364.

Hajra, J. P., & Divakar, M. (1996). Applicability of Butler's equation in interpreting the thermodynamic behaviour of surfaces and adsorption in Fe−S−O melts. *Metallurgical Materials Transactions B,* 27, 241−253.

Harris, L. A. (1968). Analysis of materials by electron−excited anger electrons. *Journal of Applied Physics,* 39, 1419−1427.

Hildebrand, J. R., Praunitz, R. L., & Scott, R. L. (1970). *Regular and related solutions.* New York: Van. Nostrand Reinhold Corporation.

Hildebrand, J. R., & Scott, R. L. (1950). *The solubility of non−electrolytes* (3 ed.). New York: Reinhold Publishing Corporation.

Hoar, T. P., & Melford, D. A. (1957). The surface tension of binary liquid mixtures: lead+tin and lead+indium alloys. *Transactions of the Faraday Society,* 53, 315−326.

Hoch, M. (1985). Application of the complex model to liquid metal-salt systems. *CALPHAD,* 9, 59−70.

Hoch, M., & Arpshofen, I. (1984). A modified aggregation model for the calculation of thermodynamic state functions of liquid alloys. *Zeitschrift für Metallkunde,* 75, 23−29.

Holtyn, C. H. (1996). The age of ship. *Transactions, Society of Noval Architects and Marine Engineers*, 74, 356−391.

Holtyn, C. H. (1972). *The construction and service records of a 306 Ft. aluminum trailer ship*. New York: Transactions, Society of Naval Architects and Marine Engineers.

Hoshino, K. (1982). Entropy of mixing of compound forming liquid binary alloys with two types of compounds. *Journal Physics F: Metal Physics,* 12, 1891−1896.

Hoshino, K., & Young, W. H. (1980). Entropy of mixing of compound forming liquid binary alloys. *Journal Physics F: Metal Physics,* 10, 1365−1374.

Huggins, M.L. (1942). Thermodynamic properties of solutions of long−chain compounds. *Annals of New York Academy of Sciences,* 43, 1−32.

Hultgren, R., Desai, P. D., Hawkins, D. T., Gleiser, M., & Kelley, K. K. (1973). *Selected Values of the Thermodynamic Properties of Binary Alloy*. Metal Park, Ohio: ASM.

Hume−Rothery, W., Mabbott, G. W., & Channel−Evans, K. M. (1934). The freezing points, melting points, and solid solubility limits of the alloys of silver and copper with the elements of the B sub−groups. *Philosophical Transactions of the Royal Society of London A,* 233, 1−97.

Hume−Rothery, W., & Powell, H. M. (1935). The theory of superlattice structures in alloys. *Zeitschrift für Kristallogr,* 91, 23−47.

Hume−Rothery, W., Smallman, R. E., & Haworth, C. W. (1988). *The structure of metals and alloys.* London: Institute of Metals.

Jha, I. S. (1989). *Stability of binary molten alloys* (Unpublished doctoral dissertation). Bhagalpur University, Bhagalpur, India.

Jha, I. S., Adhikari, D., & Singh, B. P. (2012). Mixing behaviour of sodium−based liquid alloys. *Physics and Chemistry of Liquids,* 50, 199−209.

Jha, I. S., Singh, R. N., Shrivastava, P. L., & Mitra, N. R. (1990). Local order in Cd−based liquid alloys. *Philosophical Magazine,* 61, 15−24.

Joarder, R.N., Pachandhari, S., & Gopala Rao, R.V. (1984). Thermodynamics of liquid noble−metal alloys through a pseudo−potential approach. *Physical Review B,* 30, 4417−4421.

Jordan, A. S. (1970). A theory of regular associated solution applied to the liquidus curve of the Zn−Te and Cd−Te system. *Metallurgical Transactions,* 1, 239−249.

Kaptay, G. (2012). On the tendency of solutions to tend towards ideal solutions at high temperatures. *Metallurgical and Materials Transactions A,* 43, 531−543.

Kaptay, G. (2015). Partial surface tension of components of a solution. *Langmuir,* 31, 5796−5804.

Kaptay, G. (2016). Modelling equilibrium grain boundary segregation, grain boundary energy and grain boundary segregation transition by the extended Butler equation. *Journal of Material Science,* 51, 1738−1755.

Kellogg, H.H. (1987). Thermochemistry of nickel−matte converting. *Canadian Metallurgical Quarterely,* 26, 285−298.

Kerker, G., Moran−Lopez, J. L., & Bennemann, K. H. (1977). Electronic theory for segregation at the surface of transition−metal alloys. *Physical Review B,* 15, 638−642.

Kerr, H.W. & Winegard, W.C. (1967). The structure of some eutectics with high ratios of the volume fraction. *Canadian Metallurgical Quarterly,* 6, 67−70.

Khanna, K. N., & Singh, P. (1982). Entropy of mixing of liquid metal alloys. *Physica B+C,* 114, 174−180.

Kirschner, I., Bankuti, J., Kiss, G., Kovacs, I., Laszloffy, L., Remenyi, G., & Sajo, K. (1974). Magnetic properties of superconducting In−Bi alloys. *Soviet Physics −Journal of Experimental and Theoretical Physics,* 39, 1054−1058.

Kleppa, O. J. (1960). The volume change on mixing in liquid metallic solutions. I. Alloys of cadmium with indium, tin, thallium, lead and bismuth. *Journal of Physical Chemistry,* 64, 1542−1546.

Koirala, R. P. (2016). *Phase separation in binary liquid alloys* (Unpublished doctoral dissertation), T. M. Bhagalpur University, Bhagalpur, India

Koirala, R. P., Jha, I. S., Singh, B. P., & Adhikari, D. (2013). Thermodynamic and structural behaviours of liquid Al−Ga alloys. *Advanced Materials Letters,* 4, 283−287.

Koirala, R. P., Kumar, J., Singh, B. P., & Adhikari, D. (2014). Bulk and surface properties of Co−Fe and Fe−Pd liquid alloys. *Journal of Non−Crystalline Solids,* 394−395, 9−15.

Komarek, K. L. (1973). Experimental methods for the thermodynamics of metals and alloys. *Zeitschrift für Metallkunde,* 64, 325−341.

Koo, J., Erlkamp, M., Grobelny, S., Steitz, R., & Czeslik, C. (2013). Pressure induced protein adsorption at aqueous−solid interface. *Langmuir,* 29, 8025−8030.

Kubaschewki, O. (1981). Experimental thermochemistry of alloys. *Physica B,* 103, 101−112.

Kubaschewski, O. (1976). *Phase stability in metals and alloys*. New York: McGraw−Hill.

Kubaschewski, O., Aclock, C. B., & Spencer, P. J. (1993). *Materials Thermochemistry*. New York: Pergaman Press.

Kumar, A., Jha, I. S., & Singh, B. P. (2011). Quasi−lattice model for the thermodynamic properties and microscopic structure of molten Fe−Si alloy. *Physica B: Condensed Matter,* 406, 4338−4341.

Kumar, A., Jha, I. S., & Singh, B. P. (2013). Thermodynamic and atomic order in molten Mg−Bi alloy. *Advanced Materials Letters,* 4, 155−159.

Kumar, A. & Ojha, D.P. (2010). Electric, transport and thermodynamic properties of binary liquid alloy: Sb initio approach. *Metallurgical and Materials Transactions B,* 41, 574−582.

Kumar, A. & Ojha, D.P. (2011). Electrical transport and electric structure calculation of Al−Ga binary alloys. *Acta Physica Polonica A,* 119, 408−415.

Langmuir, I. (1917). The constitution and fundamental properties of solids and liquids. II. Liquids. *Journal of American Chemical Society,* 39, 1848−1906.

Lee, H. K., Frohberg, M. G., & Hajra, J. P. (1993). The determination of the surface tensions of liquid iron, nickel and iron−nickel alloys using the electromagnetic oscillating droplet technique. *Steel Research International,* 64, 191−196.

Lee, J., Shimoda, W., & Tanaka, T. (2004). Surface tensions and its temperature coefficient of liquid Sn−X (X=Ag, Cu) alloys. *Materials Transactions,* 45, 2864−2870.

Lele, S., & Ramchandrarao, P. (1981). Estimation of complex concentration in a regular associated solution. *Metallurgical and Materials Transactions,* 12, 659−666.

Lewis, G. M. (1907). Outlines of a new system of thermodynamic chemistry. *Proceedings of Americal Academy of Arts and Sciences,* 43, 259−293.

Li, H., Wang, G., Ding, F., Wang, J., & Shen W. (2001). Molecular dynamics computation of clusters in liquid Fe−Al alloy. *Physics Letters A*, 280, 325−332.

Li, H., Xiufang, B., & Wang, G. (2001). Molecular dynamics computation of the liquid structure of $Fe_{50}Al_{50}$ alloy. *Materials Science and Engineering A*, 298, 245−250.

Lin, S., Nie, Z., Huang, H., Zhan, C., Xing, Z., & Wang, W. (2010). Thermodynamic calculations of Er−X and Al−Er−X compounds existing in Al−Mg−Mn−Zr−Er alloys. *Transactions of Non ferrous Metals Society of China,* 20, 682−687.

Liu, X. Y., & Adams, J. B. (1998). Grain−boundary segregation in Al−Mg alloys at hot working temperatures. *Acta Materilia*, 46, 3467−3476.

Liu, X. J., Yamaki, T., Ohnuma, I., Kainuma, R., & Ishida, K. (2004). Thermodynamic calculations of phase equilibrias, surface tension and viscosity in In−Ag−X (X=Bi; Sb) systems. *Materials Transactions,* 45, 637−645.

Longuet−Higgins, H.C. (1951). The statistical thermodynamics of multicomponent systems. *Proceedings of the Royal Society of London A,* 205, 247−269.

Luka, H. L., Fries, S. G., & Sundman, B. (2007). *Computational thermodynamics: the CALPHAD method.* United Kingdom: Cambridge University Press.

Lukas, H. L., Fries, S. G., & Sundman, B. (2007). *Computational Thermodynamics: The Calphad Method.* United Kingdom: Cambridge University Press.

Mansoori, G. A., Carnahan, N. F., Starling, K. E., & Leland, T. W. J. (1971). Equilibrium thermodynamic properties of mixtures of hard spheres. *Journal of Chemical Physics,* 54, 1523−1525.

March, N. H. (1968). *Liquid Metals*. Oxford: Pergamon Press.

March, N. H., & Alonso, J. A. (2008). Non−monotomic behaviour with concentration of the surface tension of certain binary liquid alloys. *Physics and Chemistry of Liquids,* 46, 522−526.

March, N. H., & Josi, M. P. (1976). *Atomic Dynamics in Liquids*. London: Mac Millan Press Limited.

Matsunaga, S., Ishiguro, T. & Tamaki, S. (1983). Thermodynamic properties of liquid Na−Pb alloys. *Journal of Physics F: Metal Physics,* 13, 587−596.

Mc Cormack, M., Jin, S., & Chen, H. S. (1994). New lead free Sn−Zn−In solder alloys. *Journal of Electronic Materials,* 23, 715−720.

Mc Lean, D. (1957). *Grain Boundaries in Metals.* Oxford: Oxford University Press.

Mc Alister, S. P., & Crozier, E. D. (1974). The concentration-concentration correlation function in the long−wavelength limit for binary liquid alloys. *Journal of Physics C: Solid State Physics,* 7, 3509−3519.

Mekler, C., & Kaptay, G. (2008). Calculation of surface tension and surface phase transition line in binary Ga−Tl system. *Material Science and Engineering A,* 495, 65−69.

Mendelev, M. I. (2009). Molecular dynamics simulation of diffusion in supercooled Cu-Zr alloys. *Philosophical Magazine*, 89, 109-126.

Mendelev, M. I., Asta, M., Rahman, M. J., & Hoyt, J. J. (2009). Development of interatomic potentials appropriate for simulation of solid−liquid interface properties in Al−Mg alloys. *Philosophical Magazine*, 28, 3269−3285.

Miedema, A. R., De Boer, F. R., & Boom, R. (1981). Predicting heat effects in alloys. *Physica B+C,* 103, 67−81.

Miedema, A. R., De Chatel, P. F., & De Boer, F. R. (1980). Cohesion in alloys−fundamentals of a semi−emperial model. *Physica B,* 100, 1−28.

Miki, T., Ogawa, N., Nagasaka, T., & Hino, M. (2001). Activity Measurement of the Constituents in Molten Ag−In−Sn Ternary Alloy by Mass Spectrometry. *MaterialsTransactions,* 42, 732−738.

Mishra, A. K., Singh, R. N., & Sahay, B. B. (1993). Electrical resistivity and thermodynamic properties of alkali−alkali liquid binary alloys. *Physics and Chemistry of Liquids,* 25, 153−168.

Monma, K., & Sudo, H. (1961). Thermodynamics of surface tension. *Journal of Japan Institute of Metals,* 25, 65−68.

Morris, D.G. & Munoz−Morris, M. (2005). The stress anomaly in FeAl-Fe3Al alloys. *Intermetallics,* 13, 1269−1274.

Mudry, S., Sklyarchuk, V., Yakymovych, A., & Schtablavy I. (2007). The structure and viscosity features in In−Bi near−eutectic melts. *Physics and Chemistry of Liquids*, 45, 675−681.

Novakovic, R. (2010). Thermodynamic, surface properties and microscopic functions of liquid Al−Nb and Nb−Ti alloys. *Journal of Non−Crystalline Solids,* 356, 1593−1598.

Novakovic, R., & Brillo, J. (2014). Thermodynamics, thermophysical and structural properties of liquid Fe−Cr alloys. *Journal of Molecular Liquids,* 200, 153−159.

Novakovic, R., Giuranno, D., Ricci, E., Delsante, S., Li, D., & Borzone, G. (2011). Bulk and surface properties of liquid Sb−Sn alloys. *Surface Science,* 605, 248−255.

Novakovic, R., Muolo, M. L., & Dasserone, A. (2004). Bulk and surface properties of liquid X−Zr (X=Ag, Cu) compound forming alloys. *Surface Science,* 549, 281−293.

Novakovic, R., Ricci, E., Giuranno, D., & Passerone, A. (2005). Surface and transport properties of Ag−Cu liquid alloys. *Surface Science,* 576, 175−187.

Odusote, Y.A., Fayose, O.O., & Odigie, P.J. (2007). Mixing properties of X−Pb, (X= Cd, In) liquid binary alloys. *Journal of Non−Crystalline Solids,* 353, 4666−4671.

Ogawa, T. (1993). Alloying behaviour among V, Np, Pu and Am predicted with Brewer valence bond model. *Journal of Alloys and Compounds,* 194, 1−7.

Ohno, S. & Tamaki, S. (2016). Electronic properties of liquid In−Bi alloys. *Journal of the Physical Society of Japan,* 38, 538−543.

Osamura, K., & Predel, B. (1977). Association in Metallic solution. *Transactions of the Japan Institute of Metals,* 118, 765−774.

Osman, S. M., & Singh, R. N. (1993). Concentration fluctuations at the liquid-vapour coexistence in Ne−Ar mixture. *Journal of Non−Crystalline Solids,* 156−158, 459−462.

Osman, S. M., & Singh, R. N. (1995). Description of concentration fluctuations in liquid binary mixtures with nonadditive potentials. *Physical Review E,* 51, 332−338.

Ouyang, Y. F., Zhang, B. W., Jin, Z. P., & Liao, S. Z. (1996). The formation enthalpies of rare earth−aluminum alloys and intermetallic components. *Zeitschrift für Metallkunde,* 87, 802−805.

Overbury, J. H., Bertrand, P. A., & Somorjai, G. A. (1975). Surface composition of binary−systems−prediction of surface phase−diagrams of solid−solutions. *Chemical Reviews,* 75, 547−560.

Passerone, A., Muolo, M.L., Valenza, F., & Novakovic R. (2009). Thermodynamic and surface properties of liquid Cu−B alloys. *Surface Science,* 603, 2725−2733.

Picha, R., Vrestal, J., & Kroupa, A. (2004). Prediction of alloy surface tension using a thermodynamic database. *CALPHAD,* 28, 141−146.

Plevachuk, Y., Sklyarchuk, V., Gerbeth, G., Eckert, S., & Novakovic, R. (2011). Surface tension and density of liquid Bi−Pb, Bi−Sn and Bi−Pb−Sn eutectic alloys. *Surface Science,* 605, 1034−1042.

Prasad, L. C., & Jha, R. K. (2005). Surface tension and viscosity of Sn−based binary liquid alloys. *Physica Status Solidi,* 202, 2709−2719.

Prasad, L. C., & Singh, R. N. (1990). A quasi-lattice model for the thermodynamic properties of Au−Zn liquid alloys. *Physics and Chemistry of Liquids,* 22, 1−9.

Prasad, L. C., & Singh, R. N. (1991). Surface segregation and concentration fluctuation at the liquid−vapour interface of molten Cu−Ni alloys. *Physical Review B,* 44, 13768−13771.

Prasad, L. C., Singh, R. N., & Singh, G. P. (1994). The role of size effects on surface properties. *Physics and Chemistry of Liquids,* 27, 179−185.

Predel, B. (1982). Recent trends and developments of experimental methods for the determination of thermodynamic quantities of alloys. *CALPHAD,* 6, 199−216.

Prigogine, I., & Defay, R. (1954). *Chemical Thermodynamics.* London: Longmans Green and Company.

Pstrus′, J., Moser, Z. & Gasior, W. (2011). Surface properties of liquid In−Zn alloys. *Applied Surface Science,* 257, 3867−3871.

Rais, A., Cusack, N. E., & Neale, F. E. (1982). Simultaneous measurement of resistivity and thermodynamic properties of liquid binary alloys application to Na−In, Na−Sn. *Journal of Physics F: Metal Physics,* 12, 1091−1100.

Ramchandrarao, P., Suryanarayana, C., & Anantharaman, T. R. (1971). On the Origin of metastable intermediate phases in splat−cooled binary Alloys. *Metallurgical Transactions,* 2, 617−619.

Ratti, V. K., & Bhatia, A. B. (1978). Concentration fluctuations and structure factors of alloys. *II Nuovo Cimento B,* 43, 1−12.

Raychaudhari, P.K. & Stafford, F.E. (1975). Alloys thermodynamics by mass spectrometry. *Materials Science and Engineering A,* 20, 1−18.

Rehn, L. E., Robrock, K. –H., & Jacques, H. (1978). Interstitial-solute complexes in an irradiated Al−Fe alloy. *Journal of Physics F: Metal Physics*, 8, 1835−1844.

Richardson, F. D., & Alcock, C. B. (1959). *Physicochemical Measurements at High Temperature*. New York: Academic Press.

Ruppersberg, H. & Egger, H.J. (1975). Short−range order in liquid Li−Pb alloys. *Journal of Chemical Physics,* 63, 4095−4103.

Ruppersberg, H. & Reiter, H.J. (1982). Chemical short range order in liquid LiPb alloys. *Journal of Physics F: Metal Physics,* 12, 1311−1325.

Rusanov, A. I. (2007). The essence of new approach to the equation of monolayer state. *Colloid Journal,* 69, 131−143.

Rusanov, A. I. (2014). New thermodynamic potentials for surface science. *Colloids Surface A,* 441, 363−367.

Saboungi, M. L., & Corbin, T. P. (1984). Dilute solution of sodium in molted bismuth and tin: EMF measurement and interpretation. *Journal of Physics F: Metal Physics,* 14, 13−21.

Saboungi, M. L., Geertsman, W., & Price, D. L. (1990). Ordering in Liquid Alloys. *Annual Review of Physics and Chemistry,* 41, 207−244.

Sachter, W. M. H., & Van Der Plank, P. (1969). The role of individual surface atoms in chemisorptions and catalysis by nickel−copper alloys. *Surface Science,* 18, 62−79.

Sakurai, T., Hashizume, T., Jimbo, A., Sakai, A., & Hyodo, S. (1985). New result in surface segregation in Ni−Cu binary alloys. *Physical Review Letters,* 55, 514−517.

Sandor, T., Mekler, C., Dobranszky, J., & Kaptay, G. (2013). An improved theoretical model for A−TIG welding based on surface phase transition and reversed Marangoni flow. *Metallurgical and Materials Transactions A,* 44, 351−361.

Schmitz, J., Brillo, J., Egrs, I. E., & Schmid-Fetzer, R. (2009). Surface tension of liquid Al−Cu binary alloys. *International Journal of Materials Research,* 100, 1529−1535.

Schmid, R. & Chang, Y.A. (1985). A thermodynamic of an associated solution model for liquid alloys. *CALPHAD,* 9, 363−382.

Schwitzgebel, G., & Langen, G. (1981). Application of the hard sphere throey to diffusion of binary liquid alloy systems. *Zeitschrift für Naturforsch,* 36, 1225−1232.

Shubin, A. B., & Shunyaev, K. Y. (2010). Enthalpies of mixing of rare earth metal-aluminium alloys: model calculations. *Rosplay,* 1, 44−50.

Sinfelt, J. H., Carter, J. L., & Yates, D. J. C. (1974). Catalytic hydrogenolysis and dehydrogenation over copper−nickel alloys. *Journal of Catalysis,* 24, 283−296.

Singh, B. P., Adhikari, D., & Jha, I. S. (2010). Concentration dependence of the structure and thermodynamic properties of silver−antimony alloys. *Journal of Non−Crystalline Solids,* 356, 1730−1734.

Singh, B. P., Koirala, R. P., Jha, I. S., & Adhikari, D. (2015). Thermodynamic, structure and surface properties in Sn−Zn melt at 750 K. *Applied Physics A−Material Science and Processing,* 120, 1347−1356.

Singh, P., & Khanna, K. N. (1984). Calculation of entropy of mixing of liquid metal alloys in a hard sphere system. *Pramana: Journal of Physics,* 23, 511−518.

Singh, R. N. (1981). Free energy and heat of mixing of alloys. *Journal Physics F: Metal Physics,* 11, 389−396.

Singh, R. N. (1987). Short−range order and concentration fluctuations in binary molten alloys. *Canadian Journal of Physics,* 65, 309−325.

Singh, R. N., & Bhatia, A. B. (1984). Flory's formula for the entropy of mixing of NaCs alloy. *Journal of Physics F: Metal Physics,* 14, 2309−2314.

Singh, R. N., & Choudhary, R. B. (1981). Entropies of molten alloys. *Journal Physics F: Metal Physics,* 11, 1577−1584.

Singh, R. N., Jha, I. S., & Sinha, S. K. (1991). The segregation−ordering transformation in CdNa liquid alloys. *Journal of Physics: Condensed Matter,* 3, 2787−2794.

Singh, R. N., & Sommer, F. (1997). Segregation and immiscibility in liquid binary alloys. *Reports in Progress in Physics,* 60, 57−150.

Skapski, A. S. (1948). The surface tensions of liquid metals. *Journal of Chemical Physics,* 16, 389−393.

Smith, L. A., Thorton, T. A., Stafford, C. F., Storto, J. M., & Holaday, V. D. (1980). CALPHAD: Compter coupling phase diagrams. *Thermochemistry,* 4, 201−218.

Sommer, F. (1982). Association model for the description of the thermodynamic functions of liquid alloys I: basic concepts. *Zeitschrift für Metallkunde,* 73, 72−77.

Sommer, F., Singh, R. N., & Witusiewicz, V. (2001). On the entropy of mixing. *Journal of Alloys and Compounds,* 325, 118−128.

Sommerfeld, A., & Beth, H. (1933). *Elektronentheorie Der Metalle.* Berlin: Springer.

Spieser, R., Poirier, D. R., & Yeum, K. (1987). Surface tension of binary liquid alloys. *Scripta Metallurgica,* 21, 687−692.

Srikanth, S., Goel, R.P., & Ramchandrarao, P. (1999). Limitations of a regular associated solution approximation in describing the thermodynamic behaviour of complex liquid alloys. *CALPHAD,* 23, 85−100.

Srikanth, S., & Jacob, K. T. (1988). Volume effects and associations in liquid alloys. *Metallurgical Transactions B,* 19, 465−470.

Stevenson, D.J. (1975). Thermodynamics and phase separation of dense fully ionized hydrogen−helium fluid mixtures. *Physical Review B,* 12, 3999−4007.

Stroud, D. (1973). Theory of phase separation in liquid−metal alloys. *Physical Review B,* 7, 4405−4408.

Suganuma, K. (2001). Advances in lead free electronics soldering. *Current Opinion in Solid State and Materials Science,* 5, 55−64.

Sun, S. P., Yi, D. Q., Liu, H. Q., Zang, B., & Jiang, Y. (2010). Calculation of glass forming ranges in Al−Ni−RE (Ce, La, Y) ternary alloys and their sub−binaries on Miedema model. *Journal of Alloys and Compounds,* 506, 377−387.

Tamaki, S., Mitsunaga, S., Ishiguro, T. &Takeda, S. (1984). Thermodynamic properties of liquid Na-VI B alloys: Li(x) Na(1-x). *Journal of Non−Crystalline Solids,* 61, 225−229.

Tanaka, T., Gokcen, N. A., & Morita, Z. (1990). Relationship between enthalpy of mixing and excess entropy in liquid binary alloys. *Zeitschrift für Metallkunde/Materials Research Advanced Techniques,* 81, 49−54.

Tanaka, T., Hack, K., Iida, T., & Hara, S. (1996). Application of a thermodynamic database to the evaluation of surface tensions of molten alloys, salt mixture and oxide mixtures. *Zeitschrift für Metallkunde,* 87, 380−389.

Tanaka, T., & Iida, T. (1994). Application of a thermodynamic database to the calculation of surface tension for iron−based liquid alloys. *Steel Research International,* 65, 21−28.

Tang, A., Pan, F., Yang, M., & Cheng, R. (2008). Mechanical properties and microstructure of magnesium−aluminium based alloys containing strontium. *Materials Transactions,* 49, 1203−1211.

Taylor, A., & Jones, R. M. (1958). Constitution and magnetic properties of iron−rich iron−aluminium alloys. *Journal of Physics and Chemistry of Solids,* 6, 16−37.

Thakur, A., Negi, N. S., & Ahluwalia, P. K. (2005). Electrical resistivity of NaPb compound-forming liquid alloy using abinitio pseudopotentials. *Pramana: Journal of Physics,* 65, 349−358.

Tiwari, B.L. (1987). Thermodynamic properties of liquid Al−Mg alloys measured by the e.m.f. method. *Metallurgical Transactions A,* 18, 1645−1651.

Trybula, M., Gancarz, T., & Gasior, W. (2014). Bulk and surface properties of liquid Al−Li and Li−Zn alloys. *Metallurgical and Materials Transactions A,* 45, 5517−5530.

Umar, I.H., Meyer, A., Watabe, M. & Young, W.H. (1974). Thermodynamic calculations for liquid alloys with an application to sodium-potassium. *Journal of Physics F: Metal Physics,* 4, 1691−1706.

Umar, I. H., Yokoyama, I., & Young, W. H. (1976). Entropies of mixing of liquid metals: A hard sphere description. *Philosophical Magazine,* 34, 535−548.

Van Hove, L. (1954). Correlations in space and time born approximation scattering in systems of interacting particles. *Physical Review,* 95, 249−262.

Vora, A. M. (2010). Study of thermodynamics of liquid noble−metals alloys through a pseudopotential theory. *Romanian Journal of Physics,* 55, 137−151.

Wagner, C.M.J. (1978). Direct method for the determination of atomic−scale structure of amorphous solids (X−ray, electron and neutron scatter). *Journal of Non−Crystalline Solids,* 31, 1−40.

Wang, C. C., & Wong, C. H. (2011). Short−to−medium range order of Al−Mg metallic glasses studied by molecular dynamics simulations. *Journal of Alloys and Compounds*, 509, 10222−10229.

Wang, J., Mia, M., Chartrand, P., & Jung, I. (2013). Thermodynamic evaluations and optimization of the Na−X binary systems (X=Ag, Ca, In, Sn, Zn) using combined CALPHAD and first principle methods of calculations. *Journal of Chemical Thermodynamics,* 66, 22−33.

Wang, S., Lai, S. K., & So, C. B. (1980). A self−consistent pseudopotential applied to transport coefficient of liquid binary alloys of alkali metals. *Journal of Physics F: Metal Physics,* 10, 445−460.

Warren, B. E. (1969). *X−Ray Diffraction.* Reading, Mass: Addison-Wesley Pub. Co.

Waseda, Y. (1980). *The Structure of Non−Crystalline Materials, Liquids and Amorphous Solid*. New York: McGraw−Hill.

Weltsch, Z., Lovas, A., Takacs, J., Cziraki, A., Toth, A., & Kaptay, G. (2013). Measurement and modeling of the wettability of graphite by a silver−tin liquid alloy. *Applied Surface Science,* 268, 52−60.

Williams, F. L., & Nason, D. (1974). Binary alloy surface compositions from bulk alloy thermodynamic data. *Surface Science,* 45, 377−408.

Wilson, J. R. (1965). The structure of liquid metals and alloys. *Metallurgical Review,* 10, 381−590.

Witusiewicz, V. T. (1995). Thermodynamics of liquid binary alloys of the 3d transition metals with metalloids: generalization. *Journal of Alloys and Compounds,* 221, 74−85.

Witusiewicz, V. T., & Sommer, F. (2000). Estimation of the excess entropy of mixing and the excess heat capacity of liquid alloys. *Journal of Alloys and Compounds,* 312, 228−237.

Woodward, C. W., Lill, J., Asta, M., & Trinkle, D. R. (2012). Molecular−dynamics simulations of molten Ni−based superalloys. *The Minerals, Metals and Materials*, 12, 537−545.

Wu, H. F., & Brewer, L. (1996). Calculation of binary phase diagrams of refractory metals, Ta, W, Tc, and Re with liquid metals, Am, Cm, and Bk, using a regular solution theory modification. *Journal of Phase Equlibria,* 17, 36−39.

Xi, Y., Zu, F.Q., Li, X.F., Yu, J., Liu, L.J., Li, Q., & Chen, Z.H. (2004). High−temperature abnormal behaviour of resistivities for Bi−In melts. *Physics Letters,* 329, 221−225.

Yadav, S. K., Lamichhane, S., Jha, L. N., Adhikari, N. P. & Adhikari, D. (2015). Mixing behaviour of Ni−Al melt at 1873 K. *Physics and Chemistry of Liquids,* 54, 370−383.

Yadav, S. K., Jha, L. N. & Adhikari, D. (2015). Segregation to ordering transformation of In−Sn melt. *Physics and Chemistry of Liquids,* 53, 443−454.

Yadav, S. K., Jha, L. N. & Adhikari, D. (2015). Thermodynamic and structural properties of Bi−based liquid alloys. *Physica B,* 475, 40−47.

Yadav, S. K., Jha, L. N. & Adhikari, D. (2014). Thermodynamic and structural behaviour of Mg−Ga melt at 923 K. *Journal of Advanced Physics,* 3, 248−253.

Yadav, S. K., Jha, L. N., Jha, I. S., Singh, B. P., Koirala, R. P. & Adhikari, D. (2016). Prediction of thermodynamic and surface properties of Pb−Hg liquid alloys at different temperatures. *Philosophical Magazine,* 96, 1909−1925.

Yadav, S. K., Jha, L. N. & Adhikari, D. (2016). Thermodynamic, structural, transport and surface properties of Pb−Tl liquid alloy. *BIBECHANA,* 13, 100−113.

Yang, H. W., Tao, D. P., & Zhou, Z. H. (2008). Prediction of the mixing enthalpies of binary liquid alloys by molecular interaction volume model. *Acta Metallurgica Sinica,* 21, 336−340.

Yih, T. S., & Thompson, J. C. (1982). Chemical potentials and related thermodynamic properties of molten Na−Cs and Na−Bi alloys. *Journal of Physics F: Metal Physics,* 12, 1625−1636.

Young, W. H. (1976). *Liquid metalls.* London: Institute of Physics.

Young, W. H. (1992). Structural and thermodynamic properties of NFE liquid metals and binary alloys. *Reports on Progress in Physics*, 55, 1769−1853.

Zhang, B., & Jesser, W. A. (2002). Formation energy of ternary alloy systems calculated by an extended Miedema model. *Physica B: Condensed Matter,* 315, 123−132.

Zhou, G. J., Liu, Z. W., Zeng, D. C., & Jin, Z. P. (2010). Thermodynamic assessment of the Fe−Er systems. *Physica B: Condensed Matter,* 405, 3590−3593.

Zuo, Y., & Chang, Y.A. (1993). Thermodynamic calculation of the Al−Mg phase diagram. *CALPHAD,* 17,161−174.

APPENDIX A

A: PARTIAL EXCESS AND EXCESS FREE ENERGIES OF MIXING

Table a: The computed values of excess free energy of mixing (G_M^{XS}/RT) for Bi−Tl liquid alloy at different temperatures

Concentration of Tl (x_1)	G_M^{XS}/RT			
	T = 750 K	T = 850 K	T = 950 K	T = 1050 K
0.1	-0.1746	-0.1537	-0.1372	-0.1239
0.2	-0.3794	-0.3382	-0.3072	-0.2821
0.3	-0.5531	-0.5064	-0.4636	-0.4289
0.4	-0.6721	-0.6232	-0.5729	-0.5323
0.5	-0.7340	-0.6884	-0.6359	-0.5934
0.6	-0.7460	-0.6990	-0.6498	-0.6099
0.7	-0.7360	-0.6908	-0.6492	-0.6156
0.8	-0.6204	-0.5907	-0.5606	-0.5364
0.9	-0.2713	-0.2529	-0.2368	-0.2237

Table b: The computed values of partial excess free energy of Tl (G_{Tl}^{XS}/RT) and Bi (G_{Bi}^{XS}/RT) of Bi−Tl liquid alloy at different temperatures

Conc. of Tl (x_1)	T = 750 K		T = 850 K		T = 950 K		T = 1050 K	
	G_{Tl}^{XS}/RT	G_{Bi}^{XS}/RT	G_{Tl}^{XS}/RT	G_{Bi}^{XS}/RT	G_{Tl}^{XS}/RT	G_{Bi}^{XS}/RT	G_{Tl}^{XS}/RT	G_{Bi}^{XS}/RT
0.1	-1.6919	-0.0060	-1.4886	-0.0054	-1.3281	-0.0049	-1.1982	-0.0045
0.2	-1.7718	-0.0313	-1.5754	-0.0289	-1.4278	-0.0270	-1.3084	-0.0255
0.3	-1.6357	-0.0891	-1.4951	-0.0827	-1.3639	-0.0777	-1.2578	-0.0737
0.4	-1.3850	-0.1968	-1.2841	-0.1826	-1.1752	-0.1714	-1.0871	-0.1624
0.5	-1.0759	-0.3921	-1.0128	-0.3639	-0.9301	-0.3416	-0.8632	-0.3236
0.6	-0.7501	-0.7397	-0.7060	-0.6885	-0.6509	-0.6481	-0.6062	-0.6155
0.7	-0.4485	-1.4069	-0.4200	-1.3227	-0.3891	-1.2562	-0.3641	-1.2024
0.8	-0.1783	-2.3890	-0.1731	-2.2611	-0.1608	-2.1600	-0.1509	-2.0782
0.9	-0.0335	-2.4110	-0.0328	-2.2342	-0.0304	-2.0945	-0.0284	-1.9815

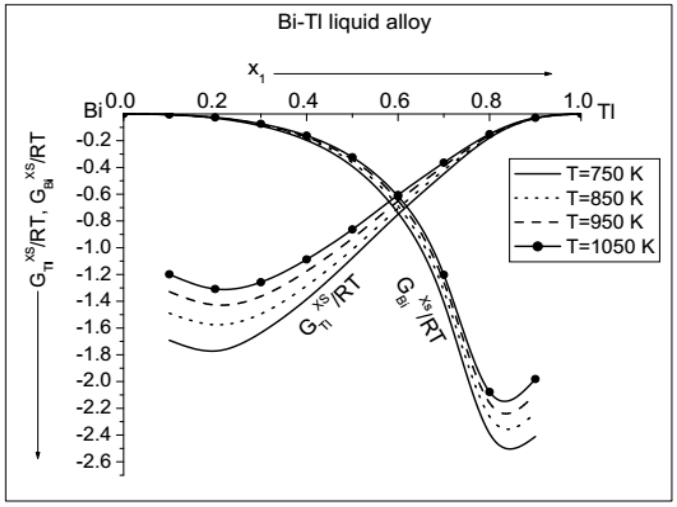

Figure a: G_{Tl}^{XS}/RT and G_{Bi}^{XS}/RT versus x_1 for Bi−Tl liquid alloy at different temperatures.

Table c: The computed values of excess free energy of mixing (G_M^{XS}/RT) for In–Bi liquid alloy at different temperatures

Concentration of In (x_1)	G_M^{XS}/RT			
	T = 900 K	T = 1000 K	T = 1100 K	T = 1200 K
0.1	-0.0697	-0.0623	-0.0563	-0.0512
0.2	-0.1374	-0.1240	-0.1131	-0.1041
0.3	-0.1940	-0.1764	-0.1621	-0.1501
0.4	-0.2348	-0.2146	-0.1981	-0.1844
0.5	-0.2539	-0.2329	-0.2156	-0.2013
0.6	-0.2542	-0.2340	-0.2174	-0.2036
0.7	-0.2332	-0.2155	-0.2010	-0.1890
0.8	-0.2029	-0.1893	-0.1783	-0.1690
0.9	-0.0962	-0.0887	-0.0826	-0.0775

Table d: The computed values of partial excess free energies of In (G_{In}^{XS}/RT) and Bi (G_{Bi}^{XS}/RT) of In–Bi liquid alloy at different temperatures

x_1	T = 900 K		T = 1000 K		T = 1100 K		T = 1200 K	
	G_{In}^{XS}/RT	G_{Bi}^{XS}/RT	G_{In}^{XS}/RT	G_{Bi}^{XS}/RT	G_{In}^{XS}/RT	G_{Bi}^{XS}/RT	G_{In}^{XS}/RT	G_{Bi}^{XS}/RT
0.1	-0.6963	-0.0001	-0.6282	0.0006	-0.5724	0.0011	-0.5259	0.0016
0.2	-0.6636	-0.0058	-0.6074	-0.0032	-0.5613	-0.0011	-0.5230	0.0006
0.3	-0.5819	-0.0277	-0.5368	-0.0220	-0.4999	-0.0173	-0.4692	-0.0134
0.4	-0.4745	-0.0750	-0.4401	-0.0643	-0.4119	-0.0556	-0.3885	-0.0483
0.5	-0.3501	-0.1576	-0.3259	-0.1398	-0.3060	-0.1252	-0.2895	-0.1130
0.6	-0.2350	-0.2829	-0.2196	-0.2555	-0.2069	-0.2331	-0.1964	-0.2144
0.7	-0.1356	-0.4610	-0.1272	-0.4215	-0.1204	-0.3891	-0.1147	-0.3622
0.8	-0.0662	-0.7498	-0.0627	-0.6959	-0.0599	-0.6518	-0.0575	-0.6151
0.9	-0.0122	-0.8526	-0.0114	-0.7846	-0.0108	-0.7288	-0.0103	-0.6824

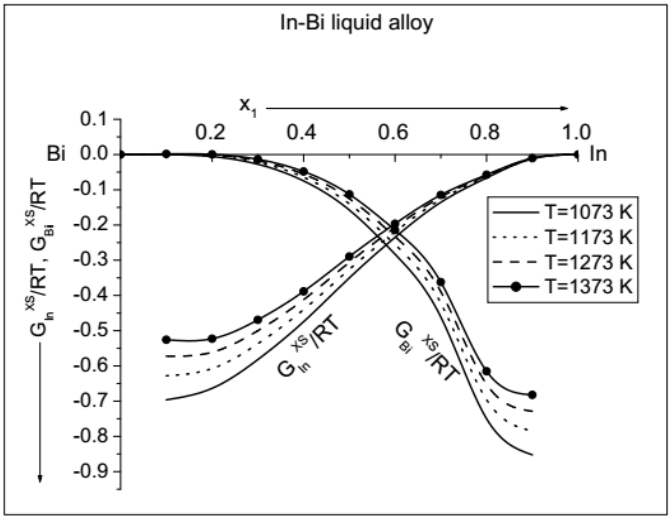

Figure b: G_{In}^{XS}/RT and G_{Bi}^{XS}/RT versus x_1 for In–Bi liquid alloy at different temperatures.

Table e: The computed values of excess free energy of mixing (G_M^{XS}/RT) for Al–Fe liquid alloy at different temperatures

Concentration of Al (x_1)	G_M^{XS}/RT			
	T = 1873 K	T = 1973 K	T = 2073 K	T = 2173 K
0.1	-0.2632	-0.2435	-0.2257	-0.2096
0.2	-0.4720	-0.4371	-0.4055	-0.3769
0.3	-0.6216	-0.5757	-0.5343	-0.4967
0.4	-0.7193	-0.6670	-0.6196	-0.5767
0.5	-0.7600	-0.7054	-0.6561	-0.6115
0.6	-0.7433	-0.6910	-0.6437	-0.6008
0.7	-0.6682	-0.6223	-0.5809	-0.5433
0.8	-0.5290	-0.4937	-0.4619	-0.4329
0.9	-0.3371	-0.3166	-0.2983	-0.2816

Table f: The computed values of partial excess free energies of Al (G_{Al}^{XS}/RT) and Fe (G_{Fe}^{XS}/RT) of Al–Fe liquid alloy at different temperatures

x_1	T = 1873 K		T = 1973 K		T = 2073 K		T = 2173 K	
	G_{Al}^{XS}/RT	G_{Fe}^{XS}/RT	G_{Al}^{XS}/RT	G_{Fe}^{XS}/RT	G_{Al}^{XS}/RT	G_{Fe}^{XS}/RT	G_{Al}^{XS}/RT	G_{Fe}^{XS}/RT
0.1	-2.4209	-0.0234	-2.2431	-0.0213	-2.0825	-0.0194	-1.9367	-0.0177
0.2	-1.9870	-0.0933	-1.8450	-0.0851	-1.7168	-0.0777	-1.6003	-0.0710
0.3	-1.5478	-0.2246	-1.4387	-0.2058	-1.3402	-0.1889	-1.2507	-0.1735
0.4	-1.1911	-0.4048	-1.1108	-0.3711	-1.0383	-0.3405	-0.9725	-0.3129
0.5	-0.8602	-0.6597	-0.8055	-0.6053	-0.7560	-0.5562	-0.7112	-0.5117
0.6	-0.5671	-1.0077	-0.5342	-0.9262	-0.5045	-0.8526	-0.4775	-0.7858
0.7	-0.3214	-1.4775	-0.3055	-1.3615	-0.2912	-1.2568	-0.2782	-1.1617
0.8	-0.1378	-2.0940	-0.1328	-1.9375	-0.1283	-1.7961	-0.1242	-1.6677
0.9	-0.0357	-3.0493	-0.0355	-2.8469	-0.0354	-2.6640	-0.0353	-2.4980

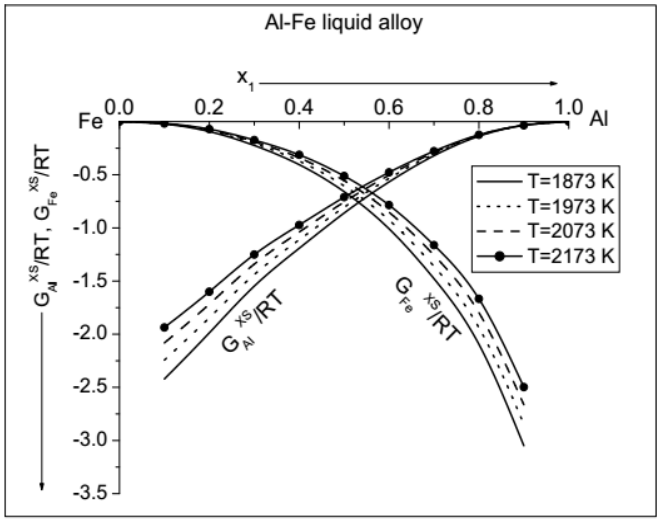

Figure c: G_{Al}^{XS}/RT and G_{Fe}^{XS}/RT versus x_1 for Al–Fe liquid alloy at different temperatures.

Table g: The computed values of excess free energy of mixing (G_M^{XS}/RT) for Al–Mg liquid alloy at different temperatures

Concentration of Al (x_1)	G_M^{XS}/RT			
	T = 1073 K	T = 1173 K	T = 1273 K	T = 1373 K
0.1	-0.0665	-0.0558	-0.0473	-0.0397
0.2	-0.1292	-0.1107	-0.0951	-0.0817
0.3	-0.1875	-0.1630	-0.1425	-0.1249
0.4	-0.2359	-0.2081	-0.1847	-0.1646
0.5	-0.2775	-0.2499	-0.2268	-0.2069
0.6	-0.2672	-0.2418	-0.2204	-0.2022
0.7	-0.1993	-0.1753	-0.1550	-0.1374
0.8	-0.1385	-0.1200	-0.1044	-0.0912
0.9	-0.0751	-0.0647	-0.0559	-0.0484

Table h: The computed values of partial excess free energies of Al (G_{Al}^{XS}/RT) and Fe (G_{Mg}^{XS}/RT) of Al–Mg liquid alloy at different temperatures

x_1	T = 1073 K		T = 1173 K		T = 1273 K		T = 1373 K	
	G_{Al}^{XS}/RT	G_{Mg}^{XS}/RT	G_{Al}^{XS}/RT	G_{Mg}^{XS}/RT	G_{Al}^{XS}/RT	G_{Mg}^{XS}/RT	G_{Al}^{XS}/RT	G_{Mg}^{XS}/RT
0.1	-0.6538	-0.0012	-0.5589	0.0001	-0.4789	0.0007	-0.4105	0.0015
0.2	-0.6342	-0.0030	-0.5555	0.0005	-0.4892	0.0034	-0.4326	0.0060
0.3	-0.5896	-0.0151	-0.5252	-0.0078	-0.4709	-0.0017	-0.4245	0.0035
0.4	-0.5050	-0.0565	-0.4544	-0.0439	-0.4117	-0.0333	-0.3753	-0.0242
0.5	-0.3938	-0.1611	-0.3572	-0.1426	-0.3264	-0.1271	-0.3000	-0.1138
0.6	-0.1171	-0.4923	-0.0993	-0.4556	-0.0842	-0.4247	-0.0714	-0.3983
0.7	-0.0390	-0.5733	-0.0300	-0.5143	-0.0223	-0.4647	-0.0158	-0.4212
0.8	-0.0084	-0.6590	-0.0045	-0.5820	-0.0013	-0.5170	0.0014	-0.4615
0.9	0.0032	-0.7797	0.0041	-0.6838	0.0049	-0.6029	0.0055	-0.5338

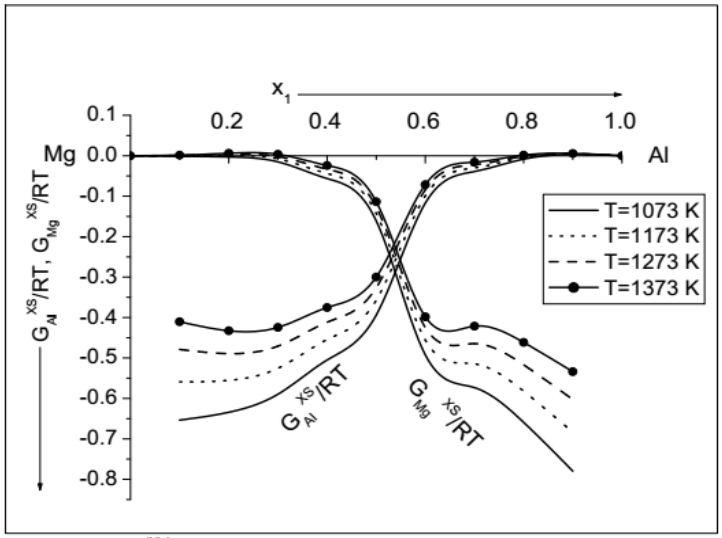

Figure d: G_{Al}^{XS}/RT and G_{Mg}^{XS}/RT versus x_1 for Al–Mg liquid alloy at different temperatures.

APPENDIX B

B: LIST OF PUBLICATIONS

1. **Prediction of thermodynamic and surface properties of Pb−Hg liquid alloys at different temperatures.**
   S.K. Yadav, L.N. Jha, I.S. Jha, B.P. Singh, R.P. Koirala and D. Adhikari
   Philosophical Magazine, 96(18) (2016) 1909−1925.

2. **Thermodynamic, structural, transport and surface properties of Pb−Tl liquid alloy**.
   S.K Yadav, L.N. Jha and D. Adhikari
   BIBECHANA, 13 (2016) 100−113.

3. **Mixing behaviour of Ni−Al melt at 1873 K**.
   S.K. Yadav, S. Lamichhane, L.N. Jha, N.P. Adhikari and D. Adhikari
   Physics and Chemistry of Liquid, 54(3) (2015) 370−383.

4. **Thermodynamic and structural properties of Bi−based liquid alloys**.
   S.K. Yadav, L.N. Jha and D. Adhikari
   Physica B: Condensed Matter, 475 (2015) 40−47.

5. **Thermo−physical properties of Mg−Tl melt**.
   D. Adhikari, S.K. Yadav and L.N. Jha
   Journal of Basic and Applied Research International, 9(2) (2015) 103−110.

6. **Segregation to ordering transformation in In−Sn melt**.
   S.K. Yadav, L.N. Jha and D. Adhikari
   Physics and Chemistry of Liquids, 53(4) (2015) 443−454.

7. **Thermodynamic and structural behaviour of Tl−Na liquid alloy**.
   S.K. Yadav, L.N. Jha and D. Adhikari
   BIBECHANA, 12 (2014) 20−29.

8. **Thermo−physical properties of Al-Fe melt**.
   D. Adhikari, S.K. Yadav and L.N. Jha
   Journal of the Chinese Advanced Material Society, 2(3) (2014) 149−153.

9. **Thermodynamic and Structural behaviour of Mg−Ga Melt at 923 K**.
   S.K. Yadav, L.N. Jha and D. Adhikari
   Journal of Advanced Physics, 3 (2014) 248−253.

10. **Segregation in Fe−Pd melt at 1873 K**.
    S.K. Yadav, L.N. Jha and D. Adhikari
    Bibechana, 11 (2014) 86−93**.**

C: LIST OF CONFERENCES ATTENDED

a: International Conferences

1. **Emerging Trends in Condensed Matter Physics,** University Department of Physics, 17−18 January, 2014, T. M. Bhagalpur University, Bhagalpur, India.

2. **Fourth International Science Congress,** 8−9 December, 2014, Udaipur, Rajasthan, India.

b: National Conferences

1. **Seminar on Modern Trends of Science and Technology,** 28−29 December, 2012, Biratnagar, Nepal.

2. **International Conference on Emerging Trends in Science and Technology,** 22–23 March, 2014, Biratnagar, Nepal.

3. **The Seventh National Conference on Science and Technology,** 29–31 March, 2016, Kathmandu, Nepal.